

Clinical Medicine Section

Department of Medicine

# "Multimodal Immunomonitoring of Hematopoietic Stem Cell Transplantation and Cellular Therapies for Hematological Malignancies"

Thesis submitted to the Faculty of Medicine of the University of Geneva

for the degree of Privat-Docent by

Federico SIMONETTA

Genève

2023

# **TABLE OF CONTENT**

1. Summary	3
2. Introduction	4
2.1. Immunomonitoring in allogeneic hematopoietic stem cell transplantation	4
(HSCT) and cellular therapies	
2.1.1 Immunomonitoring in allogeneic HSCT	4
2.1.2 Immunomonitoring after cellular therapies	10
2.2. Molecular imaging in allogeneic HSCT	12
2.2.1 Imaging metabolism	13
2.2.2. Molecular imaging of T cell responses	14
2.2.2.1 Small molecules	16
2.2.2.2 Imaging T cell lineage markers	17
2.2.2.3 Imaging T cell activation markers	17
2.2.3 Imaging tissue damage	18
3. Publications	20
3.1. Publication 1 (Xiao*, Alam*, Simonetta* et al., Blood Adv 2022)	20
3.2. Publication 2 (Maas-Bauer, [], Simonetta*, Negrin*, Blood 2021)	33
3.3. Publication 3 (Simonetta et al., Clin Can Res 2021)	48
3.4. Publication 4 (Lohmeyer, [], Negrin*, Simonetta*, Blood 2022)	61
3.5. Publication 5 ( <i>Pradier*</i> , <i>Mamez*</i> , [], <i>Simonetta</i> , <i>Ann Oncol</i> 2022)	88
4. Conclusion and perspectives	92
4.1. Molecular imaging of allogeneic HSCT and cellular therapies - summary	92
of the results and future directions	
4.2. Immune-effector and immuno-regulatory cellular therapies - summary of	94
the results and future directions	
5 References	98

# 1. Summary

Allogeneic hematopoietic stem cell transplantation (HSCT) and other cellular therapies are a broadly used therapeutic strategy employed against a wide range of hematological malignancies. However, these therapies are associated with significant toxicities and their efficacy is still not optimal. Our ability to study the immune system at steady state, during physiological responses and in immunopathological diseases greatly increased during the last decades thanks to the technological advances coming from different fields including cytometry, genomics and molecular imaging. In this work, we will discuss the application of these techniques to the study of the immune system after allogeneic HSCT and cellular therapies. In particular, we will see how these approaches can be applied to the understanding of new diagnostic and therapeutic strategies and exploited for their optimization. We will discuss the development of molecular imaging strategies for the immunomonitoring of T cells during GvHD. We will apply the use of multiple genomic techniques to the understanding of GvHD suppression by immune-regulatory T cells, namely regulatory T cells (Treg) and invariant natural killer T (iNKT) cells. We will study the immunomodulatory effects of engineered CAR iNKT cells on host immune-cells leading to an amplification of their antitumoral effect. We will apply high-throughput T cell receptor (TCR) sequencing to the understanding of the immunological defects during anti-SARS-CoV-2 responses in allogeneic HSCT. Finally, we will discuss the future applications of this acquired knowledge to improve the efficacy and safety of allogeneic HSCT and cellular therapies.

#### 2. Introduction

# 2.1. Immunomonitoring in allogeneic hematopoietic stem cell transplantation (HSCT) and cellular therapies

# 2.1.1 Immunomonitoring in allogeneic HSCT

Allogeneic hematopoietic stem cell transplantation (HSCT) is a well-established and potentially curative therapy for a broad range of hematologic malignancies thanks to its **Graft-versus-Tumor** (**GvT**) effect. Unfortunately, allogeneic HSCT is still associated with significant morbidity and mortality related to cancer relapse and transplant complications, namely **Graft-versus-Host Disease** (**GvHD**).

Cancer relapse after allogeneic HSCT results from disease resistance to chemotherapy but also from tumor escape from the immune control by the allogeneic immune system (Zeiser and Vago, 2019). Tumor immune evasion involves tumor specific factors, including loss of HLA genes, production of immune-suppressive molecules and/or acquisition of novel driver mutations, as well as immunological factors leading to an impaired alloreactive immune response. The quantitative or qualitative delay in post-transplant immune-reconstitution of the allogeneic immune system (Storek et al., 2008) are potential immunological factors contributing to cancer relapse. At the same time, the allogeneic immune system can react abnormally against host tissues resulting in **GvHD**. During GvHD, the interaction with host tissues induces donor-derived T cells activation, proliferation and migration to target organs, notably skin, liver and intestine (Zeiser and Blazar, 2017). The same immunological mechanism, donor T cell alloreactivity toward host antigens, is responsible for the beneficial GvT effect of allogeneic HSCT (Negrin, 2015; Figure 1).

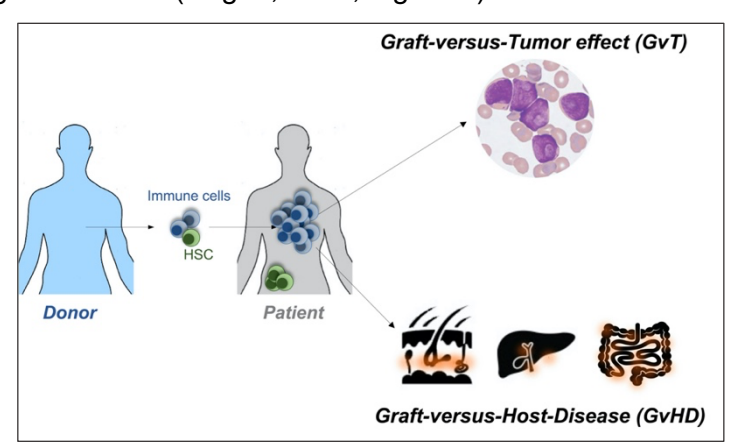


Figure 1. Graphical summary of the principles of allogeneic HSCT.

HSC: hematopoietic stem cells. Personal material.

Our ability to successfully prevent and treat relapse and GvHD strictly depends on our capacity to predict which patients will suffer post-transplant complications before clinical manifestations occur. To this aim, it is critically important to have immunomonotoring strategies capable of detecting in advance immune-defects leading to cancer relapse or excessive immune-activation leading to GvHD.

The advent of **systems immunology** dramatically expanded our ability to investigate the immune system in health and disease (Benoist et al., 2006; Davis et al., 2017). High-throughput analytical techniques can now extract extensive knowledge at the genomic, epigenomic, transcriptomic, and proteomic level from very limited amounts of materials. Such technological advances led over the last decade to an expansion of studies focusing of **biomarkers** for post-HSCT outcomes (reviewed in Paczesny, 2018). We will discuss some of the seminal studies that attempted to define cellular makers able to predict post-transplant complications.

Cytometry — Cytometry, using Fluorescence activated cell sorting (FACS) and more recently mass cytometry by time of flight (CyTOF), is the most widely employed technique to evaluate quantitatively and qualitatively post-transplant immune-reconstitution. Most centers routinely employ flow cytometry to measure the **number of immune cells**, mainly T cells and in some centers other lymphocyte subsets, recovering after transplantation. In most centers these values are clinically employed to guide the interruption of anti-infectious prophylactic treatments. Few centers adopted qualitative analysis of T cells subpopulations, namely naïve CD4 T cells, in the follow-up of patients to gain further insights into the quality of T cell reconstitution. However, absolute lymphocyte numbers do not provide qualitative information useful for prediction of GvHD or relapse. Although it is well established that immune-cells recovering after allogeneic HSCT display many phenotypic abnormalities, ranging from reduced proportion of naïve T cells and increased cell differentiation increased expression of proliferation (Ki-67) markers (Latis et al., 2020) to upregulation of immune-exhaustion markers such as PD-1, 2B4 and CD160 (Noviello et al., 2019; Simonetta et al., 2019), none of these markers appear to be predictive of post-transplant complications.

Based on the potency of several **immunoregulatory T cell subsets** to prevent and suppress GvHD in murine models and in clinical trials, several groups investigated the relationship between their immune-reconstitution and GvHD.

**Regulatory T cells** are a subpopulation of CD4 T cells characterized in human and mice by the constitutive expression of CD25, the alpha chain of the IL-2 receptor, and the transcription factor FOXP3 (Sakaguchi et al., 2020). Early studies in murine models of GvHD demonstrated

that the co-administration of Treg at time of transplant significantly reduced GvHD severity and mortality in major MHC-mismatch models of GvHD without blocking the ability of T cells to eradicate tumor cells (Edinger et al., 2003). These results, subsequently confirmed and extended by many other studies, motivated the analysis of FOXP3+ CD4+ CD25+ regulatory T cells reconstitution after allogeneic HSCT in humans. Several studies showed the association between reduced frequencies of FOXP3+ CD4+ CD25+ regulatory T cells in patients suffering from acute (Magenau et al., 2010) and chronic (Zorn et al., 2005) GvHD. Such abnormalities seem to be mainly related to an altered Treg homeostasis in allogeneic HSCT recipients (Matsuoka et al., 2010). Based on these data, effort have been made to restore Treg homeostasis using pharmacological approaches such as low dose interleukin-2 (IL-2; Koreth et al., 2011) eventually combined to the administration of Treg (Whangbo et al., 2022).

Invariant natural killer T cells are a second population of T cells able to suppress GvHD in animal models (Du et al., 2017; Leveson-Gower et al., 2011; Schneidawind et al., 2015, 2014; reviewed in Mavers et al., 2017). Although experimental evidence of the efficacy of iNKT cells to prevent GvHD in human is still lacking, several groups demonstrated the association between early recovery of iNKT cells after HSCT (Rubio et al., 2012), higher numbers of iNKT cells in the graft (Malard et al., 2016) and/or increased homeostatic potential of iNKT cells in donor cells (Rubio et al., 2017) and reduced risk of GvHD.

<u>Transcriptomic analyses</u> – Several studies attempted to identify biomarkers of post-transplant complications using **transcriptomic** analysis conducted on cells recovered from the peripheral blood, on bone marrow or on GvHD-target tissues.

Pidala and colleagues conducted the first attempts to use RNA microarrays (Pidala et al., 2015)(*Pidala et al., PLoS One. 2015*) or PCR on a small list of genes (Pidala et al., 2017) to distinguish patients at risk of developing GvHD or after diagnosis.

More recently, Latis and colleagues performed a transcriptomic analysis using of CD4+ and CD8+ T cells sorted from donors before transplant and from HSCT recipients (Latis et al., 2020). Comparison of the transcriptome of cells from HSCT recipients with cells from donors revealed the upregulation of gene sets involved in T cell activation, tissue migration and effector functions even in the absence of GvHD. More importantly, comparison of cells from patients with acute GvHD at disease onset with cells from patients without GvHD revealed a downregulation of transforming growth factor- $\beta$  (TGF- $\beta$ ) signaling in GvHD and an increase of signaling pathways and transcription factors associated with NF- $\kappa$ B.

In a very elegant and comprehensive multiomics study, Dubouchet and colleagues employed, among other techniques, transcriptomic analyses on recipients of HLA-matched grafts to

investigate the immune landscape associated with operational tolerance after transplantation, defined by lack of acute and chronic GvHD (Dubouchet et al., 2022). Comparison of tolerant versus non-tolerant patients by RNA sequencing analysis revealed an overexpression of genes associated with T cell differentiation (IL23R and ICOS) as well as the ectoenzyme NT5E (ecto-5'-nucleotidase, CD73), known to catabolize adenosine 5'-monophosphate (AMP) into adenosine, thus exerting immunosuppression.

Until recently limited to the study of bulk populations, next-generation sequencing approaches can now be employed at the single cell level. By deconvoluting immune system heterogeneity, single-cell technologies are particularly suited to the study of immunopathological processes as they allow the identification of abnormalities that would otherwise be masked by major skewing in cell subsets observed in pathological settings. Single-cell RNA sequencing (scRNA-seq) provides an analysis of the transcriptome at the single-cell level, scRNAseq allows for qualitative analyses of cells to define their classification in subsets, their differentiation and activation status and to infer insights about their biological activity. Assmann and colleagues employed for the first time this technology on samples recovered at day 30 post-HSCT from two patients, one patient who developed GvHD within 7 days from sampling and a second patient who did not develop GvHD (Assmann et al., 2021). Such analysis revealed increased expression of genes associated with T-cell activation, including CD69 and GADD45B as well as the upregulation of JUN and FOS in CD4 T cells from the patient who subsequently developed GvHD. Moreover, there was an upregulation of SLC2A3, encoding the glucose transporter GLUT3, in the "pre-GVHD" patient sample. Results in CD8 T cells showed a similar trend for activation gene sets but failed to observe the upregulation of SLC2A3 transcription. Importantly, the authors reported an enrichment in glycolysis gene sets, including PKM, ENO1, and LDHA, in CD4 T cells from the pre-GvHD patient. Although still quite preliminary and obtained from just 2 samples from 2 patients, this work showed the great potential of scRNAseq for the study of GvHD, both for the better understanding of its physiopathology and for biomarkers identification. A second study employed scRNAseq of bone marrow cells from two HSCT recipients before and after undergoing HSCT for AML (Zheng et al., 2017). After defining the donor or the recipient origin of the cells, the transcriptomic analysis revealed a decrease in T cells and an increase in erythroid cells and monocytes in post-transplant samples from AML-patients.

Few studies applied transcriptomics to the analysis of GvHD target tissues. Holtan and colleagues performed gene expression profiling on rectosigmoid biopsies from normal controls as well as from HSCT recipients at onset of stage 3–4 lower intestinal acute GvHD and, in some patients, after the GvHD became steroid refractory (Holtan et al., 2019). The analysis identified two genes encoding molecules previously reported to be involved in inflammatory

bowel disease pathogenesis, namely chitinase 3-like 1 (CHI3L1) as the most highly upregulated gene and aquaporin-8 (AQP8) as the most significantly decreased gene in acute GVHD compared with normal tissue. The analysis found as well modulation of some genes suggesting a potential interaction of host mucosa with microbiota, in particular upregulation of aryl hydrocarbon receptor (AhR) gene expression and amphiregulin (AREG) gene expression in acute GVHD samples compared with normal rectosigmoid biopsies. Gene set enrichment analysis indicated an increase in T cells gene expression as well as genes involved in inflammatory responses, both findings consistent with the known pathophysiology of acute GVHD. Interestingly, when the authors applied a cell deconvolution method, CIBERSORT, to estimate cell composition out of bulk transcriptomic analysis, they observed an increase in CD4+ activated memory T cells and of macrophages in acute GVHD samples compared with normal rectosigmoid biopsies. Moreover, while both onset and steroid-refractory acute GvHD displayed increased M1 macrophages compared with normal tissues, only steroid-refractory acute GvHD displayed increased M2 macrophages compared with both acute GvHD onset and normal biopsies. These findings are of particular interest as they move beyond the classical T-cell centric paradigm of GvHD pathogenesis and suggest a potential role of macrophages in GvHD. Finally, the authors were able to show an association of gene expression with early mortality finding that samples form patients surviving less than the median time of 82.5 days. expressed higher levels of glycerol kinase (GK), phosphoglycerate kinase 1 pseudogene 2 (PGK1P2), histone cluster 1 H1 family member A (HIST1H1A), and cytochrome C oxidase subunit 7B pseudogene 2 (COX7BP2). Based on enrichment analysis, this gene signature was associated with higher DNA damage and stress patterns in samples from patients with poor survival.

Very recently Zouali and colleagues performed bulk RNA sequencing analysis on chronic GvHD skin lesions (Zouali et al., 2022). By comparing the transcriptome of lichen planus chronic GvHD, morphea chronic GvHD and skin from healthy controls, the authors demonstrated that the up regulation in both chronic GvHD subtypes of common inflammatory pathways, including genes involved in the IFN-gamma signaling pathway. In addition, genes involved in the triggering receptor expressed on myeloid cells 1 (TREM-1) pathway were specifically upregulated in lichen planus suggesting their potential contribution to its pathogenesis.

<u>T-cell receptor sequencing</u> – Analysis of the sequences originating from the recombination of the variable (V), joining (J) and diversity (D) gene regions of T cell receptor (TCR), also known as TCR sequencing (TCRseq), is a powerful technique for the study of T cell biology. This approach allows the identification of TCR clonotypes composed by cells with the same specificity that can be followed over time to reconstruct the dynamics of a cell population

during an immune response or, in some cases, to predict the targeted antigen by inferring the specificity of the receptor. Given the importance of T cell reconstitution dynamics after allogeneic HSCT for the success of the transplant procedure and in the development of posttransplant complications, allogeneic HSCT has been one of the first settings where TCRseq was employed. Overall, TCR diversity appears to be reduced in allogeneic HSCT recipients compared with healthy donors (Buhler et al., 2020; Kanakry et al., 2016; Leick et al., 2020; Meier et al., 2013, 2019; van Heijst et al., 2013) with progressive although only partial recovery over time (Kanakry et al., 2016; Meier et al., 2013; van Heijst et al., 2013). Such diversity reduction is mainly the result of the expansion of phenotypically effector memory T cells with lower TCR repertoire diversity than the administered donor cells (Kanakry et al., 2016; van Heijst et al., 2013). Several factors influencing the TCR-repertoire reconstitution have been reported including the graft stem cell source (van Heijst et al., 2013; Yew et al., 2015; Leick et al., 2020), conditioning intensity and use of antithymocyte globulin (Leick et al., 2020) and donor age (Buhler et al., 2020). In addition, donor/recipient CMV serostatus and event more CMV infection/reactivation are considered as major drivers of T-cell clonal expansion and diversity loss after allogeneic HSCT (Kanakry et al., 2016; Suessmuth et al., 2015; van Heijst et al., 2013; Buhler et al., 2020). Regarding the relationship between the TCR repertoire and GvHD, acute GvHD has been associated with further reduced TCR diversity (van Heijst et al., 2013; Yew et al., 2015; Meier et al., 2019; Leick et al., 2020) leading some investigators to propose T cell clonal expansion as a potential biomarker for acute GvHD prediction (Leick et al., 2020). Only one study reported an inverse association, describing higher TCR diversity in patients with acute GvHD and prior systemic steroid treatment (van Heijst et al., 2013), a difference that could be due to the different patient cohort and stem cell source investigated. The analysis of the TCR repertoire in GvHD-target tissues showed little correlation with the TCR repertoire in peripheral blood (Meyer et al., 2013; Koyama et al., 2019; Kanakry et al., 2016) and revealed that T-cell repertoire in biopsies from patients suffering acute gastrointestinal GvHD are quite unique for each single patient with little overlap among patients (Meyer et al., 2013; Koyama et al., 2019). This was true even in experimental animal models employing mice of the same strain combinations (Zheng et al., 2020). More importantly, higher clonal expansion in biopsies from gastrointestinal tract was associated with more severe GvHD in terms of histological grade and of steroid-refractoriness (Meyer et al., 2013; Koyama et al., 2019). Little is known about the relationship between TCR repertoire reconstitution and risk of relapse, with one study reporting a correlation between higher TCR diversity and lower relapse rates (Yew et al., 2015).

TCR-sequencing has been recently employed in two studies evaluating the impact of adoptive transfer of manipulated CD45RA-depleted donor lymphocytes infusions (DLI) on the repertoire

of HSCT recipients (Blagov et al., 2021; van Beek et al., 2022). Surprisingly, the studies did not reveal a positive impact of CD45RA-depleted DLI T cell clonal diversity (van Beek et al., 2022). However, both studies were able to demonstrate the engraftment and persistence of pathogen-specific memory T cells, mainly cytomegalovirus (CMV)-specific cells (Blagov et al., 2021; van Beek et al., 2022).

Collectively, these and other results obtained using a wide range of technological approaches provided important clues on GvHD pathogenesis leading in some cases to the development of new therapeutic approaches but so far failed to provide a reliable cellular biomarker for post-transplant immunomonitoring. Moreover, most of these analyses were conducted on samples recovered from the peripheral blood which do not necessarily reflect the cell states at the tissue sites where tumor control and/or immunopathological reactions of GvHD take place. Whole-body immunomonitoring strategies are therefore urgently needed.

# 2.1.2 Immunomonitoring after cellular therapies

Over the last decades we witnessed a great progress in the development of cellular therapies for hematological malignancies ranging from immune effector to immunoregulatory cellular therapies. Most importantly, over the last five years, several cellular immunotherapies products were approved by the different regulatory authorities and are now part of the routine clinical practice.

Chimeric antigen receptor (CAR) T cells are T lymphocytes engineered to express synthetic receptors (CARs) specific to a predetermined tumor antigen. CAR T cells revolutionized the way we treat several refractory hematological malignancies are now clinically available for the treatment of relapsed/refractory large B cell lymphoma (LBCL), B-cell acute lymphoblastic leukemia, mantle cell lymphoma and multiple myeloma (MM). A summary of the currently available products approved by any of the regulatory agencies is provided in Table 1.

For some of these diseases, LBCL in particular, CAR T cells represent a potentially curative option for an important fraction of heavily pretreated patients. However, they show high patient-to-patient variability in expansion, activity, and overall efficacy, with only 30-50% of patients with LBCL experiencing long-term remission. CAR T cells are targeted 'living drugs' that need to migrate to tumor-infiltrated tissues and bind tumor-associated antigens on cancer cells to exert their function. Therefore, measuring their expansion and their persistence after administration can have prognostic significance and might impact clinical care.

PRODUCT	SPECIFICITY	DISEASE (APPROVAL)
TISAGENLECLEUCEL	CD19	B-ALL (FDA, EMA, CH) LBCL (FDA, EMA, CH) FL (FDA, EMA)
AXICABTAGENE CILOLEUCEL	CD19	LBCL (FDA, EMA, CH) FL (FDA, EMA, CH)
LISOCABTAGENE MARALEUCEL	CD19	LBCL (FDA, EMA, CH)
BREXUCABTAGENE AUTOLEUCEL	CD19	MCL (FDA, EMA, CH) B-ALL (FDA, EMA)
IDECABTAGENE VICLEUCEL	BCMA	MM (FDA, EMA, CH)
CILTACABTAGENE AUTOLEUCEL	BCMA	MM (FDA)

Table 1. CAR T cell products approved by different regulatory agencies for different indications. Personal material.

Current strategies to monitor CAR T cells include flow cytometry and PCR approaches, mainly performed on peripheral blood (PB) samples or, in some cases, at the tumor site when this is easily accessible to sampling (ex. bone marrow in B-ALL and MM).

Molecular quantification of CAR T cells, mainly using quantitative **PCR** (qPCR) or droplet digital PCR (ddPCR) to quantify sequences from the CAR construct, is a very sensitive approach to detect CAR T cells and one of the most widely employed both in clinical trials and clinical practice. As quantified by PCR, the early expansion of CAR-T cells upon infusion appeared to be a predictor of response to therapy after anti-CD19 CAR T cell therapies in B-cell malignancies (Fraietta et al., 2018; Neelapu et al., 2017; Park et al., 2018). Another pharmacokinetic parameter of potential clinical interest is CAR T cell persistence that in some settings, especially B-ALL, appears to be a predictor of long-term remissions (Gardner et al., 2017; Fraietta et al., 2018; Finney et al., 2019; Schultz, 2020). CD19 CAR T cell persistence can be predicted by the duration of B-cell aplasia, but the use of this parameter is limited by the pre-infusion existence of B-cell aplasia as a result of previous B-cell depleting treatments in patients with B cell malignancies.

Although less sensitive and potentially less specific than molecular techniques, **flow cytometry**, and more recently mass cytometry, can provide additional useful qualitative information in addition to CAR T cell quantification on molecules preferentially and ideally specifically expressed by T cells when they undergo activation during the biological process studied. Three main approaches are employed to specifically identify and analyze CAR T cells:

protein L staining, anti-idiotype staining or recognition of recombinant protein target. The three approaches allow phenotypic characterization of CAR T cells and comparison with endogenous non-CAR transduced cells. Moreover, these approaches allow the isolation of the CAR T cell population for in depth, high-throughput analysis.

Collectively, the aforementioned analyses have a great potential to offer new insights into the biology of CAR T cells but they unfortunately lack spatial information. Indeed, among the challenges hindering the success of CAR T cells is an incomplete understanding of cell fate *in vivo*, including their ability to traffic to and infiltrate the tumor, and persist. Such insight into the mechanisms underlying treatment success or failure would be invaluable. Strategies for non-invasive, sensitive, real-time monitoring of CAR T cell fate post-infusion in vivo are therefore urgently needed.

# 2.2. Molecular imaging in allogeneic HSCT

Current approaches for the diagnosis of GvHD are based on clinical and pathological elements that are therefore restricted to later, symptomatic stages of the disease. Given the importance of timely therapeutic interventions for GvHD treatment, prediction and early detection of GvHD before symptoms actually occur using non-invasive imaging modalities would have a great impact on patients' outcome. Conventional radiology using ultrasound, contrast-enhanced CT or MRI is of limited utility for accurate diagnosis of acute GvHD given the lack of specificity of morphological changes (Lubner et al., 2017).

Molecular imaging is a branch of medical imaging focusing on non-invasively measuring biological processes *in vivo*. Molecular imaging is widely employed in clinical medicine for different applications, ranging from neuroimaging to cardiology. In oncology, the evaluation of glucose metabolism is a routinely employed tool for staging, evaluation of responses and follow-up of a wide range of solid and hematologic malignancies.

Although still experimental, the application of molecular imaging to the study of the immune system is a rapidly expanding field. Positron emission tomography (PET) imaging is a highly sensitive and quantitative clinical molecular imaging modality, perfectly poised to provide non-invasive, whole-body mechanistic insights into disease pathogenesis. For this reason, molecular imaging using tracers specifically allowing detection of cellular and/or molecular processes involved in GvHD pathogenesis represent a promising approach to develop new strategies for early GvHD detection at pre-symptomatic stages.

# 2.2.1 Imaging metabolism

# 18F-fluorodeoxyglucose ([18F]FDG)

18F-fluorodeoxyglucose ([18F]FDG) is the most widely employed molecular imaging tracer in clinical practice which takes advantage of the higher glucose consumption by metabolically active cells and tissues.

Early reports suggested that molecular imaging by 18F-fluorodeoxyglucose ([18F]FDG) PET can visualize tissue inflammation associated with acute gastrointestinal GVHD (Stelljes et al., 2008). Using a murine model of GvHD induced by enhanced green fluorescent protein (EGFP)-expressing donor cells, Stelljes and colleagues showed that increased FDG uptake as measured by PET correlated with tissue infiltration by histology and with results of fluorescence reflectance imaging. In an effort to translate these preclinical results to the clinic, the authors conducted PET/CT imaging in 30 patients with suspected intestinal GVHD beyond 20 days after transplantation. Fourteen out of 17 patients (82%) with histologically proven GvHD displayed gut hypermetabolism compatible with GvHD. Conversely, the 13 patients in which biopsies did not reveal histological evidence of GvHD did not display any increased FDG uptake in the gut, pointing to an excellent negative predictive value of the approach.

Such very encouraging results led to further investigation of [18F]FDG PET for GvHD diagnosis. Bodet-Milin and colleagues conducted a prospective pilot study evaluating the use of [18F]FDG PET one month after allogeneic HSCT in 42 consecutive allogeneic HSCT recipients (Bodet-Milin et al., 2014). [18F]FDG was detected in 15 out of 43 patients (36%) but only 9 of them resulted to be true positive (TP) cases based on histological findings while 6 were false positive (FP) cases. [18F]FDG PET was negative in 27 cases (64%) 26 of them being true negative (TN) cases and 1 being a false negative (FN) case. These results pointed to a 96% negative predictive value but only a 60% positive predictive value. Moreover, no significant differences in SUVmax values were observed between grade 1-2 and grade 3-4 gastrointestinal acute GvHD.

A retrospective analysis conducted on 101 patients with clinically suspected acute intestinal GVHD, 74 of which with clinically and/or histologically proven intestinal acute GVHD 18F-FDG-PET had a sensitivity of 93% and specificity of 73% (Roll et al., 2021a). Moreover, tracer uptake quantification using maximum standard uptake value (SUVmax) discriminated between patients with a fast or slow/no response.

In a more recent prospective study, 51 allogeneic HSCT recipients with clinically suspected gastrointestinal acute GvHD underwent PET/CT followed by endoscopy and histological analysis (Cherk et al., 2022). Out of the 23 patients with histologically proven upper and/or lower gastrointestinal acute GvHD, 18F-FDG PET was not able to distinguish between acute gastrointestinal GVHD and non-GVHD inflammatory changes in the colon, yielding a sensitivity of 69%, a specificity of 57%, a NPV of 73% and a PPV of 59%.

Collectively, these prospective and retrospective analysis failed to provide convincing evidence for a role of 18F-FDG PET/CT for GvHD diagnosis. In an effort to increase sensitivity and specificity, Roll and colleagues conducted a pilot study on 21 patients with acute intestinal GvHD using 18F-FDG-PET-MRI (Roll et al., 2021b). The detection rate for acute intestinal GvHD raised from 57% of 18F-FDG-PET alone or 61% of MRI alone to 100% for 18F-FDG-PET-MRI. Future prospective studies on larger cohorts are needed to confirm these promising but still preliminary results.

Molecular imaging of tissue metabolism for GvHD detection was also assessed by Assmann and colleagues using MRI in murine models of syngeneic and allogeneic HSCT (Assmann et al., 2021). Given the role of glycolytic metabolism of pathogenic T cells in GvHD pathogenesis (Nguyen et al., 2016), the investigators employed hyperpolarized 13C-pyruvate (13C-MRI) to detect the conversion of pyruvate to lactate in GvHD target tissues. They show that 13C-MRI allows noninvasive detection of liver GVHD as a result of activated CD4 T cell trafficking into the target organ.

# 2.2.2. Molecular imaging of T cell responses

From the aforementioned studies, lack of ability to distinguish between GvHD and non-GvHD inflammation seems to be the biggest limitation to the use of 18F-FDF-PET for GvHD diagnosis. Given the central role of T cells in GvHD, a metabolic tracer more specifically targeting T cells would potentially circumvent such limitation. Pre-clinical and clinical evidence indicate that molecular imaging approaches are particularly promising for the immunomonitoring of T cell responses providing mechanistic insights into T cell responses ranging from T cell trafficking to T cell activation and persistence (Li et al., 2022). Several approaches to track T cell *in vivo* have been attempted in different settings and they are graphically summarized in Figure 2.

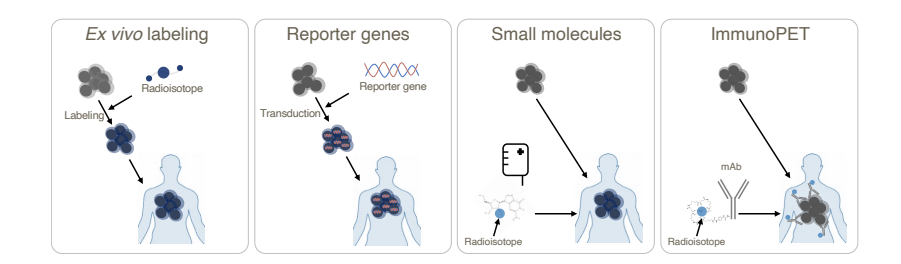


Figure 2. Graphical summary of the possible approaches for molecular imaging of T cell responses. Personal material.

A first approach involves the **ex vivo** radio-labeling of T cells before infusion. Such approach has the major limitation of the limited time-frame that it is possible to analyze, due to the

radioisotope decay as well as to the T cell proliferation that leads to the dilution of the tracer. Given the very variable timeframe at which GvHD develop after HSCT that can range from days to months, such approach does not seem to be appropriate for GvHD detection.

A way to overcome these limitations is to transduce T cells with **reporter genes** specifically designed to allow the imaging option. This strategy has been attempted using several approaches and made prove of great sensitivity in the experimental setting. However, regulatory and safety concerns around the potential immunogenicity of foreign reporters necessitates a stringent approval process. Moreover, the potential for clinical translation remains limited due to the high level of cell manipulation required that does not seem justified in the case of allogeneic HSCT.

Strategies not requiring pre-infusion manipulation of the cell therapy product would definitely be more adapted for clinical translation. One approach would be the use of radiolabeled **small molecules** uptaken by T cells. Alternatively, **immunoPET** is gaining more and more attention as an approach to monitor T cells without the need of manipulating the cells before administration. ImmunoPET exploits the great specificity of monoclonal antibodies to selectively bind cells expressing the targeted antigen and imaging them thanks to their radiolabeling with a radiotracer. T-cell targeting immunoPET tracers developed so far can be classified based on the antigen they target as in two major categories: 1) tracers targeting T-cell lineage defining molecules such as CD3, CD4 or CD8; 2) tracers targeting T-cell activation makers (ex. CD69, OX40, 41BB, ICOS).

The challenge to image T cells using one or the other of such "manipulation-free" imaging approach is to develop a T cell specific tracer that would satisfy three main requirements (summarized in Table 2).

	Small molecules	Lineage defining molecules	Activation markers
Preferential expression/uptake by the target cell population	+/-	-	+
Sustained expression/uptake during the biological activity	+/-	+/-	+
Not interfering with cellular biology (homeostasis and function)	+/-	+/-	+/-

Table 2. T-cell molecular imaging target selection requirements. Personal material.

First, the biological process or the antigen targeted by the tracer needs to be preferentially and ideally uniquely expressed by T cells when they undergo activation during the biological process studied. Second, the pathway or antigen targeted by the tracer should be upregulated in a sustained way during the whole biological process studied, in order to increase the time-window targeted and therefore the sensitivity of the approach. Finally, and most importantly, the radiotracer should not interfere with the biology of T cells that are targeted, in terms of expansion, survival and/or function.

#### 2.2.2.1 Small molecules

# 18F-30-deoxy-30-fluorothymidine

Given the high proliferation rates of T cells during GvHD, the use of 18F-30-deoxy-30-fluorothymidine (FLT) has been attempted in murine models of HSCT (Lee et al., 2018). FLT is a thymidine analog that is incorporated into the DNA at time of replication and therefore reflects cellular proliferation. In murine models of GvHD, 18F-FLT allowed the differentiation of mice developing GvHD after receiving alloreactive T cells and control mice by detecting higher tracer uptake in lymphnodes and spleen of GvHD mice. However, tracer uptake in GvHD target organs, namely the gastrointestinal tract, did not differ between GvHD and control mice because of high variability. This represents a major limitation for the use of this tracer for GvHD diagnosis given that signal outside target organs can originate from proliferation of hematopoietic cells other than T cells during engraftment as previously shown in a rat model of bone marrow transplantation (Awasthi et al., 2010).

# 2'-deoxy-2'-[18F]fluoro-9-β-D-arabinofuranosyl guanine ([18F]F-AraG)

9-β-D-arabinofuranosyl guanine (AraG) is the water-soluble prodrug of nelarabine, a drug known for its specific cytotoxicity towards T cells and clinically employed in T cell malignancies. AraG enters cells using two nucleoside transporters and is phosphorylated by either cytosolic deoxycytidine kinase (dCK) or mitochondrial deoxyguanosine kinase (dGK). At high doses, phosphorylated AraG-inhibits DNA synthesis thus inducing T cell death. At the very low mass levels required for imaging, AraG specifically enters T cells without inducing detectable cell death (Namavari et al., 2011). The Gambhir group at Stanford University developed the radiotracer 2'-deoxy-2'-[18F]fluoro-9-β-D-arabinofuranosyl guanine ([18F]F-AraG) (Namavari et al., 2011). Ronald and colleagues employed for the first time 18F-AraG in a mouse model of GvHD (Ronald et al., 2017). After confirming *in vitro* that 18F-AraG preferentially accumulates in activated T cells, they show that 18F-AraG allows to efficiently measure T cell expansion in secondary lymphoid organs during GvHD. Unfortunately, the important background noise coming from the liver precludes any analysis of the liver itself and of the gastrointestinal tract, two major GvHD-target organs. Given the easier spatial resolution

in and the favorable kinetics observed with 18FAraG in humans (Ronald et al., 2017), an attempt to clinically translate this approach for GvHD diagnosis is currently ongoing at Stanford University (NCT03367962).

# 2.2.2.2 Imaging T cell lineage markers

Targeting T cell lineage defining markers such as CD3, CD4 and/or CD8 is an obvious approach for immunoPET molecular imaging of T cell mediated processes, including GvHD. The high levels of expression of T cell lineage defining markers at cell surface represents one of the main advantages of this strategy. So far only CD3 immunoPET has been tested in murine models of GvHD.

# CD3

Pektor and colleagues employed PET/MRI imaging with a 89Zr-labeled anti-human CD3 mAb in a murine model of xenogeneic GvHD (Pektor et al., 2020). They demonstrated higher tracer uptake in GvHD target organs, namely the liver, as well in secondary lymphoid organs at different timepoints after human PBMC administration into lymphodepleted mice. Interestingly, they employed Treg administration as GvHD prophylaxis and they were able to show significantly reduced T cell infiltration in Treg treated mice. Although promising, this proof-of-concept report did not address one of the major risks of targeting CD3 in immunopathogenic contexts such as GvHD, namely the risk of interfering with T cell biology eventually by exacerbating the disease. Moreover, targeting CD3 might also interfere with T cells by chronically stimulating them, eventually leading to T cell exhaustion and therefore potentially limiting the graft versus tumor effect.

#### 2.2.2.3 Imaging T cell activation markers

Targeting T cell restricted markers upregulated during T cell activation display the potential significant advantage of providing qualitative information in addition to the quantitative one.

# HLA-DR

HLA-DR is a human Class II MHC molecule expressed on a variety of immune cells, including T cells during activation. Van Elssen and colleagues developed radiolabeled Variable Fragments of Heavy Chain Antibodies (VHH) to target human HLA-DR and employed it to image T cell activation in a murine model of xenogeneic GVHD (Van Elssen et al., 2017) in mice reconstituted with human fetal thymus, liver, and liver-derived hematopoietic stem cells (BLT mice). PET uptake was higher within the liver of mice displaying signs of severe GVHD versus control mice but the authors were unable to correlate early PET findings with subsequent GvHD before the overt disease occurred. Moreover, the authors attribute tracer

uptake deriving from HLA-DR binging to tissue infiltration by activated T cells, although the contribution of other non-T cells HLA-DR+ immune compartment, such as monocytes and macrophages, could not be excluded given the lack of specificity of HLA-DR as a T cell lineage marker.

# OX40

OX40 (CD134) is a member of the TNF receptor superfamily and its expression is highly restricted to activated T cells in which it acts as a costimulatory molecule. Because of its Tcell specificity, OX40 was identified as a target for immunoPET detection. Alam and colleagues developed a murine OX40-specific monoclonal antibody (64Cu-OX40mAb) that enables noninvasive imaging of murine OX40+ activated T cells (Alam et al., 2018). Based on previous studies showing an increase in OX40 expression at the T-cell surface during acute GvHD (Tittle et al., 1997; Lamb et al., 1999; Kotani et al., 2001; Sanchez et al., 2004; Paz Morante et al., 2006; Tkachev et al., 2017) and considered the role OX40 plays in acute GvHD pathogenesis (Stüber et al., 1998; Blazar et al., 2003; Tkachev et al., 2017; Tripathi et al., 2019), we tested the ability of OX40-immunoPET to image activated T cells in vivo in a major MHC-mismatch murine model of acute GvHD (Alam et al., 2020). We showed that OX40immunoPET successfully detected T-cell activation, expansion, and target-tissue infiltration in a murine model of acute GvHD. Importantly, owing to its high sensitivity, OX40-immunoPET could detect signs of GvHD even before clinical symptoms manifest. A major limitation of our approach however was that our 64Cu-OX40mAb tracer interfered with T cell biology and, given the agonistic nature of the monoclonal antibody employed, led to further T-cell activation and to exacerbation of GvHD when administered early after HSCT. These results stress the need to develop biologically inert tracers for imaging purposes and to carefully select imaging targets to avoid interfering with T cell activation and therefore with disease pathogenesis.

### 2.2.3 Imaging tissue damage

Once considered a passive target of T cell cytotoxic function during GvHD, the target tissue epithelium is more and more recognized as an active player in GvHD pathogenesis. Such attention to the phenotypic and functional changes of enterocytes during acute GvHD led Scott and colleagues to the identification of tryptophan-rich sensory protein oxygen sensor (TSPO) protein as a marker expressed by enterocytes during gastrointestinal acute GvHD (Scott et al., 2022). TSPO is an outer mitochondrial membrane protein previously reported to be overexpressed by enterocytes after stimulation with inflammatory mediators such as tumour necrosis factor-alpha (TNF-alpha) and IL-8, leading to its overexpression in inflammatory bowel diseases (IBD). After demonstrating enterocytic TSPO expression in tissue biopsies from patients with gastrointestinal acute GvHD, the authors performed a prospective pilot

study of PET/CT using [18F]GE-180, an already reported third-generation high-affinity TSPO radiotracer, in eight allogeneic HSCT adult recipients with a clinical suspicion of gastrointestinal acute GvHD. They demonstrated tracer uptake specifically at the intestinal level and correlation between uptake and histology in six out of eight participants. Although preliminary and despite the fact that TSPO detection might not be completely specific to enterocytes in this system given TSPO expression by other cells during inflammation, such as macrophages, this proof-of-concept study provides for the first-time evidence for molecular imaging of target epithelium during GvHD as a strategy to detect tissue damage and potentially to monitor response to treatment during the healing process.

Collectively, we have seen how different molecular imaging strategies can be applied to the study of different phases of GvHD pathogenesis (Figure 3). Clinical trials will identify one or more tracers and approaches with the highest sensitivity and specificity for GvHD diagnosis and monitoring.

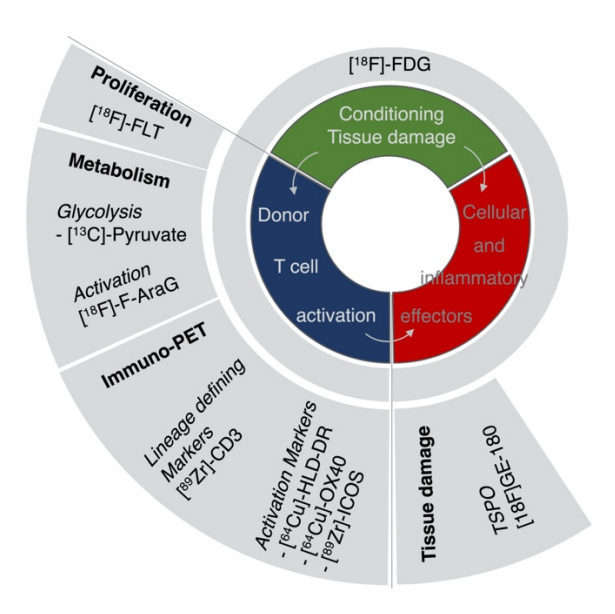


Figure 3. Graphical summary of the approaches and radiotracers tested in preclinical models of GvHD. Personal material.

#### 3. Publications

#### 3.1. Publication 1

Xiao Z\*, Alam IS\*, <u>Simonetta F</u>\*, Chen W, Scheller L, Murty S, Lohmeyer JK, Ramos TL, James ML, Negrin RS, Gambhir SS. ICOS ImmunoPET Enables Visualization of Activated T Cells and Early Diagnosis of Murine Acute Gastrointestinal GvHD. *Blood Advances* **2022**;6(16):4782-4792.

(\*co-first author)

In this study we investigated the use of ICOS-immunoPET for the detection of T cell activation and GvHD diagnosis in a murine model of acute gastrointestinal GvHD. In a previous work, we had shown that using an immunoPET tracers targeting the T-cell activation marker and costimulatory molecule OX40 allowed the detection of T cell expansion and tissue infiltration in murine models of GvHD (Alam et al., 2020). Unfortunately, such approach presented a major limitation related to the toxicity of our tracer that, despite the very low dose of antibody employed, interfered with T cell biology and exacerbated GvHD. To circumvent this limitation we looked for alternative target molecules for which immunoPET tracers were previously reported using available RNAseg datasets of T cells during GvHD that we and others previously generated. Our analysis identified the Inducible T-cell COStimulator (ICOS), a T cell activation marker and costimulatory molecule of the CD28/cytotoxic T lymphocyte antigen 4 (CTLA-4) family, as a marker selectively upregulated in activated T cells during GvHD. After confirming at the protein level ICOS upregulation on T cells during GvHD, we employed a tracer generated by the Gambhir group using a murine ICOS-specific antagonistic monoclonal antibody radiolabeled with 89Zr (Xiao et al., 2020) (Xiao et al, Cancer Res 2020) that we have previously employed in a CAR T cell immunomonitoring study (Simonetta et al., 2021a). We demonstrated that ICOS-immunoPET efficiently allowed monitoring of alloreactive T cell activation, expansion, and tissue infiltration in a major MHC-mismatch murine model of acute GvHD (Figure 4). Importantly, our approach was not associated with any detectable toxicity thus circumventing the major limitation of our previous study using OX40-immunoPET. Moreover, we were able to show that the use of ICOS-immunoPET did not interfere with the antitumor of allogeneic T cells. In conclusion, thanks to the high specificity and sensitivity, without any detectable toxicity, ICOS-immunoPET represents a compelling method for the early detection of GvHD that we aim to translate to clinical studies.

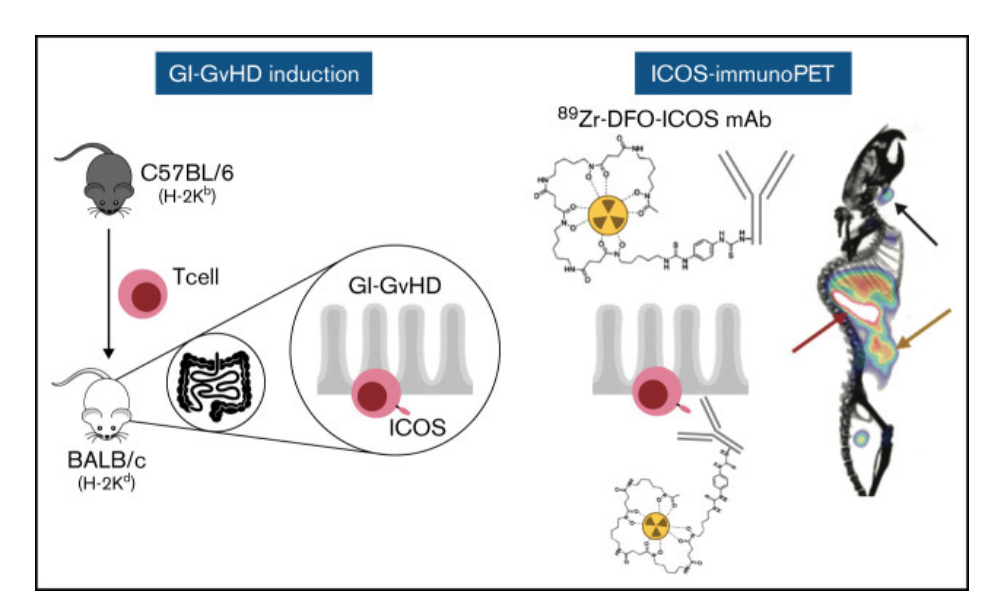


Figure 4. Graphical representation of the ICOS-immunoPET approach for early detection of T cell activation and expansion in a murine model of **GvHD**. Personal material published as graphical abstract in Blood Advances 2022.

# ICOS immunoPET enables visualization of activated T cells and early diagnosis of murine acute gastrointestinal GvHD

Zunyu Xiao, <sup>1,2,\*</sup> Israt S. Alam, <sup>1,\*</sup> Federico Simonetta, <sup>3-6,\*</sup> Weiyu Chen, <sup>1</sup> Lukas Scheller, <sup>3</sup> Surya Murty, <sup>1,7</sup> Juliane K. Lohmeyer, <sup>3</sup> Teresa L. Ramos, <sup>3</sup> Michelle L. James, <sup>1</sup> Robert S. Negrin, <sup>3,†</sup> and Sanjiv S. Gambhir<sup>1,7-9,†</sup>

<sup>1</sup>Molecular Imaging Program at Stanford (MIPS), Department of Radiology, Stanford University School of Medicine, Stanford, CA; <sup>2</sup>Molecular Imaging Research Center of Harbin Medical University, Harbin, China; <sup>3</sup>Division of Blood and Marrow Transplantation and Cellular Therapy, Department of Medicine, Stanford University, Stanford, CA; <sup>4</sup>Division of Hematology, Department of Oncology, Geneva University Hospitals and Faculty of Medicine, <sup>5</sup>Department of Medicine, Translational Research Center for Oncohematology, and <sup>6</sup>Department of Pathology and Immunology, Faculty of Medicine, University of Geneva, Geneva, Switzerland; <sup>7</sup>Department of Bioengineering, Stanford University, Stanford, CA; <sup>8</sup>Canary Center at Stanford for Cancer Early Detection, Department of Radiology, Stanford University School of Medicine, Stanford, CA; and <sup>9</sup>Bio-X Program at Stanford, Department of Radiology, Stanford University, Stanford, CA

#### **Key Points**

- ImmunoPET imaging of ICOS allows for in vivo visualization of T cells in the gastrointestinal tract in a murine model of acute GvHD.
- ICOS targeting with the immunoPET tracer does not affect GvHD pathogenesis or the GvT effect.

Allogeneic hematopoietic cell transplantation (HCT) is a well-established and potentially curative treatment for a broad range of hematological diseases, bone marrow failure states, and genetic disorders. Acute graft-versus-host disease (GvHD), mediated by donor T cells attacking host tissues, still represents a major cause of morbidity and mortality following allogeneic HCT. Current approaches to diagnosis of gastrointestinal acute GvHD rely on clinical and pathological criteria that manifest at late stages of disease. New strategies allowing for GvHD prediction and diagnosis, prior to symptom onset, are urgently needed. Noninvasive antibody-based positron emission tomography (PET) (immunoPET) imaging of T-cell activation post-allogeneic HCT is a promising strategy toward this goal. In this work, we identified inducible T-cell costimulator (ICOS) as a potential immunoPET target for imaging activated T cells during GvHD. We demonstrate that the use of the Zirconium-89-deferoxamine-ICOS monoclonal antibody PET tracer allows in vivo visualization of donor T-cell activation in target tissues, namely the intestinal tract, in a murine model of acute GvHD. Importantly, we demonstrate that the Zirconium-89-deferoxamine-ICOS monoclonal antibody PET tracer does not affect GvHD pathogenesis or the graft-versus-tumor (GvT) effect of the transplant procedure. Our data identify ICOS immunoPET as a promising strategy for early GvHD diagnosis prior to the appearance of clinical symptoms.

#### Introduction

Allogeneic hematopoietic cell transplantation (HCT) is an effective treatment for a broad range of hematological diseases. Despite its success, allogeneic HCT is still associated with a significant transplant-related morbidity and mortality related to posttransplant complications, namely graft-versus-host disease (GvHD). Acute GvHD results from the activation of donor T cells and subsequent cytolytic attack of host tissues, mainly skin, liver, and intestine. Unfortunately, current methods for GvHD diagnosis do not enable early diagnosis at a presymptomatic stage because they mostly rely on the assessment of clinical symptoms combined with tissue biopsies of target organs.

Submitted 23 February 2022; accepted 23 June 2022; prepublished online on *Blood Advances* First Edition 5 July 2022; final version published online 17 August 2022. DOI 10.1182/bloodadvances.2022007403.

 $^{\star}$ Z.X., I.S.A., and F.S. are joint first authors.

tR.S.N. and S.S.G. are joint senior authors.

For original data, please contact israt@stanford.edu.

The full-text version of this article contains a data supplement.

© 2022 by The American Society of Hematology. Licensed under Creative Commons Attribution-NonCommercial-NoDerivatives 4.0 International (CC BY-NC-ND 4.0), permitting only noncommercial, nonderivative use with attribution. All other rights reserved.

There is, therefore, a critical need to develop noninvasive strategies to accurately diagnose GvHD at early stages. Positron emission tomography (PET) is a promising approach for whole-body molecular imaging of GvHD. [18F]Fluorodeoxyglucose (18F-FDG)-PET enables noninvasive measurement of alterations in glucose metabolism and has demonstrated high sensitivity for detecting acute GvHD prior to the appearance of pathological signs.<sup>2-4</sup> <sup>18</sup>F-FDG, however, is taken up by all cells with elevated glycolysis (eg, inflammatory cells, cancer cells) and thus lacks sufficient specificity to distinguish intestinal GvHD from other causes of gastrointestinal inflammation.<sup>3,4</sup> Because donor T-cell activation is considered one of the earliest events in acute GvHD pathogenesis, 1,5,6 we and others have reported the noninvasive detection of activated T cells using the small-molecule metabolic PET tracer 2'-deoxy-2'-[18F]fluoro-9-β-D-arabinofuranosyl quanine (18F-FAraG). PET imaging with <sup>18</sup>F-FAraG enabled early detection of activated T cells during murine GvHD,7 a strategy that is currently under clinical investigation for early diagnosis of acute GvHD in HCT patients at our institution (#NCT03367962; clincialtrials.gov). Although this imaging approach is more specific than <sup>18</sup>F-FDG-PET, it is still hindered by suboptimal T-cell specificity as the targeted metabolic pathways of <sup>18</sup>F-FAraG can also be upregulated in other tissues or cells.

To address the limited specificity of metabolic tracers, several groups have been exploring the use of immunoPET, which combines the high specificity of monoclonal antibodies (mAbs) or antibody fragments targeting a particular cell surface marker with PET radioisotopes. PET imaging of GvHD targeting the T-cell lineage-defining marker CD38 and the activation marker HLA-DR9 has been reported. Although CD3 imaging enables T-cell visualization, it fails to report on T-cell activation status. Conversely, HLA-DR expression reflects T-cell activation, as well as that of the myeloid compartment, thus lacking specificity for tracking activated T-cells alone. We recently reported a <sup>64</sup>Cu-labeled OX40 mAb, which noninvasively visualized murine OX40<sup>+</sup>, activated T cells<sup>10</sup> and enabled detection of acute GvHD in a major histocompatibility complex (MHC)-mismatch murine model. 11 Despite clearly delineating activated T cells in vivo, this approach unfortunately has limited utility as the immunoPET tracer, based on an agonist clone, led to the exacerbation of acute GvHD and, consequently, serious toxicity. 11

In an effort to find new potential biomarkers to successfully and safely image activated T cells in acute GvHD by immunoPET, we identified the inducible T-cell costimulatory receptor (ICOS), a T-cell activation marker in the CD28/cytotoxic T lymphocyte antigen-4 (CTLA-4) family. Employing our previously reported Zirconium-89 (<sup>89</sup>Zr)-labeled, murine ICOS-specific antagonistic monoclonal antibody, <sup>12,13</sup> we demonstrate that ICOS immunoPET successfully visualizes the dynamics of activation, expansion, and tissue distribution of alloreactive T cells in a MHC-mismatch murine model of acute GvHD, with high specificity and sensitivity and without any detectable toxicity, thus providing a compelling method for the early detection of gastrointestinal GvHD.

# **Methods**

#### Animals and animal study approval

Female BALB/cJ (H-2kd), C57BL/6J (H-2kb), and NOD.Cg-Prkdcscid-ll2rgtm1Wjl/SzJ (NSG) mice were purchased from the Jackson Laboratory. *Luciferase* (*Luc*)<sup>+</sup> transgenic C57BL/6-L2G85

mice<sup>6</sup> were bred at Stanford University. All animal procedures were approved by the Stanford Administrative Panel of Laboratory Animal Care. All federal and state regulations governing the humane care and use of laboratory animals were upheld.

#### RNA sequencing data analysis

Previously published RNA sequencing (RNA-seq) datasets from GvHD models (National Center for Biotechnology Information Gene Expression Omnibus accession number GSE172169<sup>14</sup> and EMBL-EBI ArrayExpress E-MTAB-6865<sup>15</sup>) were analyzed. Murine CD4 and CD8 T cells were analyzed pre- and 7 days post–allogeneic HCT, as previously described, 14 and data from human T cells were analyzed pre- and 14 days post–IV injection into sublethally irradiated NSG mice. 15 Differential gene expression analysis was performed using DESeq2 16 version 1.28.1, and data were visualized using ggplot2 version 3.3.4.

#### MHC-mismatch murine models of acute GvHD

Female BALB/cJ mice (8-10 weeks) received lethal total body irradiation (TBI), consisting of 2 doses of 440 cGy, 4 hours apart (total dose 880 cGy). Splenocytes were harvested from Luc<sup>+</sup> transgenic C57BL/6 or FVB/N L2G85 mice, and donor T cells were purified by positive selection (Miltenyi Biotec). T-cell-depleted bone marrow (TCD-BM) was obtained from C57BL/6J or FVB/NJ mice by homogenizing bones, collecting the bone marrow suspension, and depleting both CD4 and CD8 T cells using MicroBeads (Miltenyi Biotec). Irradiated BALB/cJ recipients were injected with  $5 \times 10^6$  TCD-BM cells and 1  $\times$  10<sup>6</sup> T cells IV to induce acute GvHD. After transplantation, mice were monitored daily, and GvHD score was assessed at day 4 and weekly thereafter as previously described. 17 In experiments evaluating the graft-versus-tumor (GvT) effect,  $2 \times 10^5 luc^+$ A20 lymphoma cells were injected IV into the BALB/c recipient mice via a tail vein at time of transplantation; GvHD mice in these experiments received T cells from wild-type C57BL/6J mice.

#### Xenogenic GvHD model

Female NSG mice were sublethally irradiated (2 Gy) and injected IV with 10<sup>7</sup> human peripheral blood mononuclear cells (PBMCs) isolated from healthy human volunteers (Stanford Blood Center) using Ficoll-Paque (GE Healthcare) gradient centrifugation. Mice were monitored daily, and GvHD score was assessed weekly as previously described.<sup>17</sup>

#### Flow cytometry

Spleens were harvested on days 4 and 7 post–allogeneic HCT, or day 14 after human PBMC injection, for the MHC-mismatch murine acute and xenogenic GVHD models, respectively. Splenocytes were resuspended in phosphate-buffered saline (PBS) buffer containing 2% fetal bovine serum. Intestines were collected at day 7, flushed with PBS, and mechanically dissected into pieces. Tissues were digested with 1 mg/mL<sup>-1</sup> Collagenase IV (Life Technologies) for 30 minutes, and lymphocyte was isolated using a Percoll (Sigma-Aldrich) gradient. Fluorescence-activated cell sorting (FACS) staining was performed at 4°C with the following antibodies: fluorescein isothiocyanate anti-mouse CD45.1 (clone A20), BV785 anti-human/mouse/rat ICOS (C398.4A) and isotype control antibody (HTK888), APC anti-mouse Thy1.1 (OX-7), APC/Fire750 anti-mouse CD19 (clone 6D5) and anti-mouse CD45.2 (104), BV421 anti-mouse CD4 (GK1.5), BV605 anti-mouse CD3 (17A2),

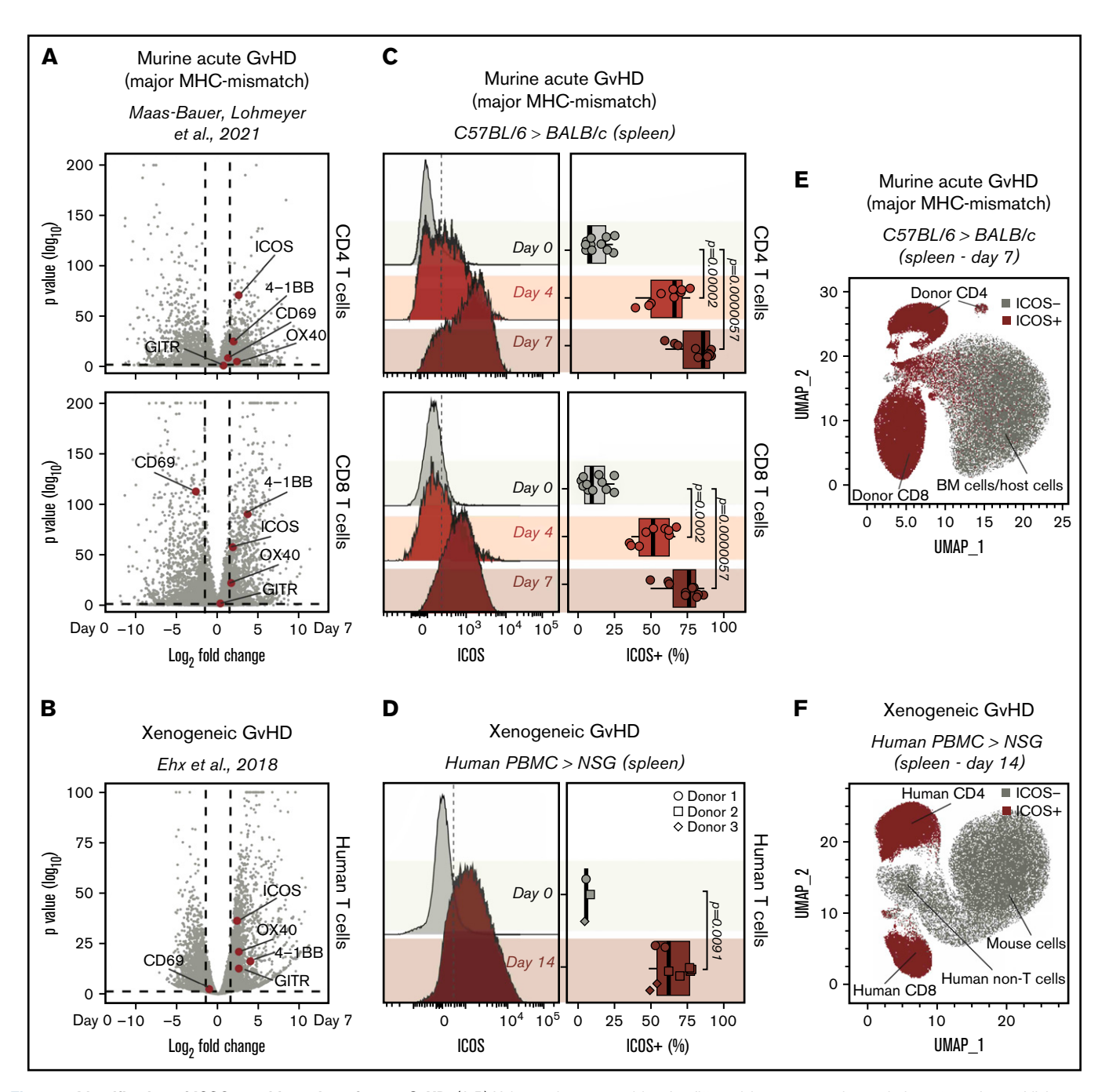


Figure 1. Identification of ICOS as a biomarker of acute GvHD. (A-B) Volcano plots summarizing the differential gene expression analysis performed on publicly available RNA-seq data comparing murine (A) and human (B) T cells recovered from murine models of acute GvHD with cells prior to adoptive transfer. Vertical dashed lines on volcano plots indicate a log<sub>2</sub> fold change of 1.5; horizontal dashed lines indicate an adjusted P value of .05. Genes encoding for selected activation markers previously employed as immunoPET targets are highlighted in red. (C) Representative FACS histograms (left panels) and summary of percentages (right panels) of ICOS expression on CD90.1+CD45.1+CD4+ (top panels) and CD8+ (bottom panels) T cells recovered from the spleen 4 and 7 days post-adoptive transfer of C57BL/6 T cells into allogeneic BALB/c recipients. Values are summarized as box plots, representing the range, first quartile, median, third quartile, and eventual outliers. Results are pooled from 2 independent experiments (n = 9-11 mice per group). Day 4 and 7 values were compared with day 0 values using a nonparametric Mann-Whitney U test. P values are indicated. (D) Representative FACS histograms (left panels) and summary of percentages (right panels) of ICOS expression on human-CD45<sup>+</sup> murine-CD45<sup>-</sup> CD3<sup>+</sup> T cells recovered from spleen 14 days post-adoptive transfer of human PBMCs from healthy donors into sublethally irradiated NSG mice. Results are pooled for a total of 9 mice (n = 2-4 mice per group). Day 14 and 0 values were compared using a nonparametric Mann-Whitney U test. P values are indicated. (E-F) Uniform Manifold Approximation and Projection plots of FACS data obtained from the analysis of spleens recovered at day 7 after MHC-mismatch murine allogeneic HCT (E) or at day 14 upon induction of xenogeneic GvHD by adoptive transfer of PBMCs into NSG mice (F). ICOS-expressing cells are depicted in red.

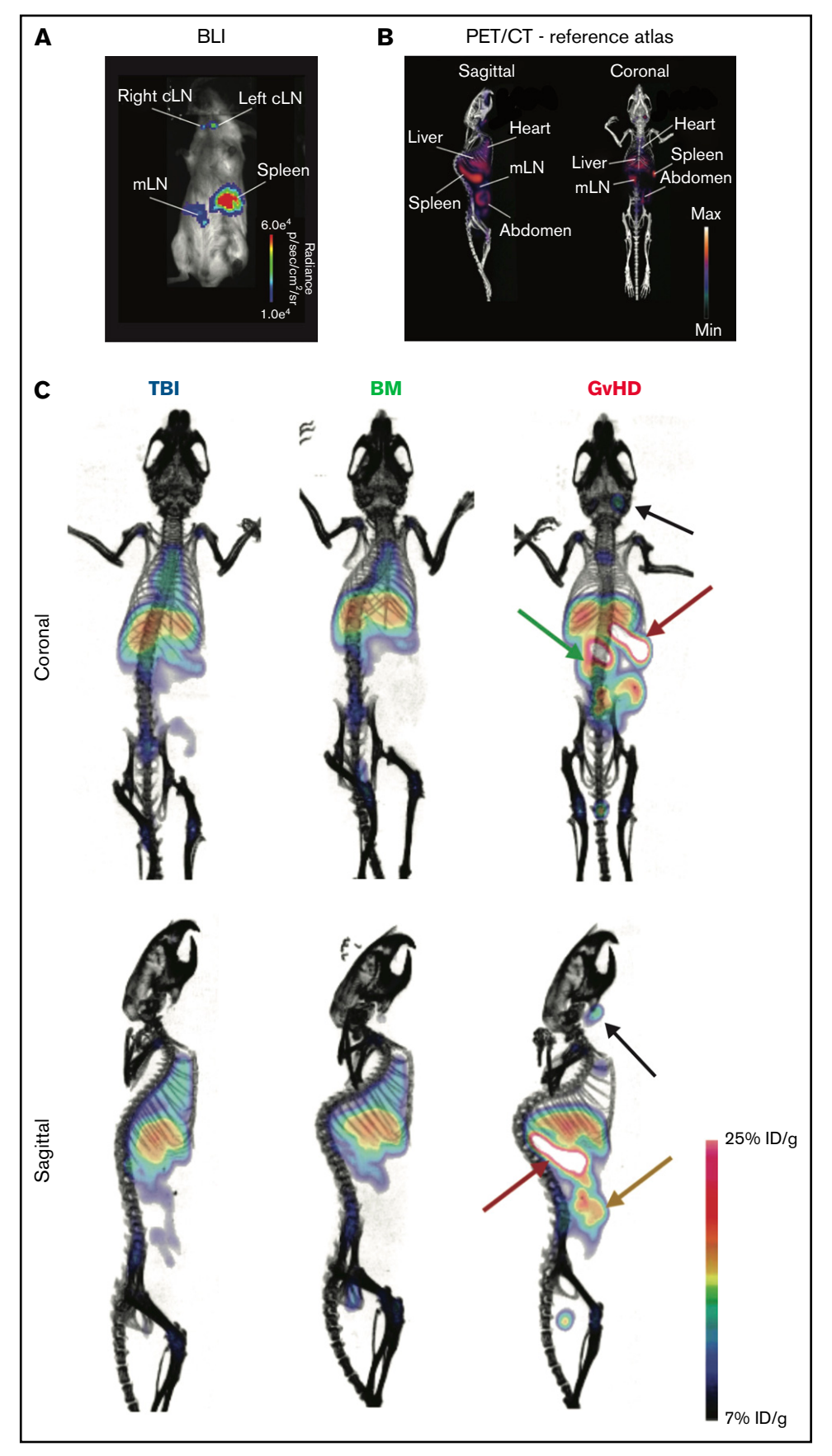


Figure 2.

BV650 anti-CD8 (53-6.7), Pacific Blue anti-human CD45 (2D1), BV605 anti-human CD3 (OKT3), BV650 anti-human CD4 (OKT4), and BV711 anti-human CD8a (RPA-T8). All antibodies were purchased from Biolegend. Data were acquired on a BD LSR II flow cytometer (BD Biosciences) and analyzed using FlowJo version 10.7.1 (BD Biosciences).

#### **Bioluminescence imaging**

Mice were anesthetized using 2% isoflurane and injected intraperitoneally with D-luciferin (10 mg/kg). Bioluminescence imaging (BLI) was performed using the IVIS Spectrum imaging system (Perkin Elmer), and data were analyzed with Living Image Software 4.1 (Perkin Elmer) or using an Ami LED-illumination-based imaging system (Spectral Instruments Imaging, Tucson, AZ) and analyzed with Aura Software (Spectral Instruments Imaging).

# Bioconjugation and 89Zr radiolabeling of monoclonal antibodies

<sup>89</sup>Zr radiolabeled ICOS antibody (rat clone 7E.17G9, Bio X cell) was prepared as previously described. 12 Briefly, 1 mg of antibody was diluted to 1 mg/mL in PBS, and the pH was adjusted to 8.8 to 9.0 prior to addition of deferoxamine-isothiocyanate (DFO-SCN) chelate (Macrocyclics) dissolved in DMSO (Thermofisher). The bioconjugation reaction was allowed to proceed for 1 hour at 37°C, after which the DFO-modified mAb was washed using a 2 mL Vivaspin filter with a 50 kDa cutoff (Sartorius) to remove unbound chelate. Matrix-assisted laser desorption/ionization (MALDI)-mass spectrometry was conducted on the bioconjugates to determine final chelate:mAb ratios (1.5-2.5 chelates per antibody), and final protein concentrations were determined using a Thermo Scientific NanoDrop UV-Vis spectrophotometer. For radiolabeling, ~1 mCi <sup>89</sup>Zr oxalate (3D Imaging), adjusted to pH 7.1 to 7.8 using 1 M Na<sub>2</sub>CO<sub>3</sub> was incubated with the DFO-ICOS mAb for 1 hour at 37°C with gentle agitation. Free <sup>89</sup>Zr oxalate was removed, and 89Zr-DFO-ICOS mAb was purified using 7K MW cutoff zeba spin desalting column (Thermofisher) and centrifuged for 1 minute at 1000g. Final radiochemical purity of >99% of  $^{89}$ Zr-DFO-ICOS mAb was determined using instant thin-layer chromatography using chromatography strips (Biodex).

# Small animal PET/CT imaging, image analysis, and biodistribution (BioD) study

All PET/computed tomography (CT) imaging studies were performed using Siemens Inveon small animal Multi-Modality-PET/CT. Mice were anesthetized using isoflurane (2% to 2.5% for induction and 1.5% to 2.0% for maintenance) delivered by 100% oxygen. 50 microcurie (μCi) (1 μCi/μL, mass dose injected; 7 μg) <sup>89</sup>Zr-DFO-ICOS mAb was administered IV via the tail vein on day 4 post-transplantation. At 24 and 48 hours post-tracer injection, 15-minute static PET scans were acquired, followed by a CT scan to provide an anatomic reference and for attenuation correction of the PET data. PET reconstruction and region of interest (ROI) analysis of the

PET images were performed using a 3-dimensional volume drawing mode.11

Mice were euthanized following completion of the PET/CT scan at 48 hours. Blood, mesenteric lymph node (mLN), liver, spleen, heart, left kidney, large intestine, bone (femur), and muscle were collected, and wet weights were immediately recorded to allow normalization of tissue-associated radioactivity to tissue weight. An automatic y counter (Hidex AMG) was used to determine the tissue-associated radioactivity for each tissue collected. Both PET and BioD data were normalized to injected dose and were expressed as percentage injected dose/g of tissue.

# Assessment of the impact of ICOS mAb on GvHD and GvT

The antibody used for PET imaging, murine-specific ICOS mAb (clone 7E.17G9), or the appropriate isotype control (clone LTF-2) were administered IV as a single dose (10 µg in 100 µL of sterile PBS) on day 4 post-HCT. The dose was determined based on the upper limit of antibody administered during PET imaging studies (7 μg antibody was injected per PET tracer dose).

#### Statistical analysis

Statistical analyses were performed using R version 4.0.2 with R studio Version 1.3.1056. Data were visualized using ggplot2 version 3.3.4. Heatmaps were generated using Pheatmap version 1.0.12. Principal component analysis (PCA) was performed using the FactoMineR package version 2.41 and visualized using the factorextra package version 1.0.7. Receiver operating characteristic(ROC) curves were calculated and plotted using plotROC version 2.2.1.

#### Results

# ICOS is strongly upregulated on murine and human T cells in models of acute GvHD

To identify surface markers of T-cell activation as potential new immunoPET targets for GvHD imaging, we interrogated an RNAseq dataset we recently published 14 containing data obtained from murine CD4 and CD8 T cells, pre- and 7 days post-MHCmismatched allogeneic HCT. After analyzing differential gene expression between cells at day 0 and at day 7, we focused our attention on genes encoding T-cell surface activation molecules previously employed as immunoPET targets, namely OX40,11 ICOS,12 CD69,<sup>18</sup> and GITR.<sup>19</sup> Among these molecules, the gene encoding ICOS was the most highly differentially expressed in CD4 (log<sub>2</sub> fold change, 2.57; adjusted P = 1.24E-71; Figure 1A) and CD8 T cells ( $log_2$  fold change, 1.90; adjusted P = 3.52E-58; Figure 1A). Interestingly, Icos transcription was upregulated to a higher extent than Tnfrsf4 (CD4:  $log_2$  fold change, 2.36; adjusted P = 2.28E-05; CD8:  $log_2$  fold change, 1.70; adjusted P = 9.30E-23), which encodes OX40, a molecule we previously reported as a target for sensitive immunoPET imaging of acute GvHD. 11 To assess whether Icos transcription was similarly upregulated on activated human T cells,

Figure 2 (continued) 89Zr-DFO-ICOS mAb immunoPET imaging of acute GvHD. (A) Representative BLI of a mouse with acute GvHD at day 4 post-HCT. (B) Reference atlas indicating the location of key clearance and lymphoid organs as well as GvHD target tissues. (C) Representative 89Zr-DFO-ICOS mAb PET/CT images acquired 48 hours after tracer administration at day 4 after HCT in TBI control (n = 5), bone marrow control (n = 7), or GvHD (n = 11) mice. Key organs, namely spleen (red arrow), cervical lymph node (cLN) (black arrow), mLN (green arrow), and intestine (yellow arrow), are highlighted. Images are representative of 2 independent experiments. %ID/g, percent injected dose per gram.

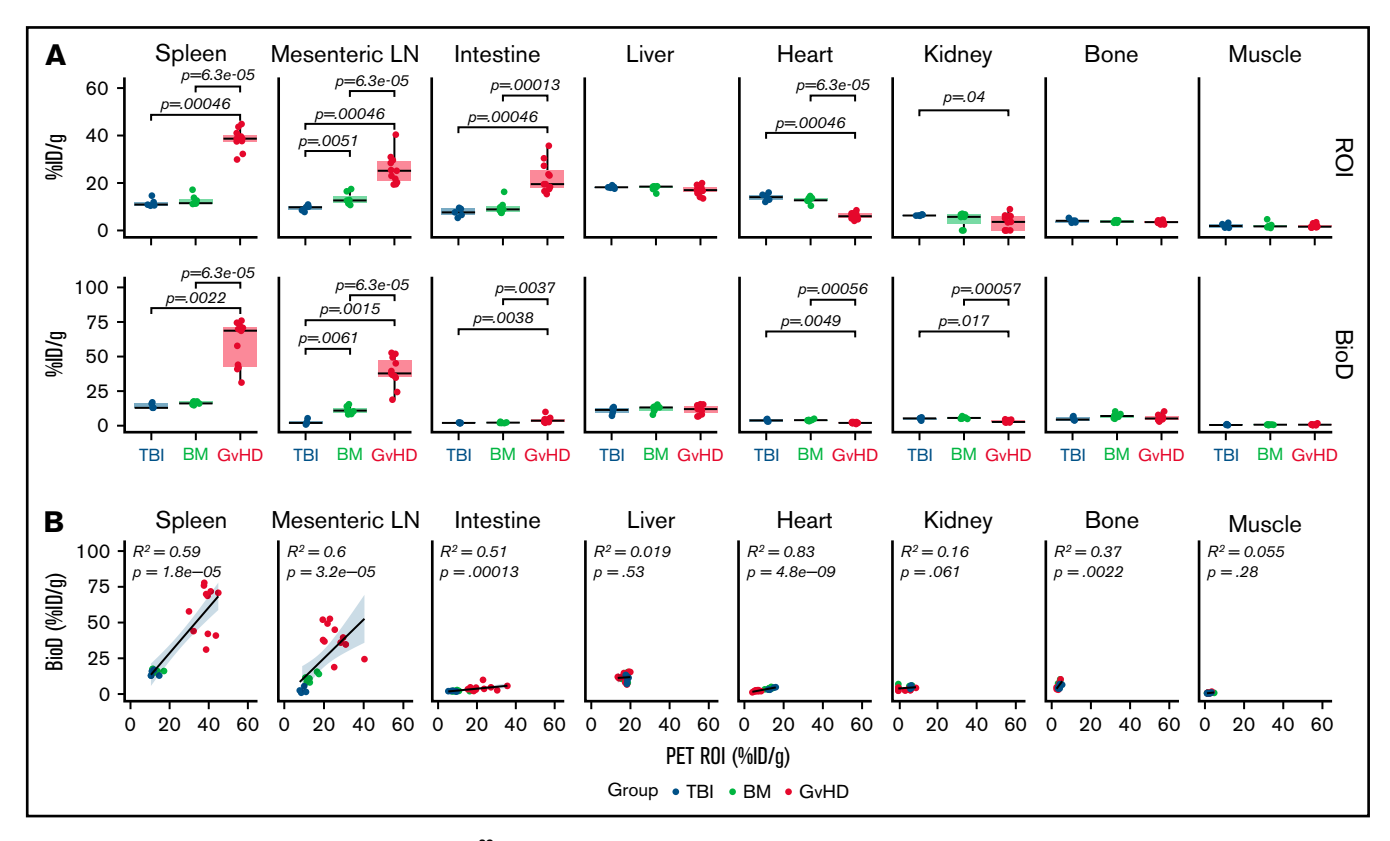


Figure 3. Quantitative PET ROI and BioD analysis of <sup>89</sup>Zr-DFO-ICOS mAb in acute GvHD. (A) Quantitative ROI analysis of PET images (upper panels) and BioD (lower panels) of spleen, mLN, intestine, liver, heart, kidney, bone, and muscle 48 hours after tracer injection in TBI (blue; n = 5), BM (green; n = 7), or GvHD mice (red; n = 11). Values are summarized as box plots, representing the range, first quartile, median, third quartile, and eventual outliers. Tracer uptake in GvHD and TBI or BM mice was compared using the Mann-Whitney *U* test. (B) Correlation between tracer uptake measured by PET ROI image analysis with that determined by BioD analysis, evaluated using a Spearman rank correlation coefficient test. Results are pooled from 2 independent experiments. %ID/g, percent injected dose per gram.

we analyzed a second publicly available RNA-seq dataset obtained from human T cells pre- and 14 days post-injection into alymphoid NSG mice induced with xenogeneic GvHD. In agreement with the murine data, *Icos* was the most significantly upregulated T-cell activation marker among those preselected ( $\log_2$  fold change, 2.30; adjusted P = 4.42E-37; Figure 1B).

We then compared murine CD4<sup>+</sup> and CD8<sup>+</sup> T cells from CD45.1 and CD90.1 C57BL/6 donor mice preinjection with those recovered at day 4 and 7 post-HCT into allogeneic CD45.2 and CD90.2 BALB/c recipients to assess ICOS expression on T cells during GvHD at the protein level. We detected significantly higher proportions of ICOS<sup>+</sup> cells among both CD4<sup>+</sup> and CD8<sup>+</sup> donor-derived CD45.1 + CD90.1 + T cells recovered at day 4 (CD4: median, 66% [range, 39%-77%], P = 1.2e-05; CD8: 52% [36%-67%], P =.0002) and at day 7 (CD4: 86% [60%-92%], P = 5.7e-06; CD8: 76% [50%-87%], P = 5.7e-06) post-HCT compared with day 0 (CD4: 9% [5%-23%]; CD8: 9% [1%-25%]; Figure 1C). Similar results were obtained when a second mouse model of acute GvHD (FVB/N into BALB/c mice) was employed (supplemental Figure 1A). Moreover, ICOS was strongly upregulated at the surface of CD4 and CD8 T cells infiltrating the intestine at day 7 after transplantation (supplemental Figure 1B). We next analyzed ICOS expression by human T cells in a model of xenogeneic GvHD. T cells recovered from spleens of NSG mice 14 days after transfer of human PBMCs showed significantly higher percentages of ICOS $^+$  cells compared with T cells prior to injection (day 14: 62% [49%-78%]; day 0: 5% [4%-8%]; P=.0091; Figure 1D). Unsupervised clustering of splenocytes recovered from GvHD mice at day 7 post–MHC-mismatch HCT showed that ICOS expression selectively identified donor-derived CD4 $^+$  and CD8 $^+$  T cells, distinguishing them from BM-derived and host-derived cells (Figure 1E). Similarly, in splenocytes recovered from xenogeneic GvHD mice at day 14 post-hPBMC transfer, ICOS expression identified activated human CD4 $^+$ and CD8 $^+$  T cells, distinguishing them from both mouse cells and other human immune cells (Figure 1F).

Collectively, these results demonstrate that ICOS expression is significantly upregulated by both mouse and human T cells in 3 murine models of acute GvHD.

# 89Zr-DFO-ICOS mAb immunoPET enables visualization of ICOS<sup>+</sup>-activated T cells in acute GvHD

We next evaluated the ability of ICOS-targeted immunoPET to visualize allogeneic T-cell activation and migration to target tissues during murine acute GvHD using <sup>89</sup>Zr-DFO-ICOS mAb. Acute GvHD was induced by adoptive transfer of  $Luc^+$  T cells, allowing in vivo T-cell detection, localization, and monitoring via BLI. On day 4 after HCT, a time point when no obvious signs of disease were observed, BLI detected donor-derived  $Luc^+$  T cells in the spleen, as

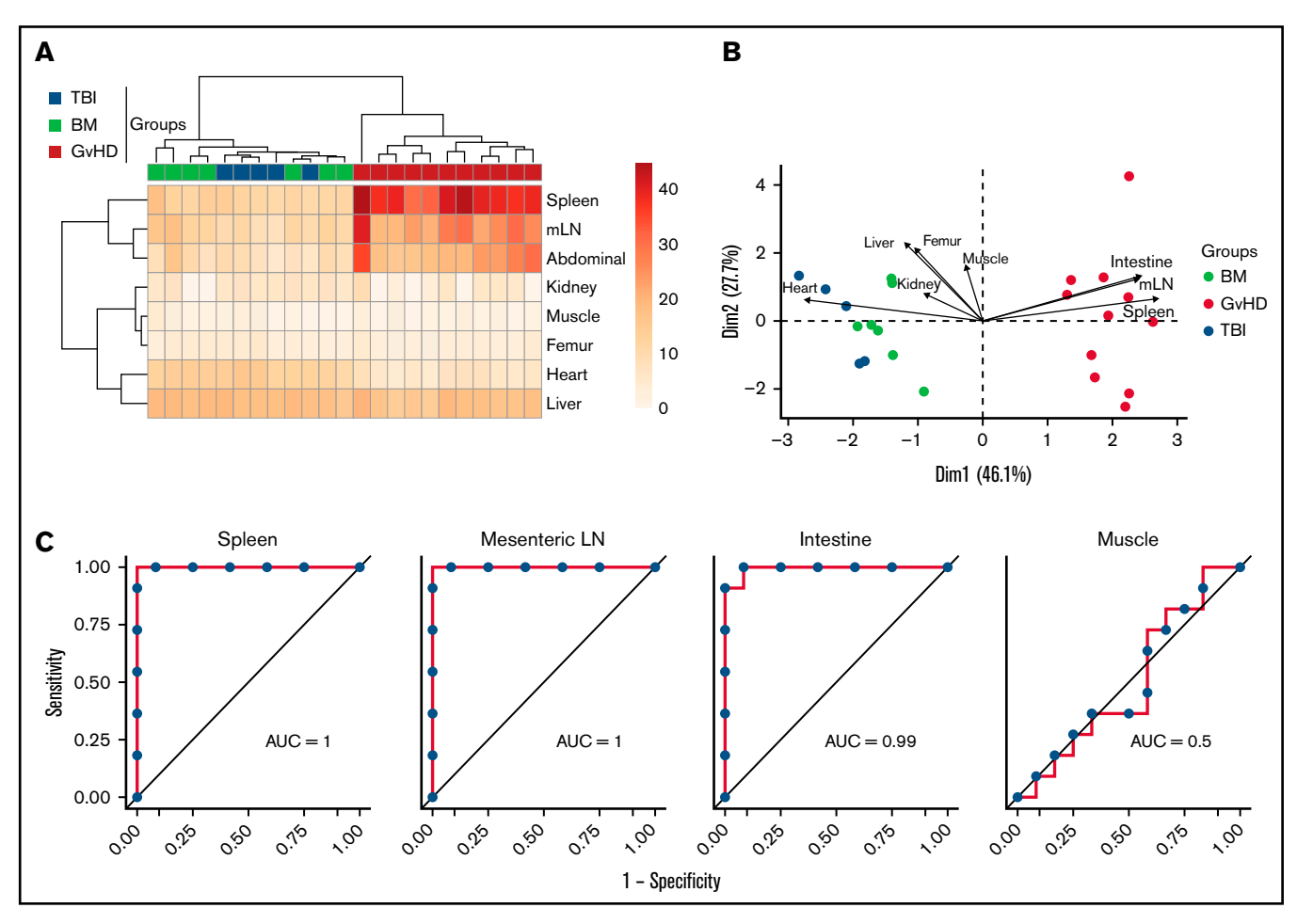


Figure 4. Assessment of 89Zr-DFO-ICOS mAb PET imaging as a potential tool for gastrointestinal GvHD early diagnosis. (A) Heatmap visualization and hierarchical clustering of normalized ICOS PET ROI values (rows) from single transplant recipients (columns). Data shown are pooled from 2 independent experiments. (B) PCA of normalized ICOS PET ROI values. Each arrow represents the relative contribution of each ROI. (C) ROC analysis showing sensitivity against 1 - specificity for distinguishing GvHD mice from other cohorts based on PET ROI values for organs identified by the PCA analysis (spleen, mLN, and intestine) and for muscle as a negative control.

well as in the mesenteric and cervical LNs (Figure 2A); this is in agreement with previously reported allogenic T-cell expansion in secondary lymphoid organs at this early stage of GvHD.6 We then evaluated the capacity of 89Zr-DFO-ICOS mAb to detect allogenic T-cell activation during GvHD. To this end, splenic T cells and TCD-BM were adoptively transferred to induce GvHD, and 50 µCi of <sup>89</sup>Zr-DFO-ICOS mAb was administrated IV at day 4 post-HCT. Mice receiving only TBI (TBI group) were used as a control to assess nonspecific tracer accumulation as a result of tissue damage and inflammation during conditioning. Mice receiving TCD-BM in the absence of T cells (BM group) were used as an additional control to evaluate signal derived from 89Zr-DFO-ICOS mAb binding to allogeneic hematopoietic cells other than T cells. PET images were acquired 24 and 48 hours after tracer administration; the 48-hour imaging timepoint was selected for further analysis due to optimal signal/noise ratios. A reference atlas of a representative volumerendered technique PET/CT image with the location of key clearance organs, lymphoid organs, and GvHD target tissues is shown in Figure 2B. PET signal was observed in the heart and the liver of all groups (Figure 2C), depicting the antibody tracer circulating in the blood and its hepatic clearance, respectively.20 Conversely,

<sup>89</sup>Zr-DFO-ICOS mAb PET signal in the spleen, mLN, and abdominal region was pronounced in GvHD mice (Figure 2C).

ROI analysis confirmed markedly increased tracer uptake in the spleen (median, 38.68% ID/g [range, 29.90-44.89]), mLN (25.15% ID/g [19.38-40.39]), and intestine (19.53% ID/g [15.31-35.67]) of GvHD mice compared with both TBI (spleen, 10.91% ID/g [10.45-14.7], P = 6.3e-05; mLN, 9.77% ID/g [7.79-10.93], P = .0005; intestine, 7.62% ID/g [5.23-9.51], P = .00046) and BM (spleen, 10.91% ID/g [10.45-14.70], P = 6.3e-05; mLN, 12.65% ID/g [10.69-17.43], P = 6.3e-05; intestine, 8.87% ID/g [7.42-16.26], P = .0001) controls (Figure 3A, upper panels). Slightly but significantly reduced levels of tracer accumulation were detected in the hearts of GvHD mice (5.96% ID/a [4.05-8.49]) compared with both TBI (14.04% ID/g [12.07-15.99], P = .00046) and BM (12.70% ID/g [10.40-14.51], P = 6.3e-05) controls; signal was also reduced in the kidney of GvHD mice (3.61% ID/g [0-9.01]) compared with TBI controls (6.30% ID/g [6.16-6.76]; P = .04; Figure 3, upper panels). These results are compatible with a sink effect, in which binding of the tracer to tissue-resident antigen effects signals reduction in the blood.

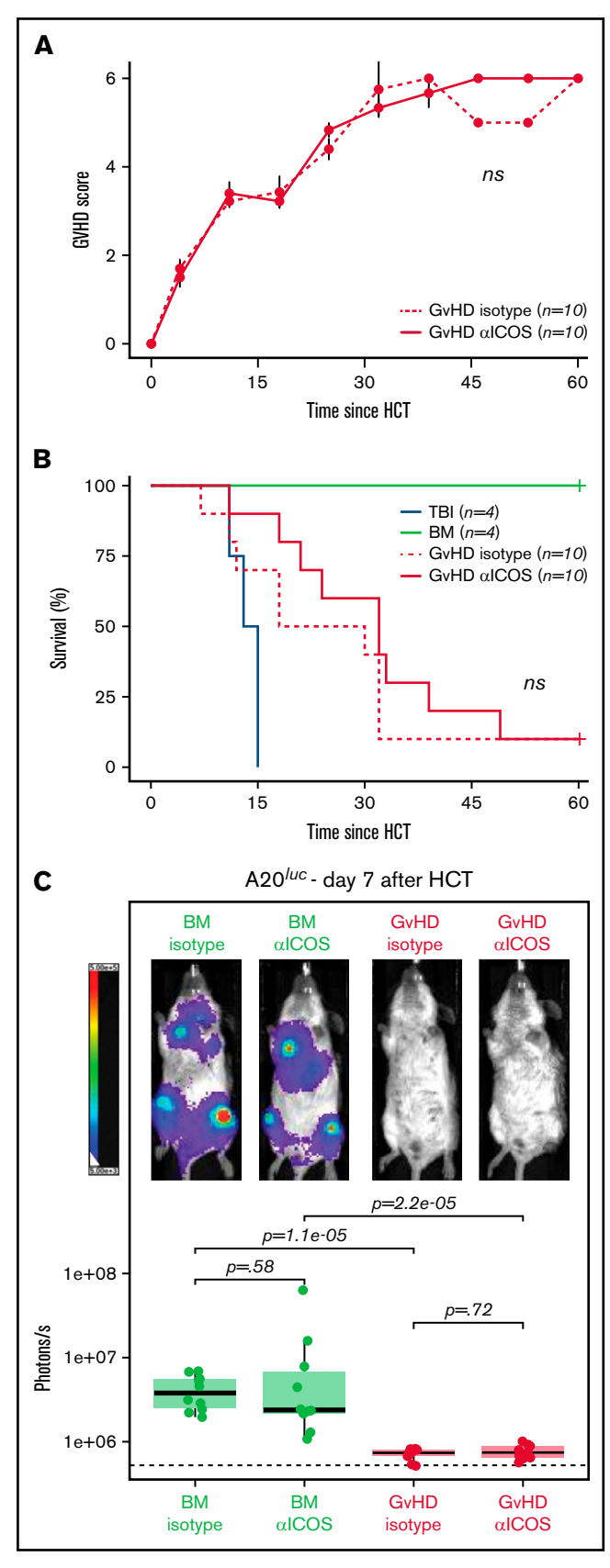


Figure 5.

Ex vivo BioD analysis using  $\gamma$  counting of tissues, performed following the 48-hour PET acquisition, showed a similar trend to the PET ROI quantification, with significantly increased tracer uptake measured in lymphoid tissues and intestines of GvHD mice vs controls (TBI: spleen P=.0022; mLN, P=.0015; intestine P=.0038; BM: spleen P=6.3e-05; mLN P=6.3e-05; intestine, P=.0037) (Figure 3A, lower panels). Correlation analysis confirmed good concordance between PET ROI and BioD measurements, showing a significant positive correlation in spleen ( $R^2$ , 0.59; P=1.8e-05), mLN ( $R^2$ , 0.6; P=3.2e-05), and intestine ( $R^2$ , 0.51, P=.0001; Figure 3B). Collectively, our data indicate that <sup>89</sup>Zr-DFO-ICOS mAb immunoPET noninvasively and specifically captures the expansion of ICOS $^+$ , activated donor-derived T cells during murine acute GvHD.

# ICOS immunoPET signals from intestine, spleen, and mLN have high diagnostic potential for early detection of murine acute gastrointestinal GvHD

We next evaluated the capability of 89Zr-DFO-ICOS mAb PET signal from different tissues to enable early diagnosis of murine acute gastrointestinal GvHD. Unsupervised hierarchical clustering based on ROI quantification of all tissues from mice in the PET dataset readily distinguished the GvHD group from TBI and BM mice (Figure 4A). Similarly, PCA clearly segregated mice from the GvHD group from other mice across the PC1, which accounted for 46% of the variance (Figure 4B). Spleen, mLN, and intestine PET ROIs were the strongest contributors in distinguishing mice in the GvHD group from other cohorts across PC1 (Figure 4B). To evaluate the diagnostic potential of 89Zr-DFO-ICOS mAb for early detection of acute GvHD, we employed ROC analysis. Spleen, mLN, and intestine ROIs had excellent diagnostic potential for GvHD diagnosis (spleen area under the curve [AUC], 1; mLN AUC, 1; intestine AUC, 0.99; Figure 4C), whereas, as predicted, muscle ROI had no diagnostic potential (AUC, 0.5). This analysis indicates that the <sup>89</sup>Zr-DFO-ICOS mAb PET signal from secondary lymphoid organs and the intestine have an optimal diagnostic potential for murine acute gastrointestinal GvHD.

# ICOS mAb does not affect murine acute GvHD pathogenesis or the GvT effect

Targeting costimulatory molecules with antibodies can potentially have perturbative effects on T-cell biology and, therefore, impact GvHD pathogenesis, leading to increased lethality. <sup>11</sup> To reduce the risk of potential toxicity of the <sup>89</sup>Zr-DFO-ICOS mAb tracer, we purposefully chose an antagonist ICOS mAb (clone 7E.17G9) for this study. <sup>21</sup> To experimentally test the safety of the ICOS mAb employed, 10 μg cold anti-ICOS or isotype control mAb was administrated at

Figure 5. Administration of ICOS mAb at tracer doses does not impact murine acute GvHD or the GvT effect. GvHD score (A) and animal survival (B) after allogeneic HCT. Two-way analysis of variance was used to compare GvHD score and log-rank test to compare survival curve between GvHD mice receiving 10 μg of cold anti-ICOS mAb (continuous red line) and isotype mAb (dashed red line) IV at day 4 post–allogenic transplantation. (C) Representative in vivo BLI images of A20<sup>luc+</sup> cell burden 7 days post-HCT in GvHD mice and BM controls having received cold anti-ICOS mAb or isotope control at day 4 post-HCT. Results are pooled from 2 independent experiments (n = 10 mice/group) and compared using a nonparametric Mann-Whitney *U* test.

day 4 post-HCT. No significant differences were observed in GvHD score (Figure 5A) or overall survival (Figure 5B) in mice injected with anti-ICOS mAb compared with those receiving the isotype control mAb, thus indicating that anti-ICOS mAb administered at imaging doses does not exacerbate acute GvHD pathogenesis.

Given the antagonistic nature of the anti-ICOS clone employed, we next assessed whether its administration at imaging doses would interfere with the antitumor potential of the allogeneic HCT. Mice were injected IV with  $luc^+$  A20 lymphoma cells (2  $\times$  10<sup>5</sup>) at the time of HCT. At day 4 after transplantation, mice were randomized and injected with unlabeled anti-ICOS or isotype control mAb (10 µg). Tumor progression was assessed by BLI at day 7. T cells transferred at the time of HCT in GvHD mice led to significantly lower tumor burden compared with mice receiving BM alone, for both isotype control and anti-ICOS mAb-treated mice (Figure 5C). Importantly, no significant differences in antitumor control in GvHD mice were observed between anti-ICOS or isotype control mAb treatment groups (Figure 5C). Collectively, these data demonstrate that the antagonistic anti-ICOS mAb used in our tracer neither alters the course of GvHD nor impairs the GvT effect of the HCT procedure, suggesting that ICOS immunoPET represents a safe, as well as a sensitive, approach for acute gastrointestinal GvHD diagnosis.

#### **Discussion**

Acute GvHD remains the major cause of nonrelapse mortality in allogeneic HCT recipients; early diagnosis would be greatly aided by the development of noninvasive approaches to detect global T-cell activation throughout different tissues in the body, given the key role of these cells in acute GvHD pathogenesis.

Although small-molecule PET tracers such as <sup>18</sup>F-FDG<sup>3,4</sup> and 18F-FAraG<sup>7</sup> have been evaluated, their utility for acute GvHD diagnosis is limited because the metabolic pathways they target are also upregulated in other tissues or cells, which can lead to low specificity. To date, other T-cell-targeted immunoPET imaging approaches in mouse models of GvHD have suffered from a lack of sensitivity or specificity<sup>8,9</sup> or from toxicity.<sup>11</sup> We previously reported the preclinical development of such an immunoPET tracer targeting OX40.11 Although this approach displayed excellent sensitivity for GvHD detection in a murine model of allogeneic HCT, the tracer also exacerbated GvHD, thus preventing its clinical translation for this particular application. To circumvent these limitations, here we assessed activation markers upregulated by both murine and human T cells in GvHD mouse models and identified ICOS as a potentially suitable target for immunoPET. Our preclinical results are in agreement with the recently reported molecular profiling of T-cell subsets from patients with acute GvHD, which demonstrated that ICOS was among the genes with the highest increase in transcript levels in both CD4 and CD8 T cells.<sup>22</sup> Consistent with our previously reported OX40-immunoPET approach, ICOS immunoPET exhibited optimal diagnostic potential in a murine model of acute GvHD. Importantly, the ICOS tracer reported here overcomes the limitations of OX40-immunoPET as the antagonistic ICOS antibody used avoids any significant toxicities on GvHD pathogenesis and does not interfere with the GvT effect, thus promoting the overall transplant success while avoiding disease relapse. These differences may be due to the use of an antagonistic mAb in lieu of an agonistic clone for the tracer, as well as the different roles of ICOS and OX40 in acute GvHD pathogenesis.<sup>23-26</sup> Notably, ICOS has a

paradoxical role in the regulation of alloreactive CD4 T cells and CD8 T cells in murine models of acute GvHD, genetic ablation of ICOS in CD4 T cells having a protective effect, and in CD8 T cells exacerbating the disease.<sup>26</sup> For this reason, we are working on the generation of a clinical tracer with a high affinity and no agonist/ antagonist and Fc-effector functions before moving to phase 1 imaging studies in HCT recipients.

Future optimization of our ICOS immunoPET imaging approach, using alternative vector formats, would allow us to minimize nonspecific binding to other cells mediated through the Fc region and also address 2 limitations of this study. First, <sup>89</sup>Zr-labeled mAbs impart higher radiation doses to patients than <sup>18</sup>F-radiolabeled tracers. The use of smaller engineered antibodies (scFv and nanobodies) and protein scaffolds with shorter serum half-lives would allow for the use of short-lived isotopes (eg, <sup>18</sup>F) for convenient same-day imaging while significantly reducing the radiation dose. Second, our <sup>89</sup>Zr-DFO-ICOS mAb tracer does not allow GvHD detection in the liver, another key target tissue, due to the hepatic accumulation of whole mAbs. The use of antibodies with a mutant Fc region, which abrogates binding to Fc receptors or smaller formats lacking the Fc region altogether and which shows renal clearance, may significantly reduce background liver signal and allow extension of this diagnostic approach beyond acute gastrointestinal GvHD. Such tracer optimization would also allow the extension of ICOS immunoPET to liver and lung imaging for diagnosis of chronic GvHD, a condition in which ICOS expression has been shown to be upregulated at the surface of pathogenic T cells.27-29

Despite the fact that our ICOS immunoPET approach specifically detects activated T cells. T-cell activation in the gastrointestinal tract is not solely restricted to GvHD and can also be observed in other transplant-related complications, namely cytomegalovirus colitis. We believe that, upon clinical translation, ICOS immunoPET will need to be integrated in the whole clinical and biological workup and that its combination with biomarkers of GvHD (ST2, REG3a) or infection (cytomegalovirus viral load) will further increase the specificity of our approach.

In conclusion, we have identified ICOS as a highly sensitive and specific imaging biomarker for the in vivo visualization of allogenic, donor-derived, activated CD4 and CD8 T cells during acute gastrointestinal GvHD. ICOS immunoPET has the potential to have significant clinical impact and improve overall management of HCT recipients by enabling early diagnosis of acute gastrointestinal GvHD.

# **Acknowledgments**

The authors would like to acknowledge Jason Lee, Frezghi Habte, and Laura Pisani at the Stanford Center for Innovation in In-Vivo Imaging (SCI<sup>3</sup>) for their assistance with the preclinical imaging studies. They are grateful to members of the Stanford FACS facility for sharing their expertise. They thank Kenneth Lau for assistance with mass spectrometry. Special thanks to Behnaz Mobashwera and Emily Deal for editing the manuscript.

This work was supported in part from funding from the Ben & Catherine Ivy Foundation (S.S.G.), the Canary Foundation (S.S.G.); National Cancer Institute (NCI), National Institutes of Health (NIH) (grants R01-CA201719-05 [S.S.G. and M.L.J.] and R01-CA23158201 and P01-CA49605 [R.S.N.]); the Parker

Institute for Cancer Immunotherapy (S.S.G. and R.S.N.); the Department of Radiology, Stanford University (I.S.A.); the Geneva University Hospitals Fellowship (F.S.); the Swiss Cancer League (BIL KLS 3806-02-2016 to F.S.); the Dubois-Ferrière-Dinu-Lipatti Foundation (F.S.); the American Society for Blood and Marrow Transplantation (New Investigator Award 2018 to F.S.); and the Geneva Cancer League (LGC 20 11 to F.S.).

We dedicate this paper to the memory of our cherished mentor and friend, Sanjiv S. Gambhir, and his extraordinary contributions to the field of molecular imaging and early disease detection.

# **Authorship**

Contribution: Z.X., I.S.A., F.S., R.S.N., and S.S.G. conceived and designed research studies; I.S.A., F.S., and Z.X. developed methodology, conducted experiments, and acquired and analyzed

data; L.S., J.K.L., and T.L.R. developed methodology, conducted experiments, and acquired data; W.C. and S.M. conducted experiments; and I.S.A., F.S., Z.X., M.L.J., and R.S.N. wrote the manuscript.

Conflict-of-interest disclosure. The authors declare no competing financial interests.

Sanjiv S. Gambhir died on 18 July 2020.

ORCID profiles: J.K.L., 0000-0003-4311-0317; T.L.R., 0000-0002-0696-7197.

Correspondence: Robert S. Negrin, Center for Clinical Sciences Research, 269 Campus Drive, Room 2205, Stanford, CA 94305; e-mail: negrs@stanford.edu; and Israt S. Alam, Stanford University, 318 Campus Drive, Clark Center, Stanford, CA 94305; e-mail: israt@stanford.edu.

#### References

- 1. Zeiser R, Blazar BR. Acute graft-versus-host disease biologic process, prevention, and therapy. N Engl J Med. 2017;377(22):2167-2179.
- Stelljes M, Hermann S, Albring J, et al. Clinical molecular imaging in intestinal graft-versus-host disease: mapping of disease activity, prediction, and monitoring of treatment efficiency by positron emission tomography. Blood. 2008;111(5):2909-2918.
- 3. Bodet-Milin C, Lacombe M, Malard F, et al. 18F-FDG PET/CT for the assessment of gastrointestinal GVHD: results of a pilot study. *Bone Marrow Transplant*. 2014;49(1):131-137.
- 4. Roll W, Evers G, Strotmann R, et al. Fluorodeoxyglucose F 18 for the assessment of acute intestinal graft-versus-host disease and prediction of response to immunosuppressive therapy. *Transplant Cell Ther.* 2021;27(7):603-610.
- 5. Hill GR, Ferrara JL. The primacy of the gastrointestinal tract as a target organ of acute graft-versus-host disease: rationale for the use of cytokine shields in allogeneic bone marrow transplantation. *Blood*. 2000;95(9):2754-2759.
- Beilhack A, Schulz S, Baker J, et al. In vivo analyses of early events in acute graft-versus-host disease reveal sequential infiltration of T-cell subsets. Blood. 2005;106(3):1113-1122.
- 7. Ronald JA, Kim B-S, Gowrishankar G, et al. A PET imaging strategy to visualize activated T cells in acute graft-versus-host disease elicited by allogenic hematopoietic cell transplant. *Cancer Res.* 2017;77(11):2893-2902.
- 8. Pektor S, Schlöder J, Klasen B, et al. Using immuno-PET imaging to monitor kinetics of T cell-mediated inflammation and treatment efficiency in a humanized mouse model for GvHD. Eur J Nucl Med Mol Imaging. 2020;47(5):1314-1325.
- 9. Van Elssen CHMJ, Rashidian M, Vrbanac V, et al. Noninvasive imaging of human immune responses in a human xenograft model of graft-versus-host disease. *J Nucl Med.* 2017;58(6):1003-1008.
- 10. Alam IS, Mayer AT, Sagiv-Barfi I, et al. Imaging activated T cells predicts response to cancer vaccines. J Clin Invest. 2018;128(6):2569-2580.
- Alam IS, Simonetta F, Scheller L, et al. Visualization of activated T Cells by OX40-ImmunoPET as a strategy for diagnosis of acute graft-versus-host disease. Cancer Res. 2020;80(21):4780-4790.
- 12. Xiao Z, Mayer AT, Nobashi TW, Gambhir SS. ICOS is an indicator of T-cell-mediated response to cancer immunotherapy. *Cancer Res.* 2020; 80(14):3023-3032.
- 13. Simonetta F, Alam IS, Lohmeyer JK, et al. Molecular imaging of chimeric antigen receptor T Cells by ICOS-ImmunoPET. Clin Cancer Res. 2021; 27(4):1058-1068.
- Maas-Bauer K, Lohmeyer JK, Hirai T, et al. Invariant natural killer T-cell subsets have diverse graft-versus-host-disease-preventing and antitumor effects. Blood. 2021;138(10):858-870.
- Ehx G, Somja J, Warnatz H-J, et al. Xenogeneic graft-versus-host disease in humanized NSG and NSG-HLA-A2/HHD mice. Front Immunol. 2018; 9:1943.
- 16. Love MI, Huber W, Anders S. Moderated estimation of fold change and dispersion for RNA-seq data with DESeq2. *Genome Biol.* 2014;15(12):
- Cooke KR, Kobzik L, Martin TR, et al. An experimental model of idiopathic pneumonia syndrome after bone marrow transplantation: I. The roles of minor H antigens and endotoxin. Blood. 1996;88(8):3230-3239.
- 18. Tako B, Knopf P, Maurer A, et al. CD69-ImmunoPET enables early response evaluation of cancer immunotherapies. In: IMAGING IMMUNITY from Nanoscale to Macroscale | Insights from Biophysics 14th ESMI Winter Conference, 12-17 January 2020, Ecole de Physique des Houches, Les Houches, France.

- 19. Krebs S, Ahad A, Carter LM, et al. Antibody with infinite affinity for in vivo tracking of genetically engineered lymphocytes. J Nucl Med. 2018; 59(12):1894-1900.
- National Institute of Diabetes and Digestive and Kidney Diseases. LiverTox: Clinical and Research Information on Drug-Induced Liver Injury. Accessed Day Month Year.
- 21. Maazi H, Patel N, Sankaranarayanan I, et al. ICOS:ICOS-ligand interaction is required for type 2 innate lymphoid cell function, homeostasis, and induction of airway hyperreactivity. Immunity. 2015;42(3):538-551.
- 22. Latis E, Michonneau D, Leloup C, et al; CRYOSTEM Consortium. Cellular and molecular profiling of T-cell subsets at the onset of human acute GVHD. Blood Adv. 2020;4(16):3927-3942.
- 23. Blazar BR, Sharpe AH, Chen AI, et al. Ligation of OX40 (CD134) regulates graft-versus-host disease (GVHD) and graft rejection in allogeneic bone marrow transplant recipients. Blood. 2003;101(9):3741-3748.
- 24. Tripathi T, Yin W, Xue Y, et al. Central roles of OX40L-OX40 interaction in the induction and progression of human T cell-driven acute graft-versus-host disease. Immunohorizons. 2019;3(3):110-120.
- 25. Taylor PA, Panoskaltsis-Mortari A, Freeman GJ, et al. Targeting of inducible costimulator (ICOS) expressed on alloreactive T cells down-regulates graft-versus-host disease (GVHD) and facilitates engraftment of allogeneic bone marrow (BM). Blood. 2005;105(8):3372-3380.
- 26. Yu X-Z, Liang Y, Nurieva RI, Guo F, Anasetti C, Dong C. Opposing effects of ICOS on graft-versus-host disease mediated by CD4 and CD8 T cells. J Immunol. 2006;176(12):7394-7401.
- 27. Zhang M, Wu Y, Bastian D, et al. Inducible T-cell co-stimulator impacts chronic graft-versus-host disease by regulating both pathogenic and regulatory T cells. Front Immunol. 2018;9:1461.
- 28. Parker MH, Stone D, Abrams K, Johnson M, Granot N, Storb R. Anti-ICOS mAb targets pathogenic IL-17A-expressing cells in canine model of chronic GVHD. Transplantation. 2021;105(5):1008-1016.
- Kong X, Zeng D, Wu X, et al. Tissue-resident PSGL1 oCD4 T cells promote B cell differentiation and chronic graft-versus-host disease-associated autoimmunity. J Clin Invest. 2021;131(1):e135468.

#### 3.2. Publication 2

Maas-Bauer K, Lohmeyer JK, Hirai T, Ramos TL, Fazal FM, Litzenburger UM, Yost KE, Ribado JV, Kambham N, Wenokur AS, Lin PY, Alvarez M, Mavers M, Baker J, Bhatt AS, Chang HY, **Simonetta F**<sup>#</sup>, Negrin RS<sup>#</sup>. Invariant natural killer T-cell subsets have diverse graft-versus-host-disease-preventing and antitumor effects. *Blood.* **2021**;138(10):858-870. doi: 10.1182/blood.2021010887.

(\* Co-senior authors)

Invariant Natural Killer T (iNKT) cells are a small subset of innate immune lymphocytes that have a great translational potential for allogeneic HSCT, as they lack any GvHD-induction potential while displaying strong antitumor as well as immune-regulatory activity. Previous studies have shown that iNKT cells are able to prevent GvHD in murine models (Leveson-Gower et al., 2011). Once considered a homogeneous population, it is now well established that murine iNKT cells differentiate during thymic development into three distinct sublineages, distinguished based on the expression of transcription factors and effector molecules and named according to the classification of conventional T cells: Th1-like iNKT (iNKT1) cells, Th2-like iNKT (iNKT2) cells, and Th-17 like iNKT (iNKT17) cells. Whether different iNKT sublineages had different GvHD suppressive effect and/or antitumor activity was not known. In this work we addressed this question.

In order to identify surface molecules whose combination would allow us to isolate viable iNKT1, iNKT2, and iNKT17 cells, we performed a single cell RNA sequencing analysis using the 10x Genomics technology on murine thymic iNKT cells isolated from 8-10 week-old FVB/N mice by flow cytometry based on PBS-57-CD1d-Tetramer staining. The results of this analysis together with previously published knowledge, allowed us to develop a sorting strategy to isolate highly purified iNKT1, iNKT2 and iNKT17 cells, whose purity was confirmed by intranuclear staining for the transcription factors PLZF and RORgT. The transcriptomic and epigenomic heterogeneity of the different iNKT sublineages was investigated by RNAseq and ATACseq (assay for transposase-accessible chromatin using sequencing) respectively. More importantly, using in vitro and in vivo assays, we demonstrated that iNKT1 cells displayed the strongest antitumor potential. Conversely, only iNKT2 and iNKT17 cells protected from GVHD, whereas iNKT1 cells lack any immune-regulatory potential (Figure 5). Our study showed for the first time functional differences between the iNKT sublineages and provided important information to guide future development of iNKT cell based immunotherapies.

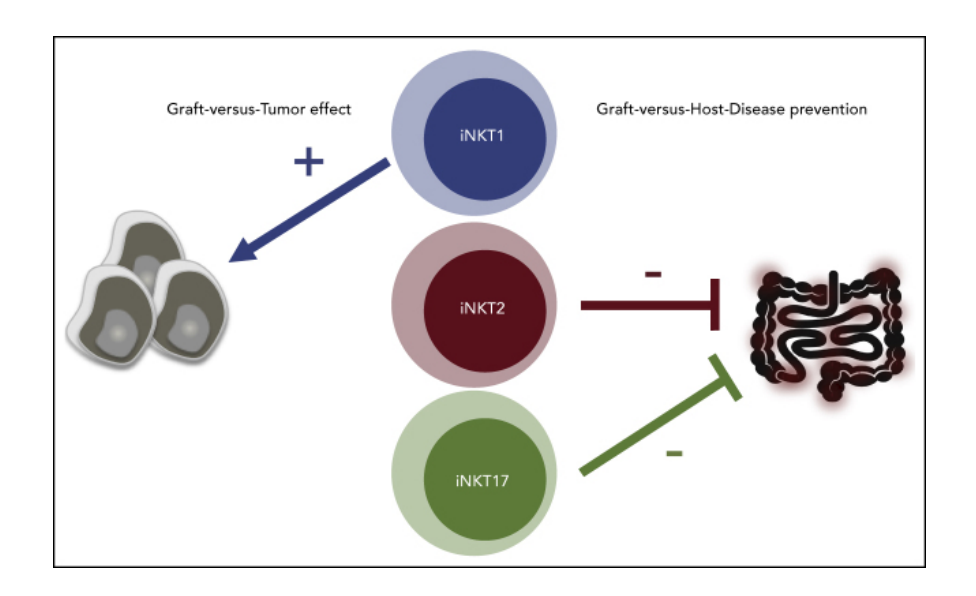


Figure 5. Graphical representation of the antitumor and immunoregulatory effects of iNKT sublineages. Personal material published as graphical abstract in Blood 2021.



# Regular Article

#### **IMMUNOBIOLOGY AND IMMUNOTHERAPY**

# Invariant natural killer T-cell subsets have diverse graft-versus-host-disease-preventing and antitumor effects

Kristina Maas-Bauer, <sup>1,2,\*</sup> Juliane K. Lohmeyer, <sup>1,\*</sup> Toshihito Hirai, <sup>1</sup> Teresa Lopes Ramos, <sup>1</sup> Furqan M. Fazal, <sup>3</sup> Ulrike M. Litzenburger, <sup>3</sup> Kathryn E. Yost, <sup>3</sup> Jessica V. Ribado, <sup>4</sup> Neeraja Kambham, <sup>5</sup> Arielle S. Wenokur, <sup>1</sup> Po-Yu Lin, <sup>1</sup> Maite Alvarez, <sup>1</sup> Melissa Mavers, <sup>1,6</sup> Jeanette Baker, <sup>1</sup> Ami S. Bhatt, <sup>1,4,7</sup> Howard Y. Chang, <sup>3,8</sup> Federico Simonetta, <sup>1,9,10,†</sup> and Robert S. Negrin <sup>1,†</sup>

<sup>1</sup>Division of Blood and Marrow Transplantation, Stanford University, Stanford, CA; <sup>2</sup>Department of Hematology, Oncology, and Stem Cell Transplantation, University of Freiburg Medical Center, Freiburg, Germany; <sup>3</sup>Center for Personal Dynamic Regulomes, <sup>4</sup>Department of Genetics, and <sup>5</sup>Department of Pathology, Stanford University, Stanford, CA; <sup>6</sup>Division of Stem Cell Transplantation and Regenerative Medicine, Bass Center for Childhood Cancer and Blood Diseases, Department of Pediatrics, Stanford University School of Medicine, Palo Alto, CA; <sup>7</sup>Division of Hematology and <sup>8</sup>Howard Hughes Medical Institute, Stanford University, Stanford, CA; <sup>9</sup>Division of Hematology, Department of Oncology, Geneva University Hospitals, Geneva, Switzerland; and <sup>10</sup>Translational Research Center for Oncohematology, Department of Internal Medicine Specialties, Faculty of Medicine, University of Geneva, Geneva, Switzerland

#### KEY POINTS

- iNKT2 and iNKT17, but not iNKT1, cells mitigate murine acute GVHD.
- iNKT1 cells exert stronger antitumor effects in vitro and in vivo.

Invariant natural killer T (iNKT) cells are a T-cell subset with potent immunomodulatory properties. Experimental evidence in mice and observational studies in humans indicate that iNKT cells have antitumor potential as well as the ability to suppress acute and chronic graft-versus-host-disease (GVHD). Murine iNKT cells differentiate during thymic development into iNKT1, iNKT2, and iNKT17 sublineages, which differ transcriptomically and epigenomically and have subset-specific developmental requirements. Whether distinct iNKT sublineages also differ in their antitumor effect and their ability to suppress GVHD is currently unknown. In this work, we generated highly purified murine iNKT sublineages, characterized their transcriptomic and epigenomic landscape, and assessed specific functions. We show that iNKT2

and iNKT17, but not iNKT1, cells efficiently suppress T-cell activation in vitro and mitigate murine acute GVHD in vivo. Conversely, we show that iNKT1 cells display the highest antitumor activity against murine B-cell lymphoma cells both in vitro and in vivo. Thus, we report for the first time that iNKT sublineages have distinct and different functions, with iNKT1 cells having the highest antitumor activity and iNKT2 and iNKT17 cells having immune-regulatory properties. These results have important implications for the translation of iNKT cell therapies to the clinic for cancer immunotherapy as well as for the prevention and treatment of GVHD.

#### Introduction

Allogeneic hematopoietic cell transplantation (HCT) is a highly effective therapy for a broad range of life-threatening hematologic malignancies, genetic abnormalities, and bone marrow failure status. It is unfortunately, however, associated with significant morbidity and mortality related to transplant complications, namely acute graft-versus-host disease (GVHD) and immune deficiencies. During acute GVHD, the interaction with host tissues induces donor-derived T-cell activation, proliferation, and migration to target organs, notably skin, liver, and intestine, leading to cell damage and clinical manifestations. Preclinical murine models of GVHD strongly support the feasibility of selectively preventing GVHD by using cellular immunotherapy.

Invariant natural killer T (iNKT) cells are an innate lymphocyte population expressing a semi-invariant T-cell receptor that recognizes glycolipids presented in the context of the non-polymorphic molecule CD1d. Through modulation of innate and adaptive immune cells, iNKT cells display an extremely versatile panel of functions, <sup>2,3</sup> ranging from antitumor effects to immune-regulatory activity. Experimental evidence in mice<sup>4-8</sup> and observational

studies in humans  $^{9,10}$  indicate that iNKT cells have the potential to suppress acute and chronic GVHD.  $^{11}$ 

It is now well established that murine iNKT cells differentiate during thymic development into at least 3 distinct sublineages, iNKT1, iNKT2, and iNKT17 cells; these sublineages are classified based on the expression of transcription factors and effector molecules. <sup>12-15</sup> Several studies provided insights into the developmental requirements <sup>16-19</sup> and molecular characteristics <sup>15,20,21</sup> of the distinct iNKT sublineages, but no formal evidence of their functional heterogeneity exists. Therefore, whether one or multiple sublineages are suitable for antitumor and/or GVHD immunotherapy is not known.

In the current work, the molecular and functional heterogeneity of murine iNKT subsets was assessed and the function of iNKT1, iNKT2, and iNKT17 cells was tested with respect to their antitumor effects. Moreover, we assessed the ability of each iNKT cell sublineage to prevent GVHD in murine models of HCT. For the first time, we show that iNKT2 and iNKT17 cells, but not iNKT1 cells, display an immune-regulatory effect

mitigating murine acute GVHD and that iNKT1 cells have the strongest antitumor effect.

# Methods

#### Mice

BALB/cJ (H-2k<sup>d</sup>), C57Bl/6J (H-2k<sup>b</sup>), and FVB/NJ (H-2k<sup>q</sup>) mice were purchased from The Jackson Laboratory. *Luc*<sup>+</sup> transgenic FVB/N L2G85 mice<sup>22</sup> were bred at Stanford University. All animal experiments were approved by the Administrative Panel on Laboratory Animal Care at Stanford University.

#### Flow cytometric analysis

Reagents used for fluorescence-activated cell sorting (FACS) analysis are summarized in the supplemental Methods (available on the *Blood* Web site). Samples were acquired on a BD LSRII (BD Biosciences) and were analyzed by using FlowJo 10.5.0 (Tree Star).

#### **Genomics analyses**

Materials and methods used for genomics analyses are detailed in the supplemental Methods.

#### Isolation of iNKT sublineages

Single-cell suspensions from thymi harvested from 6- to 8-week-old FVB/N mice were incubated with biotinylated anti-CD19, anti-CD8a, anti-CD62L, anti-TCR- $\gamma\delta$ , anti-GR-1, anti-Ter119, and streptavidin beads (BD) and negatively enriched. After staining with anti-inducible T-cell costimulator (ICOS), anti-CD27, anti-T-cell receptor (TCR)- $\beta$ , anti-CD24, anti-CD4, anti-programmed cell death protein 1 (PD-1), streptavidin, and PBS-57-CD1d tetramer, cells were sorted on an FACSAria II (BD). Cell purity was assessed by FACS after transcription factor staining with anti-PLZF and anti-ROR $\gamma$ T and was consistently >92%.

#### In vitro cytotoxicity assay

The CD1d-transduced A20 B-cell lymphoma cell line was a kind gift of Mitchell Kronenberg (La Jolla Institute for Immunology, La Jolla, CA). A20-CD1d cells were loaded for 4 hours with 250 ng/mL  $\alpha$ -galactosylceramide (KRN7000, REGiMMUNE), washed, stained by using a CellTrace CFSE Proliferation Kit (Life Technologies), and plated in round bottom 96-well plates at 10 000 cells per well. FACS-sorted iNKT1, iNKT2, and iNKT17 cells were mixed with A20-CD1d cells at an effector:target ratio of 4:1. After 24 hours, cells were stained for CD19 and B220 and viability dye, and analyzed by FACS. iNKT-mediated cytotoxicity was calculated as percentage of death compared with A20-CD1d cells cultured alone.

#### In vivo tumor model

CD1d-transduced A20 B-cell lymphoma cells (2  $\times$  10e4) resuspended in phosphate-buffered saline were injected intravenously by tail vein into alymphoid BALB/c Rag1 $^{-/-}$   $\gamma C^{-/-}$  mice or into sublethally (4.4 Gy) irradiated wild-type BALB/c mice. Sorted splenic CD4 $^+$  iNKT cells, iNKT1, iNKT2, or iNKT17 cells (5  $\times$  10e4), were injected intravenously on the same day. Mice were monitored daily and euthanized if moribund or when lower limb paralysis appeared.

#### In vitro suppressive assay

CD4<sup>+</sup> conventional T cells (Tcon) were enriched from splenocytes of *luc*<sup>+</sup> FVB/N mice with CD4 MicroBeads (Miltenyi Biotec). After

staining with a Violet Proliferation Kit (Life Technologies), cells were plated in a round bottom 96-well plate at a concentration of 30 000 cells per well with anti-CD3/anti-CD28 activation beads (1:1 ratio; Invitrogen). FACS-sorted iNKT1, iNKT2, and iNKT17 cells were mixed with CD4 Tcon at a 1:1 ratio. After 96 hours, cells were stained for CD25, ICOS, and fixable viability dye and analyzed by FACS. iNKT-mediated suppression was calculated as a percentage of reduction of mean number of cell cycles per cell compared with control cells cultured without iNKT cells.

#### Allogeneic bone marrow transplantation

Donor CD4<sup>+</sup> and CD8<sup>+</sup> conventional T cells (Tcon) were prepared from splenocytes of luc<sup>+</sup> FVB/N mice and enriched with CD4 and CD8 MicroBeads (Miltenyi Biotec). Cell purity was consistently >95%. T-cell-depleted bone marrow (TCD-BM) was prepared by crushing bones from FVB/N mice and depleting T cells with CD4 and CD8 MicroBeads. BALB/c recipient mice were lethally irradiated with 8.8 Gy in 2 doses administered 4 hours apart. On the same day, 4  $\times$  10  $^{6}$  TCD-BM cells and 1.0  $\times$  10  $^{6}$  Tcon from luc<sup>+</sup> FVB/N mice were injected intravenously. Sorted iNKT1, iNKT2, or iNKT17 cells were coinjected. Transplanted animals housed with food containing sulfamethoxazole and trimethoprim were monitored daily, and weight and GVHD scores<sup>23</sup> were assessed weekly. Survival was analyzed by using the Kaplan-Meier method and log-rank test. Weight loss and GVHD clinical score were analyzed by 2-way analysis of variance with Bonferroni correction. A value of P < .05 was considered statistically significant. All transplant experiments were performed with sexmatched mice between 8 and 12 weeks of age.

# Multiplex cytokine assays

Sera were collected from recipient mice on day 7 after transplantation. Cytokines were analyzed by using a multiplex assay system (Th1/Th2 Cytokine 11-Plex Mouse ProcartaPlex Panel; Invitrogen) and quantitated by using the Luminex 200 System (Luminex).

#### Histopathology

Tissues were fixed in 10% neutral buffered formalin. Tissue processing, staining with hematoxylin and eosin, and digital photomicrography were conducted by HistoWiz. Tissue sections were evaluated and scored for GVHD blindly by an experienced pathologist (N.K.) according to a previously published system.<sup>24</sup>

#### Statistical analysis

Statistical analyses were performed by using Prism 6 (GraphPad Software) and R 3.5.1 with R studio 1.1.453 (RStudio, Public Benefit Corporation).

#### Results

# Single-cell RNA sequencing identifies surface molecules for isolation of highly purified iNKT sublineages

In agreement with previous reports,  $^{14}$  thymic iNKT from BALB/c mice, but not C57BL/6 mice, display sizeable populations of iNKT1, iNKT2, and iNKT17, defined by the differential expression of the transcription factors PLZF and ROR $\gamma$ T (supplemental Figure 1A-B), whereas splenic iNKT cells were dominated by iNKT1 cells in both mouse strains (supplemental Figure 1A,C). Thymic iNKT cells from FVB/N mice displayed all 3 sublineages, with a slight dominance of iNKT2 cells, whereas splenic iNKT cells were mostly

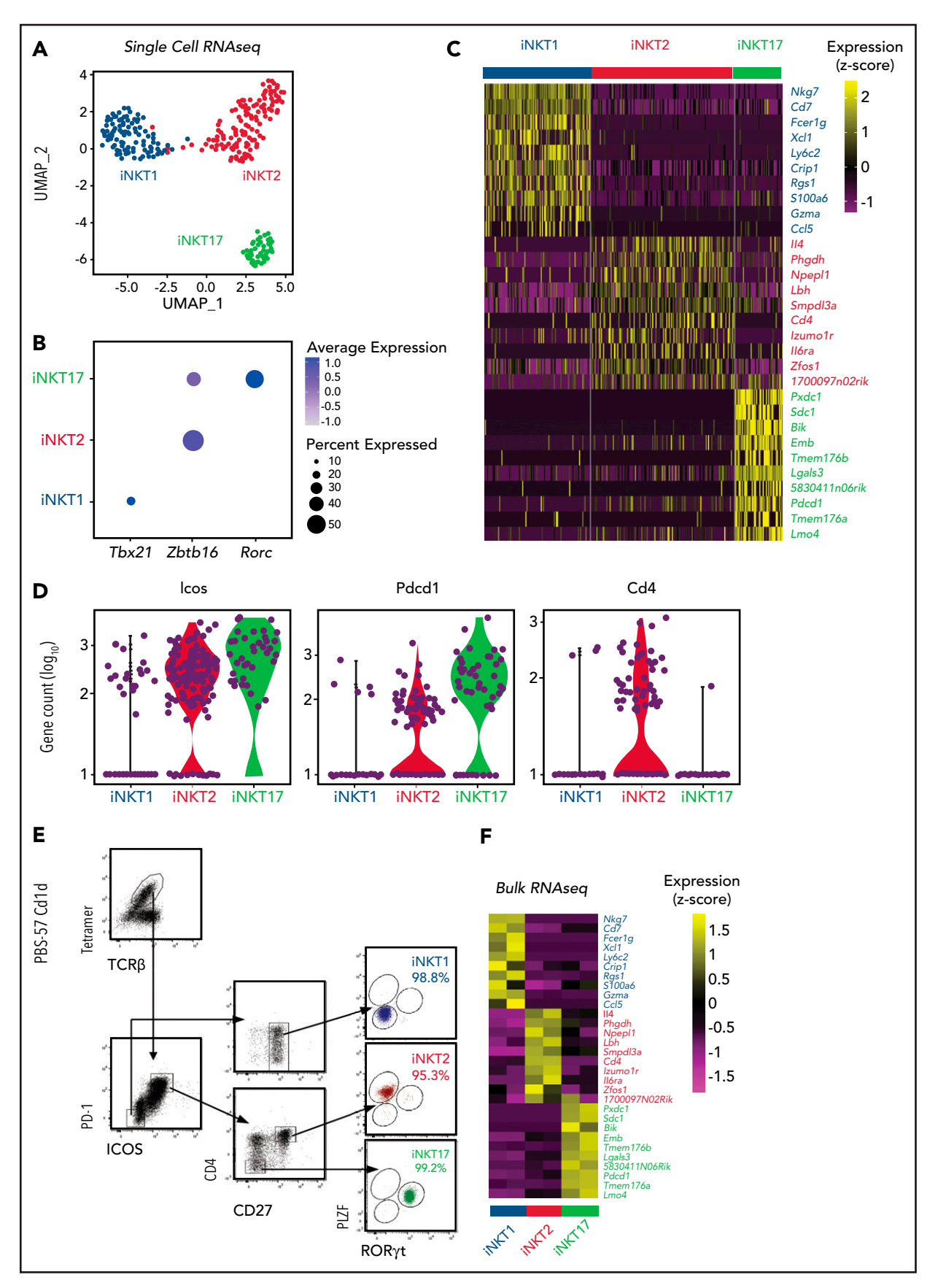


Figure 1.

represented by iNKT1 cells. Given the distribution of iNKT sublineages, FVB/N thymi were selected as a cellular source.

We next performed single-cell RNA sequencing (scRNA-seq) on thymic FVB/N iNKT cells sorted from individual animals based on PBS57-loaded tetramer staining. The cells segregated into 3 clearly defined clusters expressing genes characteristic of iNKT1, iNKT2, and iNKT17 cells (Figure 1A). Expression of *Tbx21*, *Zbtb16*, and *Rorc* genes, encoding the key lineage-defining transcription factors T-Bet, PLZF, and RORγT, respectively, further confirmed the identities of the clusters (Figure 1B). iNKT1 cells expressed the highest levels of transcripts from genes associated with cytotoxic effector function (*Nkg7*, *Gzma*, and *Ccl5*), iNKT2 cells expressed the highest level of *II4*, and iNKT17 cells preferentially expressed genes previously reported to identify Th17-like iNKT cells, namely *Sdc1* (Figure 1C).

This analysis revealed several differentially expressed transcripts encoding cell surface–expressed molecules. In particular, *Icos* and *Pdcd1* (encoding PD-1) were expressed at high levels in iNKT2 and iNKT17 cells, whereas they were barely detectable in iNKT1 cells (Figure 1D). In agreement with previous reports, iNKT1 and iNKT17 cells were almost devoid of *Cd4* transcripts. Combining these molecules with others reported in the literature (CD27 $^{12}$ ), we developed a FACS-isolation strategy yielding highly purified iNKT sublineages, as confirmed by intracellular staining for ROR $_{\gamma}$ T and PLZF (Figure 1E). Bulk RNA-seq analysis of the sorted populations confirmed the distribution of differentially expressed genes identified by scRNA-seq (Figure 1F).

# Assay for transposase-accessible chromatin sequencing reveals distinct chromatin accessibility profiles of iNKT sublineages

We next profiled the chromatin accessibility of the obtained iNKT sublineages using assay for transposase-accessible chromatin sequencing (ATAC-seq). Pairwise analyses showed that iNKT2 and iNKT17 cells had more accessibility differences compared with iNKT1 cells, with relatively fewer differences detected between iNKT2 and iNKT17 cells (Figure 2A). Hierarchical clustering further confirmed that iNKT2 and iNKT17 cells displayed closer chromatin accessibility profiles compared with iNKT1 cells (Figure 2B). Focusing on differential ATAC-seg peaks at promoter and transcription start sites for immunologically relevant genes, iNKT1 cells displayed increased accessibility at the interferon- $\gamma$ (Ifng) locus as well as at the granzyme A (Gzma) and granzyme B (Gzmb) loci. In iNKT2 cells, we observed increased chromatin accessibility in the promoter of the gene encoding the T helper 2 (Th2)-chemokine receptor CCR4, as well as in II4 promoter. Finally, iNKT17 cells selectively displayed increased chromatin accessibility at promoters of genes encoding Th17-related cytokines (II17a and II17f) and subset-specific cytokine receptors (*ll1r1* and *ll23r*). iNKT1-specific chromatin accessibility regions were enriched for Runt-related and ETS-related-gene transcription factors as well as for T-bet and Eomes binding motifs (supplemental Figure 2), as previously reported. <sup>25</sup> iNKT2-specific regions were enriched for GATA family transcription factor binding sites. Finally, iNKT17-specific regions were enriched for binding sites of the Th17-regulating factors ROR $\gamma$ T and BATF. Collectively, these data reveal that each iNKT sublineage has distinct chromatin accessibility profiles and that iNKT2 and iNKT17 cells are more epigenomically similar to one another than to iNKT1 cells.

# iNKT1 cells display epigenomic and transcriptomic potential for cytotoxic molecule production and exert the strongest antitumor effect in vitro and in vivo

We next examined chromatin accessibility and expression levels of genes encoding molecules involved in antitumor effects of iNKT cells.<sup>26</sup> iNKT1 cells were the only subset displaying high promoter chromatin accessibility and active transcription of Gzmb and Prf1 (Figure 3A). Moreover, multiple peaks were specifically enriched in iNKT1 cells at putative distal regulatory regions for the Gzmb gene (supplemental Figure 3). The promoter of the gene encoding for Fas-ligand (Fasl), a key molecule in iNKT killing of tumor cells, <sup>26,27</sup> was accessible in all three sublineages, but higher accessibility was detected in iNKT1. Similarly, we observed higher chromatin accessibility at putative distal regulatory regions both upstream and downstream of the Fasl gene in iNKT1 cells. Accordingly, iNKT1 cells uniquely expressed Fasl transcripts at detectable levels. To assess each iNKT sublineage cytotoxic activity against target tumor cells, we incubated sorted iNKT1, iNKT2, or iNKT17 cells together with α-galactosylceramide-loaded, CD1d-transduced murine A20 lymphoma cells. iNKT1 cells displayed significantly higher cytotoxic activity against CD1dexpressing A20 cells while iNKT2 and iNKT17 cells had minimal, if any, effect (Figure 3B). We next assessed the antitumor activity of iNKT sublineages in vivo. We first used spleen-derived CD4<sup>+</sup> iNKT cells in a B-cell lymphoma model allowing the use of very low numbers of iNKT cells (supplemental Figure 4A). Low numbers of spleen-derived CD4 $^+$  iNKT cells (5 imes 10e4) had no effect when coinjected with CD1d-expressing A20 cells (2  $\times$  10e4) into Rag1<sup>-/-</sup>  $\gamma C^{-/-}$  BALB/c mice. Conversely, in a fully immune competent model of partial and transient lymphopenia induced by sublethal (4.4 Gy) irradiation, low-dose splenic CD4<sup>+</sup> iNKT cells significantly extended animal survival (supplemental Figure 4B), indicating an interplay between adoptively transferred allogeneic iNKT cells and host cells. We then used this model to assess the in vivo antitumor potential of each iNKT sublineage. Invariant NKT1 cells significantly extended animal survival in this model, whereas upon adoptive transfer of iNKT2 cells and iNKT17 cells, we observed a trend toward improved survival that did not reach statistical significance (Figure 3C). Collectively, these results indicate that

Figure 1. Identification of surface molecules for sorting of iNKT sublineages using scRNA-seq. (A) Uniform manifold approximation and projection (UMAP) plot of scRNA-seq data showing distinct clusters of iNKT cell subsets: iNKT1 (blue), iNKT2 (red), and iNKT17 (green) cells. (B) Dot-plot showing the proportion of cells (dot size) and the scaled (z score) gene expression of genes encoding for the iNKT sublineage-defining transcription factors T-Bet (Tbx21), PLZF (Zbtb16), and RORγT (Rorc). (C) Single-cell heatmap representing the 10 most highly differentially expressed genes in thymic iNKT cell subsets. Expression for each gene is scaled (z scored) across single cells. (D) Normalized counts of lcos, Pdcd1, and Cd4 RNA expression. (E) FACS-sorting strategy for isolation of iNKT sublineages based on surface molecules starting from CD19°, CD8a⁻, CD62L⁻, TCRγδ⁻, GR-1⁻, Ter119⁻, and CD24⁻ cells. Cell purity of FACS-sorted iNKT sublineages assessed by intranuclear staining for the transcription factors PLZF and RORγT. (F) Heatmap representing the 10 most highly differentially expressed genes identified in scRNA-seq analysis in bulk RNA-seq analysis performed on sorted populations. Expression for each gene is scaled (z scored) across single rows.

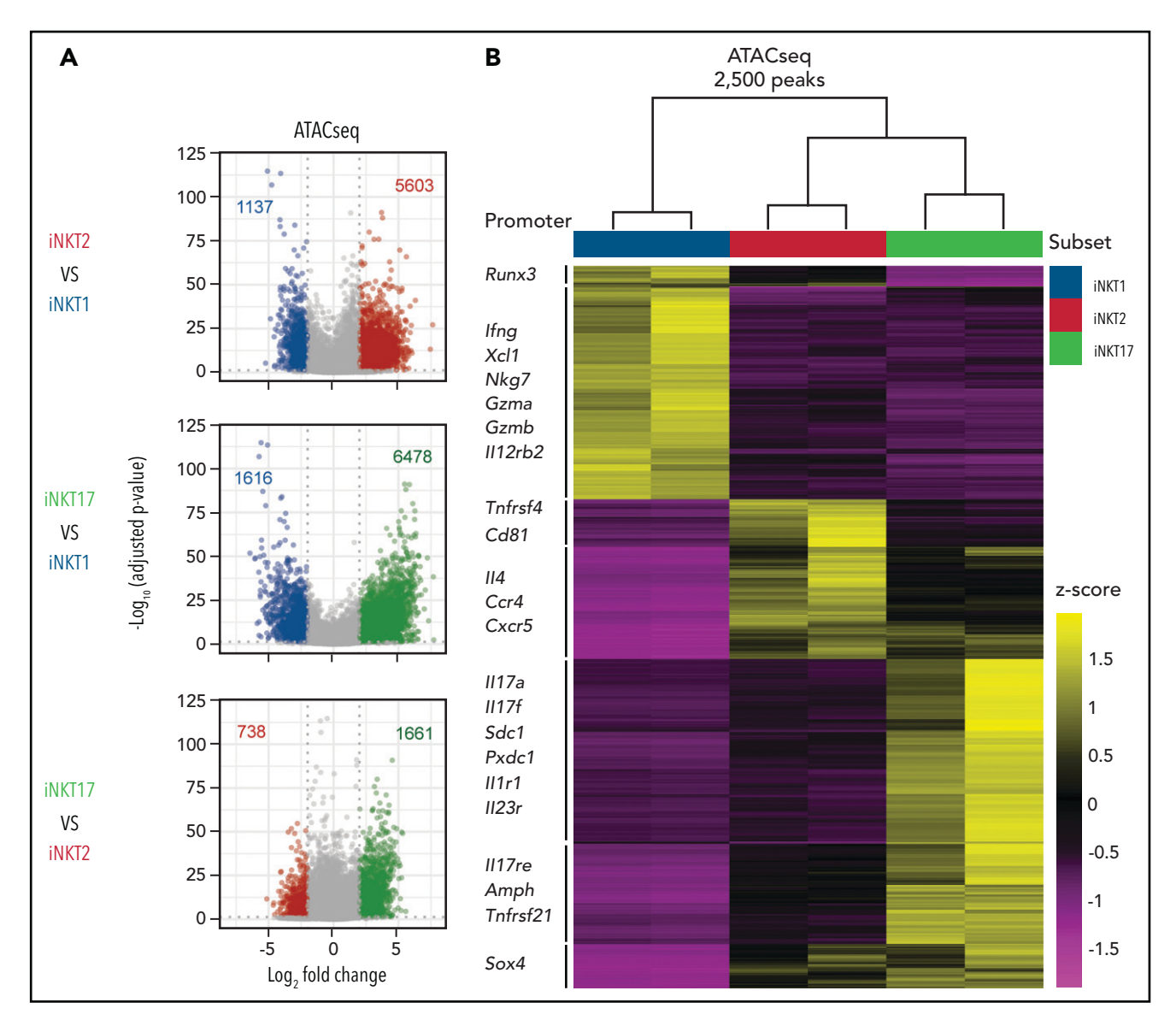


Figure 2. Analysis of the chromatin accessibility landscape in iNKT sublineages. (A) Volcano plots showing significance and  $\log_2$  fold change of ATAC-seq peaks in pairwise comparisons between iNKT sublineages. Peaks colored in gray on volcano plots indicate a  $\log_2$  fold change of -2 to +2 and/or an adjusted P value >.05. Peaks with a  $\log_2$  fold change of less than -2 or >2 and an adjusted P value <.05 are colored according to the iNKT sublineage represented (iNKT1, blue; iNKT2, red; and iNKT17, green). Vertical dotted lines on volcano plots indicate a  $\log_2$  fold change of 2; horizontal dotted line indicates an adjusted P value of .05. (B) Heatmap showing clusters for the top 2500 varying ATAC-seq peaks. Colors indicate z score of reads in each peak scaled to the mean across all iNKT cell subsets and replicates.

iNKT1 cells exert stronger antitumor activity than iNKT2 and iNKT17 cells both in vitro and in vivo.

#### iNKT sublineages display different immuneregulatory effects in vitro

We next analyzed the potential of iNKT sublineages to produce cytokines. We detected the highest *Ifng* chromatin accessibility at the promoter site (Figure 4A) and at putative distal regulatory sites (supplemental Figure 5) in iNKT1 cells. We also detected high levels of *Ifng* transcripts in iNKT1 cells, whereas this transcript was virtually undetectable in iNKT2 and iNKT17 cells. Similar levels of *Tnf* accessibility and transcripts were detectable in all 3 sublineages. Regarding the *II4* locus, encoding for interleukin-4 (IL-4), a cytokine playing a crucial role in iNKT-mediated immune-regulation, <sup>4,23</sup> iNKT2 displayed the highest chromatin accessibility at the promoter site and the highest levels of messenger RNA

transcripts. We observed at this site enrichment for binding motifs of transcription factors with highest accessibility in iNKT2, including *Gata3*, *Lef1*, and *Znf263*. iNKT17 cells partially shared with iNKT2 cells an increased accessibility at the *II4* locus compared with iNKT1 cells, which expressed the lowest levels. Conversely, chromatin accessibility and generally limited transcripts were detectable at the IL-13 (*II13*) locus in the 3 sublineages. Regarding Th17-related cytokines, both chromatin accessibility and transcription of *II17a* and *II22* genes were restricted to iNKT17 cells.

We next tested the immune-regulatory abilities of the iNKT sublineages in vitro. The 3 iNKT sublineages displayed a mild but significant inhibitory effect on CD4 Tcon proliferation (Figure 4B-C, left panels). This effect was mainly independent from cell death induction by iNKT cells, as iNKT2 cells (but not iNKT1 and iNKT17 cells) induced a slight but significant reduction in CD4

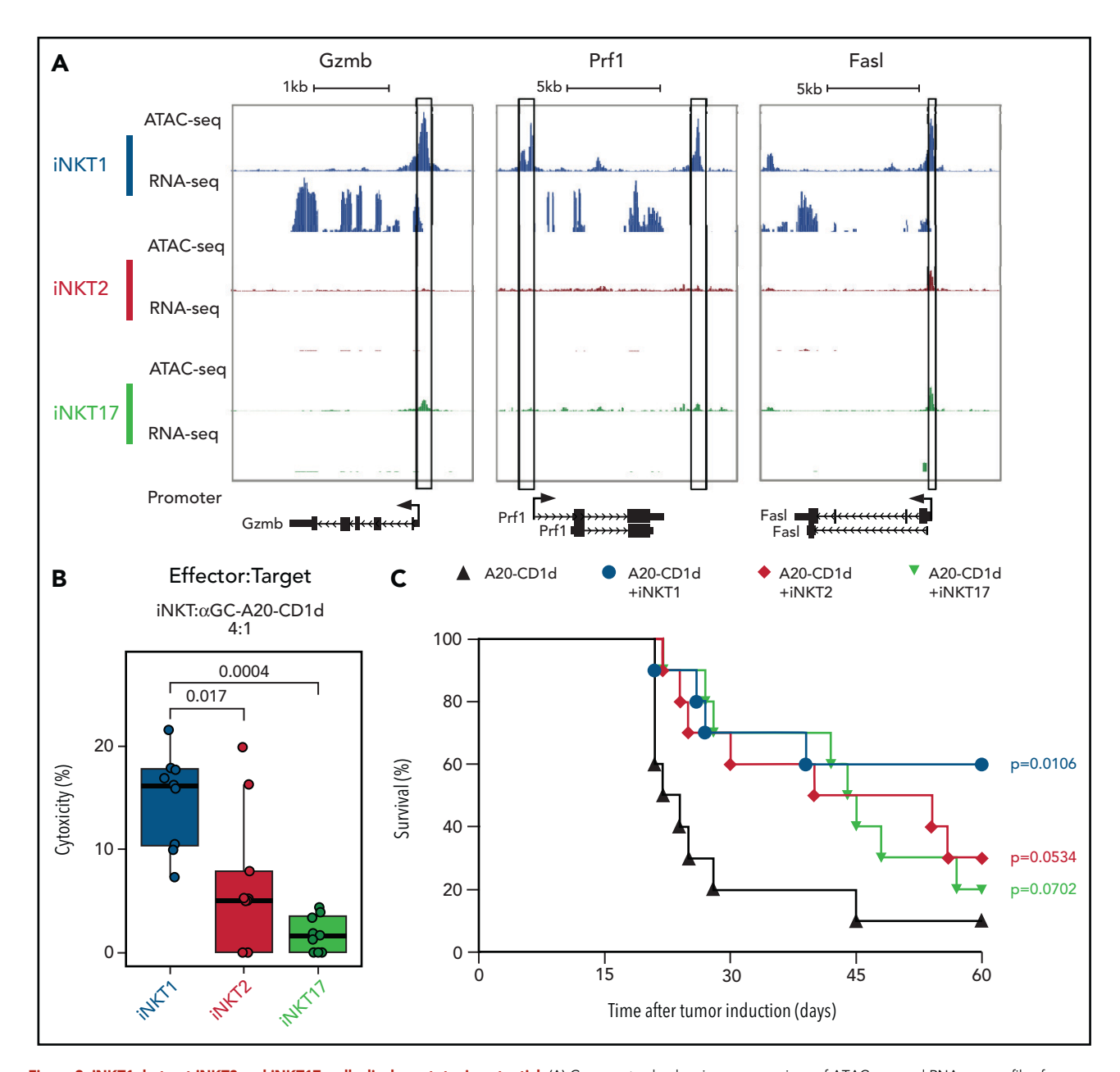


Figure 3. iNKT1, but not iNKT2 and iNKT17, cells display cytotoxic potential. (A) Genome tracks showing a comparison of ATAC-seq and RNA-seq profiles for genes encoding cytotoxic molecules in iNKT1 (blue), iNKT2 (red), and iNKT17 (green) cells. Data are merged from 2 biological replicates. Black boxes highlight differentially accessible ATAC-seq peaks. (B) In vitro cytotoxicity by iNKT sublineages against α-galactosylceramide (αGalCer)-loaded CD1d-transduced A20 lymphoma (A20-CD1d) cells after 24 hours of coculture (effector:target ratio of 4:1). Represented data are pooled from 3 independent experiments performed in triplicate. (C) Survival after A20-CD1d (2 × 10e4) cells intravenously injected into sublethally irradiated (4.4 Gy) wild-type BALB/c mice treated with iNKT cell subsets (5 × 10e4 cells; iNKT1, blue; iNKT2, red; iNKT17, green) or untreated (black). Results are pooled from 2 independent experiments with a total of 10 mice per group. Survival curves were plotted by using the Kaplan-Meier method and compared by using a log-rank test. P values are indicated when significant.

Tcon viability (supplemental Figure 6A). Interestingly, iNKT2 cells, and to a lesser extent iNKT17 cells, inhibited CD25 and ICOS upregulation on CD4 Tcon, whereas we observed no phenotypic differences in CD4 Tcon cocultured with iNKT1 cells. Similarly, coculture with iNKT2 and iNKT17 cells, but not with iNKT1 cells, induced a significant reduction in the proportion of interferon- $\gamma$  (IFN- $\gamma$ )—expressing CD4 Tcon (supplemental Figure 6B). Conversely, coculture of iNKT1 cells was associated with a slight but significant increase in tumor necrosis factor- $\alpha$  (TNF- $\alpha$ )—expressing CD4 Tcon (supplemental Figure 6B). Collectively, these results show that distinct iNKT sublineages have different cytokine production potential and immune-regulatory effects in vitro.

## iNKT2 and iNKT17 cells, but not iNKT1 cells, protect from acute murine GVHD

To assess in vivo the ability of each iNKT sublineage to protect from acute GVHD, we used a major histocompatibility complex mismatch murine model of acute GVHD, in which sorted FVB/N iNKT1, iNKT2, or iNKT17 (5  $\times$  10^4) cells were injected together with luciferase-expressing FVB/N Tcon (1  $\times$  10<sup>6</sup>; Tcon/iNKT ratio of 20:1) and TCD-BM cells (4  $\times$  10<sup>6</sup>) into lethally irradiated BALB/c mice. Compared with mice that only received Tcon, mice that received iNKT2 or iNKT17 cells displayed a significant survival benefit (Figure 5A), whereas those that received iNKT1 cells showed no survival benefit. In addition, weight and GVHD score

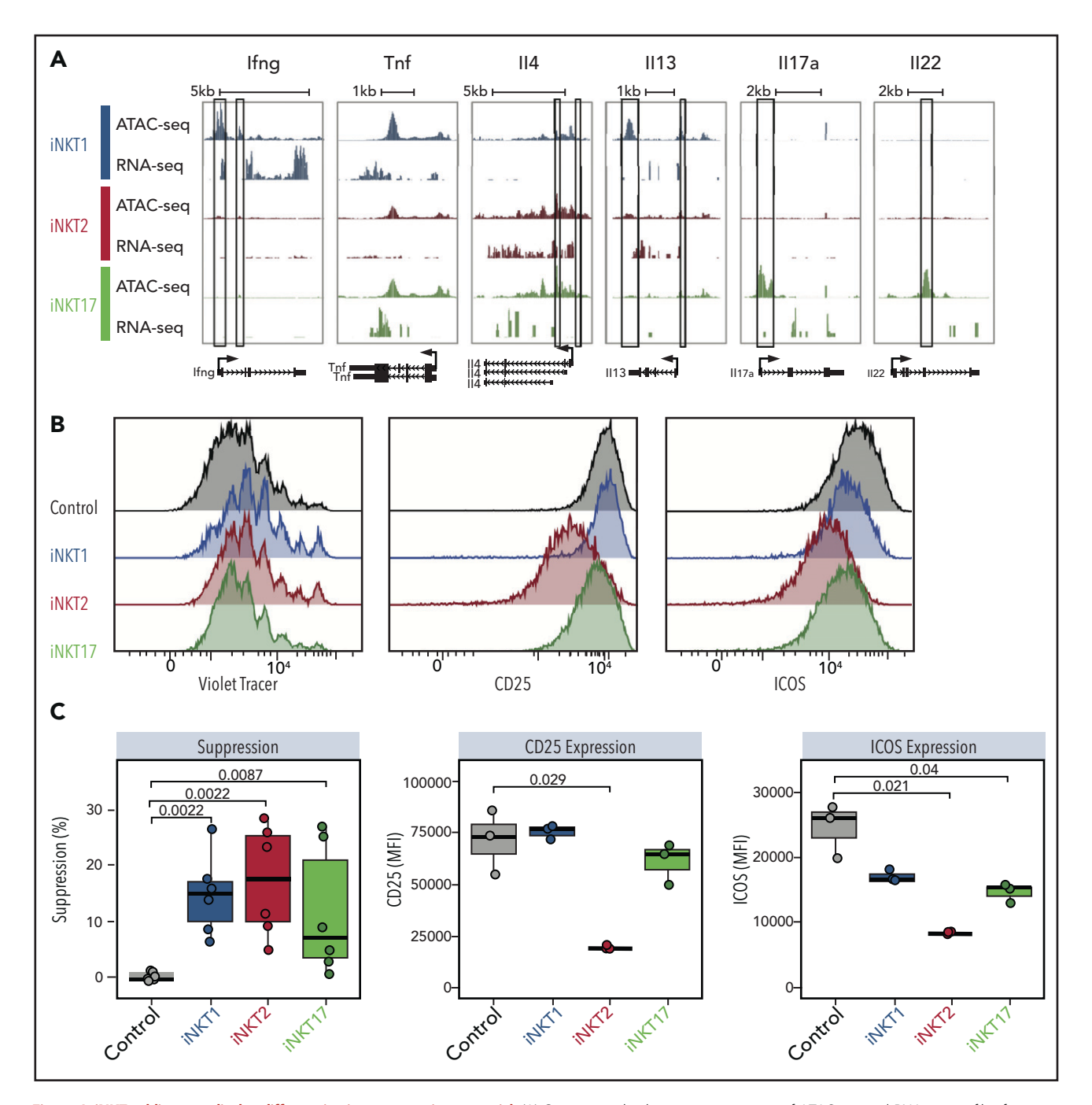


Figure 4. iNKT sublineages display different in vitro suppressive potential. (A) Genome tracks showing a comparison of ATAC-seq and RNA-seq profiles for genes encoding cytokines in iNKT1 (blue), iNKT2 (red), and iNKT17 (green) cells. Data are merged from 2 biological replicates. Black boxes highlight differentially accessible ATAC-seq peaks. In vitro suppression assay of indicated iNKT sublineages. (B-C) Representative profiles (B) and summary (C) of violet tracer dilution as well as CD25 and ICOS expression of CD4 T cells stimulated with anti-CD3/anti-CD28 activation beads in the presence or absence of FACS-sorted iNKT1, iNKT2, and iNKT17 cells. Data are representative of 2 independent experiments. MFI, mean fluorescence intensity.

were also improved in the groups that received iNKT2 or iNKT17 cells compared with mice that received iNKT1 cells. Importantly, transfer of as few as 1  $\times$  10 $^4$  (Tcon/iNKT ratio of 100:1) iNKT2 cells, but not iNKT1 or iNKT17 cells, were able to significantly suppress GVHD (Figure 5B). No significant differences were observed in cell proliferation, activation marker expression (ICOS and CD25), or cytokine production (TNF- $\alpha$  and IFN- $\gamma$ ) in CD4 and CD8 Tcon cells recovered from mice transplanted in the presence or absence of different iNKT sublineages (data not shown). Similarly, we did

not observe any significant difference in serum levels of proinflammatory cytokines, including IFN- $\gamma$ , TNF- $\alpha$ , IL-2, IL-6, and IL-18 (Figure 5C). Conversely, iNKT1 treatment was associated with a significant reduction in the Th2-like cytokines IL-5 and IL-13. These results indicate a different balance between Th1 and Th2 cytokines during GVHD depending on the iNKT sublineage administered. Collectively, these results indicate that iNKT2, and to a lesser extent iNKT17, but not iNKT1, exerted significant immune-regulatory function in a murine model of acute GVHD.

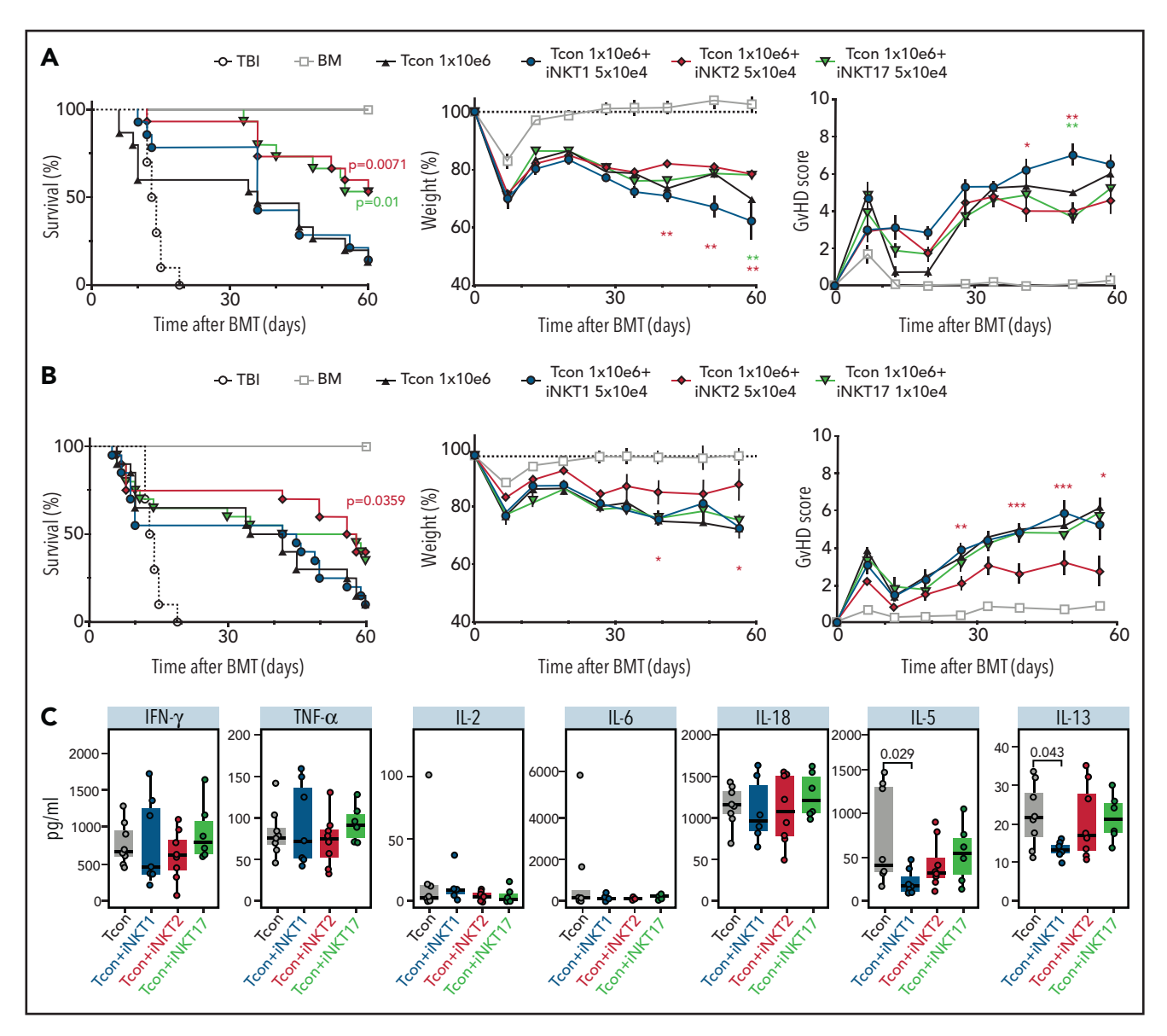


Figure 5. iNKT2 and iNKT17 cells protect from GVHD, whereas iNKT1 cells have no suppressive potential. (A) BALB/c recipient mice were irradiated with  $2 \times 4.4$  Gy, followed by transplantation of  $4 \times 10^6$  TCD-BM cells and  $1.0 \times 10^6$  Tcon from  $luc^+$  FVB/N donor mice. In addition,  $5 \times 10^4$  FACS-sorted iNKT1, iNKT2, or iNKT17 cells from FVB/N donors were transferred together with the graft. Shown are the survival curve (left graph), weight (middle graph), and GVHD score (right graph). Data are pooled from 3 independent experiments with a total of 15 mice per group (except irradiation control, n=10). Error bars indicate standard error of the mean. (B) BALB/c recipient mice were transplanted as aforementioned, and  $1 \times 10^4$  FACS-sorted iNKT1, iNKT2, or iNKT17 cells from FVB/N donors were transferred together with the graft. The survival graph is depicted on the left; the data are pooled from 3 independent experiments with a total of 20 mice per group (except total body irradiation [TBI, n=10] and BM [n=15]). For weight (middle graph) and GVHD score (right graph), data are pooled from 2 independent experiments with 10 mice per group. Error bars indicate standard error of the mean. (C) Serum Th1/Th2 cytokine levels (IFN- $\gamma$ , TNF- $\alpha$ , IL-2, IL-6, IL-18, IL-5, and IL-13) at day 7 from transplanted mice are shown (n=6-8 in each group). P values are indicated when significant. \*P < .05; \*\*P < .01; \*\*\*P < .001. BMT, BM transplantation.

# Transcriptomic analysis of Tcon during GVHD reveals differential immune-modulation induced by iNKT sublineages

To gain further insights into the functional heterogeneity of iNKT sublineages in GVHD prevention, we performed RNA-seq analysis on CD4 and CD8 Tcon recovered at day 7 after HCT with or without iNKT sublineages. Principal component analysis clearly segregated CD4 and CD8 Tcon recovered from recipients treated with iNKT cells from untreated mice along PC1 (Figure 6A-B). iNKT cell treatment was associated with higher transcription of genes encoding the immunomodulatory cytokine receptor *Il27ra*, as well as of the transcription

factor *Stat*, and reduced transcription of genes encoding *Ctla4* and *Il18r1*, as well as chemokine receptors such as *Ccc9* in CD4 Tcon and *Ccr2* in CD8 Tcon cells. Differential impact of different iNKT sublineages on Tcon transcriptome was revealed by principal component 2 that explained 14% and 21% of the variance in CD4 and CD8 Tcon, respectively. iNKT1-treated CD4 (Figure 6A,C) and CD8 (Figure 6B,D) Tcon segregated separately from iNKT2- and iNKT17-treated cells that were partially overlapping, especially for CD8 T cells. Gene Set Enrichment Analysis for Hallmark gene sets revealed that iNKT2 and iNKT17 cells, but not iNKT1 cells, induced a significant reduction in G2M checkpoint and mitotic spindle gene

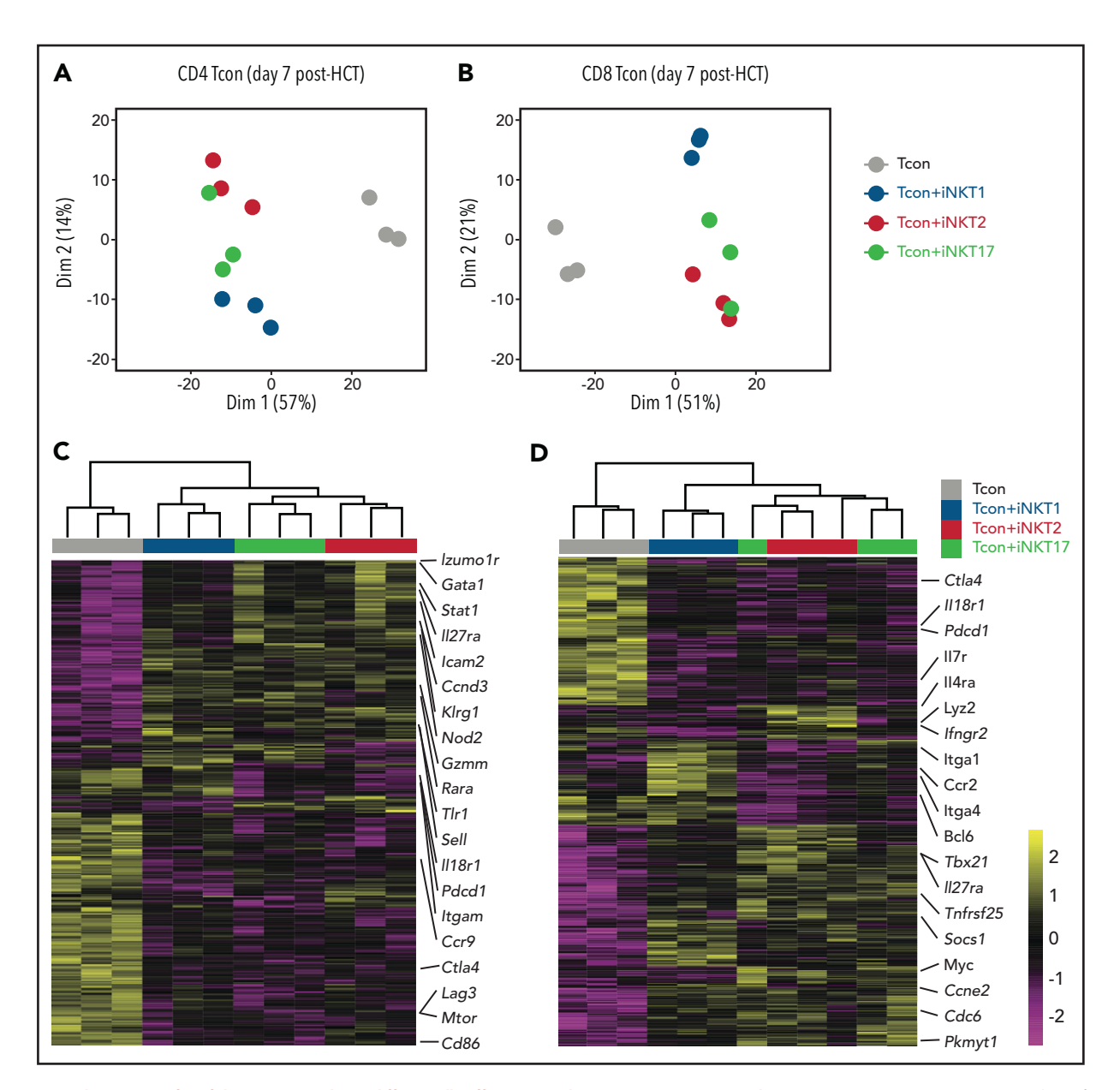


Figure 6. Adoptive transfer of distinct iNKT subsets differentially affect CD4 and CD8 Tcon transcriptome during murine acute GVHD. RNA-seq analysis of CD4 (A,C) and CD8 (B,D) Tcon recovered at day 7 post-HCT from animals treated with the indicated iNKT sublineages (untreated, gray; iNKT1, blue; iNKT2, red; iNKT17, green). (A-B) Principal component analysis of transcriptome based on the top 500 differentially expressed genes across all samples. (C-D) Heatmap and hierarchical clustering based on the 500 most highly differentially expressed genes across all samples. Immune-related genes are highlighted. Expression for each gene is scaled (z scored) across single rows. Analysis was performed on 3 biological replicates from 2 independent experiments.

sets in CD4 Tcon, whereas only iNKT2 cells suppressed the mitotic spindle gene sets in CD8 Tcon (supplemental Figure 7A-B).

Interestingly, iNKT1 cells, but not iNKT2 or iNKT17 cells, induced a downregulation of genes of the oxidative phosphorylation set both in CD4 and CD8 Tcon. iNKT2 and iNKT17 cells induced further upregulation of *Il27ra* and further downregulation of *Il18r1* in Tcon compared with Tcon treated with iNKT1 cells (Figure 6C-D). In addition, iNKT2 and iNKT17 cells induced the downregulation of genes encoding cytokine receptors and integrins involved in Tcon migration to target tissues, including *Itgam* in CD4 and Ccr2, and *Itga4* and *Itga1* in CD8 Tcon. Importantly, iNKT sublineage administration did not prevent the upregulation of gene sets involved in T-cell effector responses, namely Th1 differentiation of CD4 T cells (supplemental Figure 7C-D) and cytotoxicity of CD8

T cells (supplemental Figure 7E-F). Collectively, these results indicate that distinct iNKT sublineages differentially modulate Tcon transcriptome.

## iNKT2 and iNKT17 cells, but not iNKT1 cells, reduce intestinal tissue damage during murine acute GVHD

We next aimed to confirm at the protein level the differential modulation of molecules by different iNKT sublineages. We first focused our attention on the gene encoding for IL-18R $\alpha$ , a molecule essential for IL-18 signaling and for sustaining IFN- $\gamma$  transcription crucial in GVHD.<sup>28</sup> iNKT2 and iNKT17 cells, but not iNKT1 cells, significantly suppressed IL-18R $\alpha$  expression at CD8 and even more at the CD4 Tcon cell surface (Figure 7A). Next, we analyzed the surface expression of CD49d or integrin  $\alpha$ 4, encoded by

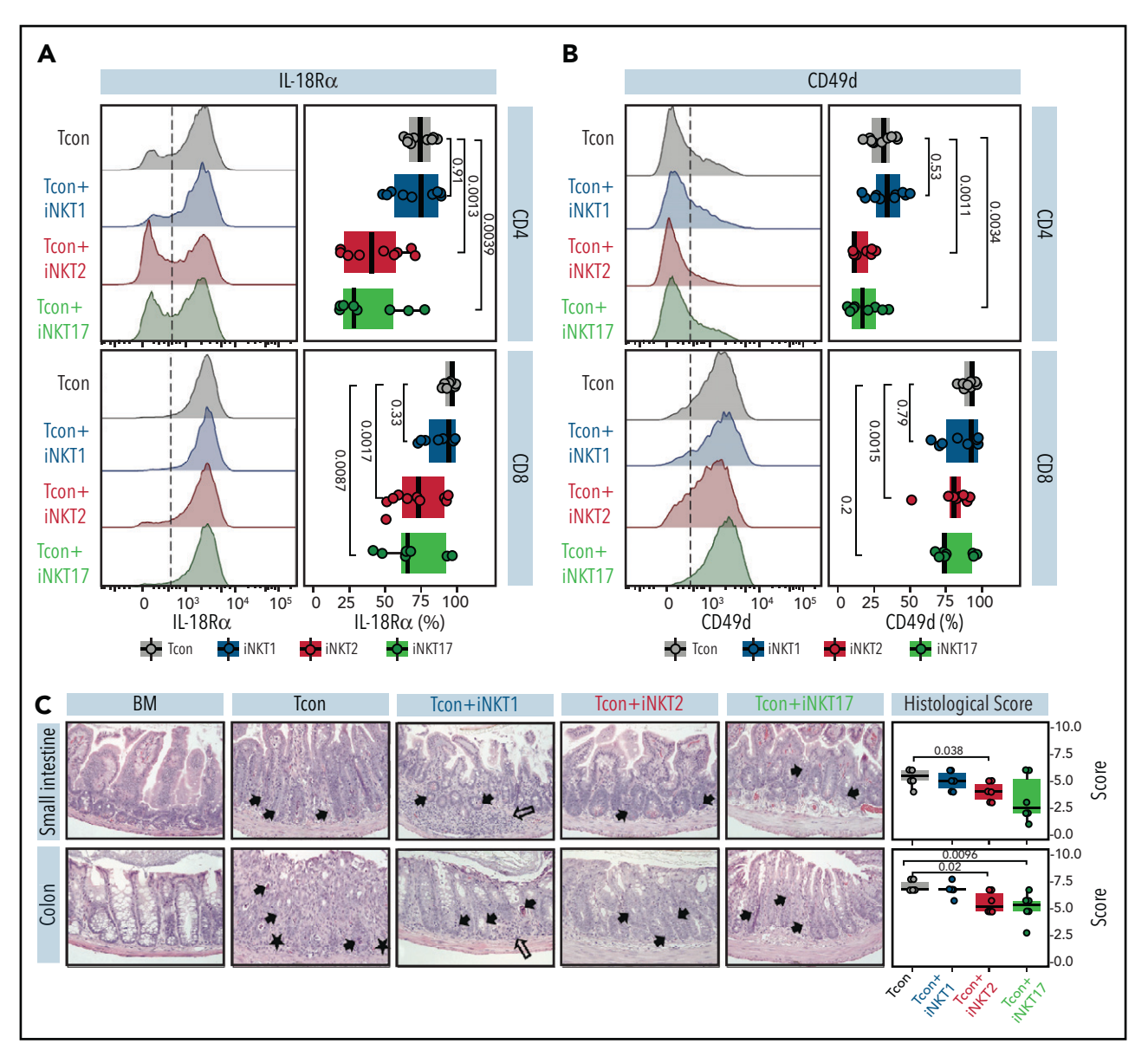


Figure 7. iNKT2 and iNKT17 cells inhibit IL-18R $\alpha$  and CD49d expression and prevent tissue damage during murine acute GVHD. IL-18R $\alpha$  (A) and CD49d (B) expression at the surface of CD4 (upper panels) and CD8 (lower panels) Tcon recovered at day 7 after HCT from spleen of mice treated with different iNKT sublineages (untreated, gray; iNKT1, blue; iNKT2, red; iNKT17, green). Representative FACS histograms (left panels) and summary bar plots (right panels) are shown. Data are pooled from 2 independent experiments with 3 to 5 mice per group. (C) Representative photomicrographs of hematoxylin and eosin–stained sections of small intestine and colon ( $\times$ 200) collected 7 days after transplantation from indicated groups. GVHD tissue damage manifests as inflammation (open arrow), crypt apoptosis (solid arrow), and crypt loss (solid arrow). Bata are pooled from 2 independent experiments with a total of 6 mice per group. P values are indicated when significant.

the *Itgam* gene and necessary for the constitution of the  $\alpha 4\beta 1$  integrin, recently reported to play a crucial role in T-cell migration to GVHD-target tissues. <sup>29</sup> As shown in Figure 7B, iNKT2 and iNKT17 cells, but not iNKT1 cells, induced a significant downregulation in CD49d expression in CD4 Tcon, with iNKT2 cells also having a significant impact on CD49d levels on CD8 Tcon cells.

To assess whether the iNKT17 cell immune-modulation observed in mice receiving iNKT2 and iNKT17 cells was associated with reduced damage at GVHD target sites, we performed a histopathologic analysis of the small intestine and colon at day 7 after transplantation. We found that recipients receiving iNKT2 and to a lesser extent iNKT17 cells displayed reduced composite GVHD pathology scores compared with recipients of conventional T cells

alone, whereas iNKT1 cells did not display any significant effect (Figure 7C). Collectively, these results indicate that iNKT2 and iNKT17 cells, but not iNKT1 cells, suppress pathways involved in GVHD pathophysiology, including IL-18R and CD49d expression, and reduce intestinal tissue damage in a murine model of acute GVHD.

#### Discussion

iNKT cells are a cell subset with pleiotropic functions ranging from cytotoxic effects to immune-regulatory activity. The demonstration of the existence of iNKT sublineages expressing distinct transcription factors and cytokines <sup>12</sup> provided a potential explanation for iNKT cell pleiotropic activity. However, our knowledge of the

functions of iNKT sublineages has been limited to observational studies, 30-33 and formal demonstration of their distinct functional roles has been missing. The current study shows, for the first time, that distinct iNKT cell sublineages display differential effector and immune-regulatory functions.

Our analyses of the potential to produce cytotoxic molecules, as well as the in vitro and in vivo tumor models, point to a preferential cytotoxic activity by iNKT1 cells compared with iNKT2 and iNKT17 cells. These results are in agreement with previous studies reporting the unique ability of iNKT1 cells to produce granzyme B upon short-term stimulation.<sup>34</sup> Moreover, after establishing an in vivo B-cell lymphoma model allowing for the analysis of the antitumor immunomodulatory effect of iNKT cells, we showed that iNKT1 cells display also the highest antitumor potential in vivo (Figure 3C).

iNKT cells have been reported to regulate GVHD through IL-4 production<sup>4,35</sup> and cytotoxic activity against recipient antigenpresenting cells.<sup>8</sup> We found that iNKT2 and iNKT17 cells, but not iNKT1 cells, are able to mitigate GVHD induced by allogeneic Tcon. According to our genomic analysis, iNKT2, and to a lesser extent iNKT17, displayed higher chromatin accessibility at the *II4* promoter site and detectable messenger RNA transcripts ex vivo, pointing to both cell subsets as potential IL-4 producers. These data are in agreement with the report from Georgiev et al,<sup>34</sup> which showed that iNKT2 and iNKT17 produce IL-4 at the protein level.

We can therefore speculate that IL-4 production ability by iNKT2 and iNKT17 is a key mechanism in their GVHD suppressive activity, although this hypothesis could not be experimentally tested as IL-4 signaling is necessary for physiological development of iNKT cell sublineages (Jung-Hyun Park, National Cancer Institute, oral presentation, 28 September 2016), and IL-4<sup>-/-</sup> cells therefore cannot be used for this purpose. Conversely, despite their higher cytotoxic potential, iNKT1 cells did not display any significant impact on GVHD progression. This scenario suggests that dendritic cell cytotoxicity might not be a major mechanism of suppression in our mouse model, although the paucity of dendritic cells after transplantation did not allow us to experimentally assess this hypothesis.

Our transcriptomic analysis points to some gene sets modulated by all iNKT subsets, including upregulation of the immunomodulatory cytokine receptor Il27ra as well as downregulation of Ctla4. At the same time, the analysis reveals the preferential modulation of cell cycle genes by iNKT2 and iNKT17 cells. Moreover, some pathways important for GVHD pathogenesis such as the IL-18/ IL-18R $\alpha$  axis, necessary for IFN- $\gamma$  transcription induction and maintenance in GVHD,  $^{28}$  and CD49d/integrin  $\alpha 4$  expression, crucial for T-cell migration to GVHD-target tissues,<sup>29</sup> were preferentially modulated by the administration of iNKT2 and iNKT17 cells. Interestingly, iNKT1 cells seemed to downregulate Tcon gene sets involved in oxidative phosphorylation, suggesting the induction of a metabolic switch toward glycolysis, a proinflammatory metabolic state in GVHD. 36,37 Collectively, our data confirm at the transcriptomic level that distinct iNKT sublineages differentially affect Tcon during GVHD and increase our knowledge about mechanisms involved in GVHD prevention by iNKT cells.

Finally, differences in iNKT sublineage tissue migration might contribute to the differences in GVHD suppression. It is well established that iNKT sublineages have tissue-specific distribution at

steady state, <sup>14</sup> and whether this might influence their immunotherapeutic potential remains to be investigated.

Recently, Erkers et al<sup>38</sup> reported an extensive characterization of human iNKT heterogeneity and identified a CD4<sup>-</sup>CD94<sup>+</sup> population with iNKT1-like properties and a CD4<sup>+</sup> population producing higher levels of IL-4. Due to the paucity of iNKT cells in human peripheral blood, current clinical trials using iNKT cells involve in vitro expansion protocols (#NCT03605953). The demonstration that iNKT2 and to a lesser extent iNKT17 cells, but not iNKT1 cells, protect from murine GVHD suggest that in vitro expansion protocols allowing the preservation or acquisition of the IL-4-producing, Th2-like phenotype should be preferred for GVHD suppression over protocols inducing a more cytotoxic cell profile that would be more suitable for antitumor applications. We provide the first complete chromatin accessibility atlas of all 3 iNKT sublineages associated with paired transcriptomic analysis. We believe that this transcriptomic and epigenomic atlas of murine iNKT sublineages will be a valuable resource to guide the development of iNKT cellular products for immunotherapy.

In summary, this study provides a formal demonstration of differential functions exerted by different iNKT sublineages. Our findings have important implications to orient clinical translation of iNKT-based therapies.

#### Acknowledgments

The authors thank Dhananjay Wagh, Xuhuai Ji, and John Coller at the Stanford Functional Genomics Facility for their excellent technical assistance in the genomics analysis. In addition, the authors acknowledge Mitchell Kronenberg for the kind gift of the A20-CD1d cell line.

This work was supported by grants from the National Institutes of Health (NIH) (National Heart, Lung, and Blood Institute, P01 HL075462, and the National Cancer Institute, R01 CA23158201, R.S.N.; National Human Genome Research Institute, RM1-HG007735, H.Y.C.), the German Cancer Aid (Mildred Scheel Postdoctoral Fellowship, K.M.-B. and J.K.L.), the Geneva University Hospitals Fellowship (F.S.), the Swiss Cancer League (BIL KLS 3806-02-2016, F.S.), the Fondation de Bienfaisance Valeria Rossi di Montelera (Eugenio Litta Fellowship, F.S.), the American Society for Blood and Marrow Transplantation (New Investigator Award 2018, F.S.), the Dubois-Ferrière-Dinu-Lipatti Foundation, F.S., the National Science Foundation (Graduate Research Fellowship DGE-114747, J.V.R.), the American Association for Cancer Research (Millennium Fellowship in Lymphoma Research 15-40-38-ALVA, M.A.), the St. Baldrick's Fellowship with generous support from the Rays of Hope Hero Fund (M.M.), and the Parker Institute for Cancer Immunotherapy (H.Y.C.). H.Y.C. is an Investigator of the Howard Hughes Medical Institute. Flow cytometry analysis for this project was conducted on instruments in the Stanford Shared FACS Facility purchased by using an NIH S10 Shared Instrumentation Grant (S10RR027431-01). Sequencing was performed on instruments in the Stanford Functional Genomics Facility, including the Illumina HiSeq 4000 purchased by using an NIH S10 Shared Instrumentation Grant (S10OD018220).

#### Authorship

Contribution: F.S., K.M.-B., T.H., and R.S.N. conceived and designed the study; K.M.-B., J.K.L., F.S., T.H., T.L.R., A.S.W., F.M.F., U.M.L., P.-Y.L., M.M., and J.B. performed the experiments; F.S., K.M.B., J.K.L., F.M.F., J.V.R., K.E.Y., A.S.W., N.K., and H.Y.C. analyzed the data; F.S., K.M.-B., J.K.L., T.H., F.M.F., J.V.R., K.E.Y., A.S.B., H.Y.C., and R.S.N. contributed to the interpretation of results; F.S., K.M.-B., and R.S.N. wrote the manuscript; F.S. and R.S.N. supervised the research; and all authors read and approved the submitted version of the manuscript.

Conflict-of-interest disclosure: H.Y.C. is a cofounder of Accent Therapeutics and Boundless Bio; and is an advisor to 10x Genomics, Arsenal

Biosciences, and Spring Discovery. The remaining authors declare no competing financial interests.

ORCID profiles: K.M.-B., 0000-0003-1788-2807; J.K.L., 0000-0003-4311-0317; T.L.R., 0000-0002-0696-7197; K.E.Y., 0000-0001-6807-950X; A.S.W., 0000-0002-6451-6140; M.A., 0000-0002-5969-9181; A.S.B., 0000-0001-8099-2975; F.S., 0000-0002-0399-689X.

Correspondence: Federico Simonetta and Robert S. Negrin, Division of Blood and Marrow Transplantation, Department of Medicine, Stanford University School of Medicine, Center for Clinical Sciences Research Building, 269 W. Campus Dr, Stanford, CA 94305; e-mails: federico.simonetta@ unige.ch or negrs@stanford.edu.

#### **Footnotes**

Submitted 19 January 2021; accepted 22 April 2021; prepublished online on Blood First Edition 25 May 2021. DOI 10.1182/blood.2021010887.

\*K.M.-B. and J.K.L. are joint first authors.

<sup>†</sup>F.S. and R.S.N. are joint senior authors.

Relevant data can be found in the Gene Expression Omnibus database (accession number GSE172169; https://www.ncbi.nlm.nih.gov/geo/ query/acc.cqi?acc=GSE172169).

The online version of this article contains a data supplement.

There is a Blood Commentary on this article in this issue.

The publication costs of this article were defrayed in part by page charge payment. Therefore, and solely to indicate this fact, this article is hereby marked "advertisement" in accordance with 18 USC section

#### **REFERENCES**

- 1. Zeiser R, Blazar BR. Acute graft-versus-host disease—biologic process, prevention, and therapy. N Engl J Med. 2017;377(22):2167-
- 2. Matsuda JL, Mallevaey T, Scott-Browne J, Gapin L. CD1d-restricted iNKT cells, the 'Swiss-Army knife' of the immune system. Curr Opin Immunol. 2008;20(3):358-368.
- 3. Crosby CM, Kronenberg M. Tissue-specific functions of invariant natural killer T cells. Nat Rev Immunol. 2018;18(9):559-574.
- 4. Leveson-Gower DB, Olson JA, Sega EI, et al. Low doses of natural killer T cells provide protection from acute graft-versus-host disease via an IL-4-dependent mechanism. Blood. 2011;117(11):3220-3229.
- 5. Schneidawind D, Pierini A, Alvarez M, et al. CD4+ invariant natural killer T cells protect from murine GVHD lethality through expansion of donor CD4+CD25+FoxP3+ regulatory T cells. Blood. 2014;124(22):3320-
- 6. Schneidawind D, Baker J, Pierini A, et al. Third-party CD4+ invariant natural killer T cells protect from murine GVHD lethality. Blood. 2015;125(22):3491-3500.
- 7. Du J, Paz K, Thangavelu G, et al. Invariant natural killer T cells ameliorate murine chronic GVHD by expanding donor regulatory T cells. Blood. 2017;129(23):3121-3125.
- 8. Coman T, Rossignol J, D'Aveni M, et al. Human CD4- invariant NKT lymphocytes regulate graft versus host disease. Oncolmmunology. 2018;7(11):e1470735.
- 9. Rubio M-T, Moreira-Teixeira L, Bachy E, et al. Early posttransplantation donor-derived invariant natural killer T-cell recovery predicts the occurrence of acute graft-versus-host disease and overall survival. Blood. 2012; 120(10):2144-2154.
- 10. Rubio M-T, Bouillié M, Bouazza N, et al. Pretransplant donor CD4<sup>-</sup> invariant NKT cell expansion capacity predicts the occurrence of acute graft-versus-host disease. Leukemia. 2017;31(4):903-912.
- 11. Mavers M, Maas-Bauer K, Negrin RS. Invariant natural killer T cells as suppressors of

- graft-versus-host disease in allogeneic hematopoietic stem cell transplantation. Front Immunol. 2017;8:900.
- 12. Lee YJ, Holzapfel KL, Zhu J, Jameson SC, Hogquist KA. Steady-state production of IL-4 modulates immunity in mouse strains and is determined by lineage diversity of iNKT cells [published correction appears in Nat Immunol. 2014;15(3):305]. Nat Immunol. 2013; 14(11):1146-1154.
- 13. Brennan PJ, Brigl M, Brenner MB. Invariant natural killer T cells: an innate activation scheme linked to diverse effector functions. Nat Rev Immunol. 2013;13(2):101-117.
- 14. Lee YJ, Wang H, Starrett GJ, Phuong V, Jameson SC, Hogquist KA. Tissue-specific distribution of iNKT cells impacts their cytokine response. Immunity. 2015;43(3):
- 15. Engel I, Seumois G, Chavez L, et al. Innate-like functions of natural killer T cell subsets result from highly divergent gene programs [published correction appears in Nat Immunol. 2019;20(12):1700]. Nat Immunol. 2016:17(6):728-739.
- 16. Wang H, Hogquist KA. How lipid-specific T cells become effectors: the differentiation of iNKT subsets. Front Immunol. 2018;9:1450.
- 17. Harsha Krovi S, Zhang J, Michaels-Foster MJ, et al. Thymic iNKT single cell analyses unmask the common developmental program of mouse innate T cells. Nat Commun. 2020;
- 18. Lee M, Lee E, Han SK, et al. Single-cell RNA sequencing identifies shared differentiation paths of mouse thymic innate T cells. Nat
- 19. Baranek T, Lebrigand K, de Amat Herbozo C, et al. High dimensional single-cell analysis reveals iNKT cell developmental trajectories and effector fate decision. Cell Rep. 2020; 32(10):108116.
- 20. Lee YJ, Starrett GJ, Lee ST, et al. Lineagespecific effector signatures of invariant NKT cells are shared amongst  $\gamma\delta$  T, innate lymphoid, and Th cells. J Immunol. 2016; 197(4):1460-1470.

46

- 21. Papadogianni G, Ravens I, Dittrich-Breiholz O, Bernhardt G, Georgiev H. Impact of aging on the phenotype of invariant natural killer T cells in mouse thymus. Front Immunol. 2020; 11:575764.
- 22. Cao Y-A, Wagers AJ, Beilhack A, et al. Shifting foci of hematopoiesis during reconstitution from single stem cells. Proc Natl Acad Sci U S A. 2004;101(1):221-226.
- 23. Cooke KR, Kobzik L, Martin TR, Brewer J, Delmonte J, Jr., Crawford JM, et al. An experimental model of idiopathic pneumonia syndrome after bone marrow transplantation: I. The roles of minor H antigens and endotoxin. Blood. 1996;88(8):3230-3239.
- 24. Lerner KG, Kao GF, Storb R, Buckner CD, Clift RA, Thomas ED. Histopathology of graft-vs.host reaction (GvHR) in human recipients of marrow from HL-A-matched sibling donors. Transplant Proc. 1974;6(4):367-371.
- 25. Tuttle KD, Krovi SH, Zhang J, et al. TCR signal strength controls thymic differentiation of iNKT cell subsets. Nat Commun. 2018;9(1): 2650.
- 26. Bassiri H, Das R, Guan P, et al. iNKT cell cytotoxic responses control T-lymphoma growth in vitro and in vivo. Cancer Immunol Res. 2014;2(1):59-69.
- 27. Wingender G, Krebs P, Beutler B, Kronenberg M. Antigen-specific cytotoxicity by invariant NKT cells in vivo is CD95/CD178-dependent and is correlated with antigenic potency. J Immunol. 2010;185(5):2721-2729.
- 28. Reichenbach DK, Schwarze V, Matta BM, et al. The IL-33/ST2 axis augments effector T-cell responses during acute GVHD [published correction appears in Blood. 2016;128(9)1311]. Blood. 2015;125(20):3183-
- 29. Alahmari B, Cooper ML, Vij K, et al. Selective targeting of  $\alpha 4\beta 1$  integrin attenuates murine graft versus host disease. Leukemia. 2020; 34(11):3100-3104.
- 30. Simoni Y, Gautron A-S, Beaudoin L, et al. NOD mice contain an elevated frequency of iNKT17 cells that exacerbate diabetes. Fur. J. Immunol. 2011;41(12):3574-3585.

- Li S, Joseph C, Becourt C, et al. Potential role of IL-17-producing iNKT cells in type 1 diabetes. PLoS One. 2014;9(4):e96151.
- Zhao M, Svensson MND, Venken K, et al. Altered thymic differentiation and modulation of arthritis by invariant NKT cells expressing mutant ZAP70. Nat Commun. 2018;9(1):2627.
- Tumes D, Hirahara K, Papadopoulos M, et al. Ezh2 controls development of natural killer T cells, which cause spontaneous asthma-like pathology. J Allergy Clin Immunol. 2019; 144(2):549-560.e10.
- 34. Georgiev H, Ravens I, Benarafa C, Förster R, Bernhardt G. Distinct gene expression patterns correlate with developmental and functional traits of iNKT subsets. *Nat Commun.* 2016;7(1):13116.
- 35. Pillai AB, George TI, Dutt S, Strober S. Host natural killer T cells induce an interleukin-4-dependent expansion of donor CD4+CD25+Foxp3+ T regulatory cells that protects against graft-versus-host disease. *Blood*. 2009;113(18):4458-4467.
- 36. Hippen KL, Aguilar EG, Rhee SY, Bolivar-Wagers S, Blazar BR. Distinct regulatory and

- effector T cell metabolic demands during graft-versus-host disease. *Trends Immunol.* 2020;41(1):77-91.
- 37. Kumari R, Palaniyandi S, Hildebrandt GC. Metabolic reprogramming—a new era how to prevent and treat graft versus host disease after allogeneic hematopoietic stem cell transplantation has begun. Front Pharmacol. 2020;11:588449.
- 38. Erkers T, Xie BJ, Kenyon LJ, et al. Highparametric evaluation of human invariant natural killer T cells to delineate heterogeneity in allo- and autoimmunity. *Blood*. 2020;135(11):814-825.

#### 3.3. Publication 3

<u>Simonetta F</u>, Lohmeyer JK, Hirai T, Maas-Bauer K, Alvarez M, Wenokur AS, Baker J, Aalipour A, Ji X, Haile S, Mackall CL, Negrin RS. Allogeneic CAR-invariant Natural Killer T Cells Exert Potent Antitumor Effects Through Host CD8 T Cell Cross-Priming. *Clin Cancer Res. 2021*; 27(21):6054-6064.

Given their potent antitumor effect and their lack of GvHD-induction potential, iNKT cells appear as a very promising cell population for the development of allogeneic cellular therapies to be used off-the-shelf. Several groups already reported the preclinical use of human iNKT cells engineered with a chimeric antigen receptor (CAR) to target several types of malignancies (Heczey et al., 2014; Rotolo et al., 2018; Heczey et al., 2020). In this work, we generated for the first time murine CAR iNKT cells to be employed in immunocompetent models of cancer. This allowed us to investigate the interplay between CAR iNKT cells and the host endogenous immune system. After showing that CD19-CAR iNKT cells were able, similarly to conventional CAR T cells, to exert a direct antitumor effect against CD19expressing lymphoma cells, we showed for the first time that allogeneic CAR iNKT cells display a potent immune-adjuvant effect toward the host immune system (Figure 6). In particular, CAR iNKT cells were able to induce activation of host CD8 T cells through their cross-priming. We showed that CAR iNKT cell treatment had an impact on host CD8 T cell transcriptome and TCR repertoire. More importantly, despite their short persistence in vivo, allogeneic CAR iNKT cells lead to the development of an antitumor immunological memory that lasted longer than the physical persistence that could be transferred to other animals in a sequential adoptive transfer experiment. Our data were published in the same period of a series of articles reporting the contribution of the epitope spreading phenomenon in conventional CAR T cell effect (Conde et al., 2021; Dhodapkar et al., 2022). Interestingly, our direct comparison between CAR iNKT cells and conventional CAR T cells suggest that CAR iNKT cells might be significantly stronger than conventional CAR T in exerting such effect in our model. If our data will be confirmed in humans, these finding might have a significant impact in the design of new, allogeneic CAR-based therapies.

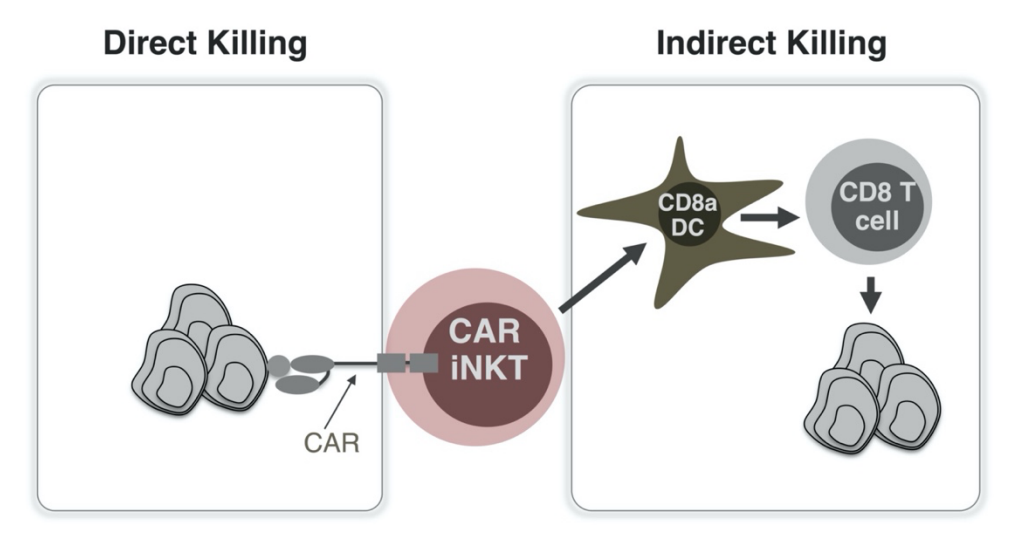


Figure 6. Graphical representation of the direct and indirect antitumor effect of CAR iNKT cells. Personal material, unpublished.

# Allogeneic CAR Invariant Natural Killer T Cells Exert Potent Antitumor Effects through Host CD8 T-Cell Cross-Priming



Federico Simonetta<sup>1,2</sup>, Juliane K. Lohmeyer<sup>1</sup>, Toshihito Hirai<sup>1</sup>, Kristina Maas-Bauer<sup>1</sup>, Maite Alvarez<sup>1</sup>, Arielle S. Wenokur<sup>1</sup>, Jeanette Baker<sup>1</sup>, Amin Aalipour<sup>3,4</sup>, Xuhuai Ji<sup>5</sup>, Samuel Haile<sup>6</sup>, Crystal L. Mackall<sup>6,7,8</sup>, and Robert S. Negrin<sup>1</sup>

#### **ABSTRACT**

**Purpose:** The development of allogeneic chimeric antigen receptor (CAR) T-cell therapies for off-the-shelf use is a major goal that faces two main immunologic challenges, namely the risk of graft-versus-host disease (GvHD) induction by the transferred cells and the rejection by the host immune system limiting their persistence. In this work we assessed the direct and indirect antitumor effect of allogeneic CAR-engineered invariant natural killer T (iNKT) cells, a cell population without GvHD-induction potential that displays immunomodulatory properties.

**Experimental Design:** After assessing murine CAR iNKT cells direct antitumor effects *in vitro* and *in vivo*, we employed an immunocompetent mouse model of B-cell lymphoma to assess the

interaction between allogeneic CAR iNKT cells and endogenous immune cells.

**Results:** We demonstrate that allogeneic CAR iNKT cells exerted potent direct and indirect antitumor activity when administered across major MHC barriers by inducing tumor-specific antitumor immunity through host CD8 T-cell cross-priming.

**Conclusions:** In addition to their known direct cytotoxic effect, allogeneic CAR iNKT cells induce host CD8 T-cell antitumor responses, resulting in a potent antitumor effect lasting longer than the physical persistence of the allogeneic cells. The utilization of off-the-shelf allogeneic CAR iNKT cells could meet significant unmet needs in the clinic.

#### Introduction

Chimeric antigen receptor (CAR) T cells have resulted in dramatic and effective therapy for a range of relapsed and refractory malignancies. The use of autologous cells for the generation of CAR T cells represents a significant limitation to their widespread use for a number of significant reasons, including the impact of disease and treatment on the T-cell product, costs of individual production, and the time required to produce the cellular product for patients with often rapidly progressive disease. The development of universal allogeneic CAR T cells could address these challenges yet faces two major limitations,

<sup>1</sup>Division of Blood and Marrow Transplantation, Department of Medicine, Stanford University School of Medicine, Stanford, California. <sup>2</sup>Division of Hematology, Department of Oncology, Geneva University Hospitals and Translational Research Centre in Onco-Haematology, Faculty of Medicine, University of Geneva, Geneva, Switzerland. <sup>3</sup>Department of Bioengineering, Stanford University School of Medicine, Stanford, California. <sup>4</sup>Molecular Imaging Program at Stanford, Stanford University School of Medicine, Stanford, California. <sup>5</sup>Human Immune Monitoring Center, Stanford University School of Medicine, Stanford, California. <sup>6</sup>Department of Pediatrics, Stanford University, Stanford, California. <sup>7</sup>Stanford Cancer Institute, Stanford University, Stanford, California. <sup>8</sup>Parker Institute for Cancer Immunotherapy, San Francisco, California.

**Note:** Supplementary data for this article are available at Clinical Cancer Research Online (http://clincancerres.aacrjournals.org/).

**Corresponding Author:** Robert S. Negrin, Medicine/BBMT, Stanford University, Stanford, CA 94305. E-mail: negrs@stanford.edu

Clin Cancer Res 2021;27:6054-64

doi: 10.1158/1078-0432.CCR-21-1329

This open access article is distributed under Creative Commons Attribution-NonCommercial-NoDerivatives License 4.0 International (CC BY-NC-ND).

 $@2021\, The\ Authors; Published\ by\ the\ American\ Association\ for\ Cancer\ Research$ 

namely the risk of graft-versus-host disease (GvHD) induction by the allogeneic cells that recognize host tissues and the rejection of the CAR modified cells by the host immune system. Ablation of the T-cell receptor (TCR; refs. 1–4) or use of non–MHC-restricted innate lymphocytes have been attempted to prevent GvHD (reviewed in ref. 5). Similarly, ablation of MHC class-I molecules to limit rejection by the host immune system (6) has been employed in preclinical models.

Invariant Natural Killer T (iNKT) cells are a rare subset of innate lymphocytes representing less than 1% of the total lymphocyte population both in humans and mice. iNKT cells express a semi-invariant TCR recognizing glycolipids presented in the context of the monomorphic, MHC-like molecule CD1d. Because of their peculiar TCR constitution and antigen recognition modality, iNKT cells do not display any GvHD induction potential and can even prevent GvHD (reviewed in ref. 7). iNKT cells display potent direct antitumor activity through production of cytotoxic molecules (8). Several groups successfully generated human CAR iNKT cells provided with antitumor potential as assessed in vitro and in xenogeneic murine models (9-13). These studies revealed several advantages of using CAR iNKT cells over conventional CAR T cells, including their lack of induction of xeno-GvHD (9), their preferential migration to tumor sites (9), and their capacity of CAR iNKT to target both the natural ligand CD1d and the CAR-targeted antigen (12). In addition to their direct cytotoxic effect, iNKT cells are known for their strong immunomodulatory effect. In particular, iNKT cells induce CD8 T-cell crosspriming (14, 15) through the licensing of CD103+ CD8alpha dendritic cells (16-18), allowing the establishment of long-lasting antitumor CD8 T-cell responses in murine models (19-22).

In this study, we tested the hypothesis that induction of host CD8 T-cell cross-priming by allogeneic CAR iNKT cells would allow the establishment of an antitumor immunity lasting beyond the physical persistence of the transferred cells. Taking advantage of the immunoadjuvant role of iNKT cells and their lack of GvHD-inducing



#### **Translational Relevance**

The use of autologous cells for the generation of chimeric antigen receptor (CAR) T cells represents a significant limitation to the widespread use of this therapeutic approach. The development of allogeneic CAR T cells for off-the-shelf use still faces two major obstacles, namely the risk of graft-versus-host disease (GvHD) induction and the rejection by the host immune system. In this work, we show that allogeneic CAR-engineered invariant natural killer T (iNKT) cells, a cell population without GvHDinduction potential and with strong immunomodulatory properties, exerted potent antitumor activity by inducing tumor-specific antitumor immunity through host CD8 T-cell cross-priming. The induction of host antitumor immunity by allogeneic CAR iNKT cells resulted in a long-lasting antitumor effect going beyond their physical persistence. We believe that allogeneic CAR iNKT cells are promising candidates for the development of off-the-shelf CAR therapies, an important unmet need in the clinic.

potential, we demonstrate that allogeneic CAR iNKT cells exert, in addition to their previously reported direct antitumor effect (9–13), an indirect effect through the induction of host CD8 T-cell cross-priming.

#### **Materials and Methods**

#### Mice

BALB/cJ (H-2K<sup>d</sup>) and FVB/NJ (H-2K<sup>q</sup>) mice were purchased from The Jackson Laboratory. Firefly Luciferase (*Luc*+) transgenic FVB/N mice have been reported previously (23) and were bred in our animal facility at Stanford University. BALB/c Rag1<sup>-/-</sup>gamma-chain<sup>-/-</sup> and BALB/c BATF3<sup>-/-</sup> mouse strains were kind gifts of Dr. Irving Weissman and Dr. Samuel Strober, respectively, and were bred in our animal facility at Stanford University. All procedures performed on animals were approved by Stanford University's Institutional Animal Care and Use Committee and were in compliance with the guidelines of humane care of laboratory animals.

#### CAR iNKT and conventional CAR T generation

Murine CD19.28z CAR iNKT and conventional CAR T cells specifically recognizing the murine CD19 molecule were generated using an adaptation of previously reported protocols (24). Murine CD19 (mCD19) CAR stable producer cell line (25) was kindly provided by Dr. Terry J. Fry. iNKT cells were negatively enriched from FVB/N mouse spleen single-cell suspensions and using a mixture of biotinylated mAbs (GR-1, clone: RB6-8C5; CD8a, clone: 53-6.7; CD19, clone: 6D5; TCRγδ, clone: GL3; TER119/erythroid cell, clone: TER-119; CD62L, clone: MEL-14; BioLegend) and negative selection by anti-biotin microbeads (BD IMag Streptavidin Particles Plus DM, BD Biosciences). The enriched fraction (typically 10–30% enrichment) was then stimulated for 5 days with a synthetic analog of α-galactosylceramide (KRN7000, 100 ng/mL, REGiMMUNE) in the presence of human IL2 (100 UI/mL; NCI Repository) and human IL15 (100 ng/mL; NCI Repository). Cells were grown in DMEM media supplemented with 10% heat-inactivated FBS, 1 mmol/L sodium pyruvate, 2 mmol/L glutamine, 0.1 mmol/L nonessential amino acids, 100 U/mL penicillin, and 100 μg/mL streptomycin at 37°C with 5% CO<sub>2</sub>. Conventional T cells were enriched from FVB/N mouse spleen single-cell suspensions using the mouse Pan T Cell Isolation Kit II (Miltenyi Biotec) according to the manufacturer's protocol. T cells were activated for 24 hours with Dynabeads Mouse T-Activator CD3/ CD28 (Life Technologies) in the presence of human IL2 (30 U/ml) and murine IL-7 (10 ng/mL; PeproTech) in RPMI1640 media supplemented with 10% heat-inactivated FBS, 1 mmol/L sodium pyruvate, 2 mmol/L glutamine, 100 U/mL penicillin, and 100 µg/mL streptomycin at 37°C with 5% CO<sub>2</sub>. Activated cells were then transduced by culturing them for 48 hours in retronectin-coated plates loaded with supernatant harvested from the stable producer line 48 hours after culture. Invariant NKT cell purity was evaluated by flow cytometry using PE-conjugated PBS-57-loaded mCD1d tetramer (NIH Tetramer Facility) and TCR-β (clone H57–597; BioLegend). Transduction efficacy was measured by flow cytometry after protein L staining (26). CAR iNKT cell numbers were adjusted based on transduction efficacy before in vitro or in vivo use and the same number of untransduced iNKT cells was used as control. In experiments comparing CAR iNKT and conventional CAR T cells, percentages of transduced cells were adjusted to the same transduction efficacy (50%).

#### In vitro cytotoxic assay

In vitro cytotoxic assays were performed as described previously (27). Briefly, murine CD19.28z CAR iNKT or conventional CAR T cells were co-cultured for 24 hours with luciferase-transduced A20 cells (A20 $^{y/p+/luc+}$ ; ref. 28). A20 $^{y/p+/luc+}$  cells tested negative for Mycoplasma by PCR in October 2017, were cryopreserved in liquid nitrogen, thawed, and cultured for maximum 1 week before use.

#### In vivo bioluminescence imaging

In vivo bioluminescence imaging (BLI) was performed as previously described (27), using an IVIS Spectrum imaging system (Perkin Elmer) and Living Image Software 4.1 (Perkin Elmer) or using an Ami LED-illumination based imaging system (Spectral Instruments Imaging) with Aura Software (Spectral Instruments Imaging).

#### In vivo murine tumor models

We employed two systemic B-cell lymphoma mouse models reported previously (28). Briefly, CD19-expressing BCL1^{luc+} ( $5\times10^4$ ) or A20^{luc+} cells ( $2\times10^4$ ) resuspended in PBS were injected intravenously by tail vein into alymphoid BALB/c (H-2K<sup>d</sup>) Rag1^-/gamma-chain^-/mice. For tumor induction in immunocompetent mice, tumor cells were injected intravenously into sublethally (4.4 Gy) irradiated BALB/c mice. For syngeneic bone marrow transplantation, BALB/c mice were lethally irradiated (8.8 Gy in 2 doses administered 4 hours apart) and transplanted with syngeneic BALB/c bone marrow cells ( $5\times10^6$ ) after T-cell depletion using CD4 and CD8 MicroBeads (Miltenyi Biotec). For retransfer experiments, bone marrow cells from alymphoid BALB/c (H-2K<sup>d</sup>) Rag1^-/gamma-chain^-/mice were used to exclude any potential contribution from bone marrow–derived T or NK cells after reconstitution.

#### Flow cytometry analysis

In vitro cultured cells or ex vivo isolated cells were resuspended in phosphate-buffered saline (PBS) containing 2% FBS. Extracellular staining was preceded by incubation with purified FC blocking reagent (Miltenyi Biotech). Cells were stained with: TIM3 (clone: RMT3–23) APC, CD62 L (clone: MEL-14) AF700, CD19 (clone: 6D5) APC-Fire750, CD44 (clone: IM7) PerCpCy5.5, PD-1 (clone: 29F.1A12) BV605, CD8a (clone: 53–6.7) BV650, NK1.1 (clone: PK136) BV711, ICOS (clone: C398.4A) BV785, CD25 (clone: PC61.5) PE, TCRβ (clone: H57–597) PE/Dazzle594, and Thy1.1 (clone: HIS51) PeCy7. All antibodies were purchased from BioLegend. Dead cells were excluded using Fixable Viability Dye eFluor 506 (eBioscience).

Samples were acquired on a BD LSR II flow cytometer (BD Biosciences), and analysis was performed with FlowJo 10.5.0 software (Tree Star).

#### RNA and TCR sequencing analysis

Host CD4 and CD8 T cells were FACS-sorted from pooled spleens from 3 mice treated with allogeneic CAR iNKT or untreated control, frozen in TRizol, and conserved at  $-80^{\circ}$ C. RNA was extracted using the TRizol RNA isolation method (Thermo Fisher Scientific) combined with the RNeasy MinElute Cleanup (Qiagen). Full-length cDNA was generated using the Clontech SMARTer v4 Kit (Takara Bio USA, Inc.) prior to library generation with the Nextera XT DNA Library Prep Kit (Illumina, Inc.). Libraries were pooled for sequencing on the Illumina HiSeq 4000 platform (75 bp, paired-end). Sequencing reads were checked using FastQC v.0.11.7. Estimated transcript counts and transcripts per million (TPM) for the mouse genome assembly GRCm38 (mm10) were obtained using the pseudo-aligner Kallisto. Transcript-level abundance was quantified and summarized into gene level using the tximport R package. Differential gene expression was performed using the DESeq2 R package version 1.22.221, using FDR < 0.05. Gene-set enrichment analysis conducted using the fgsea R package. For TCR sequencing, libraries were prepared from the synthesized full-length cDNA using the nested PCR method reported previously (29, 30). Sequencing was performed by using the Illumina MiSeq platform after Illumina paired-end adapters incorporation. TCRβ sequence analysis was performed with VDJFasta. After total count normalization, downstream analysis was performed on the 1,000 most represented clonotypes across the samples using the FactoMineR and factoextra R packages.

#### Statistical analysis

The Mann–Whitney U test was used in cross-sectional analyses to determine statistical significance. Survival curves were represented with the Kaplan–Meier method and compared by log-rank test. Statistical analyses were performed using Prism 8 (GraphPad Software) and R version 3.5.1 Comprehensive R Archive Network (CRAN) project (http://cran.us.r-project.org) with R studio version 1.1.453.

#### Results

## Allogeneic CAR iNKT cell antitumor effect is significantly enhanced in the presence of host lymphocytes

To study the interaction of allogeneic CD19-specific CAR iNKT cells with the host immune system, we utilized a fully murine experimental system and transduced murine iNKT cells expanded ex vivo from FVB/N mice with a previously reported CAR construct (24) composed of the variable region cloned from the 1D3 hybridoma recognizing murine CD19 linked to a portion of the murine CD28 molecule and to the cytoplasmic region of the murine CD3- $\zeta$  molecule (CD19.28z CAR; Fig. 1A). The cytotoxic potential of CD19.28z-CAR iNKT was confirmed by in vitro cytotoxic assays against the CD19expressing A20 lymphoma cell line, revealing dose-dependent cytotoxicity of the CD19.28z-CAR iNKT cells (Fig. 1B). As predicted, untransduced iNKT did not display any significant cytotoxic effect against A20 cells (Fig. 1B) according to their lack of expression of CD1d. We next evaluated in vivo the direct antitumor effect of allogeneic CAR iNKT cells using BALB/c (H-2Kd) Rag1<sup>-/-</sup> gamma-chain<sup>-/-</sup> mice as recipients (**Fig. 1C** and **F**). FVB/N (H-2K<sup>q</sup>) derived allogeneic CAR iNKT cells significantly controlled tumor growth (Fig. 1D) and improved animal survival (Fig. 1E) compared with both untreated mice and mice receiving untransduced iNKT cells after administration to MHC-mismatched immunodeficient mice receiving CD19-expressing BCL $_1$  B-cell lymphoma cells. In a second, more aggressive model of B-cell lymphoma using A20 cells (**Fig. 1F**), allogeneic CAR iNKT minimally affected tumor growth as revealed by BLI (**Fig. 1G**) and slightly but significantly improved survival (**Fig. 1H**) compared with untreated mice and mice treated with untransduced iNKT cells.

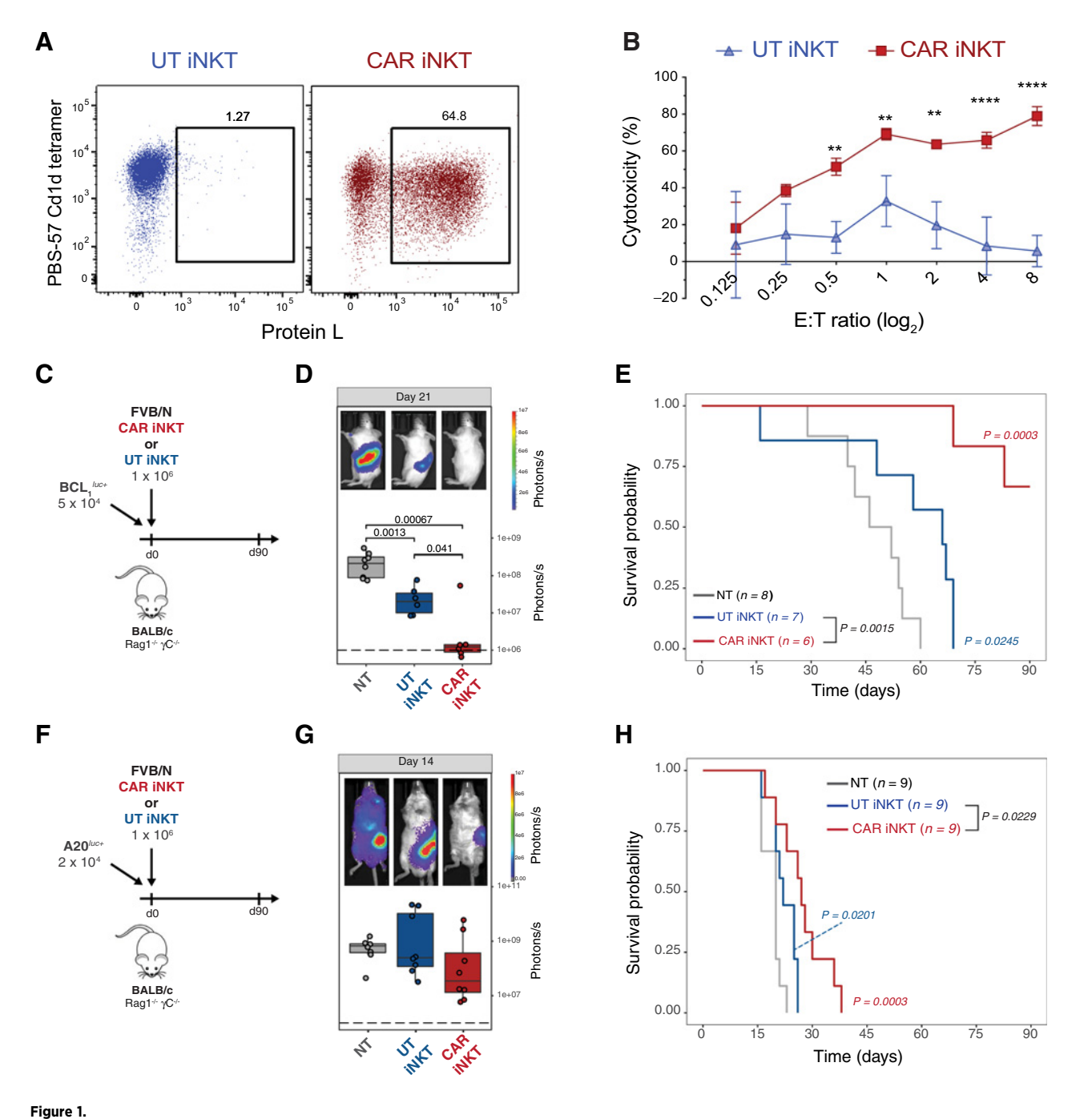
To assess the interplay between the transferred CAR iNKT cells and the host immune cells, we employed the A20 tumor model to test the antitumor activity mediated by allogeneic CAR iNKT cells in an immunocompetent model (Fig. 2A) using as recipients wild-type BALB/c mice receiving sublethal irradiation (4.4 Gy) leading to a partial and transient lymphopenia. The antitumor effect of  $1 \times 10^6$ allogeneic untransduced iNKT and CAR iNKT cells was greatly enhanced in this partially lymphopenic model, leading to long-term survival of all treated mice (Fig. 2B). Interestingly, a dose as low as  $5 \times$ 10<sup>4</sup> untransduced iNKT cells (Fig. 2C) was sufficient to significantly extend animal survival (Fig. 2D) and the addition of the CAR further improved the effect of iNKT leading to long-term survival of all CAR iNKT-treated mice (Fig. 2D). To further stress the model, we tested the antitumor effect of untransduced iNKT and CAR iNKT cells in a highburden, pre-established tumor model in which high numbers (2.5  $\times$ 10<sup>5</sup>) of A20 cells were injected 7 days before the adoptive transfer of the effector cells (Fig. 2F). In this model, untransduced iNKT displayed a minimal although statistically significant effect (Fig. 2F), whereas the administration of CAR iNKT cells significantly improved animal survival compared with both untreated mice and mice receiving untransduced iNKT cells (Fig. 2F).

Collectively, these *in vitro* and *in vivo* data confirm the direct antitumor effect of murine CAR iNKT cells and revealed an improved effect of untransduced iNKT and, even more, of CAR iNKT cells in the presence of host lymphocytes.

### Host CD8 T-cell cross-priming contributes to the indirect antitumor effect of allogeneic CAR iNKT cells

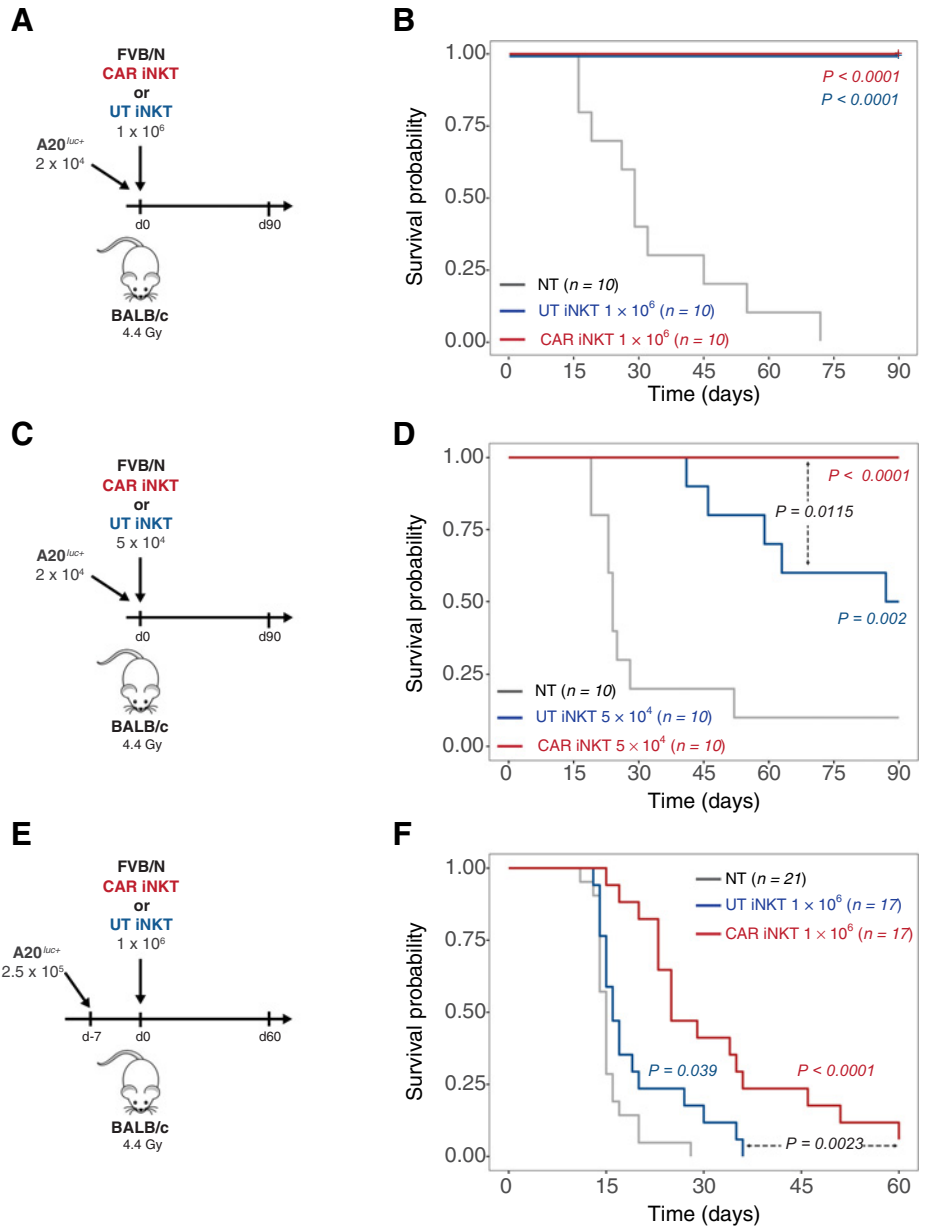
The striking difference in allogeneic CAR iNKT effect observed in mice with partial lymphopenia (**Fig. 2B** and **D**) compared with genetically alymphoid mice (**Fig. 1H**) suggested a role for host-derived lymphocytes in the antitumor effect. To test the hypothesis that host CD8 T-cell cross-priming mediates the indirect antitumor effect of allogeneic CAR iNKT cells, we employed as recipients BALB/c BATF3<sup>-/-</sup> mice, in which CD8 T-cell cross-priming is impaired as a result of the absence of BATF3-dependent CD103+ CD8alpha+dendritic cells (31).

The effect of allogeneic CAR iNKT cells was partially abrogated in A20-receiving BATF3<sup>-/-</sup> mice as compared to WT mice (Fig. 3A and B), supporting the hypothesis that the impact of allogeneic CAR iNKT cells is mediated, at least partially, by the activation of host CD8 T cells via their cross-priming. To further assess the synergistic effect of allogeneic CAR iNKT cells and host-derived CD8 T cells, we employed an autologous bone marrow transplantation model, co-administering allogeneic FVB/N CAR iNKT with syngeneic BALB/c CD8 T cells at the time of transplantation with T-cell-depleted syngeneic BALB/c bone marrow cells and transfer of A20 lymphoma cells into lethally irradiated (8.8 Gy) BALB/c recipients. Co-administration of allogeneic CAR iNKT and autologous CD8 T cells resulted in a synergistic effect, significantly improving tumor control (Fig. 3C) and animal survival (Fig. 3D) compared to mice receiving no treatment, as well as to mice receiving either allogeneic CAR iNKT or autologous CD8 T cells alone. Collectively these data indicate that CD8 T-cell cross-priming is necessary for allogeneic CAR iNKT cells to exert their full antitumor



In vitro and in vivo antitumor activity of murine CAR iNKT cells. **A,** Representative FACS-plot of untransduced (left) and mCD19.28z-CAR-transduced (right) murine iNKT cells. iNKT were identified as PBS-57 CD1d tetramer-positive cells and CAR transduction was quantified by Protein L staining. **B,** Mean and SD of cytotoxicity relative to the untreated control at different Effector:Target (E:T) ratios. Results are representative of two independent experiments performed in triplicate. **C** and **F,** Schematic representation of the BCL<sub>1</sub><sup>luc+</sup> (**C**) and A20<sup>luc+</sup> (**F**) into Rag1<sup>-/-</sup> gamma-chain<sup>-/-</sup> recipient experiments. **D** and **G,** Representative *in vivo* bioluminescence (BLI) images of BCL<sub>1</sub><sup>luc+</sup> (**D**) and A20<sup>luc+</sup> (**G**) tumor cell progression in Rag1<sup>-/-</sup> gamma-chain<sup>-/-</sup> treated with untransduced iNKT cells (blue boxes and dots), CAR iNKT cells (red boxes and dots), or untreated (gray box and dots). **E** and **H,** Survival of mice receiving BCL<sub>1</sub><sup>luc+</sup> (**E**) or A20<sup>luc+</sup> (**H**) and treated with untransduced iNKT cells (blue lines), CAR iNKT cells (red lines), or left untreated (NT, gray lines). Results are pooled from two independent experiments with a total of 6 to 9 mice per group. BLI results were compared using a nonparametric Mann–Whitney *U* test and *P* values are shown when significant. Survival curves were plotted using the Kaplan–Meier method and compared by log-rank test. *P* values are indicated when significant.

#### Simonetta et al.



employing A20<sup>luc+</sup> cells into sublethally (4.4 Gy) irradiated WT BALB/c mice. **B, D,** and **F,** Survival of mice receiving A20<sup>luc+</sup> cells and treated with untransduced iNKT cells (blue lines), CAR iNKT cells (red lines), or left untreated (NT, gray lines). Results are pooled from two independent experiments with a total of 10 to 21 mice per group. Survival curves were plotted using the Kaplan-Meier method and compared by log-rank test. *P* values are indicated when significant.

Allogeneic CAR iNKT-cell antitumor effect

is greatly enhanced by the presence of

host lymphocytes.  $\mathbf{A},\,\mathbf{C},\,\mathrm{and}\;\mathbf{E},\,\mathrm{Schematic}$ 

representation of the experiments

Figure 2.

effect and suggest a synergy between these two cytotoxic T-cell compartments.

### Allogeneic CAR iNKT-cell treatment modulates host CD8 T-cell phenotype, transcriptome, and TCR repertoire

To gain further insights into the impact of CAR iNKT cells on host T cells, we performed phenotypic analysis of host T cells recovered at day 7 and 14 after treatment with allogeneic CAR iNKT cells. At these timepoints, allogeneic CAR iNKT cells were already undetectable as revealed by *in vivo* tracking by bioluminescence (Supplementary Fig. S1A), flow cytometry (data not shown), and as suggested by the progressive increase of B-cell numbers (Supplementary Fig. S1B). We observed a significant increase in the number of CD8 T cells recovered at day 7 and day 14 from the spleen of mice treated with CAR iNKT cells compared with untreated mice (**Fig. 4A**). Immunophenotypic analysis revealed higher proportions of cells with a central memory

(CD62L+ CD44+) and reduced proportions of cells with an effector (CD62L-CD44-) or effector memory (CD62L-CD44+) phenotype in CD8 T cells recovered at day 7 after allogeneic CAR iNKT treatment compared with untreated mice (Fig. 4B). CD4 T-cell numbers were increased at day 7 but not at day 14 after allogeneic CAR iNKT treatment (Supplementary Fig. S2A), and CD4 T-cell phenotype was only minimally affected by CAR iNKT treatment (Supplementary Fig. S2B). A transcriptomic analysis performed on CD8 T cells FACSsorted at day 14 revealed the upregulation of genes associated with cytotoxic antitumor activity (Lyz2, Gzma, Gzmm, Fasl) and the downregulation of genes involved with responses to type I interferon (Irf7, Ifitm1, Ifi27l2a; Fig. 4C). Gene Set Enrichment Analysis (GSEA) for Gene Ontology (GO) Biological Processes confirmed the upregulation of antitumor gene sets (Fig. 4D) and the downregulation of the type I IFN signature. In agreement with our phenotypic results, a GSEA performed using two well-established memory CD8 T-cell gene

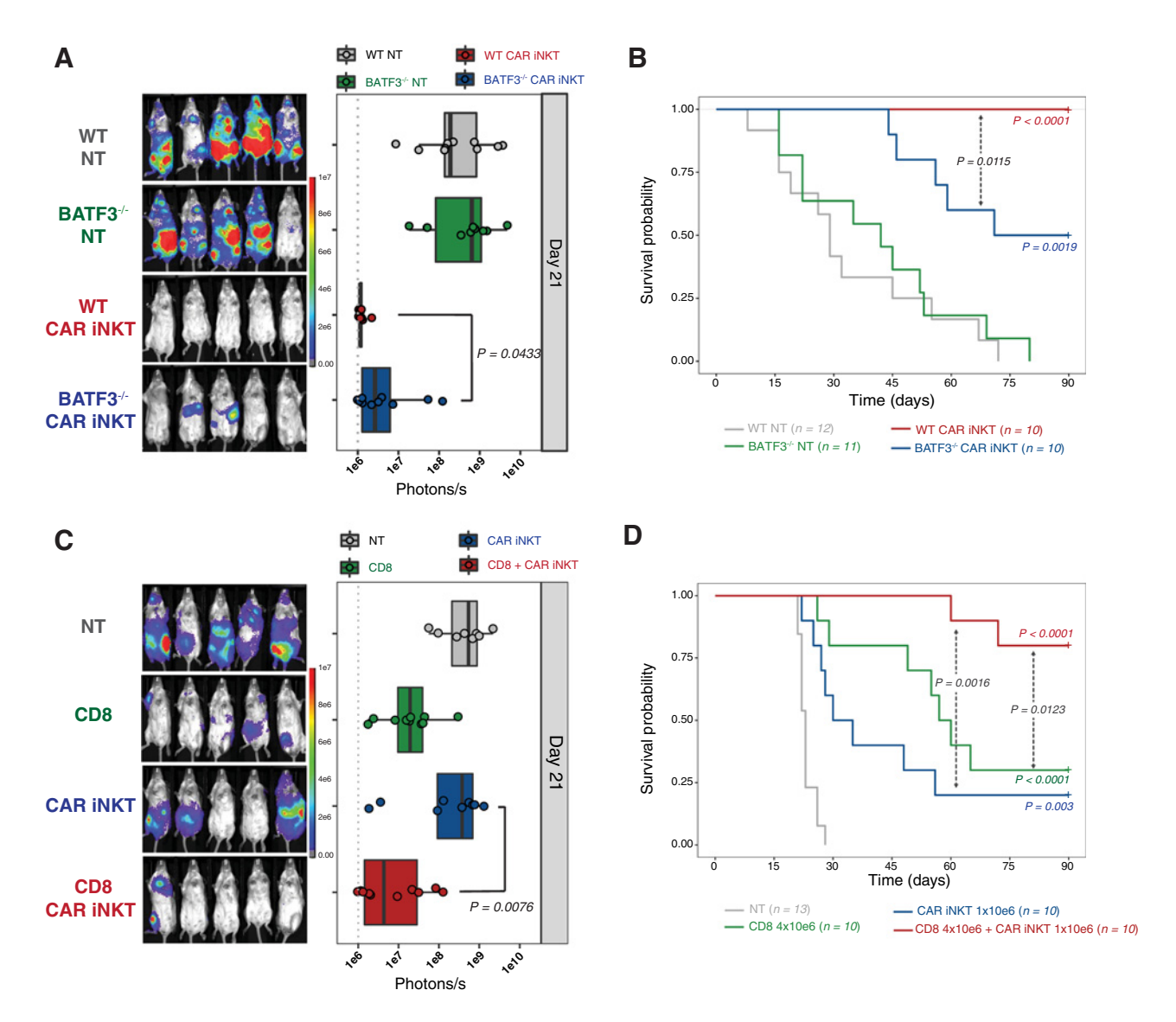


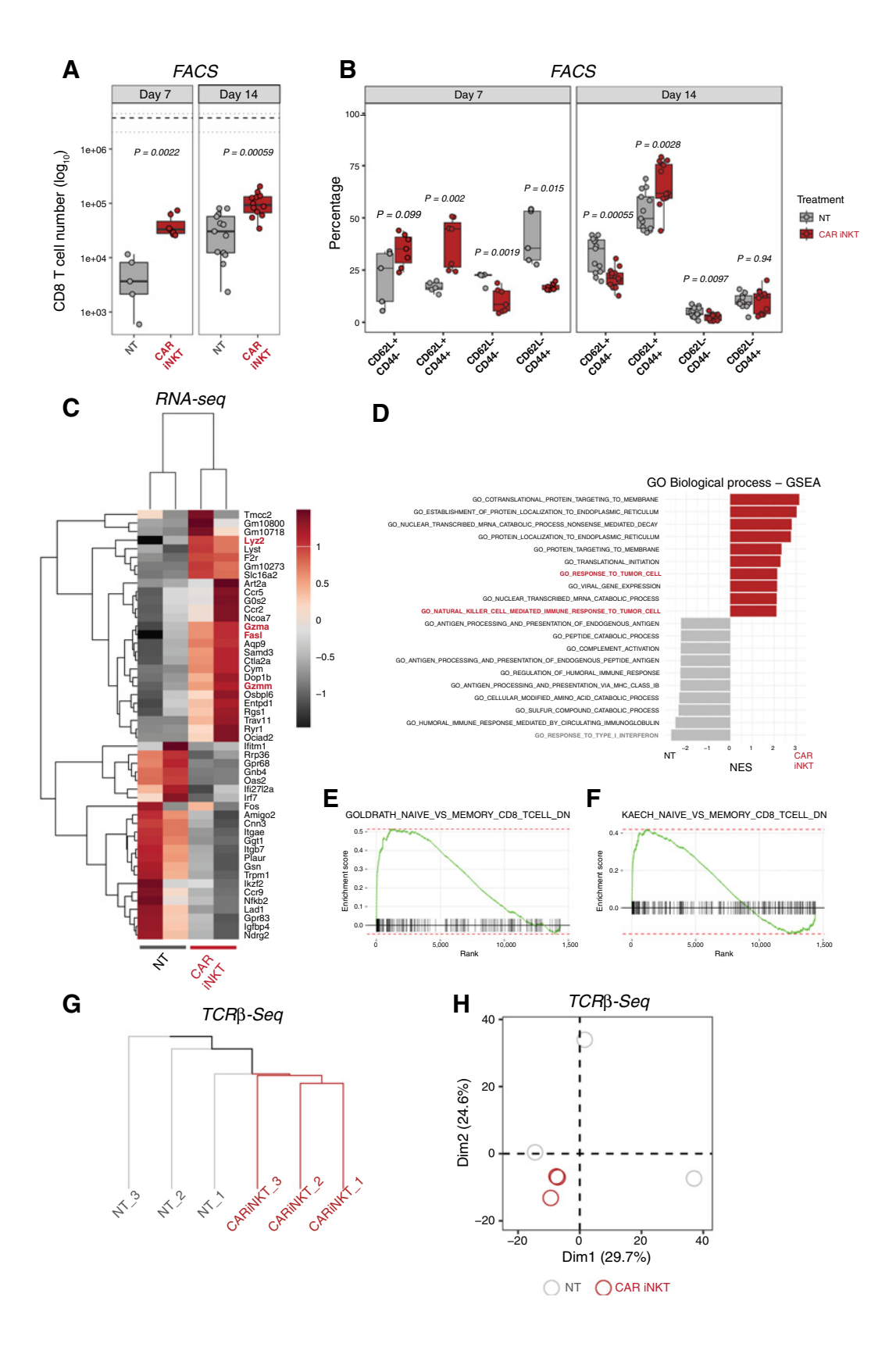
Figure 3. Indirect antitumor effect of allogeneic CAR iNKT cells is dependent on host CD8 T-cell cross-priming. Representative *in vivo* BLI images of A20  $^{luc+}$  cell progression (**A**) and survival (**B**) of sublethally (4.4 Gy) irradiated WT or BATF3 $^{-/-}$  BALB/c mice treated or not with 10 $^6$  CAR iNKT cells. Representative *in vivo* BLI images of A20  $^{luc+}$  cell progression (**C**) and survival (**D**) of lethally (8.8 Gy) irradiated WT BALB/c mice transplanted with syngeneic BALB/c TCD-BM and treated with syngeneic CD8 T cells (4 × 10 $^6$ ; green symbols and line), CAR iNKT cells (10 $^6$ ; blue symbols and line), or both (red symbols and line). Untreated controls are depicted in gray. BLI results were compared using a nonparametric Mann–Whitney U test and P values are shown. Survival curves were plotted using the Kaplan–Meier method and compared by log-rank test. P values are indicated when significant.

signatures revealed enrichment in CD8 T-cell memory genes (**Fig. 4E** and **F**). Transcriptomic analysis of CD4 T cells showed a similar downregulation of genes involved in responses to type I interferon (*Irf7, Ifit1, Ifit3*; Supplementary Fig. S2C) but did not reveal any consistent pattern of expression of genes involved in antitumor activity or cellular differentiation (Supplementary Fig. S2C). To assess the impact of CAR iNKT treatment on the TCR repertoire of CD8 T cells, we performed paired TCR- $\beta$  sequencing. Hierarchical clustering based on the 1,000 most represented TCR clonotypes revealed a closer relationship between the TCR repertoire of CD8 T cells from untreated mice (**Fig. 4G**). Accordingly, principal component analysis (PCA) showed close similarity in the TCR repertoire of CD8 T cells

from allogeneic CAR iNKT-treated mice, whereas cells from untreated mice displayed high heterogeneity (**Fig. 4H**). Analysis of the TCR repertoire of CD4 T cells did not reveal any impact of allogeneic CAR iNKT treatment (Supplementary Fig. S2D). Collectively, these results indicate that allogeneic CAR iNKT-cell treatment shaped the host CD8 T-cell compartment phenotypically, transcriptomically, and in terms of clonal repertoire.

## Allogeneic CAR iNKT-cell treatment induces long-lasting host CD8 T-cell tumor-specific responses

To formally prove that allogeneic CAR iNKT cells induce tumorspecific host immune responses, at day 60 after treatment, we recovered splenocytes from mice receiving A20 lymphoma cells and treated



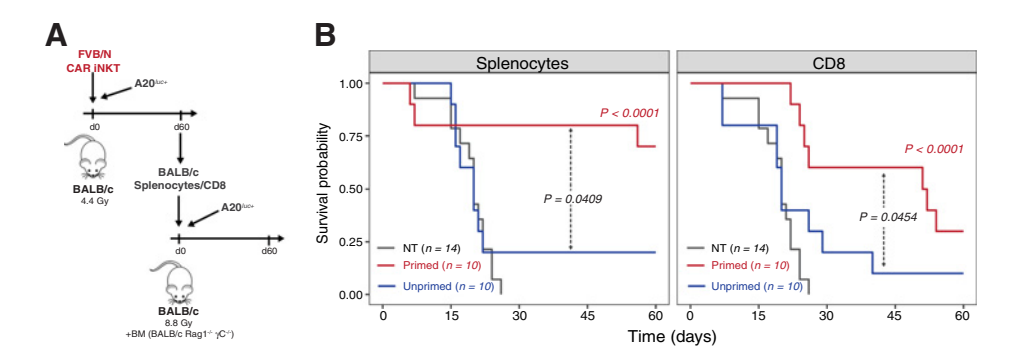


Figure 5.

Allogeneic CAR iNKT-primed host CD8 T cells display long-lasting antitumor immunity. **A,** Schematic representation of the sequential adoptive transfer experiment. Host splenocytes or CD8 T cells were recovered after 60 days from sublethally irradiated BALB/c mice, injected with A20<sup>luc+</sup> cells, and treated with CAR iNKT cells (primed cells). Splenocytes or CD8 T cells recovered after 60 days from sublethally irradiated BALB/c mice were used as controls (unprimed cells). Primed or unprimed host splenocytes ( $5 \times 10^6$  cells) were transferred, after lethal irradiation, to a new set of BALB/c mice receiving A20<sup>luc+</sup> cells together with bone marrow cells from syngeneic Rag1<sup>-/-</sup> gamma-chain<sup>-/-</sup> BALB/c mice. Alternatively, primed or unprimed host CD8 T cells ( $1 \times 10^6$  cells) were transferred. **B,** Survival of transplanted mice receiving primed (red line) or unprimed (blue line) splenocytes (left) or CD8 T cells (right). Untreated controls are depicted in gray. Results are pooled from two independent experiments with a total of 10 to 14 mice per group. Survival curves were plotted using the Kaplan–Meier method and compared by logrank test. *P* values are indicated when significant.

with allogeneic CAR iNKT cells. Recovered splenocytes were transferred into new lethally irradiated BALB/c recipients together with bone marrow from Rag1<sup>-/-</sup> gamma-chain<sup>-/-</sup> BALB/c mice and A20 cells (Fig. 5A). Unprimed splenocytes from mice receiving only sublethal irradiation were used as control. Splenocytes primed in the presence of allogeneic CAR iNKT significantly extended the survival of mice compared with both untreated mice and mice receiving unprimed splenocytes (Fig. 5B, left). To assess the contribution of CD8 T cells to this protective effect, we performed the same experiment retransferring only allogeneic CAR iNKT-primed or unprimed CD8 T cells. As shown in Fig. 5B (right), host CD8 T cells from allogeneic CAR iNKT-treated mice significantly extended animal survival compared with both mice left untreated or receiving unprimed CD8 T cells. Collectively, these experiments formally demonstrate that allogeneic CAR iNKT treatment induced a long-lasting tumor-specific host CD8-dependent antitumor immunity in allogeneic recipients.

## Allogeneic CAR iNKT cells outperform conventional CAR T cells in the presence of host lymphocytes

To assess the advantage that this indirect antitumor effect could confer to allogeneic CAR iNKT cells over allogeneic conventional CAR T cells, we compared these two populations. Given the potent direct antitumor activity of conventional CAR T cells (Supplementary Fig. S3A), a dose of as little as  $2.5\times10^5$  conventional CAR T cells was sufficient to significantly extend mouse survival when adminis-

tered into alymphoid animals (Supplementary Fig. S3B), and this dose was selected for comparison to CAR iNKT cells. As shown in Fig. 6A and B, during partial lymphopenia conventional CAR T cells significantly extended animal survival, whereas CAR iNKT cells dramatically outperformed conventional CAR T cells leading to tumor control and survival of all treated mice. Collectively, these results demonstrate that allogeneic CAR iNKT cells were significantly more effective than allogeneic conventional CAR T cells in inducing extended tumor control in immunocompetent hosts.

#### **Discussion**

In this study, we demonstrated in a murine model of CD19+ lymphoma that allogeneic CAR iNKT cells exert, in addition to their previously reported direct antitumor effect (9, 10, 12), an even stronger indirect antitumor effect mediated by the induction of host immunity.

The potential contribution of the host immune system in the effect of CAR T cells has been shown in preclinical (32–42) and clinical (43–45) studies. Recent studies indicate that immunogenic cell death eliciting endogenous cell responses contribute to the effects of adoptively transferred immune effector cells, including TCR-transgenic T cells (46, 47) and NK cells (46). We hypothesized that induction of bystander host antitumor responses might be a particularly interesting approach in the allogeneic setting, as CAR cells administered across major MHC barriers will be invariably rejected by

#### Figure 4.

Allogeneic CAR iNKT-cell treatment modulates host CD8 T-cell number, phenotype, transcriptome, and TCR repertoire. Number (**A**) and immunophenotype (**B**) of host CD8 T cells recovered from spleen 7 and 14 days after tumor induction in mice treated with allogeneic CAR iNKT cells (red boxes and symbols) or untreated (gray boxes and symbols). Median (black dashed line) and upper/lower range (gray dotted lines) of CD8 T-cell counts in naive mice are represented. Results are pooled from two independent experiments with a total of 5 to 13 mice per group. Groups were compared using a nonparametric Mann–Whitney *U* test and *P* values are shown. **C**, Heatmap representing differentially expressed genes in host CD8 T cells FACS-sorted from recipients treated or not with allogeneic CAR iNKT cells. Expression for each gene is scaled (*z*-scored) across single rows. Each column represents independent experiments with one to two biological replicates per experiment. **D**, Top 10 enriched terms/pathways in CD8 T cells from untreated (gray bars) and CAR iNKT-cell-treated (red bars) animals revealed by GO Biological Process analysis using GSEA. **E** and **F**, Enrichment plots displaying the distribution of the enrichment scores for the genes downregulated during transition from naive CD8 T cells versus memory CD8 T cells according to the Luckey and colleagues (**E**; ref. 66) or Kaech and colleagues (**F**; ref. 67) signatures. Gene signatures were obtained from Molecular Signatures Database (MSigDB; C7: immunologic signatures). **G** and **H**, Hierarchical clustering (**G**) and PCA (**H**) of the top 1,000 clonotypes based on TCRβ sequencing of CD8 T cells from hosts treated with allogeneic CAR iNKT cells (red) or left untreated (gray).

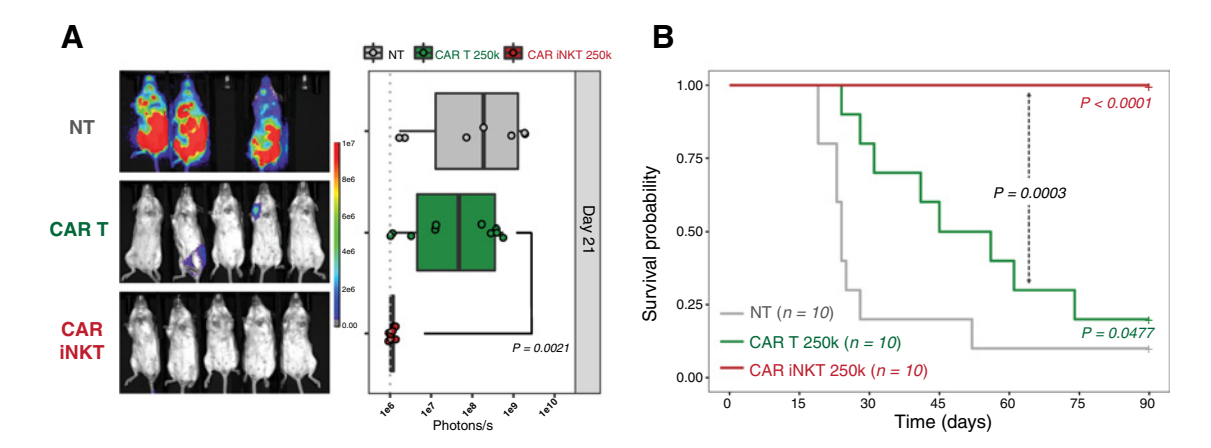


Figure 6.

Allogeneic CAR iNKT cells are more effective than allogeneic conventional CAR T cells. Representative *in vivo* BLI images of  $A20^{luc+}$  cell progression (**A**) and survival (**B**) of sublethally (4.4 Gy) irradiated BALB/c mice treated with 2.5 ×  $10^5$  allogeneic CAR iNKT cells (red curve and symbols), 2.5 ×  $10^5$  allogeneic conventional CAR T cells (green curve and symbols), or untreated (gray curve and symbols). Results are pooled from two independent experiments with a total of 10 mice per group. BLI results were compared using a nonparametric Mann–Whitney *U* test and *P* values are shown. Survival curves were plotted using the Kaplan–Meier method and compared by log-rank test. *P* values are indicated when significant.

the host immune system. After confirming in a fully murine model the previously reported direct cytotoxic effect of CAR iNKT cells (9-13), we demonstrate that allogeneic CAR iNKT cells efficiently induce antitumor immune responses in the recipient. Using BATF3<sup>-/-</sup> mice, a classically employed model of conventional type 1 dendritic cell (cDC1) deficiency (38, 46, 31, 48), we show that host CD8 T-cell crosspriming is necessary for the full action of CAR iNKT cells. However, BATF3 deficiency affects several lineages, including CD8 T cells (49,50) and Treg (51). To circumvent this limitation, we completed our analysis with an adoptive transfer model using wild-type recipients and wild-type CD8 T cells, indicating a synergy between allogeneic CAR iNKT cells and host-type CD8 T cells. Importantly, we show that retransfer of CAR iNKT-primed CD8 T cells allow for the transfer of protective antitumor immunity. In our study, we focused our attention on the induction of host CD8 T-cell responses that, lasting longer than the physical persistence of the administered allogeneic cells, would provide long-term antitumor protection. However, we cannot exclude that other mechanisms, including host NK-cell activation (52) or killing of tumor-associated macrophages (53), can contribute to the early effects of CAR iNKT cells in our model.

iNKT cells are an ideal platform for off-the-shelf immunotherapies given their lack of GvHD-induction potential (7) without need for deletion of their endogenous TCR, a manipulation that has been recently shown to alter the CAR T-cell homeostasis and persistence (54). Moreover, despite being a rare lymphocyte population, iNKT cells can be easily expanded ex vivo to numbers needed for clinical uses (55-58) and several clinical trials using ex vivo expanded autologous iNKT cells have been already successfully conducted (59-61). However, previous reports indicate that the ability of iNKT cells to expand in vitro may vary widely among individuals (62), a potential limitation for generation of autologous or allogeneic MHC-matched products. Use of allogeneic, off-the-shelf iNKT cells to be administered across MHC barriers will circumvent this potential limitation as universal donors whose iNKT cells display optimal expansion potential can be selected. Moreover, our results indicate that extremely low numbers of CAR iNKT cells persisting for a very limited time are able to induce a potent, long-lasting antitumor effect through their immunomodulatory role. Such an effect is in accordance with what we previously reported in the GvHD settings, where similarly low numbers ( $5 \times 10e4$ ) of CD4+ iNKT cells were able to efficiently prevent GvHD induced by conventional T cells in a major MHC-mismatch mouse model of bone marrow transplantation (63, 64), even when rapidly rejected third-party cells were employed (65).

A phase I clinical trial employing CD19-specific allogeneic CAR iNKT cells for patients with relapsed or refractory B-cell malignancies is currently ongoing (ANCHOR; NCT03774654). In analogy to what performed with conventional CAR T cells, this clinical trial involves the administration of a lymphodepleting regimen containing fludarabine and cyclophosphamide before CAR iNKT-cell infusion. Our results indicate that a major component of allogeneic CAR iNKT cells' effect derives from their interplay with the host immune system, an interaction that can significantly be impaired by the lymphodepleting conditioning. Future studies will determine whether the conventional fludarabine/cyclophosphamide lymphodepletion interferes with CAR iNKT-cell effect and will test alternative regimens to optimize both the homeostasis and the immunoadjuvant effect of the administered product.

In conclusion, our results represent the first demonstration of an immunoadjuvant effect exerted by an allogeneic CAR cell product toward the host immune system, resulting in long-lasting antitumor effects that go beyond the physical persistence of the allogeneic cells.

#### **Data and Materials Availability**

Sequencing data can be found under accession number PRJNA742379 (https://www.ncbi.nlm.nih.gov/bioproject/PRJNA742379).

#### **Authors' Disclosures**

F. Simonetta reports grants from Swiss Cancer League and American Society for Transplantation and Cellular Therapy during the conduct of the study. C.L. Mackall reports grants from NIH, California Institute for Regenerative Medicine, and Parker Institute for Cancer Immunotherapy during the conduct of the study. C.L. Mackall also reports grants and personal fees from Lyell Immunopharma, as well as personal fees from Syncopation Life Sciences, Neoimmune Tech, Immatics, GlaxoSmithKline, Bristol Myers Squibb, Apricity Health, Allogene, Vor, Bryologyx, and Red Tree Capital outside the submitted work. No disclosures were reported by the other authors.

#### **Authors' Contributions**

F. Simonetta: Conceptualization, data curation, formal analysis, funding acquisition, investigation, visualization, methodology, writing-original draft, project administration. J.K. Lohmeyer: Investigation, writing-review and editing. T. Hirai: Conceptualization, investigation, methodology, writing-review and editing. K. Maas-Bauer: Investigation, writing-review and editing. A.S. Wenokur: Investigation, writing-review and editing. J. Baker: Investigation, methodology, project administration, writing-review and editing. A. Aalipour: Resources, investigation, methodology, writing-review and editing. X. Ji: Methodology, writing-review and editing. S. Haile: Methodology, writing-review and editing. R.S. Negrin: Conceptualization, resources, supervision, funding acquisition, validation, writing-review and editing.

#### **Acknowledgments**

This work was supported by funding from R01 CA23158201 (to R.S. Negrin), P01 CA49605 (to R.S. Negrin), the Parker Institute for Cancer Immunotherapy (to R.S. Negrin), an American Society for Blood and Marrow Transplantation New Investigator Award 2018 (to F. Simonetta), the Geneva University Hospitals Fellowship (to F. Simonetta), the Swiss Cancer League BIL KLS 3806-02-2016 (to

F. Simonetta), the Fondation de Bienfaisance Valeria Rossi di Montelera Eugenio Litta Fellowship (to F. Simonetta), the Dubois-Ferrière-Dinu-Lipatti Foundation (to F. Simonetta), the Virginia and D.K. Ludwig Fund for Cancer Research (to C.L. Mackall), and a St Baldrick's/Stand Up to Cancer Pediatric Dream Team Translational Cancer Research Grant (to C.L. Mackall). Stand Up to Cancer is a program of the Entertainment Industry Foundation administered by the American Association for Cancer Research. C.L. Mackall is a member of the Parker Institute for Cancer Immunotherapy, which supports the Stanford University Cancer Immunotherapy Program. Flow cytometry analysis and sorting were performed on instruments in the Stanford Shared FACS Facility purchased using a NIH S10 Shared Instrumentation Grant (S10RR027431–01). Sequencing was performed on instruments in the Stanford Functional Genomics Facility, including the Illumina HiSeq 4000 purchased using a NIH S10 Shared Instrumentation Grant (S100D018220).

The costs of publication of this article were defrayed in part by the payment of page charges. This article must therefore be hereby marked *advertisement* in accordance with 18 U.S.C. Section 1734 solely to indicate this fact.

Received April 10, 2021; revised June 13, 2021; accepted July 30, 2021; published first August 10, 2021.

#### References

- Poirot L, Philip B, Schiffer-Mannioui C, Le Clerre D, Chion-Sotinel I, Derniame S, et al. Multiplex genome-edited T-cell manufacturing platform for "Off-the-Shelf" adoptive T-cell immunotherapies. Cancer Res 2015;75: 3853–64.
- Eyquem J, Mansilla-Soto J, Giavridis T, van der Stegen SJC, Hamieh M, Cunanan KM, et al. Targeting a CAR to the TRAC locus with CRISPR/Cas9 enhances tumour rejection. Nature 2017;543:113–7.
- MacLeod DT, Antony J, Martin AJ, Moser RJ, Hekele A, Wetzel KJ, et al. Integration of a CD19 CAR into the TCR alpha chain locus streamlines production of allogeneic gene-edited CAR T cells. Mol Ther 2017;25: 949–61.
- 4. Wiebking V, Lee CM, Mostrel N, Lahiri P, Bak R, Bao G, et al. Genome editing of donor-derived T-cells to generate allogenic chimeric antigen receptor-modified T cells: Optimizing  $\alpha\beta$  T cell-depleted haploidentical hematopoietic stem cell transplantation. Haematologica 2021;106:847–58.
- Daher M, Rezvani K. Outlook for new CAR-based therapies with a focus on CAR NK cells: What lies beyond CAR-engineered T cells in the race against cancer. Cancer Discov 2021;11:45–58.
- Torikai H, Reik A, Soldner F, Warren EH, Yuen C, Zhou Y, et al. Toward eliminating HLA class I expression to generate universal cells from allogeneic donors. Blood 2013;122:1341–9.
- Mavers M, Maas-Bauer K, Negrin RS. Invariant natural killer T cells as suppressors of graft-versus-host disease in allogeneic hematopoietic stem cell transplantation. Front Immunol 2017;8:900.
- 8. Wingender G, Krebs P, Beutler B, Kronenberg M. Antigen-specific cytotoxicity by invariant NKT cells in vivo is CD95/CD178-dependent and is correlated with antigenic potency. J Immunol 2010;185:2721–9.
- Heczey A, Liu D, Tian G, Courtney AN, Wei J, Marinova E, et al. Invariant NKT cells with chimeric antigen receptor provide a novel platform for safe and effective cancer immunotherapy. Blood 2014;124:2824–33.
- Tian G, Courtney AN, Jena B, Heczey A, Liu D, Marinova E, et al. CD62L+ NKT cells have prolonged persistence and antitumor activity in vivo. J Clin Invest 2016;126:2341–55.
- Ngai H, Tian G, Courtney AN, Ravari SB, Guo L, Liu B, et al. IL-21 selectively protects CD62L+ NKT cells and enhances their effector functions for adoptive immunotherapy. J Immunol 2018;201:2141–53.
- Rotolo A, Caputo VS, Holubova M, Baxan N, Dubois O, Chaudhry MS, et al. Enhanced anti-lymphoma activity of CAR19-iNKT cells underpinned by dual CD19 and CD1d targeting. Cancer Cell 2018;34:596–610.e11.
- Xu X, Huang W, Heczey A, Liu D, Guo L, Wood M, et al. NKT cells coexpressing a GD2-specific chimeric antigen receptor and IL15 show enhanced in vivo persistence and antitumor activity against neuroblastoma. Clin Cancer Res 2019; 25:7126–38.
- 14. Fujii S, Shimizu K, Smith C, Bonifaz L, Steinman RM. Activation of natural killer T cells by  $\alpha$ -galactosylceramide rapidly induces the full maturation of dendritic cells in vivo and thereby acts as an adjuvant for combined CD4 and CD8 T cell immunity to a coadministered protein. J Exp Med 2003;198:267–79.

- Hermans IF, Silk JD, Gileadi U, Salio M, Mathew B, Ritter G, et al. NKT cells enhance CD4+ and CD8+ T cell responses to soluble antigen in vivo through direct interaction with dendritic cells. J Immunol 2003;171:5140-7.
- Farrand KJ, Dickgreber N, Stoitzner P, Ronchese F, Petersen TR, Hermans IF. Langerin+CD8α+ dendritic cells are critical for cross-priming and IL-12 production in response to systemic antigens. J Immunol 2009;183:7732–42.
- Semmling V, Lukacs-Kornek V, Thaiss CA, Quast T, Hochheiser K, Panzer U, et al. Alternative cross-priming through CCL17-CCR4-mediated attraction of CTLs toward NKT cell-licensed DCs. Nat Immunol 2010;11:313–20.
- Valente M, Dölen Y, van Dinther E, Vimeux L, Fallet M, Feuillet V, et al. Crosstalk between iNKT cells and CD8 T cells in the spleen requires the IL-4/CCL17 axis for the generation of short-lived effector cells. Proc Natl Acad Sci U S A 2019; 116:25816–27.
- Nishimura T, Kitamura H, Iwakabe K, Yahata T, Ohta A, Sato M, et al. The interface between innate and acquired immunity: glycolipid antigen presentation by CD1d-expressing dendritic cells to NKT cells induces the differentiation of antigen-specific cytotoxic T lymphocytes. Int Immunol 2000;12:987–94.
- Fujii S, Shimizu K, Okamoto Y, Kunii N, Nakayama T, Motohashi S, et al. NKT cells as an ideal anti-tumor immunotherapeutic. Front Immunol 2013;4:409.
- Dashtsoodol N, Shigeura T, Tashiro T, Aihara M, Chikanishi T, Okada H, et al. Natural killer T cell-targeted immunotherapy mediating long-term memory responses and strong antitumor activity. Front Immunol 2017;8:1206.
- Ghinnagow R, Meester JD, Cruz LJ, Aspord C, Corgnac S, Macho-Fernandez E, et al. Co-delivery of the NKT agonist α-galactosylceramide and tumor antigens to cross-priming dendritic cells breaks tolerance to self-antigens and promotes antitumor responses. OncoImmunology 2017;6:e1339855.
- Beilhack A, Schulz S, Baker J, Beilhack GF, Wieland CB, Herman EI, et al. In vivo analyses of early events in acute graft-versus-host disease reveal sequential infiltration of T-cell subsets. Blood 2005;106:1113–22.
- Kochenderfer JN, Yu Z, Frasheri D, Restifo NP, Rosenberg SA. Adoptive transfer of syngeneic T cells transduced with a chimeric antigen receptor that recognizes murine CD19 can eradicate lymphoma and normal B cells. Blood 2010;116: 3875–86.
- Qin H, Ishii K, Nguyen S, Su PP, Burk CR, Kim B-H, et al. Murine pre-B-cell ALL induces T-cell dysfunction not fully reversed by introduction of a chimeric antigen receptor. Blood 2018;132:1899–910.
- Zheng Z, Chinnasamy N, Morgan RA. Protein L: a novel reagent for the detection of chimeric antigen receptor (CAR) expression by flow cytometry. J Transl Med 2012;10:29.
- Simonetta F, Alam IS, Lohmeyer JK, Sahaf B, Good Z, Chen W, et al. Molecular imaging of chimeric antigen receptor T cells by ICOS-ImmunoPET. Clin Cancer Res 2021;27:1058–68.
- Edinger M, Cao Y-A, Verneris MR, Bachmann MH, Contag CH, Negrin RS. Revealing lymphoma growth and the efficacy of immune cell therapies using in vivo bioluminescence imaging. Blood 2003;101:640–8.
- Han A, Glanville J, Hansmann L, Davis MM. Linking T-cell receptor sequence to functional phenotype at the single-cell level. Nat Biotechnol 2014;32:684–92.

#### Simonetta et al.

- Saligrama N, Zhao F, Sikora MJ, Serratelli WS, Fernandes RA, Louis DM, et al. Opposing T cell responses in experimental autoimmune encephalomyelitis. Nature 2019;572:481–7.
- Hildner K, Edelson BT, Purtha WE, Diamond M, Matsushita H, Kohyama M, et al. Batf3 deficiency reveals a critical role for CD8alpha+ dendritic cells in cytotoxic T cell immunity. Science 2008;322:1097–100.
- Wang L-CS, Lo A, Scholler J, Sun J, Majumdar RS, Kapoor V, et al. Targeting fibroblast activation protein in tumor stroma with chimeric antigen receptor T cells can inhibit tumor growth and augment host immunity without severe toxicity. Cancer Immunol Res 2014;2:154–66.
- Sampson JH, Choi BD, Sanchez-Perez L, Suryadevara CM, Snyder DJ, Flores CT, et al. EGFRvIII mCAR-modified T-cell therapy cures mice with established intracerebral glioma and generates host immunity against tumor-antigen loss. Clin Cancer Res 2014;20:972–84.
- Kueberuwa G, Kalaitsidou M, Cheadle E, Hawkins RE, Gilham DE. CD19 CART cells expressing IL-12 eradicate lymphoma in fully lymphoreplete mice through induction of host immunity. Mol Ther Oncolytics 2018;8:41–51.
- Brossart P. The role of antigen-spreading in the efficacy of immunotherapies. Clin Cancer Res 2020;26:4442-7.
- Lai J, Mardiana S, House IG, Sek K, Henderson MA, Giuffrida L, et al. Adoptive cellular therapy with T cells expressing the dendritic cell growth factor Flt3L drives epitope spreading and antitumor immunity. Nat Immunol 2020;21:914–26.
- Kuhn NF, Purdon TJ, van Leeuwen DG, Lopez AV, Curran KJ, Daniyan AF, et al. CD40 ligand-modified chimeric antigen receptor T cells enhance antitumor function by eliciting an endogenous antitumor response. Cancer Cell 2019;35: 473–88.
- Kuhn NF, Lopez AV, Li X, Cai W, Daniyan AF, Brentjens RJ. CD103+ cDC1 and endogenous CD8+ T cells are necessary for improved CD40L-overexpressing CAR T cell antitumor function. Nat Commun 2020;11:6171.
- Alizadeh D, Wong RA, Gholamin S, Maker M, Aftabizadeh M, Yang X, et al. IFNg is critical for CAR T cell mediated myeloid activation and induction of endogenous immunity. Cancer Discov 2021;11:2248–65.
- Boulch M, Cazaux M, Loe-Mie Y, Thibaut R, Corre B, Lemaître F, et al. A crosstalk between CAR T cell subsets and the tumor microenvironment is essential for sustained cytotoxic activity. Sci Immunol 2021;6:eabd4344.
- Murad JP, Tilakawardane D, Park AK, Lopez LS, Young CA, Gibson J, et al. Preconditioning modifies the TME to enhance solid tumor CAR T cell efficacy and endogenous protective immunity. Mol Ther 2021;29:2335–49.
- Rodriguez-Garcia A, Lynn RC, Poussin M, Eiva MA, Shaw LC, O'Connor RS, et al. CAR-T cell-mediated depletion of immunosuppressive tumor-associated macrophages promotes endogenous antitumor immunity and augments adoptive immunotherapy. Nat Commun 2021;12:877.
- Beatty GL, Haas AR, Maus MV, Torigian DA, Soulen MC, Plesa G, et al. Mesothelin-specific chimeric antigen receptor mRNA-engineered T cells induce anti-tumor activity in solid malignancies. Cancer Immunol Res 2014;2:112–20.
- Wang X, Hu Y, Liu X, Yu J, Xu P, Wei G, et al. Quantitative characterization of Tcell repertoire alteration in Chinese patients with B-cell acute lymphocyte leukemia after CAR-T therapy. Bone Marrow Transplant 2019;54:2072–80.
- Chen P-H, Lipschitz M, Weirather JL, Jacobson C, Armand P, Wright K, et al. Activation of CAR and non-CAR T cells within the tumor microenvironment following CAR T cell therapy. JCI Insight 2020;5:e134612.
- Minute L, Teijeira A, Sanchez-Paulete AR, Ochoa MC, Alvarez M, Otano I, et al. Cellular cytotoxicity is a form of immunogenic cell death. J Immunother Cancer 2020:8:e000325.
- Jaime-Sanchez P, Uranga-Murillo I, Aguilo N, Khouili SC, Arias MA, Sancho D, et al. Cell death induced by cytotoxic CD8+ T cells is immunogenic and primes caspase-3-dependent spread immunity against endogenous tumor antigens. J Immunother Cancer 2020;8:e000528.
- 48. Spranger S, Dai D, Horton B, Gajewski TF. Tumor-residing Batf3 dendritic cells are required for effector T cell trafficking and adoptive T cell therapy. Cancer Cell 2017;31:711–23.e4.

- Ataide MA, Komander K, Knöpper K, Peters AE, Wu H, Eickhoff S, et al. BATF3 programs CD8+ T cell memory. Nat Immunol 2020;21:1397–407.
- Qiu Z, Khairallah C, Romanov G, Sheridan BS. Cutting edge: Batf3 expression by CD8 T cells critically regulates the development of memory populations. J Immunol 2020:205:901–6.
- Zhang X, Xiao X, Lan P, Li J, Dou Y, Chen W, et al. OX40 costimulation inhibits Foxp3 expression and Treg induction via BATF3-dependent and independent mechanisms. Cell Rep 2018:24:607–18.
- Metelitsa LS, Naidenko OV, Kant A, Wu HW, Loza MJ, Perussia B, et al. Human NKT cells mediate antitumor cytotoxicity directly by recognizing target cell CD1d with bound ligand or indirectly by producing IL-2 to activate NK cells. J Immunol 2001;167:3114–22.
- Song I, Asgharzadeh S, Salo J, Engell K, Wu H, Sposto R, et al. Vα24-invariant NKT cells mediate antitumor activity via killing of tumor-associated macrophages. J Clin Invest 2009;119:1524–36.
- Stenger D, Stief TA, Käuferle T, Willier S, Rataj F, Schober K, et al. Endogenous TCR promotes in vivo persistence of CD19-CAR-T cells compared to a CRISPR/ Cas9-mediated TCR knockout CAR. Blood 2020;136:1407–18.
- Exley MA, Hou R, Shaulov A, Tonti E, Dellabona P, Casorati G, et al. Selective activation, expansion, and monitoring of human iNKT cells with a monoclonal antibody specific for the TCR α-chain CDR3 loop. Eur J Immunol 2008;38:1756-66.
- Chiba A, Cohen N, Brigl M, Brennan PJ, Besra GS, Brenner MB. Rapid and reliable generation of invariant natural killer T-cell lines in vitro. Immunology 2009;128:324–33.
- East JE, Sun W, Webb TJ. Artificial antigen presenting cell (aAPC) mediated activation and expansion of natural killer T cells. J Vis Exp 2012;29:4333.
- Mavers M, Simonetta F, Lee AW, Hirai T, Maas-Bauer K, Alvarez M, et al. IL-2 plus IL-15 leads to enhanced ex vivo expansion of human invariant natural killer T cells. Biol Blood Marrow Transplant 2018;24:S208–9.
- Motohashi S, Ishikawa A, Ishikawa E, Otsuji M, Iizasa T, Hanaoka H, et al. A phase I study of in vitro expanded natural killer T cells in patients with advanced and recurrent non-small cell lung cancer. Clin Cancer Res 2006;12: 6079–86
- Yamasaki K, Horiguchi S, Kurosaki M, Kunii N, Nagato K, Hanaoka H, et al. Induction of NKT cell-specific immune responses in cancer tissues after NKT cell-targeted adoptive immunotherapy. Clin Immunol 2011;138: 255–65.
- Exley MA, Friedlander P, Alatrakchi N, Vriend L, Yue S, Sasada T, et al. Adoptive transfer of invariant NKT cells as immunotherapy for advanced melanoma: A phase I clinical trial. Clin Cancer Res 2017;23:3510–9.
- 62. Rubio M-T, Bouillié M, Bouazza N, Coman T, Trebeden-Nègre H, Gomez A, et al. Pre-transplant donor CD4- invariant NKT cell expansion capacity predicts the occurrence of acute graft-versus-host disease. Leukemia 2017;31: 903–12.
- Schneidawind D, Pierini A, Alvarez M, Pan Y, Baker J, Buechele C, et al. CD4+ invariant natural killer T cells protect from murine GVHD lethality through expansion of donor CD4+CD25+FoxP3+ regulatory T cells. Blood 2014;124: 3320-8.
- Maas-Bauer K, Lohmeyer JK, Hirai T, Lopes Ramos T, Fazal FM, Litzenburger UM, et al. Invariant natural killer T cell subsets have diverse graft-versus-hostdisease-preventing and anti-tumor effects. Blood 2021;138:858–70.
- Schneidawind D, Baker J, Pierini A, Buechele C, Luong RH, Meyer EH, et al. Third-party CD4+ invariant natural killer T cells protect from murine GVHD lethality. Blood 2015;125:3491–500.
- Luckey CJ, Bhattacharya D, Goldrath AW, Weissman IL, Benoist C, Mathis D. Memory T and memory B cells share a transcriptional program of self-renewal with long-term hematopoietic stem cells. Proc Natl Acad Sci USA 2006;103: 3304–9.
- Kaech SM, Hemby S, Kersh E, Ahmed R. Molecular and functional profiling of memory CD8 T cell differentiation. Cell 2002;111:837–51.

#### 3.4. Publication 4

Lohmeyer JK, Hirai T, Turkoz M, Buhler S, Lopes Ramos T, Köhler N, Baker J, Ji X, Villard J, Melotti A, Wagner I, Pradier A, Wang S, Ji X, Becattini S, Villard J, Merkler D, Chalandon Y, Negrin RS<sup>#</sup>, <u>Simonetta F</u><sup>#</sup>. Analysis of T cell Repertoire and Transcriptome Identifies Mechanisms of Regulatory T cell (Treg) Suppression of GvHD. *Blood 2022*, Accepted (\*co-senior author)

CD4+ CD25+ FOXP3+ regulatory T cells (Treg) were the first immunoregulatory T cell population to be reported to suppress GvHD in murine models of HSCT without interfering with the graft-versus-tumor effect (GvT) of the transplantation procedure (Edinger et al., 2003). Leveraging on these preclinical experiments, several groups successfully transferred the Treg-immunotherapy concept for GvHD prevention to the human setting in pilot clinical trials (Di lanni et al., 2011; Martelli et al., 2014; Meyer et al., 2019; Pierini et al., 2021) and the first multicentric randomized phase III clinical trial (NCT05316701) is currently ongoing. However, the cellular and molecular mechanisms underlying this dissociation of GvHD from GvT by Treg are not fully understood. This knowledge appeared essential for the further development of Treg-based therapies in GvHD and, more broadly, to generate new therapies that would prevent and treat GvHD without interfering with the GvT effect of the transplant procedure. In this work we addressed this issue by using paired transcriptomic and TCR repertoire analysis of CD4 and CD8 Tcon as well as Treg in the previously reported murine model of GvHD suppression by Treg. Our analysis identified several potential mechanisms through which Treg modulate Tcon function after allogeneic HSCT (Figure 7). First, we observed an increased transcription of IL-10 and IL-35 encoding genes in Treg mirrored by a downstream upregulation in genes involved in IL-10 and IL-35 signaling in Tcon, suggesting that these two molecular pathways are involved in the Treg/Tcon interaction during GvHD suppression. Second, we found a transcriptional metabolic switch induced in Tcon by the Treq coadministration characterized by the upregulation of genes involved in oxidative phosphorylation and the downregulation of genes involved in glycolysis. Interestingly, such changes in the transcription of genes involved in T cell metabolism were detected also at the target tissue level when our sequencing analysis was performed on colon tissues from mice with GvHD treated or not with Treg. In addition, in colon tissues from mice treated with Treg, we observed a downregulation of genes part of the signaling cascade of several inflammatory molecules including IFN- $\gamma$ , IL-6 and TNF- $\alpha$ . Collectively, our results identified multiple non redundant potential mechanisms of GvHD suppression by Treg. Moreover, in addition to these positive results, some negative results are as well of particular interest in understanding mechanisms of GvHD suppression by Treg. First, our analysis of the Tcon TCR repertoire in the presence or absence of Treg indicate that Treg coadministration does not preclude the

expansion of alloreactive Tcon clonotypes. Second, despite the fact that Treg as well undergo clonal restriction during GvHD suppression, we did not find evidence of increased similarity between the Treg and Tcon TCR repertoire during GvHD suppression, suggesting that the antigens recognized by Treg and Tcon differ and/or that Treg and Tcon have distinct activation modalities after allogeneic HSCT.

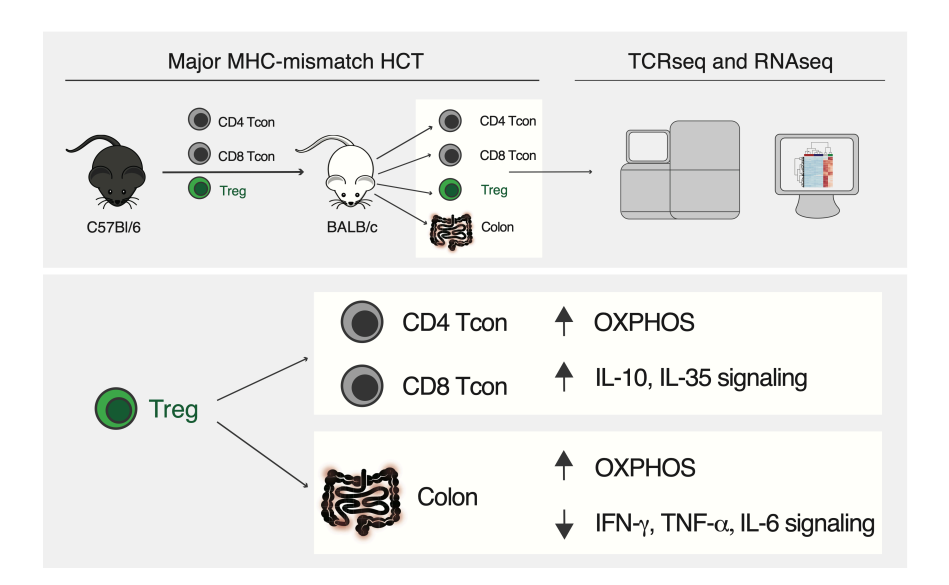


Figure 7. Graphical representation of the immunoregulatory effects of Treg on conventional T cell transcriptome and repertoire during murine acute GvHD. Personal material to be published as graphical abstract in Blood 2023.



American Society of Hematology 2021 L Street NW, Suite 900, Washington, DC 20036 Phone: 202-776-0544 | Fax 202-776-0545

#### Analysis of T cell Repertoire and Transcriptome Identifies Mechanisms of Regulatory T cell (Treg) Suppression of GvHD

Tracking no: BLD-2022-017982R1

Juliane Lohmeyer (Stanford University School of Medicine, United States) Toshihito Hirai (Stanford University, United States) Mustafa Turkoz (Stanford University, United States) Stephane Buhler (Geneva University Hospitals, Switzerland) Teresa Lopes Ramos (Stanford University School of Medicine, United States) Natalie Köhler (Stanford University, United States) Jeanette Baker (Stanford University, United States) Astrid Melotti (Geneva University Hospital and Geneva Medical School, Switzerland) Ingrid Wagner (University of Geneva, Switzerland) Amandine Pradier (Geneva University Hospital and Geneva Medical School, Switzerland) Sisi Wang (Geneva Medical School, Switzerland) Xuhuai Ji (Stanford University, United States) Simone Becattini (Geneva Medical School, Switzerland) Jean Villard (Transplantation Immunology Unit and National Reference Laboratory for Histocompatibility, Switzerland) Doron Merkler (Geneva University Hospital and Geneva Medical School, Switzerland) Yves Chalandon (University Hospital of Geneva, Switzerland) Robert Negrin (Stanford University Medical Center, United States) Federico Simonetta (Geneva University Hospital and Geneva Medical School, Switzerland)

#### Abstract:

CD4+FOXP3+ regulatory T cells have demonstrated efficacy in graft-versus-host disease (GvHD) prevention and treatment. Preclinical and clinical studies indicate that Treg are able to protect from GvHD without interfering with the graft-versus-tumor (GvT) effect of hematopoietic cell transplantation (HCT), although the underlying molecular mechanisms are largely unknown. To elucidate Treg suppressive function during in vivo suppression of acute GvHD, we performed paired T cell receptor (TCRa, TCRb genes) repertoire sequencing and RNA sequencing analysis on conventional T cells (Tcon) and Treg before and after transplantation in an MHC major-mismatch mouse model of HCT. We show that both Treg and Tcon underwent clonal restriction and that Treg did not interfere with the activation of alloreactive Tcon clones and the breadth of their TCR repertoire, however, markedly suppressed their expansion. Transcriptomic analysis revealed that Treg predominantly affected the transcriptome of CD4 Tcon and to a lesser extent of CD8 Tcon, modulating the transcription of genes encoding pro- and anti-inflammatory molecules as well as enzymes involved in metabolic processes, inducing a switch from glycolysis to oxidative phosphorylation. Finally, Treg did not interfere with the induction of gene sets involved in the GvT effect. Our results shed light into the mechanisms of acute GvHD suppression by Treg and will support the clinical translation of this immunoregulatory approach.

Conflict of interest: No COI declared

COI notes:

Preprint server: Yes; Biorxiv https://doi.org/10.1101/2022.07.26.501553

Author contributions and disclosures: JKL, TH, MT, FS conceived and designed research studies; JKL, TH, MT, TLR, AM, IW, AP, SW, FS conducted experiments; JKL, SB, NK, SW, FS analyzed data; XJ, developed methodology and analyzed data; JB, developed methodology and provided essential reagents; SB, JV, DM, YC provided essential tools and intellectual input; JKL, FS and RSN wrote the manuscript; FS and RSN supervised the research.

Non-author contributions and disclosures: No;

Agreement to Share Publication-Related Data and Data Sharing Statement: Relevant data can be found in the Gene Expression Omnibus database (accession number GSE205375; https://www.ncbi.nlm.nih.gov/geo/ query/acc.cgi?acc= GSE205375)

Analysis of T cell Repertoire and Transcriptome Identifies Mechanisms of Regulatory T cell 1 2 (Treg) Suppression of GvHD 3 Juliane K. Lohmeyer<sup>1</sup>, Toshihito Hirai<sup>1,2</sup>, Mustafa Turkoz<sup>1</sup>, Stephane Buhler<sup>3</sup>, Teresa Lopes Ramos<sup>1</sup>, 4 Natalie Köhler<sup>1,4</sup>, Jeanette Baker<sup>1</sup>, Astrid Melotti<sup>5,6</sup>, Ingrid Wagner<sup>6</sup>, Amandine Pradier<sup>5,6,7</sup>, Sisi 5 Wang<sup>5,6</sup>, Xuhuai Ji<sup>8</sup>, Simone Becattini<sup>6</sup>, Jean Villard<sup>3,6</sup>, Doron Merkler<sup>6,9</sup>, Yves Chalandon<sup>5,7</sup>, Robert 6 S. Negrin<sup>1#</sup>, Federico Simonetta<sup>1,5,6,7#</sup> 7 8 <sup>1</sup> Division of Blood and Marrow Transplantation and Cellular Therapy, Stanford University, 9 10 Stanford, CA <sup>2</sup> Department of Urology, Tokyo Women's Medical University, Tokyo, Japan 11 <sup>3</sup> Transplantation Immunology Unit and National Reference Laboratory for Histocompatibility, 12 Department of Diagnostic, Geneva University Hospitals, Geneva, Switzerland 13 <sup>4</sup> Department of Medicine I, Medical Center - University of Freiburg, Faculty of Medicine, 14 University of Freiburg, Freiburg, Germany 15 <sup>5</sup> Translational Research Center for Oncohematology, Department of Medicine, Faculty of Medicine, 16 University of Geneva, Geneva, Switzerland 17 <sup>6</sup> Department of Pathology and Immunology, Faculty of Medicine, University of Geneva, Geneva, 18 19 Switzerland <sup>7</sup> Division of Hematology, Department of Oncology, Geneva University Hospitals, Geneva, 20 Switzerland 21 <sup>8</sup> Human Immune Monitoring Center, Stanford University, Stanford, CA 22 23 <sup>9</sup> Division of Clinical Pathology, Geneva University Hospitals, Geneva, Switzerland 24 25 <sup>#</sup> R.S.N and F.S. are co-senior authors. 26 27 28 Word count: Abstract: 212 29 Main text: 3909 30 Figures: 7 31 Supplemental Figures: 5 32 Supplemental Methods: 1 33 References: 42 34 Running title: Analysis of Treg suppression mechanisms of GvHD 35 \*Corresponding authors: Robert S. Negrin, MD (negrs@stanford.edu) and Federico Simonetta, MD, 36 37 PhD (federico.simonetta@unige.ch), Division of Blood and Marrow Transplantation and Cellular

Therapy, Department of Medicine, Stanford University School of Medicine, Center for Clinical

Sciences Research Building, Room 2205, 269 W. Campus Drive, Stanford, CA 94305 (USA).

38

39

40

#### Abstract

41 42 43

44

45

46

47

48 49

50

51

52

53

54

5556

CD4+FOXP3+ regulatory T cells have demonstrated efficacy in graft-versus-host disease (GvHD) prevention and treatment. Preclinical and clinical studies indicate that Treg are able to protect from GvHD without interfering with the graft-versus-tumor (GvT) effect of hematopoietic cell transplantation (HCT), although the underlying molecular mechanisms are largely unknown. To elucidate Treg suppressive function during in vivo suppression of acute GvHD, we performed paired T cell receptor (TCRα, TCRβ genes) repertoire sequencing and RNA sequencing analysis on conventional T cells (Tcon) and Treg before and after transplantation in an MHC major-mismatch mouse model of HCT. We show that both Treg and Tcon underwent clonal restriction and that Treg did not interfere with the activation of alloreactive Tcon clones and the breadth of their TCR repertoire, however, markedly suppressed their expansion. Transcriptomic analysis revealed that Treg predominantly affected the transcriptome of CD4 Tcon and to a lesser extent of CD8 Tcon, modulating the transcription of genes encoding pro- and anti-inflammatory molecules as well as enzymes involved in metabolic processes, inducing a switch from glycolysis to oxidative phosphorylation. Finally, Treg did not interfere with the induction of gene sets involved in the GvT effect. Our results shed light into the mechanisms of acute GvHD suppression by Treg and will support the clinical translation of this immunoregulatory approach.

585960

61

62

63

64

656667

57

#### **Key Points**

- Regulatory T cells modulate conventional T cells transcriptome during GvHD suppression by affecting several, non-redundant pathways.
- Regulatory T cells undergo activation and clonal expansion during GvHD suppression.

#### Introduction

 Allogeneic hematopoietic cell transplantation (HCT) is a well-established and potentially curative therapy for a broad range of hematologic malignancies due to the graft-versus-tumor (GvT) effect. Unfortunately, allogeneic HCT is still associated with significant morbidity and mortality related to cancer relapse and transplant complications, namely graft-versus-host disease (GvHD). The immunological mechanism responsible for GvHD, i.e. donor T cell alloreactivity toward host antigens, is also responsible for the beneficial GvT effect of allogeneic HCT<sup>1</sup>. Because of the interconnection between these two phenomena, none of the currently employed strategies to GvHD prevention and treatment can efficiently target GvHD without affecting GvT.

Immunoregulatory cellular therapies are a promising approach for GvHD prevention and treatment<sup>2</sup>,<sup>3</sup>. We and others have previously shown in preclinical murine models that CD4+FOXP3+ regulatory T cells (Treg) are able to protect from GvHD without interfering with the GvT effect of HCT<sup>4-6</sup>. Efforts are ongoing to translate the use of Treg adoptive transfer for GvHD prevention<sup>7-10</sup> and treatment<sup>11,12</sup> to the clinic with promising results.

The precise cellular and molecular mechanisms underlying GvHD suppression by Treg are incompletely understood. Two non-exclusive and potentially complementary models exist: Treg could quantitatively affect T cell responses by limiting the activation and expansion of alloreactive T cell clones and/or might qualitatively modulate T cell function by selectively interfering with pathways responsible for GvHD but dispensable for GvT. To gain further insights supporting one or the other of these models, we performed paired T cell receptor (TCR) and RNA sequencing analysis on Tcon and Treg before and after transplantation using an MHC major-mismatch mouse model of acute GvHD.

#### Material and methods

93 94 95

#### **Acute GvHD murine model**

Donor CD4<sup>+</sup> and CD8<sup>+</sup> conventional T cells (Tcon) were separately isolated from splenocytes 96 harvested from CD45.1 Thy1.1 luc<sup>+</sup> C57Bl/6 mice by negative enrichment (Stemcell). T cell-97 98 depleted bone marrow (TCD-BM) cells were prepared from CD45.1 Thy1.2 C57Bl/6 mice by first 99 crushing bones followed by T cell depletion using CD4 and CD8 MicroBeads (Miltenyi Biotec). CD45.2 Thy1.2 FoxP3/GFP<sup>+</sup> CD4<sup>+</sup> Treg were FACS sorted from CD8/CD19-depleted single cell 100 101 suspensions from spleens and lymph nodes from CD45.2 Thy1.2 FoxP3GFP<sup>+</sup> C57Bl/6 using a BD 102 FACS Aria II. CD45.2 Thy1.2 BALB/c mice were lethally irradiated (8.8 Gy) and transplanted with 103 5x10e6 TCD-BM cells from CD45.1 Thy1.2 C57Bl/6 mice alone or together with CD45.2 Thy1.2 C57Bl/6 FoxP3/GFP<sup>+</sup> Treg (1x10e6) on day 0. On day 2, CD45.1<sup>+</sup> Thy1.1<sup>+</sup> C57Bl/6 Tcon (1x10e6; 104 105 CD4:CD8 ratio = 2:1) were injected to induce GvHD. Irradiated (11 Gy) syngeneic C57Bl/6 106 recipients receiving C57Bl/6 CD45.1<sup>+</sup> Thy1.2<sup>+</sup> TCD-BM and CD45.1<sup>+</sup> Thy1.1<sup>+</sup> Tcon alone were 107 used as controls. Mice were monitored daily, and body weight and GvHD score were assessed 108 weekly.

109110

#### Cell isolation

Recipient mice were euthanized 8 days after HCT (6 days after Tcon adoptive transfer) and single 111 112 cell suspensions obtained from spleens and lymph nodes. Cells from 3 animals per group were pooled to obtain 2 biological replicates in each of the two independent experiments. After Fc block 113 (Miltenyi), cells were incubated with the following antibodies (BioLegend): CD4 (BV421), CD8 114 115 (BV605), Thy1.1 (PE), CD45.1 (PE-Cy7), CD45.2 (APC), H-2kd (biotin) and CD19 (biotin) 116 followed by streptavidin APC-Fire. Donor-derived Thy1.1 CD45.1 CD4 and CD8 Tcon as well as Thy1.2<sup>+</sup> CD45.2<sup>+</sup> CD4<sup>+</sup> FoxP3/GFP<sup>+</sup> Treg were FACS-sorted. Tcon and Treg taken from the donor 117 118 aliquot before injection or recovered at day 8 post-HCT were frozen in Trizol (Thermo Fisher 119 Scientific) and conserved at -80°C until analysis.

120

- 121 Supplemental Methods
- Animals employed in the study as well as materials and methods used for bioluminescent imaging (BLI), genomics analyses, histopathological analyses and statistical analyses are detailed in the Supplemental Methods.

125126

127

#### **Results**

128 129 130

131

132

133

134

135 136

137

138 139

140

141

142

143

144

145

146 147

#### Treg treatment inhibited Tcon expansion and target tissue infiltration without affecting their TCR repertoire breadth

We employed a well-established mouse model of GvHD in which Treg were transferred at time of HCT, two days prior the adoptive transfer of Tcon<sup>13</sup>. As previously described, mice treated with Treg prior to Tcon transfer showed significantly improved survival and GvHD scores compared to mice receiving Tcon alone (Supplemental Figure 1A). The use of Tcon isolated from luciferase<sup>+</sup> donors revealed that this effect was associated with a significant reduction of Tcon expansion at day 8 after transplantation (day 6 after Tcon administration; Supplemental Figure 1B-C). At this time point, previously reported to be the peak of Tcon expansion<sup>14</sup>, Treg treatment also affected the localization of luc<sup>+</sup> Tcon. The Tcon derived signal was mainly restricted to secondary lymphoid organs (spleen and lymph nodes) and reduced in the abdominal region in mice receiving Treg compared to untreated mice with GVHD (Supplemental Figure 1B). Based on these results, we first hypothesized that Treg would inhibit the expansion of alloreactive clones during GvHD by controlling the TCR repertoire breadth, similarly to what was previously shown during antiviral responses<sup>15</sup>. To this aim, at day 8 after HCT, we re-isolated donor-derived CD45.1<sup>+</sup> Thy 1.1<sup>+</sup> CD4 and CD8 Tcon previously administered to syngeneic CD45.2<sup>+</sup> C57Bl/6 mice or allogeneic CD45.2<sup>+</sup> BALB/c mice in the presence or absence of CD45.2<sup>+</sup> FOXP3<sup>gfp+</sup> Treg (Figure 1A). As expected, the analysis of the TCR repertoire based on sequencing of the TCR alpha and beta

148 chains revealed a significant clonal restriction of both CD4 (Figure 1B, left panel) and CD8 (Figure 1C, left panel) Tcon recovered from allogeneic HCT recipients compared with Tcon from syngeneic 149 150 HCT recipients. Importantly, such clonal restriction in allogeneic HCT recipients was not inhibited

151 by Treg treatment (Figure 1B-C, left panels). Clonal overlap between Tcon collected at day 8 and

152 those before injection was reduced in allogeneic HCT recipients compared to syngeneic controls

153 (Figure 1B-C, middle panels) and Treg did not inhibit such reduction in clonal overlap (Figure 1B-C, 154

right panels). Collectively, our data indicate that Treg affected the expansion and the localization of

Tcon after HCT without impacting the TCR repertoire breadth of Tcon and the initial activation of alloreactive T cell clones during GvHD.

156 157 158

159

160 161

162

163

164

165

166

167

168

169

170

171

155

#### Treg treatment affected CD4 and to a lesser extent CD8 Tcon transcriptome during GvHD

We next evaluated the impact of Treg treatment on CD4 and CD8 Tcon at the transcriptomic level. Principal component analysis (PCA) of the top 1000 most differentially expressed genes across all samples revealed that 68% of the variance was explained by PC1, which clearly segregated CD4 and CD8 Tcon recovered at day 8 from allogeneic recipients from cells before injection or recovered from syngeneic recipients (Figure 2A), revealing a dominant effect of the allogeneic transplant procedure on the different T cell populations. PC1 was mainly driven by naïve T cell genes (Ccr7, Sell, Il6ra, Il6st, Foxo1) that were progressively downregulated along PC1, pointing to T cell activation/effector differentiation as a main element affected by the transplantation into allogeneic mice and, to a lesser extent, into syngeneic recipients (Figure 2A). Treg impact on CD4 and CD8 Tcon transcriptome was revealed by PC2 (Figure 2A) which contributed to 14.8% and 17.3% of the variance in CD4 and CD8 Tcon, respectively. Treg treatment mainly affected CD4 Tcon transcriptome (Figure 2A, left panel) inducing the downregulation of 219 genes and the upregulation of 111 genes (Figure 2B, left panel) compared to Tcon in the absence of Treg. In particular, Treg coadministration induced the downregulation of proinflammatory genes (*Il18rap*) and of Th1-signature genes (*Tbx21*, *Il12rb1*, *Il12rb2*) compared to Tcon injected alone. However, compared to resting cells (day 0) or to cells injected into syngeneic recipients, Treg still allowed significant upregulation of *Tbx21*, encoding for the Th1-master regulator transcription factor T-bet (Supplemental Figure 2). Treg promoted the up-regulation of anti-inflammatory genes (*Il18bp*) and Th2 signature genes (*Ccr4*, *Il4*) in CD4 Tcon (Figure 2B left panel, Supplemental Figure 2). Conversely, only a limited impact of Treg treatment was observed on CD8 Tcon (Figure 2A, right panel) with only 19 genes upregulated and 17 genes downregulated (Figure 2B, right panel) in Treg-treated CD8 Tcon compared to untreated CD8 Tcon. Collectively, these results revealed that Treg did not interfere with the major transcriptomic changes associated with T cell activation/effector differentiation during GvHD but exerted a CD4-dominant immunomodulatory effect on lineage-specific genes suppressing Th1 differentiation.

#### Treg underwent clonal restriction and activation during GvHD suppression

We next performed the same integrated analysis of the TCR repertoire and the transcriptome on Treg during GvHD suppression. Similar to what we observed in Tcon, Treg underwent clonal restriction during GvHD suppression, as revealed by a significantly increased  $TCR\alpha$  and  $TCR\beta$  clonality index at day 8 compared to before injection (Figure 3A). Accordingly, we observed only limited TCR overlap between day 0 and day 8 Treg (Figure 3B-C). These results indicated that during GvHD suppression Treg underwent clonal restriction at a similar extent as CD4 Tcon (figure 1B). To assess whether Treg and CD4 Tcon reacted to the same antigens during GvHD, we next compared the TCR repertoire of these two subpopulations. We observed a small clonal overlap between Treg and CD4 Tcon before injection and this was further reduced at day 8 after transplantation (Figure 3D-E), suggesting that Treg and CD4 Tcon responses during GvHD are engaging different cell clonotypes triggered by different epitopes or antigens. The increased activation state of Treg during GvHD suppression was further supported by the transcriptomic analysis revealing down-regulation of genes characterizing naive Treg (Sell) and up-regulation of several genes involved in activation such as Icos, Tnfrsf4 (encoding the costimulatory molecule OX40), Ccr2, Klrg1 and Gzmb (Figure 3F). After transplantation, Treg preserved the distinct transcriptomic signature observed before injection (Supplemental Figure 3A) further enhanced by the up regulation of genes involved in Treg activation and suppressive function (Ccr4, Ccr8, Gata3, Il9r, Il2ra, Il10, Tnfrsf18, Tnfrsf4, Areg) (Supplemental Figure 3B). Collectively, these data indicate that during GvHD suppression Treg undergo activation and clonal restriction similarly to what was observed in CD4 Tcon, although the analysis of the TCR repertoire of the two populations indicated divergence rather than increased similarity between Treg and CD4 Tcon during GvHD.

## Paired transcriptomic analysis of Treg and Tcon identified IL-10 and IL-35 as potential mechanisms of GvHD suppression

Treg employ a wide range of mechanisms to suppress immunopathological processes, ranging from production of immunosuppressive molecules to metabolic modulation of target cells  $^{16,17}$ . To infer the dominant mechanisms of suppression employed by Treg to control GvHD from transcriptomic data, we analyzed the transcript expression of suppressive molecules in Treg before and after HCT as well as the expression of gene sets induced by such molecules in Tcon. We did not observe any differences in Tgfb gene expression between Treg before injection (day 0) and Treg recovered at day

216 8 after HCT (Figure 4A). Accordingly, Gene Set Enrichment Analysis (GSEA) of TGFβ-induced 217 genes did not reveal any differences between Tcon treated or not with Treg (Figure 4B). Conversely, 218 Treg at day 8 after HCT expressed higher transcript levels of Il10 and Ebi3, encoding for one of the 219 two subunits constituting IL-35, compared to Treg before injection (Figure 4A). Accordingly, GSEA 220 revealed a significant enrichment of IL-10-induced genes in CD4 Tcon and IL-35-induced genes in 221 CD4 and CD8 Tcon (Figure 4B). Finally, day 8 Treg displayed a significant upregulation of the *Il2ra* 222 gene, encoding the alpha chain of the Il-2 receptor (Figure 4A). In addition to being a constitutively 223 expressed marker in Treg that is further upregulated during activation, IL-2RA expression is also essential in IL-2 deprivation of Tcon, an additional Treg mechanism of suppression 18,19. GSEA for 224 225 IL-2 induced genes in Tcon did not reveal any significant difference between Tcon recovered from 226 mice treated or not with Treg (Figure 4B). Collectively, our transcriptomic results support the 227 involvement of IL-10 and IL-35 production by Treg and their downstream signaling in Tcon as 228 major mechanisms of suppression of GvHD by Treg.

## Treg modulated genes involved in metabolic pathways favoring oxidative phosphorylation and suppressing glycolysis in CD4 and CD8 Tcon

To look for additional mechanisms of Treg suppression during GvHD, we performed GSEA for Hallmark gene sets on CD4 and CD8 Tcon in the presence or absence of Treg. This analysis identified the oxidative phosphorylation gene set as the top one induced in CD4 Tcon (Figure 5A) and the top third in CD8 Tcon (Figure 5B). Given the recently discovered importance of T cellmetabolism in GvHD<sup>20-22</sup>, we analyzed in detail the impact of Treg on genes involved in the main metabolic pathways (Figure 5C). Treg treatment significantly suppressed the transcription of genes involved in glycolytic processes including Slc2a1, encoding for the glucose receptor GLUT1, and Pkm, encoding for the key glycolytic enzyme pyruvate kinase, in both CD4 and CD8 Tcon (Figure 5C). Conversely, Treg treatment led to a global up-regulation of genes encoding for enzymes involved in oxidative phosphorylation (OXPHOS; Figure 5C). We did not observe any significant impact of Treg on Tcon transcription of genes involved in fatty acid oxidation (FAO) or the tricarboxylic acid (TCA) cycle (Figure 5C). Analysis of metabolic gene sets in Treg at day 8 post-HCT compared to Treg before injection revealed an enrichment in both OXPHOS and glycolysis gene signatures and a trend toward enrichment of FAO gene signatures (Supplemental Figure 4). Collectively, our results demonstrated that Treg significantly modulated genes involved in Tcon metabolism, leading to the downregulation of genes involved in glycolysis and the upregulation of the ones responsible for oxidative phosphorylation, pointing to a metabolic shift of Tcon induced by Treg during GvHD.

## 250251

229230

231

232

233

234

235

236

237238

239

240241

242

243

244

245

246

247

248

249

252

253

254

255

256

257

258

259

## Treg reduced infiltration by activated T cells and inflammation in intestinal tissues while inducing oxidative phosphorylation

To assess the impact of Treg treatment in GvHD-target organs, we performed a transcriptomic analysis of colonic tissues harvested at day 8 after transplantation from mice receiving Tcon in the presence or absence of Treg. We detected significantly reduced *Cd3e* transcripts in the colon from mice receiving Treg compared to mice receiving Tcon alone (Figure 6A). Similarly, we observed a reduction in transcripts of the *Trac*, *Trbc1* and *Trbc2* genes, encoding TCR subunits (Supplemental Figure 5A). Immunohistochemistry staining for CD3 of colonic tissues from mice receiving Treg confirmed a reduction in T cell infiltration compared with tissues from mice receiving Tcon alone

(Supplemental Figure 5B-C). We have previously shown that expression of the T-cell activation markers ICOS and OX40 is a sensitive parameter for GvHD monitoring (<sup>23,24</sup>). We detected reduced transcript levels of both *Icos* and *Tnfrsf4*, encoding ICOS and OX40 respectively, whose expression positively correlated with *Cd3e* expression (Figure 6A).

PCA performed on the top 1000 most differentially expressed genes clearly segregated tissues from mice receiving Tcon and Treg from mice receiving Tcon alone, with a PC1 explaining 79.4% of the variance (Figure 6B). Differential gene expression analysis identified 106 down-regulated genes and 54 up-regulated genes in the colon from mice receiving Treg treatment compared to mice receiving Tcon in the absence of Treg (Supplemental Figure 5D). GSEA for Hallmark gene sets on colonic tissues from mice receiving Treg identified the oxidative phosphorylation gene set as the top one induced (Figure 6C-D). Conversely, the top Hallmark gene signature suppressed by Treg was allograft rejection (Figure 6C-D). In addition, Treg administration was associated with a significant downregulation of gene signatures involved in the signaling pathways of several proinflammatory molecules including TNFα, IFNγ, IL-2/STAT5 and IL-6/JAK/STAT3 (Figure 6C).

Collectively, the transcriptomic analysis of colonic tissues revealed an impact of Treg on colon infiltration by activated Tcon, suppression of tissue inflammation and induction of oxidative phosphorylation during GvHD.

#### Treg treatment did not affect the induction of effector gene sets involved in GvT effect

We and others have previously shown that Treg are capable of suppressing GvHD without impairing the GvT effect of the transplant procedure<sup>5</sup>. We therefore hypothesized that Treg treatment would have minimal if any impact on Tcon transcription of effector molecules involved in the GvT effect. To test this hypothesis, we compared the transcription of effector molecules in Tcon recovered at day 8 from allogeneic mice treated or not with Treg. As shown in Figure 7A, the addition of Treg did not inhibit but further increased the transcription of *Ifng*, *Il2* and *Tnf* in CD4 Tcon. Accordingly, Treg did not prevent the upregulation of gene sets involved in leukocyte mediated cytotoxicity after HCT (Figure 7B). Similar results were observed in CD8 Tcon where Treg did not prevent the upregulation of cytotoxic genes including *Ifng*, *Gzmb* and *Prf1* (Figure 7C), nor the enrichment in genes involved in leukocyte mediated cytotoxicity (Figure 7D). Collectively, these results demonstrate that Treg treatment did not interfere with the induction of genes encoding effector molecules involved in the GvT effect of HCT.

#### Discussion

293294295

296

297

298

299

In this work we used integrated TCR repertoire and transcriptomic analysis of murine Tcon and Treg to gain further insights into the mechanisms of acute GvHD suppression by Treg. Our results indicate that Treg treatment did not interfere with the activation and differentiation of alloreactive Tcon clones during GvHD. Treg predominantly affected the CD4 Tcon and to a lesser extent the CD8 Tcon transcriptome, modulating the transcription of genes encoding pro- and anti-inflammatory molecules as well as enzymes involved in glycolytic processes.

300 301 302

303

304 305

306

307

308

309

310

311312

CD4+CD25+FOXP3+ regulatory T cells are a well-established immunomodulatory cell population able to suppress conventional T cell responses employing several, non-mutually exclusive, mechanisms <sup>16</sup>. Our analysis identified multiple pathways potentially involved in Treg suppression of GvHD, namely anti-inflammatory cytokine production mirrored by downstream Tcon signaling of IL-10 and IL-35 as well as a metabolic switch of Tcon from glycolysis to oxidative phosphorylation. Conversely, we did not find evidence for a role of TGFβ production and competition for IL-2 as dominant mechanisms of Treg suppression. The study of Tcon and Treg transcriptome during GvHD limited our analysis to T cell intrinsic mechanisms of suppression while it did not allow us to evaluate the relevance of cytolysis of effectors and APCs. Previous studies addressing the role of cytolysis mediated by Treg through production of cytotoxic molecules failed to find evidence for a role of granzyme B<sup>25</sup> and showed experimental<sup>26</sup> and clinical<sup>27</sup> evidence for a role of granzyme A in Treg mediated suppression of GvHD. Our transcriptomic analysis found an upregulation of *Gzmb* and *Gzma* in Treg after transplantation (Figure 3F).

314315316

317318

319

320321

322

323

324

325

326327

328

329330

331332

333

334

313

Recent studies point to an important role of metabolic regulation of T cells during GvHD (reviewed in Mohamed et al<sup>28</sup>). Murine studies revealed that donor T cells undergo metabolic reprogramming after allogeneic HCT, switching from fatty acid β-oxidation (FAO) and pyruvate oxidation via the tricarboxylic (TCA) cycle to aerobic glycolysis<sup>20</sup>. Using transcriptomic and metabolomic analysis, Assmann and colleagues<sup>21</sup> confirmed that murine donor CD4+ T cells acquired a highly glycolytic profile during acute GvHD and showed increased transcription of glycolytic enzymes in human CD4+ T cells isolated from allogeneic HSCT recipients just before the onset of acute GvHD. Our transcriptomic results suggest that Treg inhibit the metabolic switch of Tcon toward glycolysis by interfering at different crucial points. We observed a decrease in the transcription of the gene encoding the glucose transporter GLUT1, which contributes to the pathogenicity of allogeneic Tcon during GvHD<sup>22,29</sup>. Moreover, Treg inhibited the induction of genes encoding several glycolytic enzymes, including 6-phosphofructo-2-kinase/fructose-2,6-biphosphatase 3 (PFKFB3), the ratelimiting factor in glycolytic metabolism whose specific pharmacological inhibition using 3-(3pyridinyl)-1-(4-pyridinyl)-2-propen-1-one (3-PO) has been shown to protect against acute GvHD<sup>20</sup>. T cell metabolic fitness through glycolysis and oxidative phosphorylation (OXPHOS) has been recently shown to play an essential role in the GvT effect after allogeneic HCT<sup>30</sup>. In our experiments, Treg not only inhibited the transcription of glycolytic genes but also increased the transcription of OXPHOS-related genes, suggesting a metabolic switch toward mitochondrial respiration as a source of energy. These results, so far entirely based on transcriptomic analysis, will need functional validation before being exploited to improve the efficacy of Treg-based therapies.

335336

The need for TCR activation as well as the nature of the antigens recognized by Treg during GvHD is still debated. The beneficial effects of low dose IL-2 treatment on Treg numbers and function in chronic GvHD<sup>31-33</sup> suggest that cytokine-mediated Treg activation is sufficient for GvHD suppression without the need for TCR triggering. However, we previously showed that MHC disparities between Treg and the host were necessary as both donor and third-party Treg but not host Treg protect from GvHD in murine allogeneic HCT<sup>34</sup> pointing to a critical role of TCR activation for alloreactive Treg suppression of GvHD. Our present study further supports a model of TCR-mediated Treg activation for GvHD suppression, given the clonal restriction that Treg undergo after allogeneic HCT. Interestingly, we observed a divergence rather than a convergence of Tcon and Treg clonotypes detected after HCT compared to the steady state, suggesting that Tcon and Treg react against different antigens during GvHD. The contribution of Tcon derived IL-2 to this process is not excluded.

Our results have clinical implications given the increasing interest in Treg-based therapies for GvHD prevention and treatment. The Perugia group pioneered the adoptive transfer of fresh Treg followed by Tcon in a T cell depleted, CD34-selected HLA-haploidentical HCT platform<sup>7,10,35</sup> demonstrating the potential of human Treg to prevent GvHD but to still allow the GvT effect in patients. We reported a similar approach in HLA-matched recipients<sup>9</sup>. Recently, therapeutic adoptive transfer of Treg-enriched donor lymphocyte infusion combined with low-dose IL-2 has been reported in chronic GvHD<sup>11</sup>. A better understanding of the mechanisms of GvHD suppression by Treg is particularly relevant now that, after years of monocentric early-phase clinical trials and now multicentric phase III clinical trials.

Given the rarity of Treg, several groups attempted to *ex vivo* expand them from cord-blood<sup>8,36</sup> or from peripheral blood<sup>12</sup>. Our results point to the need of optimizing culture conditions to favor the expansion of IL-10 and IL-35 producing Treg<sup>37</sup>.

Our data reveal that, during GvHD suppression, Treg preserved a transcriptomic signature distinct from CD4 and CD8 Tcon (Supplemental Figure 3). Among differentially expressed genes, we identified genes encoding several surface markers, including Killer cell lectin-like receptor family molecules (*Klrc1*, *Klrd1*, *Klrk1*, *Klrb1b*), *CD160* and cytotoxic and regulatory T cell molecule (*Crtam*). Efforts are ongoing to target these and other markers to selectively deplete alloreactive T cells while sparing Treg.

Our analysis on Treg and Tcon was conducted on cells recovered from secondary lymphoid organs (SLO) and not on GvHD-target tissues as previously reported by other groups who focused on Tcon<sup>38–41</sup>. We decided to study SLO because this is the site where Treg suppression of Tcon mediating GvHD is believed to take place<sup>6,42</sup>. Moreover, the reduction in Tcon tissue infiltration upon Treg treatment precluded the isolation of sufficient numbers of Tcon and Treg from the GvHD-target tissues sites to conduct this kind of analysis. However, our bulk analysis of the colon recovered from mice receiving Tcon in the presence or absence of Treg supports the results we obtained in SLO, identifying the OXPHOS signature as the most strongly upregulated one upon Treg treatment and identifying several inflammatory molecules signaling pathways suppressed by Treg administration.

Our study has several limitations. First, our analysis was performed at the peak of Tcon expansion and lacks the dynamic information about the early impact of Treg during the very first days of GvHD suppression. Unfortunately, the limited number of cells that is possible to recover at earlier time points represent an obstacle to this analysis. Second, the strain combination of C57Bl/6 donors into BALB/c recipients is known to be more dependent on CD4+ T cells where it is possible that other strain combinations more dependent on CD8+ T cells may show more impact of Treg on this cell population.

In conclusion, our results provide further insights into the mechanisms of Treg suppression of GvHD. Moreover, our data support a model in which Treg qualitatively modulate Tcon function through several mechanisms rather than preventing the activation of alloreactive clones, providing a potential explanation for the ability of Treg to suppress GvHD while allowing GvT.

#### 394 Funding

- This work was supported from funding from the R01 CA23158201 (RSN), P01 CA49605 (RSN), the
- 396 Parker Institute for Cancer Immunotherapy (RSN), the German Cancer Aid Mildred Scheel
- Postdoctoral Fellowship (JKL), the Swiss Cancer League BIL KLS 3806-02-2016 (FS), the Geneva
- 398 Cancer League LGC 20 11 (FS), the American Society for Blood and Marrow Transplantation New
- 399 Investigator Award 2018 (FS), the Dubois-Ferrière-Dinu-Lipatti Foundation (FS), the ChooseLife
- 400 Foundation (FS), the Fondation Gustave & Simone Prévot (to FS), the Fondation Henriette Meyer (to
- 401 FS), the Gruenewald-Zuberbier Foundation (NK). Flow cytometry analysis and sorting were
- 402 performed on instruments in the Stanford Shared FACS Facility purchased using a NIH S10 Shared
- 403 Instrumentation Grant (S10RR027431-01). Sequencing was performed on instruments in the
- 404 Stanford Functional Genomics Facility, including the Illumina HiSeq 4000 purchased using a NIH
- 405 S10 Shared Instrumentation Grant (S10OD018220).

406 407

#### **Author contributions**

- JKL, TH, MT, FS conceived and designed research studies; JKL, TH, MT, TLR, AM, IW, AP, SW,
- 409 FS conducted experiments; JKL, SB, NK, SW, FS analyzed data; XJ, developed methodology and
- analyzed data; JB, developed methodology and provided essential reagents; SB, JV, DM, YC
- 411 provided essential tools and intellectual input; JKL, FS and RSN wrote the manuscript; FS and RSN
- 412 supervised the research

413

#### 414 Competing interests

415 All other authors have declared that no relevant conflict of interest exist.

416

#### 417 Data and materials availability

- 418 Relevant data can be found in the Gene Expression Omnibus database (accession number
- 419 GSE205375; https://www.ncbi.nlm.nih.gov/geo/ query/acc.cgi?acc= GSE205375).

#### 420 References

- 1. Negrin RS. Graft-versus-host disease versus graft-versus-leukemia. *Hematology*. 2015;2015(1):225–230.
- 2. Blazar BR, MacDonald KPA, Hill GR. Immune regulatory cell infusion for graft-versus-host disease prevention and therapy. *Blood*. 2018;131(24):2651–2660.
- 3. Negrin RS. Immune regulation in hematopoietic cell transplantation. *Bone Marrow Transplant*. 2019;54(2):765–768.
- 427 4. Hoffmann P, Ermann J, Edinger M, Fathman CG, Strober S. Donor-type CD4+CD25+ 428 Regulatory T Cells Suppress Lethal Acute Graft-Versus-Host Disease after Allogeneic Bone 429 Marrow Transplantation. *J Exp Med.* 2002;196(3):389–399.
- 5. Edinger M, Hoffmann P, Ermann J, et al. CD4+CD25+ regulatory T cells preserve graft-versus-tumor activity while inhibiting graft-versus-host disease after bone marrow transplantation. *Nat Med.* 2003;9(9):1144–1150.
- 433 6. Taylor PA, Panoskaltsis-Mortari A, Swedin JM, et al. L-Selectinhi but not the L-selectinlo CD4+25+ T-regulatory cells are potent inhibitors of GVHD and BM graft rejection. *Blood*. 2004;104(12):3804–3812.
- 7. Di Ianni M, Falzetti F, Carotti A, et al. Tregs prevent GVHD and promote immune reconstitution in HLA-haploidentical transplantation. *Blood*. 2011;117(14):3921–3928.
- 8. Brunstein CG, Miller JS, Cao Q, et al. Infusion of ex vivo expanded T regulatory cells in adults transplanted with umbilical cord blood: safety profile and detection kinetics. *Blood*. 2011;117(3):1061–1070.
- 9. Meyer EH, Laport G, Xie BJ, et al. Transplantation of donor grafts with defined ratio of conventional and regulatory T cells in HLA-matched recipients. *JCI Insight*. 4(10):.
- 10. Pierini A, Ruggeri L, Carotti A, et al. Haploidentical age-adapted myeloablative transplant and regulatory and effector T cells for acute myeloid leukemia. *Blood Advances*. 2021;5(5):1199–1208.
- 11. Whangbo J, Nikiforow S, Kim HT, et al. A phase 1 study of donor regulatory T-cell infusion plus low-dose interleukin-2 for steroid-refractory chronic graft-vs-host disease. *Blood Advances*.
   2022;bloodadvances.2021006625.
- 449 12. Landwehr-Kenzel S, Müller-Jensen L, Kuehl J-S, et al. Adoptive transfer of ex vivo expanded 450 regulatory T cells improves immune cell engraftment and therapy-refractory chronic GvHD. *Mol* 451 *Ther*. 2022;S1525-0016(22)00153–8.
- 452 13. Nguyen VH, Zeiser R, daSilva DL, et al. In vivo dynamics of regulatory T-cell trafficking and survival predict effective strategies to control graft-versus-host disease following allogeneic transplantation. *Blood*. 2007;109(6):2649–2656.
- 14. Beilhack A, Schulz S, Baker J, et al. In vivo analyses of early events in acute graft-versus-host disease reveal sequential infiltration of T-cell subsets. *Blood*. 2005;106(3):1113–1122.
- 15. Fontaine M, Vogel I, Van Eycke Y, et al. Regulatory T cells constrain the TCR repertoire of antigen-stimulated conventional CD4 T cells. *EMBO J.* 2018;37(3):398–412.
- 16. Vignali DAA, Collison LW, Workman CJ. How regulatory T cells work. *Nat Rev Immunol*. 2008;8(7):523–532.
- 17. Sakaguchi S, Mikami N, Wing JB, et al. Regulatory T Cells and Human Disease. *Annu Rev Immunol*. 2020;38:541–566.
- 18. Pandiyan P, Zheng L, Ishihara S, Reed J, Lenardo MJ. CD4+CD25+Foxp3+ regulatory T cells induce cytokine deprivation-mediated apoptosis of effector CD4+ T cells. *Nat Immunol*. 2007;8(12):1353–1362.
- 466 19. McNally A, Hill GR, Sparwasser T, Thomas R, Steptoe RJ. CD4+CD25+ regulatory T cells
   467 control CD8+ T-cell effector differentiation by modulating IL-2 homeostasis. *Proc Natl Acad Sci* 468 USA. 2011;108(18):7529–7534.

- 20. Nguyen HD, Chatterjee S, Haarberg KMK, et al. Metabolic reprogramming of alloantigenactivated T cells after hematopoietic cell transplantation. *J Clin Invest*. 2016;126(4):1337–1352.
- 21. Assmann JC, Farthing DE, Saito K, et al. Glycolytic metabolism of pathogenic T cells enables early detection of GVHD by 13C-MRI. *Blood*. 2021;137(1):126–137.
- 473 22. Huang Y, Zou Y, Jiao Y, et al. Targeting Glycolysis in Alloreactive T Cells to Prevent Acute Graft-Versus-Host Disease While Preserving Graft-Versus-Leukemia Effect. *Front Immunol*. 2022;13:751296.
- 476 23. Alam IS, Simonetta F, Scheller L, et al. Visualization of Activated T Cells by OX40-477 ImmunoPET as a Strategy for Diagnosis of Acute Graft-versus-Host Disease. *Cancer Res.* 478 2020;80(21):4780–4790.
- 479 24. Xiao Z, Alam IS, Simonetta F, et al. ICOS immunoPET enables visualization of activated T cells and early diagnosis of murine acute gastrointestinal GvHD. *Blood Adv.* 2022;6(16):4782–4792.
- 25. Cai SF, Cao X, Hassan A, Fehniger TA, Ley TJ. Granzyme B is not required for regulatory T cell-mediated suppression of graft-versus-host disease. *Blood*. 2010;115(9):1669–1677.
- 483 26. Velaga S, Ukena SN, Dringenberg U, et al. Granzyme A Is Required for Regulatory T-Cell 484 Mediated Prevention of Gastrointestinal Graft-versus-Host Disease. *PLoS One*. 485 2015;10(4):e0124927.
- 486 27. Ukena SN, Velaga S, Geffers R, et al. Human regulatory T cells in allogeneic stem cell transplantation. *Blood*. 2011;118(13):e82-92.
- 488 28. Mohamed FA, Thangavelu G, Rhee SY, et al. Recent Metabolic Advances for Preventing and Treating Acute and Chronic Graft Versus Host Disease. *Front Immunol*. 2021;12:757836.
- 490 29. Macintyre AN, Gerriets VA, Nichols AG, et al. The Glucose Transporter Glut1 Is Selectively 491 Essential for CD4 T Cell Activation and Effector Function. *Cell Metabolism*. 2014;20(1):61–72.
- 492 30. Uhl FM, Chen S, O'Sullivan D, et al. Metabolic reprogramming of donor T cells enhances graft-493 versus-leukemia effects in mice and humans. *Sci. Transl. Med.* 2020;12(567):eabb8969.
- 494 31. Koreth J, Matsuoka K, Kim HT, et al. Interleukin-2 and regulatory T cells in graft-versus-host disease. *N Engl J Med*. 2011;365(22):2055–2066.
- 496 32. Matsuoka K, Koreth J, Kim HT, et al. Low-dose interleukin-2 therapy restores regulatory T cell homeostasis in patients with chronic graft-versus-host disease. *Sci Transl Med*. 2013;5(179):179ra43.
- 33. Kennedy-Nasser AA, Ku S, Castillo-Caro P, et al. Ultra low-dose IL-2 for GVHD prophylaxis after allogeneic hematopoietic stem cell transplantation mediates expansion of regulatory T cells without diminishing antiviral and antileukemic activity. *Clin Cancer Res.* 2014;20(8):2215–2225.
- 34. Pierini A, Colonna L, Alvarez M, et al. Donor Requirements for Regulatory T Cell Suppression of Murine Graft-versus-Host Disease. *The Journal of Immunology*. 2015;195(1):347–355.
- 35. Martelli MF, Di Ianni M, Ruggeri L, et al. HLA-haploidentical transplantation with regulatory and conventional T-cell adoptive immunotherapy prevents acute leukemia relapse. *Blood*. 2014;124(4):638–644.
- 36. Brunstein CG, Miller JS, McKenna DH, et al. Umbilical cord blood-derived T regulatory cells to prevent GVHD: kinetics, toxicity profile, and clinical effect. *Blood*. 2016;127(8):1044–1051.
- 510 37. Ulbar F, Villanova I, Giancola R, et al. Clinical-Grade Expanded Regulatory T Cells Are 511 Enriched with Highly Suppressive Cells Producing IL-10, Granzyme B, and IL-35. *Biol Blood* 512 *Marrow Transplant*. 2020;26(12):2204–2210.
- 38. Zhou V, Agle K, Chen X, et al. A colitogenic memory CD4+ T cell population mediates gastrointestinal graft-versus-host disease. *J Clin Invest*. 2016;126(9):3541–3555.
- 515 39. Tkachev V, Kaminski J, Potter EL, et al. Spatiotemporal single-cell profiling reveals that invasive and tissue-resident memory donor CD8+ T cells drive gastrointestinal acute graft-versus-host disease. *Sci Transl Med.* 2021;13(576):eabc0227.

- 518 40. Gerdemann U, Fleming RA, Kaminski J, et al. Identification and Tracking of Alloreactive T Cell 519 Clones in Rhesus Macaques Through the RM-scTCR-Seq Platform. *Frontiers in Immunology*. 520 2022;12:.
- 521 41. Piper C, Hainstock E, Yin-Yuan C, et al. Single-cell immune profiling reveals a developmentally 522 distinct CD4+ GM-CSF+ T-cell lineage that induces GI tract GVHD. *Blood Adv*. 523 2022;6(9):2791–2804.
- 42. Ermann J, Hoffmann P, Edinger M, et al. Only the CD62L+ subpopulation of CD4+CD25+ regulatory T cells protects from lethal acute GVHD. *Blood*. 2005;105(5):2220–2226.

526527528

#### Figure legends

529530531

532

533

534

535536

537

538

539

540

541

542

543

544

545

Figure 1. Treg did not affect the TCR breadth of Tcon after HCT. (A) Schematic representation of the experimental pipeline. On day 0, Balb/c or C57Bl/6 recipient mice were lethally irradiated and transplanted with  $5x10^6$  CD45.1<sup>+</sup> Thy 1.2<sup>+</sup> T cell depleted bone marrow cells (TCD-BM) with or without 1x10<sup>6</sup> Foxp3<sup>GFP</sup> Treg cells from C57Bl6 donors. On day 2, 1x10<sup>6</sup> CD45.1<sup>+</sup> Thy1.1<sup>+</sup> Tcon from C57Bl/6 donors were injected. GFP<sup>+</sup> donor Treg and CD45.1<sup>+</sup> Thy1.1<sup>+</sup> CD4 and CD8 donor Tcon before transplantation (day 0/2) and isolated on day 8 were used for sequencing analysis (B, C) Clonality of the TCRA and TCRB repertoire in CD4 (B) and CD8 (C) Tcon recovered at day 8 after HCT in syngeneic recipients (green box and symbols), allogeneic recipients (blue box and symbols) and allogeneic recipients receiving Treg (red box and symbols). Representative example of overlap of the TCRA and TCRB repertoire in CD4 and CD8 Tcon prior to transplantation and at day 8 after HCT (left panels). Scatter plots (middle panels) represent clone frequencies before and after HCT and number of unique clones (dot size). Clones that are only observed at one time point are colored in light grey, while overlapping clones are colored in dark grey. Repertoire overlap in CD4 and CD8 (right panels) Tcon recovered at day 8 after HCT and before injection quantified using the Jaccard index of similarity. Groups were compared using a nonparametric Mann-Whitney U test and p values are shown.

546547548

549

550551

# Figure 2. Treg modulated CD4 and to a lesser extent CD8 Tcon transcriptome during GvHD. (A) Principal component analysis of transcriptome based on the top 1000 differentially expressed genes across all CD4 (left panel) and CD8 (right panel) Tcon samples. (B) Volcano plots showing significance and Log2 fold change of transcripts from Treg treated CD4 (left panel) and CD8 (right panel) Tcon compared to untreated Tcon. Vertical dashed lines on volcano plots indicate a Log2 fold

Figure 3. Treg underwent clonal restriction of the TCR repertoire and activation during GvHD

change of 1.5; horizontal dashed line indicates an adjusted p-value of 0.05.

552553554

555

556

557

558

559

560

561

562

563

564

565

566

567

568

569

570

(z scored) across single rows.

suppression. (A) Clonality of the TCRA and TCRB repertoire in Treg at day 0 (light pink box and symbols) and day 8 (purple box and symbols) after HCT. (B) Representative example of overlap of the TCRA and TCRB repertoire in Treg prior to transplantation and at day 8 after HCT. Scatter plots represent clones' frequencies before and after HCT and number of unique clones (dot size). Clones that are observed at only one time point are colored in light grey, while overlapping clones are colored in dark grey. (C) Venn diagram representing the number of overlapping and non-overlapping clones between day 0 (light pink box and symbols) and day 8 (purple box and symbols) Treg. (D) Representative example of overlap of the TCRA and TCRB repertoire in CD4 Tcon (x axis) and Treg (y axis) at day 8 after HCT in allogeneic mice receiving both Tcon and Treg. Scatter plots represent clones' frequencies in Tcon and Treg and number of unique clones (dot size). Clones that are observed in only one population are colored in light grey, while overlapping clones are colored in dark grey. Jaccard indexes are indicated. (E) Venn diagram representing the number of overlapping

571572

and non-overlapping clones between Treg and Tcon treated or not with Treg recovered at day 8 after

HCT. (F) Heatmap and hierarchical clustering based on the 500 most highly differentially expressed

genes across all samples. Immune-related genes are highlighted. Expression for each gene is scaled

- 573 Figure 4. Paired transcriptomic analysis of Tcon and Treg identified mechanisms of GvHD 574 suppression. (A) Transcript expression of genes encoding for molecules involved in classical Treg 575 mechanisms of suppression. (B) Enrichment plots displaying enrichment scores for the genes 576 involved (HALLMARK TGF BETA SIGNALING), *Tgfb* Il10577 (REACTOME INTERLEUKIN 10 SIGNALING), *Il35* 578 (GSE24210 CTRL VS IL35 TREATED TCONV CD4 TCELL DN) Il2 and
- 579 (HALLMARK IL2 STAT5 SIGNALING) in CD4 (left panels) and CD8 (right panels) Tcon 580 recovered at day 8 after HCT in the presence or absence of Treg. Gene signatures were obtained

581 from Molecular Signatures Database (MSigDB).

582 583

584

585

586

587

Figure 5. Treg modulated genes regulating metabolic patterns in CD4 and CD8 Tcon during GvHD. (A-B) Top 10 enriched terms/pathways in CD4 (A) and CD8 (B) Tcon from mice receiving Tcon and Treg (positive NES, red bars indicate the significant patways) or Tcon alone (negative NES, blue bars indicate the significant pathways) revealed by Hallmark GSEA. (C) Map of genes regulating CD4 and CD8 Tcon metabolisms before and after HCT. Single genes heatmap represent the row-scaled gene expression expressed in FPKM. Genes and enzymes are indicated.

588 589 590

591

592

593

594

595

596

597

598

599

600

601

Figure 6. Treg modulated colon T-cell infiltration and gene expression. (A) Scatter plots and marginal bar plots correlating and comparing the transcript expression of Cd3e, Icos and Tnfrsf4 in the colon from mice receiving Tcon alone (blue dots and bars) or Tcon and Treg (red dots and bars). Differences between groups were assessed using DESeq2. Correlations were evaluated using a Spearman rank correlation coefficient test. (B) Principal component analysis of transcriptome based on the top 1000 differentially expressed genes across colon tissues isolated at day 8 from mice receiving Tcon alone (blue dots) or Tcon and Treg (red dots). (C) Top 10 enriched terms/pathways in colon Tcon from mice receiving Tcon and Treg (positive NES, red bars indicate the significant patways) or Tcon alone (negative NES, blue bars indicate the significant pathways) revealed by Hallmark GSEA. (D) Enrichment plots displaying enrichment scores for the genes involved in allograft rejection (HALLMARK ALLOGRAFT REJECTION) and oxidative phosphorylation (HALLMARK OXIDATIVE PHOSPHORILATION) from colon tissues recovered at day 8 after HCT in the presence or absence of Treg.

602 603 604

605

606

607

608

609

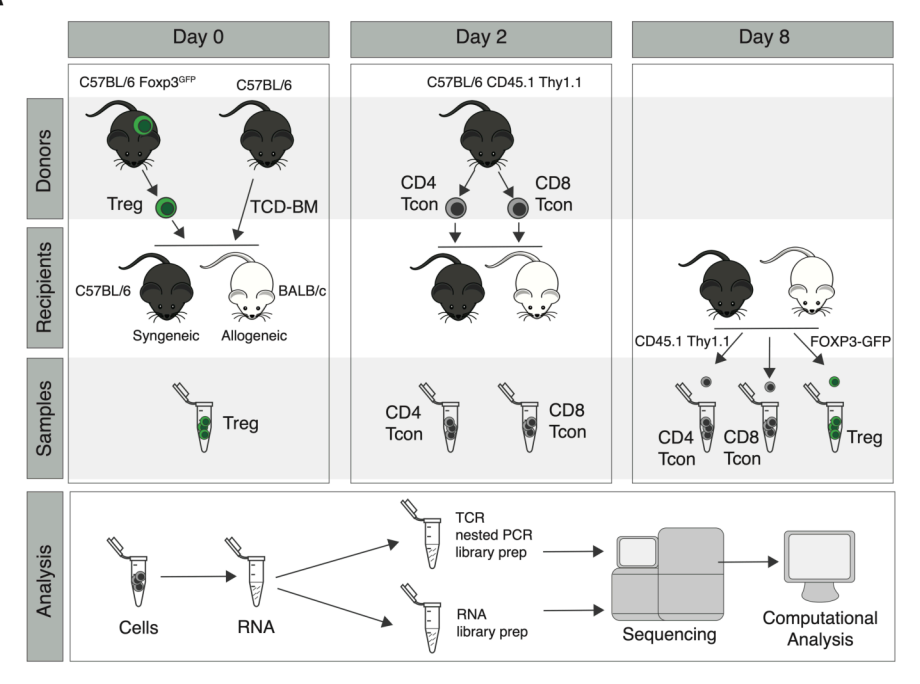
610

611

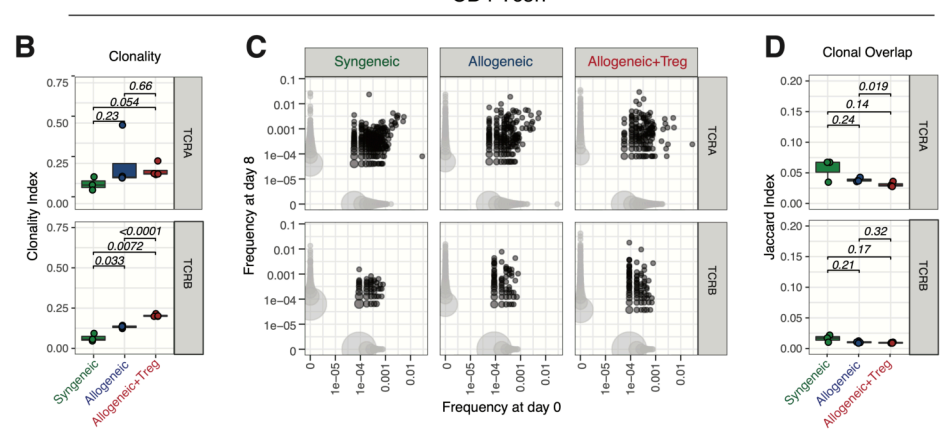
612

Figure 7. Treg did not inhibit the upregulation of gene sets involved in the GvT effect. (A) Transcript expression of effector molecules (Ifng, Il2, Tnf) in CD4 Tcon. (B) Enrichment plots enrichment scores for the genes involved in leucocyte (GO LEUKOCYTE MEDIATED CYTOTOXICITY) from CD4 Tcon recovered at day 8 after HCT in the presence or absence of Treg. (C) Transcript expression of effector molecules (Ifng. Gzmb, Prf1) in CD8 Tcon. (D) Enrichment plots displaying enrichment scores for the genes involved in leucocyte cytotoxicity (GO LEUKOCYTE MEDIATED CYTOTOXICITY) from CD8 Tcon recovered at day 8 after HCT in the presence or absence of Treg. Gene signatures were obtained from Molecular Signatures Database (MSigDB).

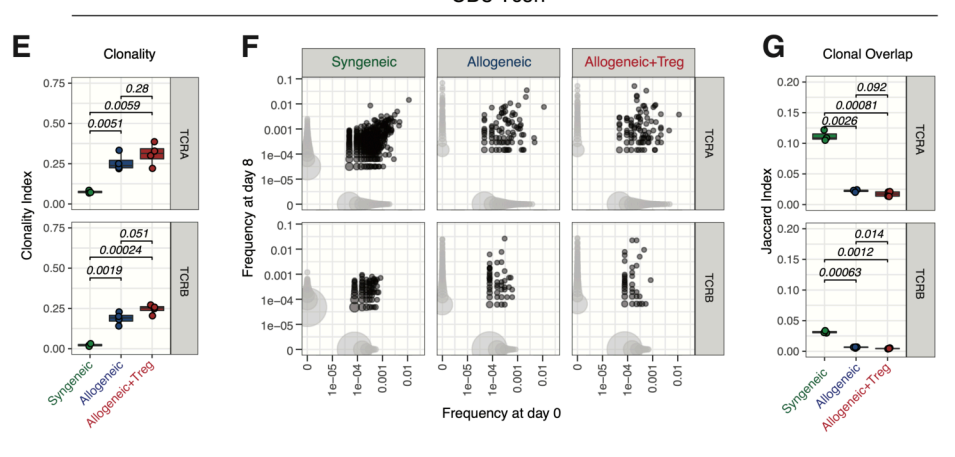
Α

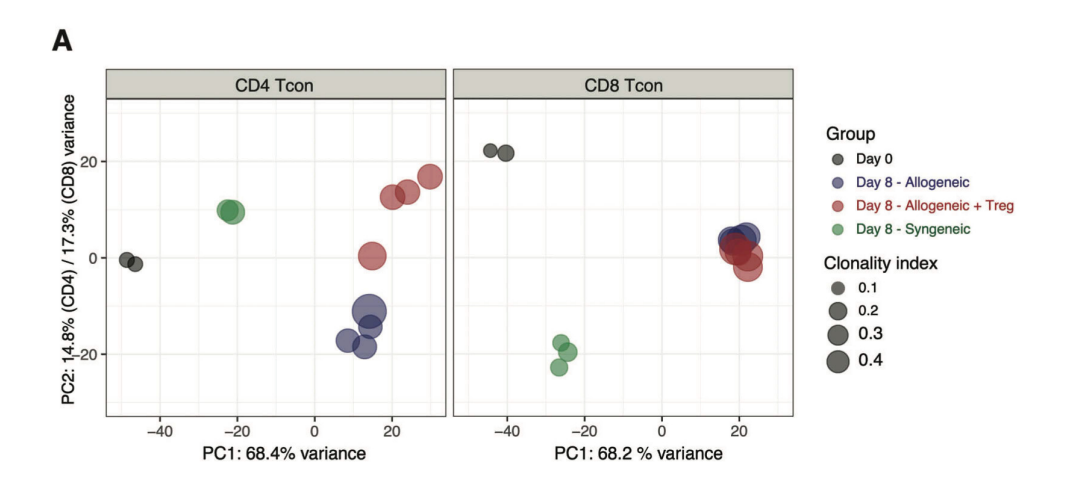


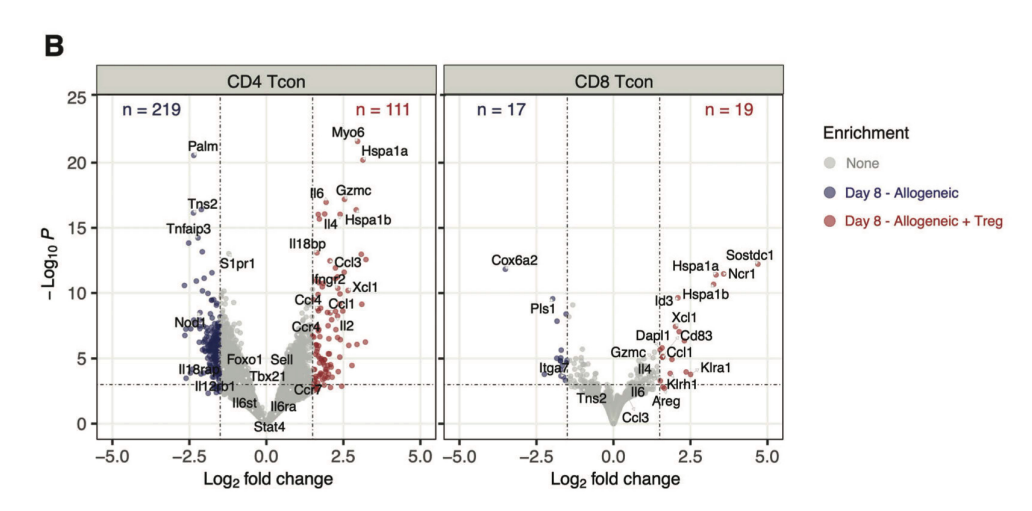
CD4 Tcon

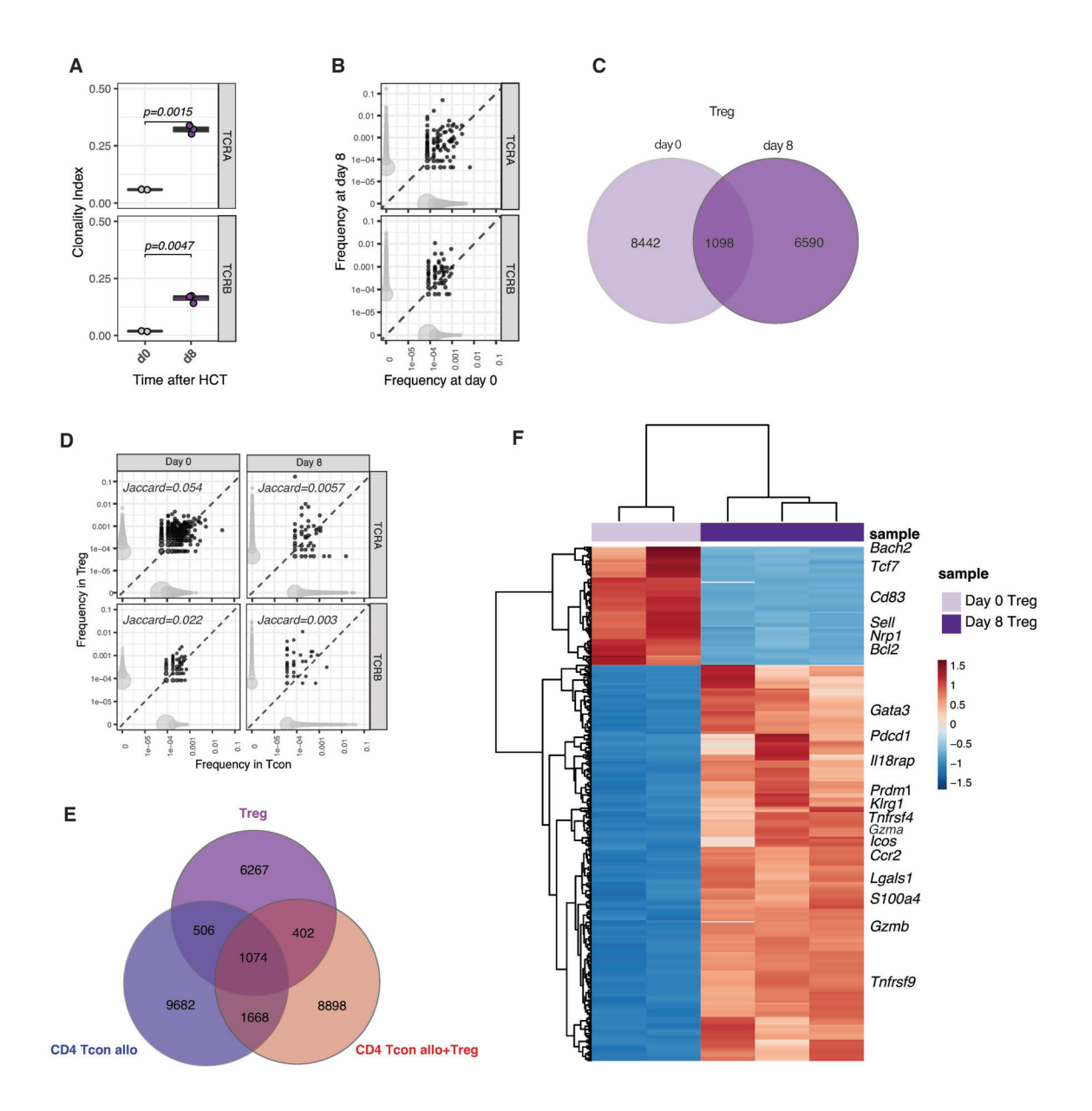


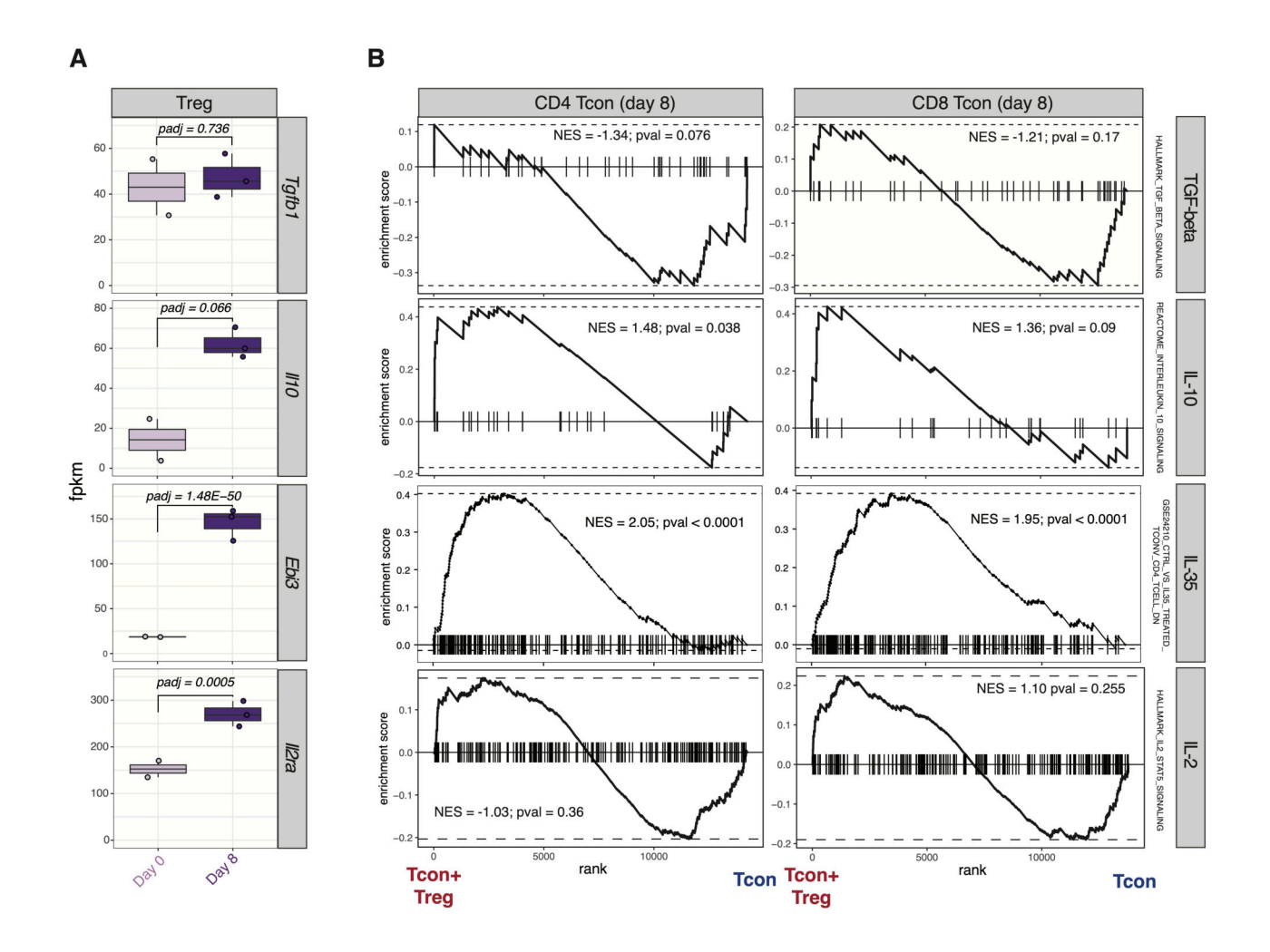
CD8 Tcon

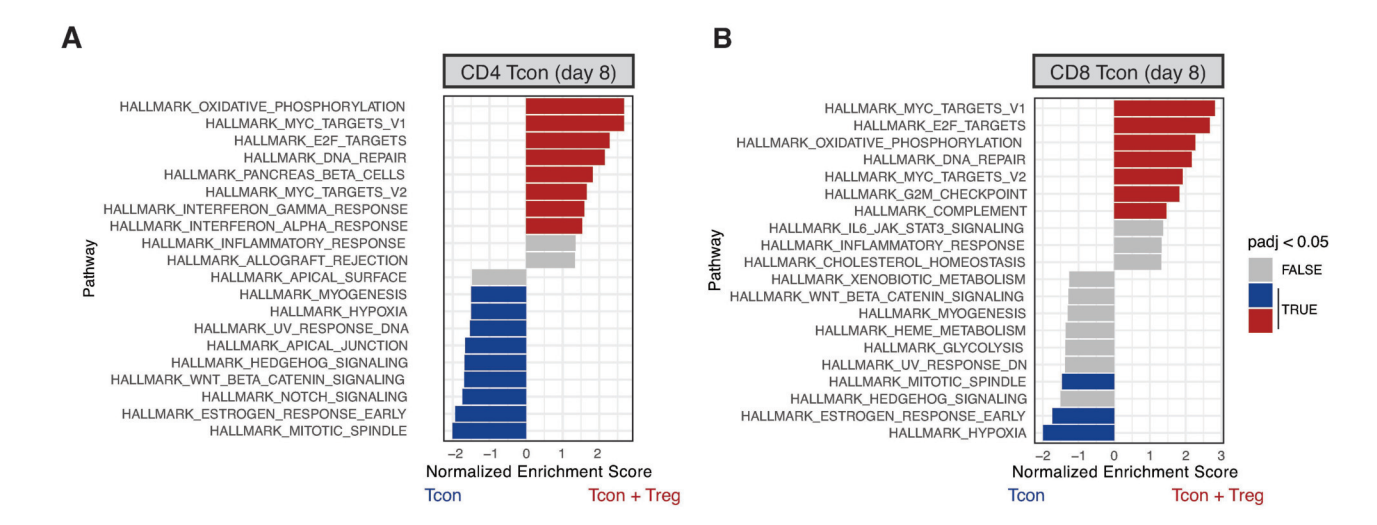


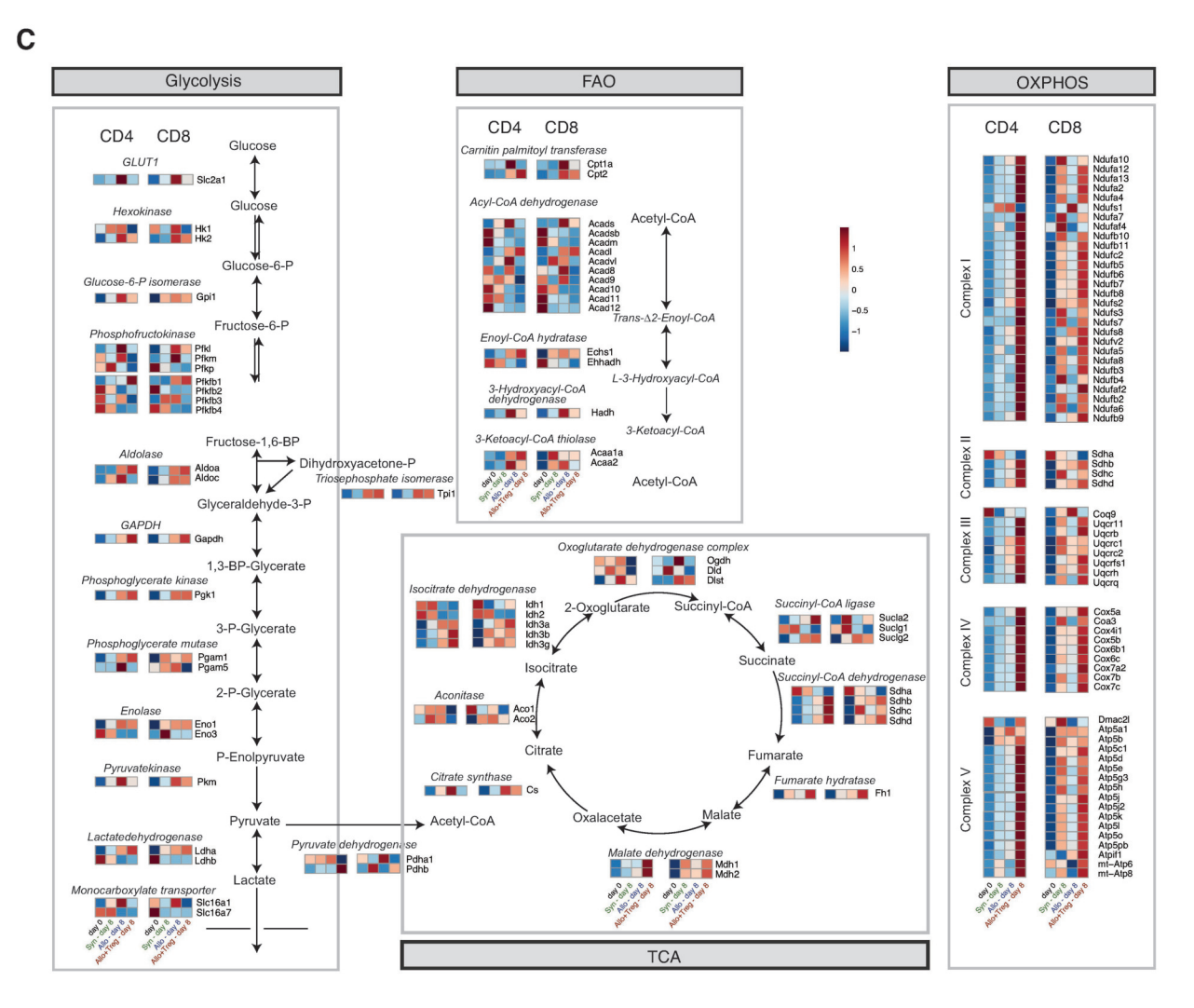


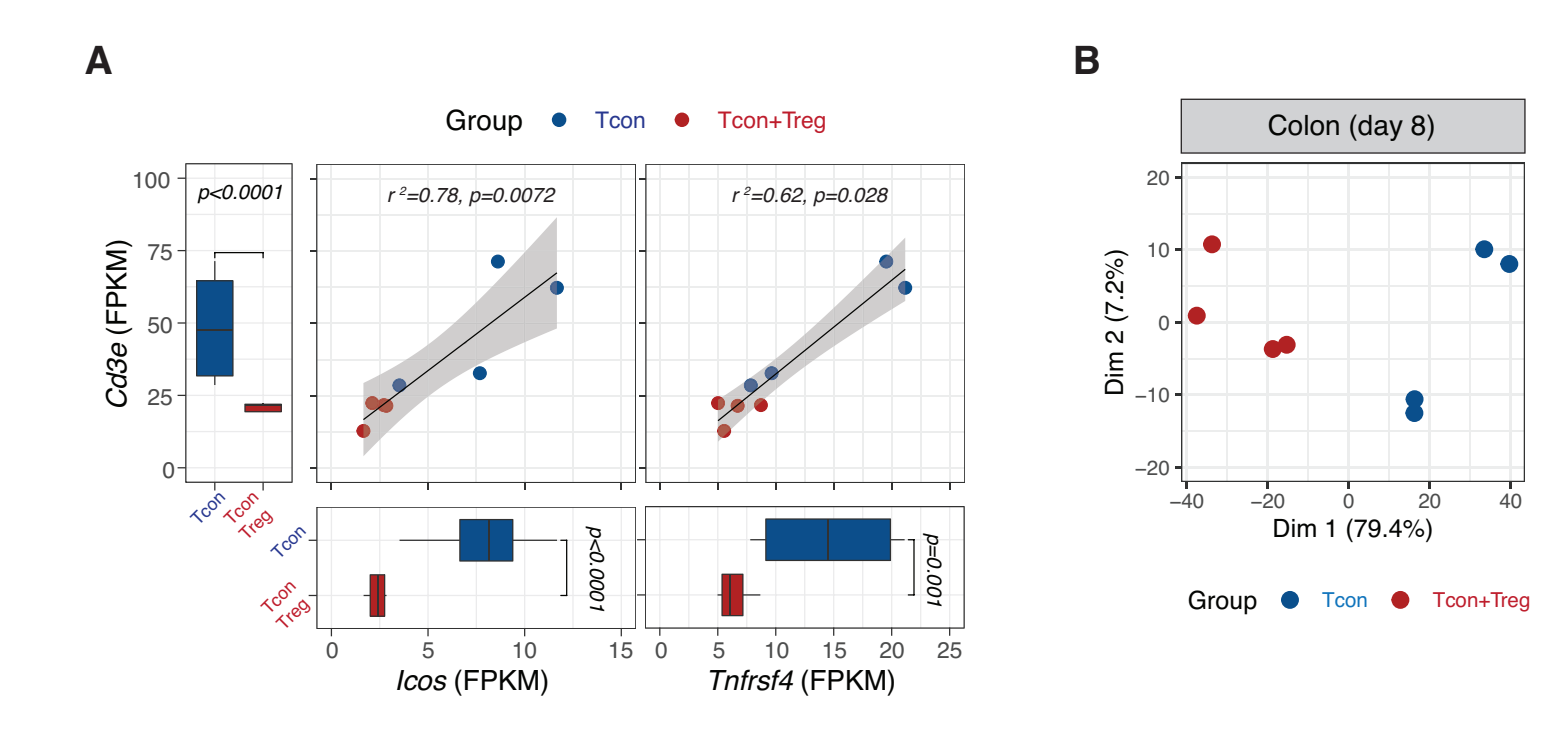


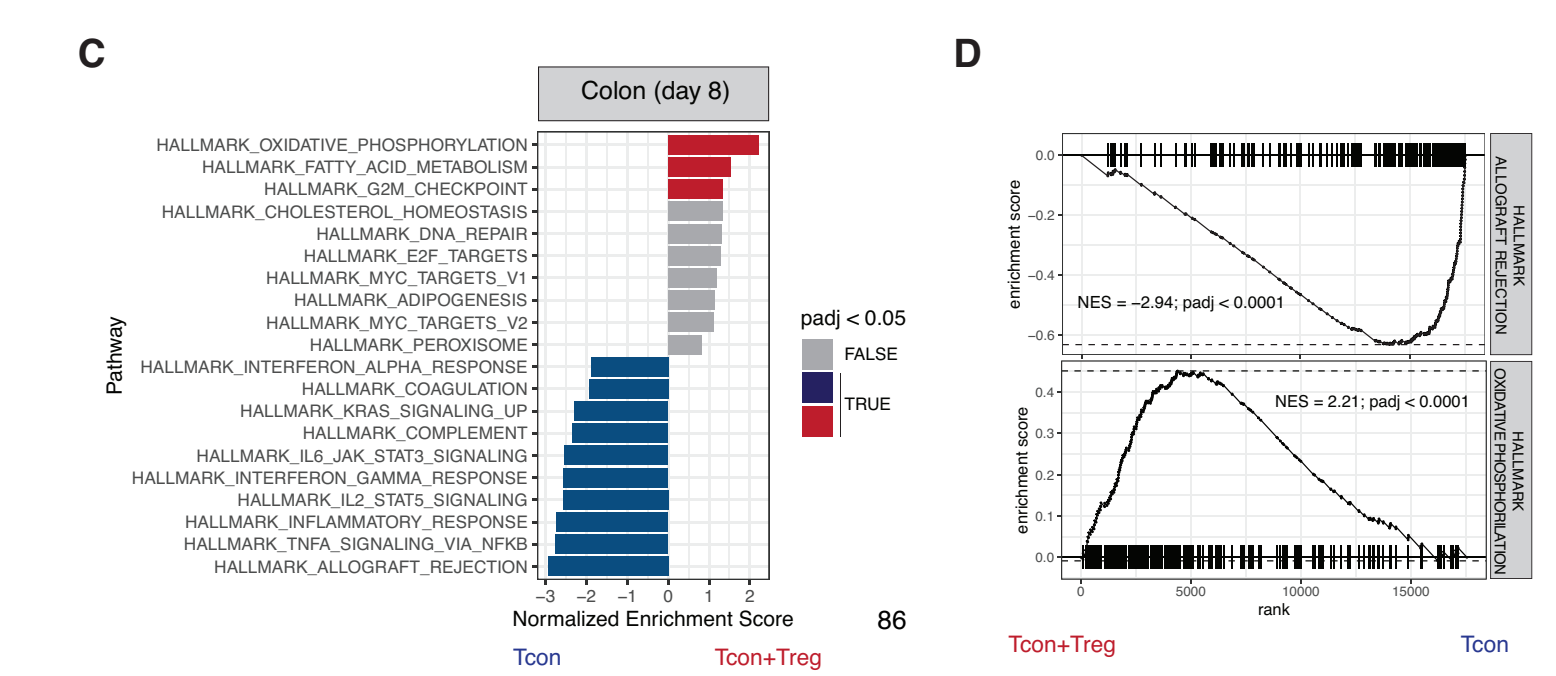


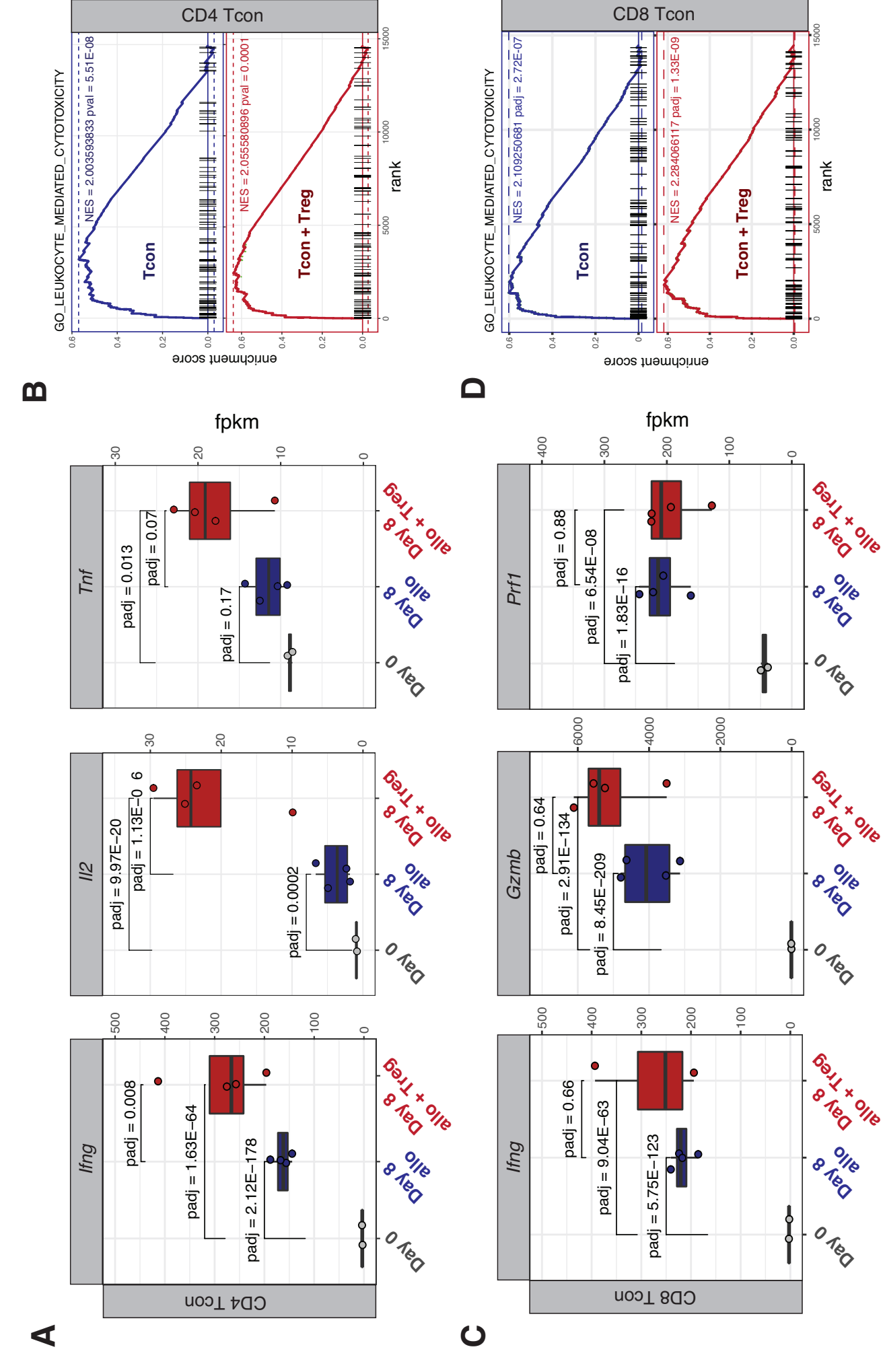












#### 3.5. Publication 5

Pradier A, Mamez AC, Stephan C, Giannotti F, Masouridi-Levrat S, Wang S, Morin S, Neofytos D, Vu DL, Melotti A, Arm I, Eberhardt CS, Tamburini J, Kaiser L, Chalandon Y, <u>Simonetta F.</u> T cell receptor sequencing reveals reduced clonal breadth of T-cell responses against SARS-CoV-2 after natural infection and vaccination in allogeneic hematopoietic stem cell transplant recipients. **Ann Oncol. 2022** S0923-7534(22)04144-8. doi: 10.1016/j.annonc.2022.09.153.

The SARS-CoV-2 pandemic represented an unprecedented opportunity to investigate the ability of allogeneic HSCT recipients to react to antigens, presented in the context of natural infection and/or vaccination, toward which neither the donor nor the recipient had been previously exposed. After the mRNA-based vaccines became available we were among the first groups reporting reduced antibody response rates in allogeneic HSCT recipients in comparison with the general population (Mamez et al., 2021). Subsequently, in this second work we extended our analysis to SARS-CoV-2 specific T cell responses. We used for the first time high-throughput TCR beta sequencing to identify, quantify and characterize SARS-CoV-2-specific T cell clonotypes in allogeneic HSCT recipients and healthy controls after both COVID-19 natural infection and vaccination. Our analysis revealed a reduced breadth of SARS-CoV-2 specific T cell responses to infection and vaccination in allogeneic HSCT recipients compared to healthy controls. Such a reduction in different SARS-CoV-2-specific T cell clonotypes was associated with a reduction in the number of T cells producing IFN-γ after restimulation with SARS-CoV-2 peptides as measured by ELISpot. Conversely, no relationship between SARS-CoV-2 specific T cell clonal breath and humoral responses was observed. As previously reported, allogeneic HSCT recipients displayed an increased clonality and a reduced TCR diversity. Importantly, the inverse correlation between the breadth of SARS-CoV-2 specific T cell clonotypes and the clonality of the TCR repertoire pointed to the impaired immune-reconstitution and reduced TCR diversity after allogeneic HSCT as a main cause of reduced responses against SARS-CoV-2. Our results demonstrate, for the first time using a new pathogen as a model, that allogenic HSCT recipients have a reduced ability to mount physiological T cell responses against new epitopes as a consequence of their impaired immune-reconstitution.

tumor event: a propensity score-matched cohort analysis of the GEC-ESTRO Breast Cancer Working Group Database. *Int J Radiat Oncol Biol Phys.* 2021;110(2):452—461.

T cell receptor sequencing reveals reduced clonal breadth of T-cell responses against SARS-CoV-2 after natural infection and vaccination in allogeneic hematopoietic stem cell transplant recipients



Allogeneic hematopoietic stem cell transplantation (HSCT) recipients have a higher risk of developing severe coronavirus disease (COVID-19) and a higher mortality rate compared with the general population (Ljungman et al.¹) potentially also as a consequence of their reduced ability to respond to vaccination (Mamez et al.²; Redjoul et al.³; Einarsdottir et al.⁴). To evaluate the magnitude and breadth of T-cell responses against SARS-CoV-2 in allogeneic HSCT recipients, we carried out high-throughput T cell receptor (TCR) repertoire profiling on cells recovered from allogeneic HSCT recipients or healthy controls (HC) after COVID-19 natural infection or messenger RNA (mRNA)-based vaccination.

Peripheral blood samples were obtained after COVID-19 infection from allogeneic HSCT recipients (n = 11; Supplementary Tables S1 and S2, available at https://doi. org/10.1016/j.annonc.2022.09.153) or HC (n = 10; Supplementary Material, available at https://doi.org/10. 1016/j.annonc.2022.09.153). A total of 6 out of 11 patients were under immunosuppression for active (n = 3) or resolved (n = 3) graft-versus-host disease. T-cell receptor (TCR) beta sequencing (Supplementary Material, available at https://doi.org/10.1016/j.annonc.2022.09.153) identified SARS-CoV-2 specific T-cell clonotypes in both HC and HSCT recipients after COVID-19 infection (Figure 1A). No difference was observed in the proportion of T cells specific for SARS-CoV-2 between HSCT recipients and HC (data not shown). The diversity of the SARS-CoV-2-specific T-cell clonotypes, a measure previously shown to be inversely associated with severity of the disease (Elyanow et al.<sup>5</sup>), however, was significantly reduced in HSCT recipients compared with HC (Figure 1B). Enzyme-Linked ImmunoSpot (ELISpot) assay (Supplementary Material, available at https://doi.org/10.1016/j.annonc.2022.09.153) showed significantly lower numbers of interferon-  $\gamma$  (IFN- $\gamma$ ) spot forming units (SFU) after stimulation of PBMCs from HSCT recipients with peptides from both the SARS-CoV-2 spike (S) protein (Figure 1B, upper panel) and the membrane glycoprotein (M) plus the nucleocapsid phosphoprotein (N) proteins (data not shown) compared with HC. A significant positive correlation between SARS-CoV-2-specific T-cell clonotypes and IFN-γ SFU was observed (Figure 1B, upper panel). Conversely, we detected no significant difference in anti-S immunoglobulin G (IgG) titers and no correlation

between antibody titers and different clonotypes (Figure 1B, middle panel). HSCT recipients displayed a less diverse TCR repertoire compared with HC as revealed by higher Simpson clonality and the Simpson clonality negatively correlated with the number of different SARS-CoV-2-specific T-cell clonotypes (Figure 1B, lower panel).

We next carried out the same analysis on samples recovered from allogeneic HSCT recipients (n = 11; Supplementary Tables S1 and S2, available at https://doi. org/10.1016/j.annonc.2022.09.153) or from healthy controls (n = 10) after vaccination with three doses of mRNAbased SARS-CoV-2 vaccines (Supplementary Material, available at https://doi.org/10.1016/j.annonc.2022.09.153). We observed a significant reduction in different S-proteinspecific T-cell clonotypes in allogeneic HSCT recipients compared with HC (Figure 1C and D). ELISpot analysis revealed significantly lower numbers of IFN-γ SFU in HSCT recipients compared with HC and a slightly significant positive correlation between the ELISpot and the TCR-seq results (Figure 1D, upper panel). We observed slightly reduced anti-S titers in HSCT recipients compared with HC and a trend toward a positive correlation between S-specific clonotypes and anti-S titers (Figure 1D, middle panels). We detected a negative correlation between the Simpson clonality and the number of different S-protein-specific Tcell clonotypes after vaccination (Figure 1D).

Our results indicate that allogeneic HSCT recipients display reduced breadth of SARS-CoV-2-specific T-cell clonotypes after COVID-19 infection and vaccination. No clear correlation was detected between TCR clonal breadth and anti-S IgG titers. The clonal breadth defect was associated with increased T-cell clonality after HSCT, pointing to the reduced diversity of the TCR repertoire as a mechanism leading to impaired cellular responses against SARS-CoV-2 in HSCT recipients.

A. Pradier<sup>1,2,†</sup>, AC. Mamez<sup>1,\*†\*</sup>, C. Stephan<sup>1</sup>, F. Giannotti<sup>1</sup>, S. Masouridi-Levrat<sup>1</sup>, S. Wang<sup>2</sup>, S. Morin<sup>1</sup>, D. Neofytos<sup>3</sup>, D. L. Vu<sup>3</sup>, A. Melotti<sup>2</sup>, I. Arm<sup>4</sup>, C. S. Eberhardt<sup>5</sup>, J. Tamburini<sup>2</sup>, L. Kaiser<sup>3,4,6</sup>, Y. Chalandon<sup>1,2</sup> & F. Simonetta<sup>1,2\*\*</sup>

<sup>1</sup>Division of Hematology, Department of Oncology, Geneva University Hospitals, University of Geneva, Geneva; <sup>2</sup>Translational Research Centre in Onco-Haematology, Faculty of Medicine, University of Geneva, Geneva; <sup>3</sup>Division of Infectious Diseases, Geneva University Hospitals, Geneva;

<sup>4</sup>Laboratory of Virology, Division of Infectious Diseases and Division of Laboratory Medicine, University Hospitals of Geneva & Faculty of Medicine, University of Geneva, Geneva:

<sup>5</sup>Center for Vaccinology, University Hospitals of Geneva Division of General Pediatrics, Department of Woman, Child and Adolescent Medicine, Faculty of Medicine, University of Geneva, Geneva; Annals of Oncology

Letters to the editor

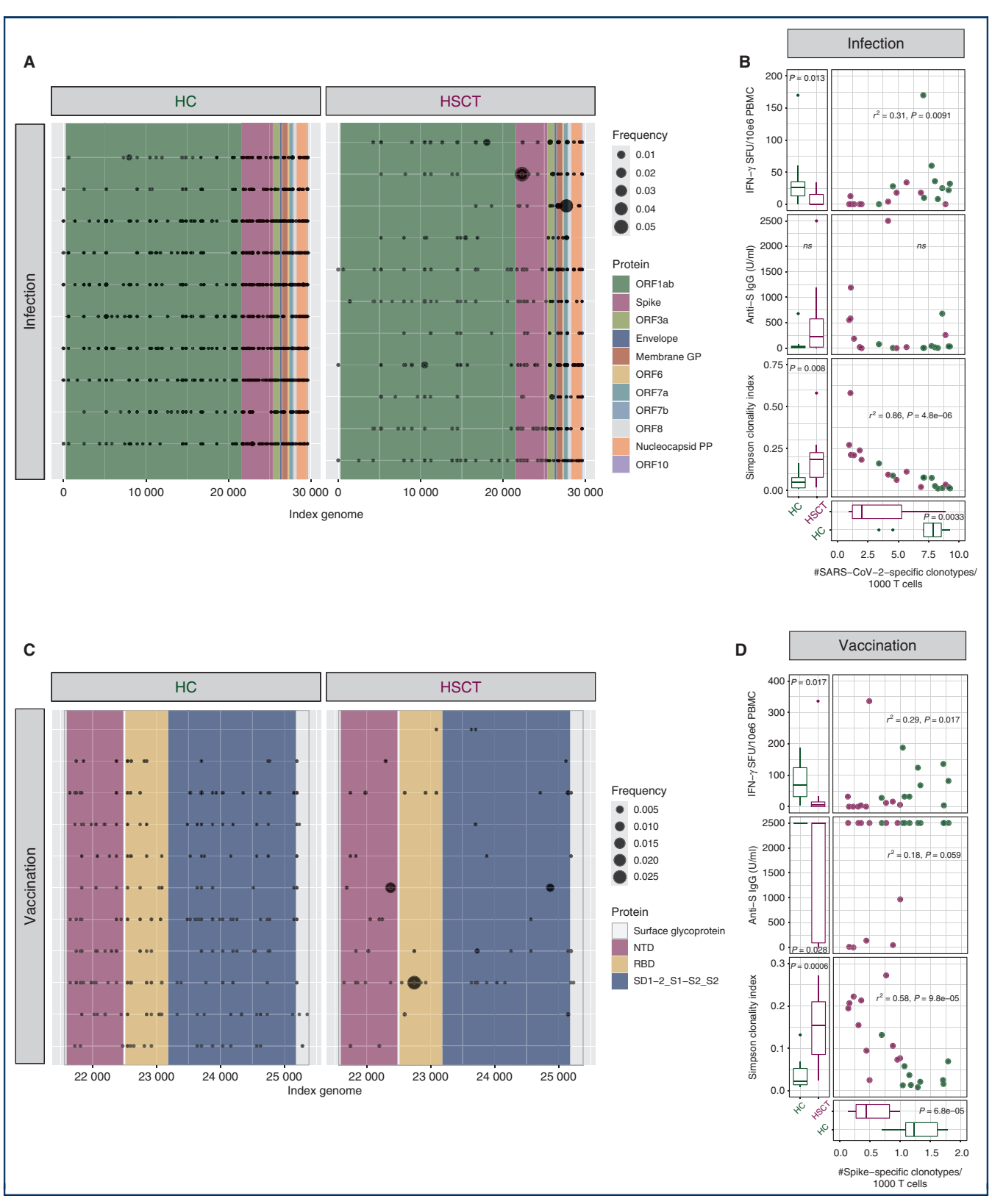


Figure 1. Reduced SARS-CoV2-specific T-cell clonotypes after COVID-19 infection and vaccination in allogeneic HSCT recipients. (A, C) SARS-CoV-2-specific T-cell clonotypes visualized based on the putative sequence of the SARS-CoV-2 genome recognized. (B, D) Scatter plots and marginal bar plots correlating and comparing the number of different SARS-CoV-2-specific T-cell clonotypes/1000 T cells, the anti-S IFN-γ SFU, the anti-S IgG titers and the Simpson clonality index in HC and HSCT. Differences between groups were assessed using the Mann—Whitney *U* test. Correlations were evaluated using a Spearman rank correlation coefficient test. GP, glycoprotein; HC, healthy controls; HSCT, hematopoietic stem cell transplantation; IFN, interferon; IgG, immunoglobulin G; NTD, N-terminal domain; PP, phosphoprotein; RBD, receptor binding domain; SFU, spot forming units.

<sup>6</sup>Geneva Centre for Emerging Viral Diseases, Geneva University Hospitals, Geneva, Switzerland (\*E-mail: anne-claire.mamez@hcuge.ch) (\*E-mail: federico.simonetta@unige.ch).

<sup>†</sup>These authors contributed equally to this work.

Available online 16 September 2022

© 2022 European Society for Medical Oncology. Published by Elsevier Ltd. All rights reserved.

https://doi.org/10.1016/j.annonc.2022.09.153

#### **FUNDING**

This work was supported by the Dubois-Ferrière-Dinu-Lipatti Foundation (no grant number) to ACM, the Geneva University Hospitals' Private Foundation (no grant number) to ACM, the Geneva University Hospitals' Clinical Research Center [grant number PRD 13-21-I] to ACM, the Choose Life Foundation (no grant number) to YC and FS, the Fondation Gustave & Simone Prévot (no grant number) to FS and the Geneva Cancer League [grant number LGC 20 11] to FS.

#### **DISCLOSURE**

The authors have declared no conflicts of interest.

#### **REFERENCES**

- Ljungman P, de la Camara R, Mikulska M, et al. COVID-19 and stem cell transplantation; results from an EBMT and GETH multicenter prospective survey. Leukemia. 2021;35(10):2885–2894.
- Mamez AC, Pradier A, Giannotti F, et al. Antibody responses to SARS-CoV2 vaccination in allogeneic hematopoietic stem cell transplant recipients. Bone Marrow Transplant. 2021;56(12):3094—3096.
- Redjoul R, Le Bouter A, Parinet V, et al. Antibody response after third BNT162b2 dose in recipients of allogeneic HSCT. Lancet Haematol. 2021;8(10):e681—e683.
- Einarsdottir S, Martner A, Waldenström J, et al. Deficiency of SARS-CoV-2
  T-cell responses after vaccination in long-term allo-HSCT survivors translates into abated humoral immunity. Blood Adv. 2022;6(9):2723—2730.
- Elyanow R, Snyder TM, Dalai SC, et al. T cell receptor sequencing identifies prior SARS-CoV-2 infection and correlates with neutralizing antibodies and disease severity. JCI Insight. 2022;7(10), e150070.

#### 4. Conclusion and perspectives

In the works summarized above we demonstrated how the use of multimodal immunomonitoring after allogeneic HSCT and cellular therapies can lead to further diagnostic and therapeutic developments. Previously restricted mainly to the quantitative evaluation of persistence and expansion of the administered cellular therapies, immunomonitoring can nowadays provide big amounts of quantitative and qualitative information about the cell therapy product as well as about its interaction with the host. We will next discuss how the knowledge acquired from these studies can be further extended in future research and hopefully exploited for clinical translation over the next years.

# 4.1. Molecular imaging of allogeneic HSCT and cellular therapies - summary of the results and future directions

In our molecular imaging studies, we exploited radiotracers for the identification of activation markers previously generated for monitoring of endogenous immune responses, such as OX40 (Alam et al., 2018) and ICOS (Xiao et al., 2020), to the field of allogeneic HSCT and adoptive cellular therapies. In a first study, we tested the use of OX40-immunoPET in murine models of HSCT and we demonstrated that this approach was able to detect T cell activation, expansion, and tissue infiltration during acute GvHD (Alam et al., 2020). However, our strategy had a major limitation related to the toxicity of the tracer employed: the 64Cu-OX40mAb was generated using an agonist anti-OX40 mAb and this led to the exacerbation of GvHD when administered early after allogeneic HSCT. These results stress the importance of testing the biological impact of radiotracers targeting immunological molecules. Given the extremely low mass doses employed for imaging purposes, very little if any biological effect is expected from the use of radiotracers. However, considered the extremely high specificity and affinity of mAb we can expect that, depending on the agonistic or antagonistic nature of the antibody employed and on the nature of the immune-process investigated (immune-effector therapy or immuno-pathological process), a given radiotracer can exert null, positive or negative effects. To circumvent this limitation we undertook two, potentially complementary approaches: 1) we used publicly available data that we and other generated in independent studies to identify alternative molecules to be used as targets; 2) given the immunopathological nature of the process investigated (GvHD) we moved from an agonistic to an antagonistic mAb. Our analysis of already available RNAseq data identified ICOS as a potential candidate for GvHD imaging both in murine and human cells. After confirming ICOS expression at the protein level on T cells during GvHD, we demonstrated that immunoPET using a 89Zr-DFO-ICOSmAb efficiently visualized T cell activation, expansion and tissue infiltration during murine GvHD (Xiao et al., 2022). Importantly, we did not observe any toxicities of our tracer. This can be due to the target molecule selected and/or to the antagonist nature of the mAb employed. Allogeneic HSCT is primarily performed for its GvT effect and the use of an antagonistic mAb might therefore results of an interference of the radiotracer of such antitumor effect. Using a classical GvT model employing the A20 lymphoma cell line in a major MHC-mismatch model of HSCT, we demonstrated that the administration of tracer doses of anti-ICOS mAb did not interfere with the ability of allogeneic T cells to control tumor growth. We cannot exclude that having switched from an agonist to an antagonist clone for OX40 might have resulted in a similar safety profile without the need to change the molecular target.

An even better approach would be to design a tracer that has no biological effect on the molecule target, neither agonistic nor antagonistic. This would allow to use a given tracer independently of the biological process investigated. However, this will need in most cases the generation of entirely new mAb clone as the great majority of already available ones were developed to activate or to block biological pathways. Alternatively, antibody fragments generated from already available clones might allow the use of previously developed mAbs after depriving them of their biological activity. No matter the approach that will be employed, for future clinical translation it will be essential to extensively test the safety of the radiotracer before employing it in patients.

Once a promising immunoPET radiotracer will be identified for molecular imaging of GvHD, it will remain the issue of how to employ it in clinical practice. One option would be to employ it as a screening strategy in all allogeneic HSCT recipients at selected time points after transplantation. Given the high complexity and the significant costs of immunoPET, it is however unlikely that this approach will prove to be cost-effective when employed as a general screening tool. A second option could be to restrict its use to patient populations at particular risk of developing GvHD based on some clinical criteria (ex. donor type employed). Alternatively, the use of immunoPET for detection of gastrointestinal GvHD, the deadliest form of GvHD, could be triggered by other clinical signs frequently preceding or accompanying it such as skin GvHD. Given the great results accomplished with the use of blood biomarkers of GvHD, such as REG3 $\alpha$  and ST2 (Levine et al., 2015), we can imagine a scenario in which immunoPET use will be triggered by positive results coming from the cheaper and more easily accessible blood biomarkers.

In addition to GvHD diagnosis, immunoPET has a great potential as a tool to assess the severity of GvHD in order to guide therapy. We have recently seen the promising results of clinical trials adjusting the intensity of anti-GvHD therapy based on the severity of GvHD assessed on clinical and biological criteria (Pidala et al., 2020; Etra et al., 2022). Similarly, immunoPET could be used to evaluate the extent and severity of GvHD in a more comprehensive way compared to endoscopy and biopsies thus allowing to identify patients at low and high risk GvHD and helping to adapt the treatment accordingly.

The use of immunoPET targeting activation molecules can be applied to other forms of T-cell based therapies such as for example CAR T cells. We were the first to attempt this using ICOS-immunoPET in a murine model of B-cell lymphoma treated by CAR T cells (Simonetta et al., 2021a). Using the aforementioned 89Zr-DFO-ICOSmAb, we showed that ICOS-immunoPET was able to detect CAR T cell activation and expansion at the tumor site. Similarly, to our GvHD-studies, we tested the safety of our tracer in this setting and showed that tracer doses of ICOS mAb did not interfere with CAR T cell expansion, persistence and, most importantly, antitumor activity.

Based on these and other (Hirai et al., 2021) preclinical results we obtained using murine specific tracers, we are now in the process of developing human specific tracers to be employed for clinical transition. This work, still conducted in collaboration with Drs Israt Alam and Michelle James at Stanford University who are leading the molecular imaging part, will aim to develop anti-human OX40- and ICOS-specific 89Zr-radiolabeled monoclonal antibodies with minimal biological activity that we will test in murine model of xenogeneic GvHD and CAR T cell therapy. Once the tracers will be developed and preclinically validated, we will proceed to their clinical translation in patients receiving allogeneic HSCT and immune-effector cellular therapies.

# 4.2. Immune-effector and immuno-regulatory cellular therapies - summary of the results and future directions

We have discussed four examples of how high-throughput sequencing technologies can provide quantitative and qualitative information about the adoptively transferred cells as well about the endogenous cells and tissues.

In Maas-Bauer et al., 2021, we employed a wide range of molecular techniques, including RNAseq, single-cell RNAseq and ATACseq, to better define the transcriptomic and epigenomic heterogeneity of iNKT cell subsets. After conducting a series of *in vitro* and *in vivo* functional assays demonstrating the functional heterogeneity of iNKT1, iNKT2 and iNKT17, we performed a transcriptomic analysis of CD4 and CD8 Tcon recovered after transplantation in the presence of the different iNKT cell subsets. This was to the best of our knowledge the first transcriptomic analysis assessing the impact of an immunoregulatory cellular therapy for GvHD prevention. Collectively, this study was important in order to define the characteristics of iNKT cellular products needed for different cellular therapy applications, namely iNKT1 for anti-tumor therapies and iNKT2 and/or iNKT17 for immune-regulatory therapies. Leveraging on these results we are now in the process of developing expansion protocols to specifically obtain human iNKT cells displaying an iNKT1 or an iNKT2 phenotype with the plan to exploit

the different cellular products for different purposes, iNKT1 as immune-effector therapy against cancer and iNKT2 as immune-regulatory therapy to prevent GvHD.

As an extension of our preclinical work on iNKT cells, we built upon the antitumor effect of iNKT1 cells by expanding splenic-derived murine iNKT cells and engineering them with a murine CD19 CAR (Simonetta et al., 2021b). Having for the first time fully murine CAR iNKT cells allowed us to study their interplay with the host immune system and to demonstrate that CAR iNKT cells have both a direct and, most importantly, an indirect antitumor effect by inducing CD8 T cell cross-priming. This effect was, in our model, stronger with CAR iNKT cells than in conventional CAR T cells. Importantly, given that the long-term antitumor effect was mediated by host T cells rather than from the allogeneic product whose persistence was extremely limited, CAR iNKT cells led to only a very transient on-target off-tumor effect on normal B cells, with prompt resolution of the B-cell aplasia. This offers a major advantage if we want to exploit the potential of CAR iNKT cells in diseases where on-target off-tumor toxicities cannot be tolerated, such as in myeloid malignancies. A major limitation to the development of CAR T cells against acute myeloid leukemia (AML) is the fact that most available targets expressed at AML cells surface are expressed by normal myeloid progenitors and/or mature cells as well. An on-target off-tumor effect would therefore lead to a nonclinically tolerable myelotoxicity. We hypothesize that taking advantage of their indirect effect and their short persistence, allogeneic CAR iNKT cells can circumvent such obstacle. We are therefore developing CAR iNKT cells targeting a series of myeloid surface antigens including CD33, CD123 and CD38 that we are testing in vitro and in vivo. Given their lack of alloreactive potential, we hypothesize that CAR iNKT cells targeting different antigens might be mixed even when originating from different donors. Being able to multiplex off-the-shelf allogeneic CAR T cells with different specificities would be extremely useful in an extremely heterogeneous disease such as AML.

CD4+ CD25+ FOXP3+ regulatory T cells (Treg) are a second immune-regulatory cell population that is currently at a more advanced stage of clinical development compared to iNKT cells for GvHD prevention. The preclinical studies demonstrating their efficacy in the experimental setting are now 20 years old (Edinger et al., 2003) and this approach is now finally tested in an ongoing phase III prospective randomized, multicenter clinical trial. Despite this, we still don't know the mechanisms through which Treg can suppress GvHD without interfering with the GvT effect of the transplant procedure. To elucidate them, we applied an analytical pipeline similar to the one employed in our iNKT study to evaluate the impact of Treg on Tcon during GvHD prevention (Lohmeyer et al., 2022). We combined the analysis of the transcriptome with the analysis of the TCR repertoire on Tcon and Treg before and after transplantation. Our results identified several qualitative transcriptomic effects of Treg on Tcon

in addition to provide strong evidence that Treg as well undergo clonal expansion and activation during GvHD suppression. Importantly, our data point to a series of non-redundant, complementary mechanisms employed by Treg to suppress GvHD. Some of them are classical Treg-suppression mechanisms such as IL-10 and IL-35 production. In addition, our analysis revealed a major impact of Treg in the modulation of the transcription of genes involved in T cell metabolism, with suppression of the transcription of genes encoding molecules involved in glycolysis and upregulation of those involved in oxidative phosphorylation. Conversely, Treg upregulated genes involved in both glycolysis and oxidative phosphorylation suggesting that they can rely on both pathways for their activation, expansion and function during GvHD suppression. We plan to build upon this finding to develop pharmacological protocols of GvHD prevention based on metabolism modulators, to either reduce glycolysis, by inhibiting hexokinase using 3-Bromopyruvate or transketolase using oxythiamine, and/or enhance oxidative phosphorylation using the pyruvate dehydrogenase kinase (PDK) inhibitor dichloroacetate for example. In particular, we are interested in combining such and immune-metabolic modulators with Treg therapy with the aim of maximizing their function. Such approach will be tested in preclinical models of GvHD using both murine and human cells.

Our Treg and iNKT studies combined offer a comprehensive analysis of the transcriptomic impact of the two main immunoregulatory T cell populations, Treg and iNKT cells, reported to suppress GvHD in murine models of HSCT and whose clinical translation is currently ongoing. Some conclusions can be drawn by the combined analysis of the two datasets to obtain a list of genes suppressed in CD4 and CD8 Tcon by both Treg and iNKT cells. We believe that this combined analysis will offer a great opportunity to identify genes involved in GvHD but dispensable for the GvT effect. We plan to use the CRISPR/Cas9 technology to knock-out one or more of these genes at the same time in Tcon to be tested in murine models of GvHD using both murine and human cells. Our hypothesis is that ablation of Treg/iNKT-modulated genes using gene editing will allow the generation of a cellular product deprived of any GvHD induction potential but retaining its antitumor capacity. There is a great interest in developing new strategies of graft and donor lymphocyte infusion engineering based on the selection of different cell population (ex. CD45RA-depletion, TCRαβ/CD19-depletion) to prevent GvHD but still provide a benefit in terms of antitumor effect. If our objective will be achieved, our future studies will pave the way to the use of gene edited grafts and donor lymphocyte infusions.

Our recent study on T cell responses to SARS-CoV-2 antigens after natural infection or vaccination investigated the mechanisms underlying the impaired responses previously reported in allogeneic HSCT recipients and incompletely understood. We used high-

throughput T cell receptor (TCR) beta sequencing and ELISpot to study SARS-CoV-2-specific T cells in allogeneic HSCT recipients and healthy controls. Our analysis revealed a reduced breadth of SARS-CoV-2 specific T cell responses to infection and vaccination in allogeneic HSCT recipients compared to healthy controls, pointing to the impaired immune-reconstitution and reduced TCR diversity after allogeneic HSCT as a main cause of reduced responses against SARS-CoV-2 (Pradier et al., 2022). Although somewhat predictable, our results demonstrate, for the first time using an infection that neither the donor nor the recipient had encountered before as a model, that the TCR restriction observed after allogeneic HSCT leads to an impaired ability of HSCT recipients to mount physiologically diverse response against new antigens. We predict that such abnormality will not be exclusive of SARS-CoV-2-specific T cell responses but will be found in T cells with other specificities and we hypothesize that this might at least in part justify the state of immune-impairment observed in allogeneic HSCT recipients against viral infections. We are testing this hypothesis in an ongoing observational study investigating immune-reconstitution in haploidentical HSCT recipients, known to display a high degree of immune-deficiency post-transplant. Moreover, we will assess the ability of haploidentical allogeneic CD45RA-depleted DLI to restore TCR diversity and, hopefully, improve protection in a phase I clinical trial currently ongoing in our Division (CE 2019-02433, Swiss Medic authorization number: 2020TpP1009, PI: Anne-Claire Mamez, MD).

#### 5. References

- Alam, I.S., Mayer, A.T., Sagiv-Barfi, I., Wang, K., Vermesh, O., Czerwinski, D.K., Johnson, E.M., James, M.L., Levy, R., Gambhir, S.S., 2018. Imaging activated T cells predicts response to cancer vaccines. J. Clin. Invest. 128, 2569–2580. https://doi.org/10.1172/JCI98509
- Alam, I.S., Simonetta, F., Scheller, L., Mayer, A.T., Murty, S., Vermesh, O., Nobashi, T.W., Lohmeyer, J.K., Hirai, T., Baker, J., Lau, K.H., Negrin, R., Gambhir, S.S., 2020. Visualization of Activated T Cells by OX40-ImmunoPET as a Strategy for Diagnosis of Acute Graft-versus-Host Disease. Cancer Res 80, 4780–4790. https://doi.org/10.1158/0008-5472.CAN-20-1149
- Assmann, J.C., Farthing, D.E., Saito, K., Maglakelidze, N., Oliver, B., Warrick, K.A., Sourbier, C., Ricketts, C.J., Meyer, T.J., Pavletic, S.Z., Linehan, W.M., Krishna, M.C., Gress, R.E., Buxbaum, N.P., 2021. Glycolytic metabolism of pathogenic T cells enables early detection of GVHD by 13C-MRI. Blood 137, 126–137. https://doi.org/10.1182/blood.2020005770
- Awasthi, V., Holter, J., Thorp, K., Anderson, S., Epstein, R., 2010. F-18-fluorothymidine-PET evaluation of bone marrow transplant in a rat model. Nucl Med Commun 31, 152–158. https://doi.org/10.1097/MNM.0b013e3283339f92
- Benoist, C., Germain, R.N., Mathis, D., 2006. A plaidoyer for "systems immunology." Immunol Rev 210, 229–234. https://doi.org/10.1111/j.0105-2896.2006.00374.x
- Blagov, S., Zvyagin, I.V., Shelikhova, L., Khismatullina, R., Balashov, D., Komech, E., Fomchenkova, V., Shugay, M., Starichkova, J., Kurnikova, E., Pershin, D., Fadeeva, M., Glushkova, S., Muzalevskii, Y., Kazachenok, A., Efimenko, M., Osipova, E., Novichkova, G., Chudakov, D., Maschan, A., Maschan, M., 2021. T-cell tracking, safety, and effect of low-dose donor memory T-cell infusions after αβ T cell-depleted hematopoietic stem cell transplantation. Bone Marrow Transplant 56, 900–908. https://doi.org/10.1038/s41409-020-01128-2
- Blazar, B.R., Sharpe, A.H., Chen, A.I., Panoskaltsis-Mortari, A., Lees, C., Akiba, H., Yagita, H., Killeen, N., Taylor, P.A., 2003. Ligation of OX40 (CD134) regulates graft-versus-host disease (GVHD) and graft rejection in allogeneic bone marrow transplant recipients. Blood 101, 3741–3748. https://doi.org/10.1182/blood-2002-10-3048
- Bodet-Milin, C., Lacombe, M., Malard, F., Lestang, E., Cahu, X., Chevallier, P., Guillaume, T., Delaunay, J., Brissot, E., Moreau, P., Kraeber-Bodere, F., Mohty, M., 2014. 18F-FDG PET/CT for the assessment of gastrointestinal GVHD: results of a pilot study. Bone Marrow Transplant 49, 131–137. https://doi.org/10.1038/bmt.2013.144
- Buhler, S., Bettens, F., Dantin, C., Ferrari-Lacraz, S., Ansari, M., Mamez, A.-C., Masouridi-Levrat, S., Chalandon, Y., Villard, J., 2020. Genetic T-cell receptor diversity at 1 year following allogeneic hematopoietic stem cell transplantation. Leukemia 34, 1422–1432. https://doi.org/10.1038/s41375-019-0654-y
- Cherk, M.H., Khor, R., Barber, T.W., Yap, K.S.K., Patil, S., Walker, P., Avery, S., Roberts, S., Kemp, W., Pham, A., Bailey, M., Kalff, V., 2022. Noninvasive Assessment of Acute Graft-Versus-Host Disease of the Gastrointestinal Tract After Allogeneic Hemopoietic Stem Cell Transplantation Using 18F-FDG PET. J Nucl Med 63, 1899–1905. https://doi.org/10.2967/jnumed.121.263688
- Conde, E., Vercher, E., Soria-Castellano, M., Suarez-Olmos, J., Mancheño, U., Elizalde, E., Rodriguez, M.L., Glez-Vaz, J., Casares, N., Rodríguez-García, E., Hommel, M., González-Aseguinolaza, G., Uranga-Murillo, I., Pardo, J., Alkorta, G., Melero, I., Lasarte, J., Hervas-Stubbs, S., 2021. Epitope spreading driven by the joint action of CART cells and pharmacological STING stimulation counteracts tumor escape via antigen-loss variants. J Immunother Cancer 9, e003351. https://doi.org/10.1136/jitc-2021-003351
- Davis, M.M., Tato, C.M., Furman, D., 2017. Systems immunology: just getting started. Nat Immunol 18, 725–732. https://doi.org/10.1038/ni.3768

- Dhodapkar, K.M., Cohen, A.D., Kaushal, A., Garfall, A.L., Manalo, R.J., Carr, A.R., McCachren, S.S., Stadtmauer, E.A., Lacey, S.F., Melenhorst, J.J., June, C.H., Milone, M.C., Dhodapkar, M.V., 2022. Changes in Bone Marrow Tumor and Immune Cells Correlate with Durability of Remissions Following BCMA CAR T Therapy in Myeloma. Blood Cancer Discov 3, 490–501. https://doi.org/10.1158/2643-3230.BCD-22-0018
- Di lanni, M., Falzetti, F., Carotti, A., Terenzi, A., Castellino, F., Bonifacio, E., Del Papa, B., Zei, T., Ostini, R.I., Cecchini, D., Aloisi, T., Perruccio, K., Ruggeri, L., Balucani, C., Pierini, A., Sportoletti, P., Aristei, C., Falini, B., Reisner, Y., Velardi, A., Aversa, F., Martelli, M.F., 2011. Tregs prevent GVHD and promote immune reconstitution in HLA-haploidentical transplantation. Blood 117, 3921–3928. https://doi.org/10.1182/blood-2010-10-311894
- Du, J., Paz, K., Thangavelu, G., Schneidawind, D., Baker, J., Flynn, R., Duramad, O., Feser, C., Panoskaltsis-Mortari, A., Negrin, R.S., Blazar, B.R., 2017. Invariant natural killer T cells ameliorate murine chronic GVHD by expanding donor regulatory T cells. Blood 129, 3121–3125. https://doi.org/10.1182/blood-2016-11-752444
- Dubouchet, L., Todorov, H., Seurinck, R., Vallet, N., Van Gassen, S., Corneau, A., Blanc, C.,
   Zouali, H., Boland, A., Deleuze, J.-F., Ingram, B., de Latour, R.P., Saeys, Y., Socié,
   G., Michonneau, D., 2022. Operational tolerance after hematopoietic stem cell transplantation is characterized by distinct transcriptional, phenotypic, and metabolic signatures.
   Sci Transl Med 14, eabg3083.
   https://doi.org/10.1126/scitranslmed.abg3083
- Edinger, M., Hoffmann, P., Ermann, J., Drago, K., Fathman, C.G., Strober, S., Negrin, R.S., 2003. CD4+CD25+ regulatory T cells preserve graft-versus-tumor activity while inhibiting graft-versus-host disease after bone marrow transplantation. Nat Med 9, 1144–1150. https://doi.org/10.1038/nm915
- Etra, A.M., Capellini, A., Alousi, A.M., Al Malki, M.M., Choe, H.K., DeFilipp, Z., Hogan, W.J., Kitko, C.L., Ayuk, F.A., Baez, J., Gandhi, I., Kasikis, S., Gleich, S., Hexner, E., Hoepting, M., Kapoor, U., Kowalyk, S., Kwon, D., Langston, A., Mielcarek, M., Morales, G., Özbek, U., Qayed, M., Reshef, R., Roesler, W., Spyrou, N., Young, R., Chen, Y.-B., Ferrara, J.L., Levine, J.E., 2022. Effective treatment of low risk acute GVHD with itacitinib monotherapy. Blood blood.2022017442. https://doi.org/10.1182/blood.2022017442
- Finney, O.C., Brakke, H.M., Rawlings-Rhea, S., Hicks, R., Doolittle, D., Lopez, M., Futrell, R.B., Orentas, R.J., Li, D., Gardner, R.A., Jensen, M.C., 2019. CD19 CAR T cell product and disease attributes predict leukemia remission durability. J Clin Invest 129, 2123–2132. https://doi.org/10.1172/JCl125423
- Fraietta, J.A., Lacey, S.F., Orlando, E.J., Pruteanu-Malinici, I., Gohil, M., Lundh, S., Boesteanu, A.C., Wang, Y., O'Connor, R.S., Hwang, W.-T., Pequignot, E., Ambrose, D.E., Zhang, C., Wilcox, N., Bedoya, F., Dorfmeier, C., Chen, F., Tian, L., Parakandi, H., Gupta, M., Young, R.M., Johnson, F.B., Kulikovskaya, I., Liu, L., Xu, J., Kassim, S.H., Davis, M.M., Levine, B.L., Frey, N.V., Siegel, D.L., Huang, A.C., Wherry, E.J., Bitter, H., Brogdon, J.L., Porter, D.L., June, C.H., Melenhorst, J.J., 2018. Determinants of response and resistance to CD19 chimeric antigen receptor (CAR) T cell therapy of chronic lymphocytic leukemia. Nat Med 24, 563–571. https://doi.org/10.1038/s41591-018-0010-1
- Gardner, R.A., Finney, O., Annesley, C., Brakke, H., Summers, C., Leger, K., Bleakley, M., Brown, C., Mgebroff, S., Kelly-Spratt, K.S., Hoglund, V., Lindgren, C., Oron, A.P., Li, D., Riddell, S.R., Park, J.R., Jensen, M.C., 2017. Intent-to-treat leukemia remission by CD19 CAR T cells of defined formulation and dose in children and young adults. Blood 129, 3322–3331. https://doi.org/10.1182/blood-2017-02-769208
- Heczey, A., Courtney, A.N., Montalbano, A., Robinson, S., Liu, K., Li, M., Ghatwai, N., Dakhova, O., Liu, B., Raveh-Sadka, T., Chauvin-Fleurence, C.N., Xu, X., Ngai, H., Di Pierro, E.J., Savoldo, B., Dotti, G., Metelitsa, L.S., 2020. Anti-GD2 CAR-NKT cells in patients with relapsed or refractory neuroblastoma: an interim analysis. Nat Med 26, 1686–1690. https://doi.org/10.1038/s41591-020-1074-2

- Heczey, A., Liu, D., Tian, G., Courtney, A.N., Wei, J., Marinova, E., Gao, X., Guo, L., Yvon, E., Hicks, J., Liu, H., Dotti, G., Metelitsa, L.S., 2014. Invariant NKT cells with chimeric antigen receptor provide a novel platform for safe and effective cancer immunotherapy. Blood 124, 2824–2833. https://doi.org/10.1182/blood-2013-11-541235
- Hirai, T., Mayer, A.T., Nobashi, T.W., Lin, P.-Y., Xiao, Z., Udagawa, T., Seo, K., Simonetta, F., Baker, J., Cheng, A.G., Negrin, R.S., Gambhir, S.S., 2021. Imaging alloreactive T cells provides early warning of organ transplant rejection. JCI Insight 6, e145360. https://doi.org/10.1172/jci.insight.145360
- Holtan, S.G., Shabaneh, A., Betts, B.C., Rashidi, A., MacMillan, M.L., Ustun, C., Amin, K., Vaughn, B.P., Howard, J., Khoruts, A., Arora, M., DeFor, T.E., Johnson, D., Blazar, B.R., Weisdorf, D.J., Wang, J., 2019. Stress responses, M2 macrophages, and a distinct microbial signature in fatal intestinal acute graft-versus-host disease. JCI Insight 5, e129762, 129762. https://doi.org/10.1172/jci.insight.129762
- Kanakry, C.G., Coffey, D.G., Towlerton, A.M.H., Vulic, A., Storer, B.E., Chou, J., Yeung, C.C.S., Gocke, C.D., Robins, H.S., O'Donnell, P.V., Luznik, L., Warren, E.H., 2016. Origin and evolution of the T cell repertoire after posttransplantation cyclophosphamide. JCI Insight 1, e86252. https://doi.org/10.1172/jci.insight.86252
- Koreth, J., Matsuoka, K., Kim, H.T., McDonough, S.M., Bindra, B., Alyea, E.P., Armand, P., Cutler, C., Ho, V.T., Treister, N.S., Bienfang, D.C., Prasad, S., Tzachanis, D., Joyce, R.M., Avigan, D.E., Antin, J.H., Ritz, J., Soiffer, R.J., 2011. Interleukin-2 and regulatory T cells in graft-versus-host disease. N Engl J Med 365, 2055–2066. https://doi.org/10.1056/NEJMoa1108188
- Kotani, A., Ishikawa, T., Matsumura, Y., Ichinohe, T., Ohno, H., Hori, T., Uchiyama, T., 2001. Correlation of peripheral blood OX40+(CD134+) T cells with chronic graft-versus-host disease in patients who underwent allogeneic hematopoietic stem cell transplantation. Blood 98, 3162–3164. https://doi.org/10.1182/blood.v98.10.3162
- Koyama, D., Murata, M., Hanajiri, R., Akashi, T., Okuno, S., Kamoshita, S., Julamanee, J., Takagi, E., Miyao, K., Sakemura, R., Goto, T., Terakura, S., Nishida, T., Kiyoi, H., 2019. Quantitative Assessment of T Cell Clonotypes in Human Acute Graft-versus-Host Disease Tissues. Biol Blood Marrow Transplant 25, 417–423. https://doi.org/10.1016/j.bbmt.2018.10.012
- Lamb, L.S., Abhyankar, S.A., Hazlett, L., O'Neal, W., Folk, R.S., Vogt, S., Parrish, R.S., Bridges, K., Henslee-Downey, P.J., Gee, A.P., 1999. Expression of CD134 (0X-40) on T cells during the first 100 days following allogeneic bone marrow transplantation as a marker for lymphocyte activation and therapy-resistant graft-versus-host disease. Cytometry 38, 238–243. https://doi.org/10.1002/(sici)1097-0320(19991015)38:5<238::aid-cyto6>3.0.co;2-o
- Latis, E., Michonneau, D., Leloup, C., Varet, H., Peffault de Latour, R., CRYOSTEM Consortium, Bianchi, E., Socié, G., Rogge, L., 2020. Cellular and molecular profiling of T-cell subsets at the onset of human acute GVHD. Blood Adv 4, 3927–3942. https://doi.org/10.1182/bloodadvances.2019001032
- Lee, Y.Z., Akinnagbe-Zusterzeel, E., Fowler, K.A., Coghill, J.M., 2018. 18F-3'-Deoxy-3'-Fluorothymidine Positron Emission Tomography Imaging for the Prediction of Acute Graft-Versus-Host Disease in Mouse Hematopoietic Stem Cell Transplant Models. Biol Blood Marrow Transplant 24, 2184–2189. https://doi.org/10.1016/j.bbmt.2018.06.032
- Leick, M., Gittelman, R.M., Yusko, E., Sanders, C., Robins, H., DeFilipp, Z., Nikiforow, S., Ritz, J., Chen, Y.-B., 2020. T Cell Clonal Dynamics Determined by High-Resolution TCR-β Sequencing in Recipients after Allogeneic Hematopoietic Cell Transplantation. Biol Blood Marrow Transplant 26, 1567–1574. https://doi.org/10.1016/j.bbmt.2020.04.026
- Leveson-Gower, D.B., Olson, J.A., Sega, E.I., Luong, R.H., Baker, J., Zeiser, R., Negrin, R.S., 2011. Low doses of natural killer T cells provide protection from acute graft-versus-host disease via an IL-4-dependent mechanism. Blood 117, 3220–3229. https://doi.org/10.1182/blood-2010-08-303008
- Levine, J.E., Braun, T.M., Harris, A.C., Holler, E., Taylor, A., Miller, H., Magenau, J., Weisdorf, D.J., Ho, V.T., Bolaños-Meade, J., Alousi, A.M., Ferrara, J.L.M., Blood and Marrow

- Transplant Clinical Trials Network, 2015. A prognostic score for acute graft-versus-host disease based on biomarkers: a multicentre study. Lancet Haematol 2, e21-29. https://doi.org/10.1016/S2352-3026(14)00035-0
- Li, C., Han, C., Duan, S., Li, P., Alam, I.S., Xiao, Z., 2022. Visualizing T-Cell Responses: The T-Cell PET Imaging Toolbox. J Nucl Med 63, 183–188. https://doi.org/10.2967/jnumed.121.261976
- Lohmeyer, J.K., Hirai, T., Turkoz, M., Buhler, S., Lopes Ramos, T., Köhler, N., Baker, J., Melotti, A., Wagner, I., Pradier, A., Wang, S., Ji, X., Becattini, S., Villard, J., Merkler, D., Chalandon, Y., Negrin, R.S., Simonetta, F., 2022. Analysis of T cell Repertoire and Transcriptome Identifies Mechanisms of Regulatory T cell (Treg) Suppression of GvHD. Blood blood.2022017982. https://doi.org/10.1182/blood.2022017982
- Lubner, M.G., Menias, C.O., Agrons, M., Alhalabi, K., Katabathina, V.S., Elsayes, K.M., Pickhardt, P.J., 2017. Imaging of Abdominal and Pelvic Manifestations of Graft-Versus-Host Disease After Hematopoietic Stem Cell Transplant. AJR Am J Roentgenol 209, 33–45. https://doi.org/10.2214/AJR.17.17866
- Maas-Bauer, K., Lohmeyer, J.K., Hirai, T., Ramos, T.L., Fazal, F.M., Litzenburger, U.M., Yost, K.E., Ribado, J.V., Kambham, N., Wenokur, A.S., Lin, P.-Y., Alvarez, M., Mavers, M., Baker, J., Bhatt, A.S., Chang, H.Y., Simonetta, F., Negrin, R.S., 2021. Invariant natural killer T-cell subsets have diverse graft-versus-host-disease-preventing and antitumor effects. Blood 138, 858–870. https://doi.org/10.1182/blood.2021010887
- Magenau, J.M., Qin, X., Tawara, I., Rogers, C.E., Kitko, C., Schlough, M., Bickley, D., Braun, T.M., Jang, P.-S., Lowler, K.P., Jones, D.M., Choi, S.W., Reddy, P., Mineishi, S., Levine, J.E., Ferrara, J.L.M., Paczesny, S., 2010. Frequency of CD4(+)CD25(hi)FOXP3(+) regulatory T cells has diagnostic and prognostic value as a biomarker for acute graft-versus-host-disease. Biol Blood Marrow Transplant 16, 907–914. https://doi.org/10.1016/j.bbmt.2010.02.026
- Malard, F., Labopin, M., Chevallier, P., Guillaume, T., Duquesne, A., Rialland, F., Derenne, S., Peterlin, P., Leauté, A.-G., Brissot, E., Gregoire, M., Moreau, P., Saas, P., Gaugler, B., Mohty, M., 2016. Larger number of invariant natural killer T cells in PBSC allografts correlates with improved GVHD-free and progression-free survival. Blood 127, 1828–1835. https://doi.org/10.1182/blood-2015-12-688739
- Mamez, A.-C., Pradier, A., Giannotti, F., Petitpas, A., Urdiola, M.F., Vu, D.-L., Masouridi-Levrat, S., Morin, S., Dantin, C., Clerc-Renaud, D., Eberhardt, C.S., Kaiser, L., Simonetta, F., Chalandon, Y., 2021. Antibody responses to SARS-CoV2 vaccination in allogeneic hematopoietic stem cell transplant recipients. Bone Marrow Transplant 56, 3094–3096. https://doi.org/10.1038/s41409-021-01466-9
- Martelli, M.F., Di lanni, M., Ruggeri, L., Falzetti, F., Carotti, A., Terenzi, A., Pierini, A., Massei, M.S., Amico, L., Urbani, E., Del Papa, B., Zei, T., Iacucci Ostini, R., Cecchini, D., Tognellini, R., Reisner, Y., Aversa, F., Falini, B., Velardi, A., 2014. HLA-haploidentical transplantation with regulatory and conventional T-cell adoptive immunotherapy prevents acute leukemia relapse. Blood 124, 638–644. https://doi.org/10.1182/blood-2014-03-564401
- Matsuoka, K., Kim, H.T., McDonough, S., Bascug, G., Warshauer, B., Koreth, J., Cutler, C., Ho, V.T., Alyea, E.P., Antin, J.H., Soiffer, R.J., Ritz, J., 2010. Altered regulatory T cell homeostasis in patients with CD4+ lymphopenia following allogeneic hematopoietic stem cell transplantation. J Clin Invest 120, 1479–1493. https://doi.org/10.1172/JCI41072
- Mavers, M., Maas-Bauer, K., Negrin, R.S., 2017. Invariant Natural Killer T Cells As Suppressors of Graft-versus-Host Disease in Allogeneic Hematopoietic Stem Cell Transplantation. Front Immunol 8, 900. https://doi.org/10.3389/fimmu.2017.00900
- Meier, J., Roberts, C., Avent, K., Hazlett, A., Berrie, J., Payne, K., Hamm, D., Desmarais, C., Sanders, C., Hogan, K.T., Archer, K.J., Manjili, M.H., Toor, A.A., 2013. Fractal organization of the human T cell repertoire in health and after stem cell transplantation. Biol Blood Marrow Transplant 19, 366–377. https://doi.org/10.1016/j.bbmt.2012.12.004

- Meier, J.A., Haque, M., Fawaz, M., Abdeen, H., Coffey, D., Towlerton, A., Abdeen, A., Toor, A., Warren, E., Reed, J., Kanakry, C.G., Keating, A., Luznik, L., Toor, A.A., 2019. T Cell Repertoire Evolution after Allogeneic Bone Marrow Transplantation: An Organizational Perspective. Biol Blood Marrow Transplant 25, 868–882. https://doi.org/10.1016/j.bbmt.2019.01.021
- Meyer, E.H., Hsu, A.R., Liliental, J., Löhr, A., Florek, M., Zehnder, J.L., Strober, S., Lavori, P., Miklos, D.B., Johnson, D.S., Negrin, R.S., 2013. A distinct evolution of the T-cell repertoire categorizes treatment refractory gastrointestinal acute graft-versus-host disease. Blood 121, 4955–4962. https://doi.org/10.1182/blood-2013-03-489757
- Meyer, E.H., Laport, G., Xie, B.J., MacDonald, K., Heydari, K., Sahaf, B., Tang, S.-W., Baker, J., Armstrong, R., Tate, K., Tadisco, C., Arai, S., Johnston, L., Lowsky, R., Muffly, L., Rezvani, A.R., Shizuru, J., Weng, W.-K., Sheehan, K., Miklos, D., Negrin, R.S., 2019. Transplantation of donor grafts with defined ratio of conventional and regulatory T cells in HLA-matched recipients. JCI Insight 4, e127244, 127244. https://doi.org/10.1172/jci.insight.127244
- Namavari, M., Chang, Y.-F., Kusler, B., Yaghoubi, S., Mitchell, B.S., Gambhir, S.S., 2011. Synthesis of 2'-deoxy-2'-[18F]fluoro-9-β-D-arabinofuranosylguanine: a novel agent for imaging T-cell activation with PET. Mol Imaging Biol 13, 812–818. https://doi.org/10.1007/s11307-010-0414-x
- Neelapu, S.S., Locke, F.L., Bartlett, N.L., Lekakis, L.J., Miklos, D.B., Jacobson, C.A., Braunschweig, I., Oluwole, O.O., Siddiqi, T., Lin, Y., Timmerman, J.M., Stiff, P.J., Friedberg, J.W., Flinn, I.W., Goy, A., Hill, B.T., Smith, M.R., Deol, A., Farooq, U., McSweeney, P., Munoz, J., Avivi, I., Castro, J.E., Westin, J.R., Chavez, J.C., Ghobadi, A., Komanduri, K.V., Levy, R., Jacobsen, E.D., Witzig, T.E., Reagan, P., Bot, A., Rossi, J., Navale, L., Jiang, Y., Aycock, J., Elias, M., Chang, D., Wiezorek, J., Go, W.Y., 2017. Axicabtagene Ciloleucel CAR T-Cell Therapy in Refractory Large B-Cell Lymphoma. N Engl J Med 377, 2531–2544. https://doi.org/10.1056/NEJMoa1707447
- Negrin, R.S., 2015. Graft-versus-host disease versus graft-versus-leukemia. Hematology Am Soc Hematol Educ Program 2015, 225–230. https://doi.org/10.1182/asheducation-2015.1.225
- Nguyen, H.D., Chatterjee, S., Haarberg, K.M.K., Wu, Y., Bastian, D., Heinrichs, J., Fu, J., Daenthanasanmak, A., Schutt, S., Shrestha, S., Liu, C., Wang, H., Chi, H., Mehrotra, S., Yu, X.-Z., 2016. Metabolic reprogramming of alloantigen-activated T cells after hematopoietic cell transplantation. J Clin Invest 126, 1337–1352. https://doi.org/10.1172/JCI82587
- Noviello, M., Manfredi, F., Ruggiero, E., Perini, T., Oliveira, G., Cortesi, F., De Simone, P., Toffalori, C., Gambacorta, V., Greco, R., Peccatori, J., Casucci, M., Casorati, G., Dellabona, P., Onozawa, M., Teshima, T., Griffioen, M., Halkes, C.J.M., Falkenburg, J.H.F., Stölzel, F., Altmann, H., Bornhäuser, M., Waterhouse, M., Zeiser, R., Finke, J., Cieri, N., Bondanza, A., Vago, L., Ciceri, F., Bonini, C., 2019. Bone marrow central memory and memory stem T-cell exhaustion in AML patients relapsing after HSCT. Nat Commun 10, 1065. https://doi.org/10.1038/s41467-019-08871-1
- Paczesny, S., 2018. Biomarkers for posttransplantation outcomes. Blood 131, 2193–2204. https://doi.org/10.1182/blood-2018-02-791509
- Park, J.H., Rivière, I., Gonen, M., Wang, X., Sénéchal, B., Curran, K.J., Sauter, C., Wang, Y., Santomasso, B., Mead, E., Roshal, M., Maslak, P., Davila, M., Brentjens, R.J., Sadelain, M., 2018. Long-Term Follow-up of CD19 CAR Therapy in Acute Lymphoblastic Leukemia. N Engl J Med 378, 449–459. https://doi.org/10.1056/NEJMoa1709919
- Paz Morante, M., Briones, J., Canto, E., Sabzevari, H., Martino, R., Sierra, J., Rodriguez-Sanchez, J.L., Vidal, S., 2006. Activation-associated phenotype of CD3 T cells in acute graft-versus-host disease. Clin Exp Immunol 145, 36–43. https://doi.org/10.1111/j.1365-2249.2006.03104.x
- Pektor, S., Schlöder, J., Klasen, B., Bausbacher, N., Wagner, D.-C., Schreckenberger, M., Grabbe, S., Jonuleit, H., Miederer, M., 2020. Using immuno-PET imaging to monitor

- kinetics of T cell-mediated inflammation and treatment efficiency in a humanized mouse model for GvHD. Eur J Nucl Med Mol Imaging 47, 1314–1325. https://doi.org/10.1007/s00259-019-04507-0
- Pidala, J., Bloom, G.C., Eschrich, S., Sarwal, M., Enkemann, S., Betts, B.C., Beato, F., Yoder, S., Anasetti, C., 2015. Tolerance associated gene expression following allogeneic hematopoietic cell transplantation. PLoS One 10, e0117001. https://doi.org/10.1371/journal.pone.0117001
- Pidala, J., Hamadani, M., Dawson, P., Martens, M., Alousi, A.M., Jagasia, M., Efebera, Y.A., Chhabra, S., Pusic, I., Holtan, S.G., Ferrara, J.L.M., Levine, J.E., Mielcarek, M., Anasetti, C., Antin, J.H., Bolaños-Meade, J., Howard, A., Logan, B.R., Leifer, E.S., Pritchard, T.S., Horowitz, M.M., MacMillan, M.L., 2020. Randomized multicenter trial of sirolimus vs prednisone as initial therapy for standard-risk acute GVHD: the BMT CTN 1501 trial. Blood 135, 97–107. https://doi.org/10.1182/blood.2019003125
- Pidala, J., Sigdel, T.K., Wang, A., Hsieh, S., Inamoto, Y., Martin, P.J., Flowers, M.E., Hansen, J.A., Lee, S.J., Sarwal, M.M., 2017. A combined biomarker and clinical panel for chronic graft versus host disease diagnosis. J Pathol Clin Res 3, 3–16. https://doi.org/10.1002/cjp2.58
- Pierini, A., Ruggeri, L., Carotti, A., Falzetti, F., Saldi, S., Terenzi, A., Zucchetti, C., Ingrosso, G., Zei, T., Iacucci Ostini, R., Piccinelli, S., Bonato, S., Tricarico, S., Mancusi, A., Ciardelli, S., Limongello, R., Merluzzi, M., Di Ianni, M., Tognellini, R., Minelli, O., Mecucci, C., Martelli, M.P., Falini, B., Martelli, M.F., Aristei, C., Velardi, A., 2021. Haploidentical age-adapted myeloablative transplant and regulatory and effector T cells for acute myeloid leukemia. Blood Adv 5, 1199–1208. https://doi.org/10.1182/bloodadvances.2020003739
- Pradier, A., Mamez, A.C., Stephan, C., Giannotti, F., Masouridi-Levrat, S., Wang, S., Morin, S., Neofytos, D., Vu, D.L., Melotti, A., Arm, I., Eberhardt, C.S., Tamburini, J., Kaiser, L., Chalandon, Y., Simonetta, F., 2022. T cell receptor sequencing reveals reduced clonal breadth of T-cell responses against SARS-CoV-2 after natural infection and vaccination in allogeneic hematopoietic stem cell transplant recipients. Ann Oncol 33, 1333–1335. https://doi.org/10.1016/j.annonc.2022.09.153
- Roll, W., Evers, G., Strotmann, R., Albring, J., Reicherts, C., Noto, B., Weckesser, M., Lenz, G., Schäfers, M., Stelljes, M., 2021a. Fluorodeoxyglucose F 18 for the Assessment of Acute Intestinal Graft-versus-Host Disease and Prediction of Response to Immunosuppressive Therapy. Transplant Cell Ther 27, 603–610. https://doi.org/10.1016/j.jtct.2021.04.011
- Roll, W., Schindler, P., Masthoff, M., Strotmann, R., Albring, J., Reicherts, C., Weckesser, M., Noto, B., Stelljes, M., Schäfers, M., Evers, G., 2021b. 18F-FDG-PET-MRI for the assessment of acute intestinal graft-versus-host-disease (GvHD). BMC Cancer 21, 1015. https://doi.org/10.1186/s12885-021-08748-x
- Ronald, J.A., Kim, B.-S., Gowrishankar, G., Namavari, M., Alam, I.S., D'Souza, A., Nishikii, H., Chuang, H.-Y., Ilovich, O., Lin, C.-F., Reeves, R., Shuhendler, A., Hoehne, A., Chan, C.T., Baker, J., Yaghoubi, S.S., VanBrocklin, H.F., Hawkins, R., Franc, B.L., Jivan, S., Slater, J.B., Verdin, E.F., Gao, K.T., Benjamin, J., Negrin, R., Gambhir, S.S., 2017. A PET Imaging Strategy to Visualize Activated T Cells in Acute Graft-versus-Host Disease Elicited by Allogenic Hematopoietic Cell Transplant. Cancer Res 77, 2893–2902. https://doi.org/10.1158/0008-5472.CAN-16-2953
- Rotolo, A., Caputo, V.S., Holubova, M., Baxan, N., Dubois, O., Chaudhry, M.S., Xiao, X., Goudevenou, K., Pitcher, D.S., Petevi, K., Kachramanoglou, C., Iles, S., Naresh, K., Maher, J., Karadimitris, A., 2018. Enhanced Anti-lymphoma Activity of CAR19-iNKT Cells Underpinned by Dual CD19 and CD1d Targeting. Cancer Cell 34, 596-610.e11. https://doi.org/10.1016/j.ccell.2018.08.017
- Rubio, M.-T., Bouillié, M., Bouazza, N., Coman, T., Trebeden-Nègre, H., Gomez, A., Suarez, F., Sibon, D., Brignier, A., Paubelle, E., Nguyen-Khoc, S., Cavazzana, M., Lantz, O., Mohty, M., Urien, S., Hermine, O., 2017. Pre-transplant donor CD4- invariant NKT cell

- expansion capacity predicts the occurrence of acute graft-versus-host disease. Leukemia 31, 903–912. https://doi.org/10.1038/leu.2016.281
- Rubio, M.-T., Moreira-Teixeira, L., Bachy, E., Bouillié, M., Milpied, P., Coman, T., Suarez, F., Marcais, A., Sibon, D., Buzyn, A., Caillat-Zucman, S., Cavazzana-Calvo, M., Varet, B., Dy, M., Hermine, O., Leite-de-Moraes, M., 2012. Early posttransplantation donor-derived invariant natural killer T-cell recovery predicts the occurrence of acute graft-versus-host disease and overall survival. Blood 120, 2144–2154. https://doi.org/10.1182/blood-2012-01-404673
- Sakaguchi, S., Mikami, N., Wing, J.B., Tanaka, A., Ichiyama, K., Ohkura, N., 2020. Regulatory T Cells and Human Disease. Annu Rev Immunol 38, 541–566. https://doi.org/10.1146/annurev-immunol-042718-041717
- Sanchez, J., Casaño, J., Alvarez, M.A., Roman-Gomez, J., Martin, C., Martinez, F., Gomez, P., Serrano, J., Herrera, C., Torres, A., 2004. Kinetic of regulatory CD25high and activated CD134+ (OX40) T lymphocytes during acute and chronic graft-versus-host disease after allogeneic bone marrow transplantation. Br J Haematol 126, 697–703. https://doi.org/10.1111/j.1365-2141.2004.05108.x
- Schneidawind, D., Baker, J., Pierini, A., Buechele, C., Luong, R.H., Meyer, E.H., Negrin, R.S., 2015. Third-party CD4+ invariant natural killer T cells protect from murine GVHD lethality. Blood 125, 3491–3500. https://doi.org/10.1182/blood-2014-11-612762
- Schneidawind, D., Pierini, A., Alvarez, M., Pan, Y., Baker, J., Buechele, C., Luong, R.H., Meyer, E.H., Negrin, R.S., 2014. CD4+ invariant natural killer T cells protect from murine GVHD lethality through expansion of donor CD4+CD25+FoxP3+ regulatory T cells. Blood 124, 3320–3328. https://doi.org/10.1182/blood-2014-05-576017
- Schultz, L., 2020. Chimeric Antigen Receptor T Cell Therapy for Pediatric B-ALL: Narrowing the Gap Between Early and Long-Term Outcomes. Front Immunol 11, 1985. https://doi.org/10.3389/fimmu.2020.01985
- Scott, A.P., Thomas, P., Pattison, D.A., Francis, L., Ridge, P., Tey, S.-K., Kennedy, G.A., 2022. [18F]GE-180 PET/CT assessment of enterocytic translocator protein (TSPO) over-expression: a pilot study in gastrointestinal GVHD. Bone Marrow Transplant 57, 517–519. https://doi.org/10.1038/s41409-022-01571-3
- Simonetta, F., Alam, I.S., Lohmeyer, J.K., Sahaf, B., Good, Z., Chen, W., Xiao, Z., Hirai, T., Scheller, L., Engels, P., Vermesh, O., Robinson, E., Haywood, T., Sathirachinda, A., Baker, J., Malipatlolla, M.B., Schultz, L.M., Spiegel, J.Y., Lee, J.T., Miklos, D.B., Mackall, C.L., Gambhir, S.S., Negrin, R.S., 2021a. Molecular Imaging of Chimeric Antigen Receptor T Cells by ICOS-ImmunoPET. Clin Cancer Res 27, 1058–1068. https://doi.org/10.1158/1078-0432.CCR-20-2770
- Simonetta, F., Lohmeyer, J.K., Hirai, T., Maas-Bauer, K., Alvarez, M., Wenokur, A.S., Baker, J., Aalipour, A., Ji, X., Haile, S.T., Mackall, C.L., Negrin, R., 2021b. Allogeneic CAR-invariant Natural Killer T Cells Exert Potent Antitumor Effects Through Host CD8 T Cell Cross-Priming. Clin Cancer Res. https://doi.org/10.1158/1078-0432.CCR-21-1329
- Simonetta, F., Pradier, A., Bosshard, C., Masouridi-Levrat, S., Dantin, C., Koutsi, A., Tirefort, Y., Roosnek, E., Chalandon, Y., 2019. Dynamics of Expression of Programmed Cell Death Protein-1 (PD-1) on T Cells After Allogeneic Hematopoietic Stem Cell Transplantation. Front Immunol 10, 1034. https://doi.org/10.3389/fimmu.2019.01034
- Stelljes, M., Hermann, S., Albring, J., Köhler, G., Löffler, M., Franzius, C., Poremba, C., Schlösser, V., Volkmann, S., Opitz, C., Bremer, C., Kucharzik, T., Silling, G., Schober, O., Berdel, W.E., Schäfers, M., Kienast, J., 2008. Clinical molecular imaging in intestinal graft-versus-host disease: mapping of disease activity, prediction, and monitoring of treatment efficiency by positron emission tomography. Blood 111, 2909–2918. https://doi.org/10.1182/blood-2007-10-119164
- Storek, J., Geddes, M., Khan, F., Huard, B., Helg, C., Chalandon, Y., Passweg, J., Roosnek, E., 2008. Reconstitution of the immune system after hematopoietic stem cell transplantation in humans. Semin Immunopathol 30, 425–437. https://doi.org/10.1007/s00281-008-0132-5

- Stüber, E., Von Freier, A., Marinescu, D., Fölsch, U.R., 1998. Involvement of OX40-OX40L interactions in the intestinal manifestations of the murine acute graft-versus-host disease. Gastroenterology 115, 1205–1215. https://doi.org/10.1016/s0016-5085(98)70092-7
- Suessmuth, Y., Mukherjee, R., Watkins, B., Koura, D.T., Finstermeier, K., Desmarais, C., Stempora, L., Horan, J.T., Langston, A., Qayed, M., Khoury, H.J., Grizzle, A., Cheeseman, J.A., Conger, J.A., Robertson, J., Garrett, A., Kirk, A.D., Waller, E.K., Blazar, B.R., Mehta, A.K., Robins, H.S., Kean, L.S., 2015. CMV reactivation drives posttransplant T-cell reconstitution and results in defects in the underlying TCRβ repertoire. Blood 125, 3835–3850. https://doi.org/10.1182/blood-2015-03-631853
- Tittle, T.V., Weinberg, A.D., Steinkeler, C.N., Maziarz, R.T., 1997. Expression of the T-cell activation antigen, OX-40, identifies alloreactive T cells in acute graft-versus-host disease. Blood 89, 4652–4658.
- Tkachev, V., Furlan, S.N., Watkins, B., Hunt, D.J., Zheng, H.B., Panoskaltsis-Mortari, A., Betz, K., Brown, M., Schell, J.B., Zeleski, K., Yu, A., Kirby, I., Cooley, S., Miller, J.S., Blazar, B.R., Casson, D., Bland-Ward, P., Kean, L.S., 2017. Combined OX40L and mTOR blockade controls effector T cell activation while preserving Treg reconstitution after transplant. Sci Transl Med 9, eaan3085. https://doi.org/10.1126/scitranslmed.aan3085
- Tripathi, T., Yin, W., Xue, Y., Zurawski, S., Fujita, H., Hanabuchi, S., Liu, Y.-J., Oh, S., Joo, H., 2019. Central Roles of OX40L-OX40 Interaction in the Induction and Progression of Human T Cell-Driven Acute Graft-versus-Host Disease. Immunohorizons 3, 110–120. https://doi.org/10.4049/immunohorizons.1900001
- van Beek, J.J.P., Puccio, S., Di Vito, C., De Paoli, F., Zaghi, E., Calvi, M., Scarpa, A., Peano, C., Basso, G., Cibella, J., De Philippis, C., Sarina, B., Timofeeva, I., Capizzuto, R., Mannina, D., Mineri, R., Mariotti, J., Crocchiolo, R., Santoro, A., Castagna, L., Bramanti, S., Mavilio, D., Lugli, E., 2022. Selected memory T cells infused post haploidentical hematopoietic stem cell transplantation persist and hyper-expand. Blood Adv bloodadvances.2022007735. https://doi.org/10.1182/bloodadvances.2022007735
- Van Elssen, C.H.M.J., Rashidian, M., Vrbanac, V., Wucherpfennig, K.W., Habre, Z.E., Sticht, J., Freund, C., Jacobsen, J.T., Cragnolini, J., Ingram, J., Plaisier, L., Spierings, E., Tager, A.M., Ploegh, H.L., 2017. Noninvasive Imaging of Human Immune Responses in a Human Xenograft Model of Graft-Versus-Host Disease. J Nucl Med 58, 1003–1008. https://doi.org/10.2967/jnumed.116.186007
- van Heijst, J.W.J., Ceberio, I., Lipuma, L.B., Samilo, D.W., Wasilewski, G.D., Gonzales, A.M.R., Nieves, J.L., van den Brink, M.R.M., Perales, M.A., Pamer, E.G., 2013. Quantitative assessment of T cell repertoire recovery after hematopoietic stem cell transplantation. Nat Med 19, 372–377. https://doi.org/10.1038/nm.3100
- Whangbo, J.S., Nikiforow, S., Kim, H.T., Wahl, J., Reynolds, C.G., Rai, S.C., Kim, S., Burden, A., Alho, A.C., Lacerda, J.F., Alyea, E.P., Cutler, C.S., Ho, V.T., Antin, J.H., Soiffer, R.J., Ritz, J., Koreth, J., 2022. A phase 1 study of donor regulatory T-cell infusion plus low-dose interleukin-2 for steroid-refractory chronic graft-vs-host disease. Blood Adv 6, 5786–5796. https://doi.org/10.1182/bloodadvances.2021006625
- Xiao, Z., Alam, I.S., Simonetta, F., Chen, W., Scheller, L., Murty, S., Lohmeyer, J.K., Ramos, T.L., James, M.L., Negrin, R.S., Gambhir, S.S., 2022. ICOS immunoPET enables visualization of activated T cells and early diagnosis of murine acute gastrointestinal GvHD. Blood Adv 6, 4782–4792. https://doi.org/10.1182/bloodadvances.2022007403
- Xiao, Z., Mayer, A.T., Nobashi, T.W., Gambhir, S.S., 2020. ICOS Is an Indicator of T-cell-Mediated Response to Cancer Immunotherapy. Cancer Res 80, 3023–3032. https://doi.org/10.1158/0008-5472.CAN-19-3265
- Yew, P.Y., Alachkar, H., Yamaguchi, R., Kiyotani, K., Fang, H., Yap, K.L., Liu, H.T., Wickrema, A., Artz, A., van Besien, K., Imoto, S., Miyano, S., Bishop, M.R., Stock, W., Nakamura, Y., 2015. Quantitative characterization of T-cell repertoire in allogeneic hematopoietic stem cell transplant recipients. Bone Marrow Transplant 50, 1227–1234. https://doi.org/10.1038/bmt.2015.133

- Zeiser, R., Blazar, B.R., 2017. Acute Graft-versus-Host Disease Biologic Process, Prevention, and Therapy. N Engl J Med 377, 2167–2179. https://doi.org/10.1056/NEJMra1609337
- Zeiser, R., Vago, L., 2019. Mechanisms of immune escape after allogeneic hematopoietic cell transplantation. Blood 133, 1290–1297. https://doi.org/10.1182/blood-2018-10-846824
- Zheng, G.X.Y., Terry, J.M., Belgrader, P., Ryvkin, P., Bent, Z.W., Wilson, R., Ziraldo, S.B., Wheeler, T.D., McDermott, G.P., Zhu, J., Gregory, M.T., Shuga, J., Montesclaros, L., Underwood, J.G., Masquelier, D.A., Nishimura, S.Y., Schnall-Levin, M., Wyatt, P.W., Hindson, C.M., Bharadwaj, R., Wong, A., Ness, K.D., Beppu, L.W., Deeg, H.J., McFarland, C., Loeb, K.R., Valente, W.J., Ericson, N.G., Stevens, E.A., Radich, J.P., Mikkelsen, T.S., Hindson, B.J., Bielas, J.H., 2017. Massively parallel digital transcriptional profiling of single cells. Nat Commun 8, 14049. https://doi.org/10.1038/ncomms14049
- Zheng, P., Tamaresis, J., Thangavelu, G., Xu, L., You, X., Blazar, B.R., Negrin, R.S., Zehnder, J.L., Iliopoulou, B.P., Meyer, E.H., 2020. Recipient-specific T-cell repertoire reconstitution in the gut following murine hematopoietic cell transplant. Blood Adv 4, 4232–4243. https://doi.org/10.1182/bloodadvances.2019000977
- Zorn, E., Kim, H.T., Lee, S.J., Floyd, B.H., Litsa, D., Arumugarajah, S., Bellucci, R., Alyea, E.P., Antin, J.H., Soiffer, R.J., Ritz, J., 2005. Reduced frequency of FOXP3+ CD4+CD25+ regulatory T cells in patients with chronic graft-versus-host disease. Blood 106, 2903–2911. https://doi.org/10.1182/blood-2005-03-1257
- Zouali, H., Lemasson, J., Calugareanu, A., Battail, C., Michonneau, D., le Buanec, H., Grolleau, C., Cassius, C., Robin, M., Merandet, M., Dobos, G., Mahevas, T., Rybojad, M., de Masson, A., Amode, R., Boland, A., Michel, L., Sicre de Fontbrune, F., Peffault de Latour, R., Bruneval, P., Ait-Oufella, H., Battistella, M., Jachiet, M., Bagot, M., Deleuze, J.-F., Socié, G., Bouaziz, J.-D., 2022. RNA sequencing of chronic GVHD skin lesions defines shared and unique inflammatory pathways characterizing lichen planus and morphea. Blood Adv 6, 2805–2811. https://doi.org/10.1182/bloodadvances.2021004707